Lecture Notes in Physics 912

Antal Jakovác
András Patkós

Resummation and Renormalization in Effective Theories of Particle Physics

Springer

Lecture Notes in Physics

Volume 912

The Lecture Notes in Physics

The series Lecture Notes in Physics (LNP), founded in 1969, reports new developments in physics research and teaching-quickly and informally, but with a high quality and the explicit aim to summarize and communicate current knowledge in an accessible way. Books published in this series are conceived as bridging material between advanced graduate textbooks and the forefront of research and to serve three purposes:

- to be a compact and modern up-to-date source of reference on a well-defined topic
- to serve as an accessible introduction to the field to postgraduate students and nonspecialist researchers from related areas
- to be a source of advanced teaching material for specialized seminars, courses and schools

Both monographs and multi-author volumes will be considered for publication. Edited volumes should, however, consist of a very limited number of contributions only. Proceedings will not be considered for LNP.

Volumes published in LNP are disseminated both in print and in electronic formats, the electronic archive being available at springerlink.com. The series content is indexed, abstracted and referenced by many abstracting and information services, bibliographic networks, subscription agencies, library networks, and consortia.

Proposals should be sent to a member of the Editorial Board, or directly to the managing editor at Springer:

Christian Caron
Springer Heidelberg
Physics Editorial Department I
Tiergartenstrasse 17
69121 Heidelberg/Germany
christian.caron@springer.com

More information about this series at http://www.springer.com/series/5304

Antal Jakovác • András Patkós

Resummation and Renormalization in Effective Theories of Particle Physics

Springer

Antal Jakovác
Institute of Physics
Roland Eötvös University
Budapest, Hungary

András Patkós
Institute of Physics
Roland Eötvös University
Budapest, Hungary

ISSN 0075-8450 ISSN 1616-6361 (electronic)
Lecture Notes in Physics
ISBN 978-3-319-22619-4 ISBN 978-3-319-22620-0 (eBook)
DOI 10.1007/978-3-319-22620-0

Library of Congress Control Number: 2015951832

Springer Cham Heidelberg New York Dordrecht London

Printed on acid-free paper

Springer International Publishing AG Switzerland is part of Springer Science+Business Media (www.springer.com)

Preface

The elective course titled "Finite-Temperature Quantum Fields" has been part of the curriculum of the master's degree in physics program at Eötvös University for about 15 years. The original one-semester course was introduced by one of the authors (A.P.) and extended to a two-semester series in 2013 by the second author (A.J.) in cooperation with Dr. Zsolt Szép. The aim of the lecturers was and remains to enable students to acquire the conceptual knowledge and the technical tools of quantum field theory at a level that allows them to participate in research projects of current international interest. That success in this goal has been achieved is indicated by the fact that several of the sections of the present monograph grew out of such joint work carried out with students attending the course.

The material covered in these notes should help to improve students' ability to deal in general with reorganizations of the perturbation series of renormalizable theories. The specific topics selected reflect the subject area of our own research. From the middle of the 1990s, thermodynamic changes occurring in the ground state of the strong and electroweak vacuum has been at the center of our scientific interest. Although the fundamental theories accounting in principle for all relevant phenomena are well established, field theories with effective degrees of freedom (such as the sigma-meson and constituent quarks) were constructed with an eye to the essential features of the underlying dynamics. These models are able to account for the qualitative changes and even to reproduce some known results semiquantitatively.

It was definitely not our goal to transform our handwritten notes into a monograph when we decided to write a book. We hoped to preserve the characteristics of a university course in which one learns both concepts and "recipes" of quantum field theory mostly by the detailed technical presentation of relevant examples. The eight chapters of this book can be divided into four parts, each of a different character. The historic introductory chapter is followed by two chapters reviewing the basics of quantum field theory necessary for following the directions of contemporary research. The next three chapters introduce three different and equally widely used approaches to improving convergence properties of renormalized perturbation theory. Finally, the last two chapters discuss some physical features of strong and

electroweak matter relying to a large extent on the theoretical tools developed in the previous chapters. Some frequently used or more complicated formulas are collected in three appendices.

Most of the presented material is widely known, which explains the relatively low number of external references. Our citations point either to papers in which specific results of central interest have appeared or to those works that we found (very subjectively) the most instructive. We are grateful to the entire community of theoretical particle physicists investigating characteristic features of strong and electroweak matter, from whom many ideas reflected in the material of the present notes originate.

Nevertheless, we would like to express our specific gratitude to a few colleagues who helped us in our work in the field of the effective models of particle physics in an essential way. For a very fruitful period of our scientific activity we thank to Professors F. Karsch (Bielefeld-Brookhaven) and K. Kajantie (Helsinki). Our research and the present lecture series were shaped in important ways by long-term collaboration with Zsolt Szép and Péter Petreczky. We thank also Szabolcs Borsányi, Tamás Herpay, Dénes Sexty, Péter Kovács, Gergely Markó, and Gergely Fejős.

This book is dedicated to the memory of Professor Péter Szépfalusy (1932–2015). His perfectionist lectures that we attended as students still represent an ideal for us. It was our privilege to have participated in joint research projects with Péter. His results on the application of the $1/N$ expansion to magnetic systems represented a constant source of intuition during our collaboration on the temperature-induced variations of the excitations in the quark–meson theory.

Budapest, Hungary — Antal Jakovác
April 2015 — András Patkós

Abbreviations

1PI	One-particle irreducible
2PI	Two-particle irreducible
2PR	Two particle reducible
3D	Three-dimensional
nPI	n-Particle irreducible
BEH-effect	Brout–Englert–Higgs effect
BSM	Beyond standard model
$\mathscr{B}$	Bubble integral (d dimensions)
$\mathscr{B}_3$	Bubble integral (3 dimensions)
$\mathscr{B}^F$	Finite part of the bubble integral (d dimensions)
$\mathscr{B}_d^{(0)}$	Logarithmically divergent part of the bubble integral (d dimensions)
CEP	Critical endpoint
CTP	Closed time path
DR	Dimensional reduction
DS	Dyson–Schwinger
ECCP	Equivalence class of constant physics
EoM	Equation of motion
EoS	Equation of state
FAC	Fastest apparent convergence
FRG	Functional renormalization group
HRG	Hadronic resonance gas
HTL	Hard thermal loop
IR-divergence	Infrared divergence
KMS-condition	Kubo–Martin–Schwinger condition
LCP	Line of constant physics
LO	Leading order
MC simulation	Monte Carlo simulation
MS-scheme	Minimal subtraction scheme
NLO	Next-to-leading order

OMS-scheme	On-mass-shell scheme
OPT	Optimized perturbation theory
PCAC	Partially conserved axial current
PMS	Principle of minimal sensitivity
RS	Resummation scheme
R/A formalism	Retarded/advanced formalism
SB limit	Stefon–Boltzmann limit
SM	Standard model
SSB	Spontaneous symmetry-breaking
QCD	Quantum chromodynamics
QED	Quantum electrodynamics
QGP	Quark gluon plasma
$\mathscr{T}$	Tadpole integral in d dimensions
$\mathscr{T}_3$	Tadpole integral in 3 dimensions
$\mathscr{T}^F$	Finite part of the tadpole integral in d dimensions
$\mathscr{T}_d^{(2)}$	Quadratically divergent part of the tadpole integral in d dimensions
TCP	Tricritical point

Contents

Chapter 1
Effective Theories from Nuclear to Particle Physics

Quantum fields $\hat{\psi}_i(\mathbf{x}, t)$ have the potential of bringing freely propagating field quanta, characterized by a set of quantum numbers compressed here into the index i, to rise or disappear from the ground state. Outgoing particles of radically different nature from the incoming ones enter the β-decay of a neutron: the neutral constituent of the nuclei disappears and the positively charged constituent emerges. The idea that neutrinos are born in the process of decay was at radical variance with earlier interpretations of the decay that assumed in the neutron the hidden preexistence of a proton and an electron. Fermi proposed for the mathematical description of this process the following interaction Hamiltonian [1] containing four different field operators:

$$\hat{H}_{\text{Fermi}} \sim \int d^3x \left(\bar{\psi}_{\text{proton}}(\mathbf{x}, t)\psi_{\text{neutron}}(\mathbf{x}, t)\right)\left(\bar{\psi}_{\text{electron}}(\mathbf{x}, t)\psi_{\text{neutrino}}(\mathbf{x}, t)\right). \tag{1.1}$$

The Hamiltonian contains many more potential reactions beyond the β-decay (for instance, the inverse β-decay) that were discovered in sequence and found to follow perfectly the statistical characterization predicted by the unique coupling constant of the Fermi theory.

The variable nature of the nuclear constituents gained ground also in the interpretation of the charge-invariance of the nuclear binding energy. This led to the postulation of the isotopic invariance of strong forces, formally accounting for the fact that the strength of nuclear interaction is invariant under proton $\leftrightarrow$ neutron exchange [2]. The origin of this interaction was modeled by Yukawa assuming the existence of a mediating quantum field very similar to the photon mediating electromagnetic interactions (QED) [3]. In analogy with QED, a bilinear coupling can be assumed of the two-component nucleon field $\Psi_N(x)$ and the quantum force field introduced by Yukawa. The principle of isotopic invariance was extended by Kemmer [4] also on the mediating field $\pi^\alpha(x)$, requiring its irreducible

A. Jakovác, A. Patkós, *Resummation and Renormalization in Effective Theories of Particle Physics*, Lecture Notes in Physics 912,
DOI 10.1007/978-3-319-22620-0_1

transformation under the $SU(2)_I$ group:

$$H_{\text{Yukawa}} \sim \int d^3x \bar{N}(\mathbf{x},t)\tau^\alpha N(\mathbf{x},t)\pi^\alpha(\mathbf{x},t),$$
$$N(x) = \begin{pmatrix}\psi_p \\ \psi_n\end{pmatrix}, \quad \pi^\alpha = (\pi^+,\pi^-,\pi^0). \tag{1.2}$$

(The pseudoscalar nature of the pions was recognized and appropriately taken into account only later.) Here the generators of the isotopic spin transformations $\tau^\alpha/2$ are introduced in analogy with the $SU(2)$ group of spatial quantum rotations. The two components of Ψ_N fit into the doublet and the three components of π^a into the triplet representation of the symmetry group.

By the end of the 1930s, Cassen and Condon, and also Wigner, carefully checked the consistency of the experimental information on nuclear reactions with the isotopic $SU(2)_I$ symmetry [5, 6]. Also, the mass of the quanta mediating the nuclear force was estimated by analyzing the relationship between the finite-range force field of a pointlike pion source and the mass of the scalar field quantum whose exchange produces the attractive nuclear potential. Everything was in place for the application of quantum field theory to nuclear phenomena. However, when a radical turn in world history actually brought nuclear science to the forefront of public interest, it also temporarily shifted the interest of physicists away from exploring the quantum field theory of strong interactions.

The return to activity in this field occurred in the early 1950s. In that epoch, the lowest-mass mesons were discovered, and experimental investigations exhibited the systematic variation of the nuclear binding energy/nucleon with increasing atomic number A. The extrapolation $A \to \infty$ led to the notion of *nuclear matter* characterized by finite energy density and pressure, and important characteristics were derived from the corresponding thermodynamic equation of state. The theoretical interpretation of the fundamental features of nuclear matter followed a dual approach.

First of all, some rather specific two-body, three-body, etc., complex interaction potentials were introduced and used in a generalization of quantum theory of atomic physics to the nuclear interactions. In competition with this approach, a quantum-field-theoretic description was introduced by Johnson and Teller [7]. In their model, the exchange of a scalar quantum (the *σ-field*) is responsible for the strong attraction. Stability against collapse is ensured by the presence of the $\omega_\mu(x)$ vector field (recall that same-sign electric charges interacting via the electrostatic vector field act on each other repulsively). The full classical Lagrangian density is given by the expression

$$L_{JT} = \bar{N}(x)\left[i\gamma_\mu(\partial^\mu - ig_\omega\omega^\mu) - m_N + g_\sigma\sigma(x)\right]N(x)$$
$$- \frac{1}{2}\sigma(x)\left(\Box + m_\sigma^2\right)\sigma(x) - \frac{1}{4}\omega_{\mu\nu}(x)\omega^{\mu\nu} + \frac{1}{2}m_\omega^2\omega_\mu(x)\omega^\mu(x). \tag{1.3}$$

The significance of this proposition can be appreciated by neglecting for a moment the effect of ω_μ and solving the sigma-nucleon theory on the level of the mean field approximation, characterized by a homogeneous nonvanishing expectation value of the σ-field.

The corresponding quantum equations in the Heisenberg picture are the following:

$$(\Box+m_\sigma^2)\sigma(x)-g_\sigma\bar{N}(x)N(x)=0, \qquad \left(i\gamma_\mu\partial^\mu-m_N+g_\sigma\sigma(x)\right)N(x)=0. \tag{1.4}$$

The mean field approximation corresponds to

$$<\sigma(x)>=\Sigma, \qquad m_{eff}=m_N-g_\sigma\Sigma. \tag{1.5}$$

It is remarkable that the mean field modifies the nucleon mass appearing in the second equation of (1.4). The plane-wave modes of the Dirac field with this modified mass fill the Fermi sphere of the nuclear matter constituents up to the momentum k_N^F determined by the nucleon density of the medium:

$$\rho_N=4\int\frac{d^3k}{(2\pi)^3}\Theta(k_N^F-k)=\frac{2}{3\pi^2}k_N^{F3}, \tag{1.6}$$

where the degeneracy factor $4=(2S_z+1)(2I_3+1)$ reflects the spin and isospin doublet nature of the nucleons. Next, one takes the expectation value of the first equation of (1.4) and finds the following *gap equation* for the mean field amplitude with the help of the relation $\langle\bar{N}N\rangle_k=m_{eff}/E(k)$, $E^2(k)=k^2+m_{eff}^2$, which can be seen to follow directly for the plane wave solutions of the Dirac equation:

$$m_\sigma^2\Sigma=\frac{2g_\sigma}{\pi^2}m_{eff}\int_0^{k_N^F}dk\frac{k^2}{(k^2+m_{eff}^2)^{1/2}}. \tag{1.7}$$

For nonzero density ($k_N^F\neq 0$), the ground state of the system is characterized by a nonzero σ-condensate. This condensate is not spontaneously formed; it is generated by the nonzero nucleon density.

It required five more years after this pioneering investigation before Y. Nambu raised the possibility of the spontaneous formation of a scalar condensate at vanishing baryon density, following the Ginzburg–Landau scenario of superconductivity. Here this condensate might emerge from the breakdown of the (approximate) chiral invariance of *NN*-interactions. According to his proposition, the mass of the nucleons would fully result from this symmetry-breaking [8].

With vanishing value for the starting nucleon mass, the Lagrangian of the nucleons decomposes into a sum of two chiral terms:

$$L_N = \bar{N}(x) i\gamma_\mu \partial^\mu N(x) = \bar{N}_L(x) i\gamma_\mu \partial^\mu N_L(x) + \bar{N}_R(x) i\gamma_\mu \partial^\mu N_R(x), \tag{1.8}$$

where

$$N_L = \frac{1-\gamma_5}{2} N, \qquad N_R = \frac{1+\gamma_5}{2} N. \tag{1.9}$$

On the two chiral components one is allowed to perform two independent $SU(2)$ symmetry transformations, the Lagrangian (1.8) has an $SU(2)_L \times SU(2)_R$ symmetry. A nonzero mass term of almost all elementary fermions, $m_N \bar{N}(x) N(x) = m_N(\bar{N}_L N_R + \bar{N}_R N_L)$, however, explicitly violates this symmetry, and it therefore cannot be an exact symmetry of nature.

The symmetry operation can be rearranged into a direct product of an axial and a vector transformation in the following way. One parameterizes the unitary transformations as

$$U_L = e^{i\Theta_{Lj}\tau^j}, \qquad U_R = e^{i\Theta_{Rj}\tau^j}, \tag{1.10}$$

which gives for the nucleon field the following transformation rule:

$$N(x) \to \left(\frac{1-\gamma_5}{2} e^{i\Theta_{Lj}\tau^j} + \frac{1+\gamma_5}{2} e^{i\Theta_{Rj}\tau^j} \right) N(x) = e^{i\Theta_{Vj}\tau^j + i\gamma_5 \Theta_{Aj}\tau^j} N(x), \tag{1.11}$$

with $\Theta_{Vj} = (\Theta_{Lj} + \Theta_{Rj})/2, \Theta_{Aj} = (\Theta_{Rj} - \Theta_{Lj})/2$. A mass term described by the quadratic form $\bar{N}_i \mathscr{M}_{ij} N_j$ transforms under a combined infinitesimal vector–axial transformation as

$$\delta L_{mass} = i\bar{N}(x) \left(\delta\Theta_{Vj} [\tau^j, \mathscr{M}]_- - \delta\Theta_{Aj} [\tau^j, \mathscr{M}]_+ \right) N(x). \tag{1.12}$$

The $-$ and $+$ indices of the square brackets refer to commutators and anticommutators respectively. If the isotopic symmetry is exact ($\mathscr{M} \sim I$), only the axial symmetry is broken. This means that a mechanism that produces mass to the nucleons leads to the symmetry-breaking pattern $SU_V(2) \times SU_A(2) \to SU_V(2)$.

An explicit relativistic field-theoretic mechanism of the chiral symmetry breakdown can be constructed by generalizing the Johnson–Teller model of nucleon–meson interactions with the help of a meson multiplet M with well-defined left–right transformation properties and defined as

$$M = \sigma(x) + i\eta(x) + (a_{0j}(x) + i\pi_j(x))\tau^j, \qquad M \to U_L M(x) U_R^\dagger. \tag{1.13}$$

(The conventional notation for the new meson fields is employed.) The invariant meson dynamics is easily rewritten in terms of the component fields:

$$\begin{aligned} L_M &= \frac{1}{4}\mathrm{Tr}\left(\partial_\mu M^\dagger(x)\partial^\mu M(x) - \mu^2 M^\dagger(x)M(x)\right) - \frac{\lambda}{16}\left(\mathrm{Tr}(M^\dagger(x)M(x))\right)^2 \\ &= \frac{1}{2}\Big[\partial_\mu\sigma\partial^\mu\sigma + \partial_\mu\eta\partial^\mu\eta + \partial_\mu a_{0j}\partial^\mu a_{0j} + \partial_\mu\pi_j\partial^\mu\pi_j \\ &\quad - \mu^2(\sigma^2+\eta^2+a_{0j}^2+\pi_j^2)\Big] - \frac{\lambda}{4}\left(\sigma^2+\eta^2+a_{0j}^2+\pi_j^2\right)^2, \end{aligned} \tag{1.14}$$

and it obviously has an orthogonal $O(8)$ symmetry. The generalization of the Yukawa interaction reads

$$L_{Yukawa} = -g\left(\bar{N}_L(x)M(x)N_R(x) + \bar{N}_R(x)M^\dagger(x)N_L(x)\right). \tag{1.15}$$

This is the matrix version of the *linear σ-model*.

The stability of the meson sector requires $\lambda > 0$, but the coefficient of the quadratic term can be negative ("wrong sign mass term" $\mu^2 < 0$). Then there is a spontaneously selected direction in the eight-dimensional field space along which the classical value is nonzero. This direction is chosen conventionally as the σ-axis: $\sigma_{class} = \Sigma$, and the Yukawa interaction provides mass for the nucleon, $m_N = g\Sigma$. The expansion of the meson Lagrangian around this classical ground state leads to massive σ excitations and seven massless mesons, which illustrates the consequences of Goldstone's theorem [9].

Though the idea of symmetry-breaking revolutionized the thinking on the generation of mass hierarchies in particle physics and was eventually honored with the Nobel Prize of the year 2008, this model is problematic, because the number of light (massless) particles is greater than what nature displays. There are two ways out of this dilemma.

Gell-Mann and Lévy simply omitted half of the mesons, reducing in this way the symmetry of the meson sector to $O(4)$. Their version of the σ-model has the following Lagrangian density [10]:

$$\begin{aligned} L_\sigma &= \bar{N}(x)i\gamma_\mu\partial^\mu N(x) + \frac{1}{2}\left[(\partial_\mu\sigma)^2 + (\partial_\mu\pi_j)^2 - \mu^2(\sigma^2+\pi_j^2)\right] \\ &\quad - \frac{\lambda}{4}(\sigma^2+\pi_j^2)^2 - g\bar{N}(x)\left(\sigma(x) + i\gamma_5\tau^j\pi_j(x)\right)N(x). \end{aligned} \tag{1.16}$$

In this case, one has three massless pions resulting from the spontaneous symmetry-breaking and

$$\sigma_{min}^2 = -\frac{\lambda}{\mu^2}, \qquad m_\sigma^2 = -2\lambda\mu^2. \tag{1.17}$$

Another alternative to the reduction to the right multiplet structure proceeds via the complete elimination of the mesons. The one-meson exchange between the nucleons results in a scalar but nonlocal 4-fermion interaction that displays the original $SU(2)_L \times SU(2)_R$ symmetry:

$$S = \int dx \bar{N}(x) i\gamma_\mu \partial^\mu N(x) - g^2 \int dx \int dy (\bar{N}_L(x) N_R(x)) K(x-y) (\bar{N}_R(y) N_L(y)), \tag{1.18}$$

where $K(x-y)$ is the invariant nonlocal kernel. Its local variant is the original Nambu–Jona-Lasinio model [11], which follows the example of the Fermi-interaction of the β-decay:

$$\begin{aligned} S_{NJL} &= \int dx \bar{N}(x) i\gamma_\mu \partial^\mu N(x) - g^2 \int dx (\bar{N}_L(x) N_R(x)) (\bar{N}_R(x) N_L(x)) \\ &= \int dx \bar{N}(x) i\gamma_\mu \partial^\mu N(x) - \frac{g^2}{8} \left[(\bar{N}(x) N(x))^2 - (\bar{N}(x) \gamma_5 N(x))^2 \right]. \end{aligned} \tag{1.19}$$

In the original investigation, the authors showed that for strong enough g^2, a nucleon condensate $\langle \bar{N} N \rangle \neq 0$ is formed in the ground state of the model that generates mass for the nucleons and provides three massless Goldstone modes that are identified with the pions in the chiral limit (with vanishing explicit symmetry-breaking term).

A complementary approach is to eliminate just the heavy modes. Then the meson matrix is nonlinearly parameterized:

$$M(x) = S(x) e^{i\tau^j \pi_j(x)/2F} \equiv S(x) U[\pi]. \tag{1.20}$$

In the expression of the potential energy of (1.14), only the invariant $S(x)$ shows up, while the kinetic density of the meson sector looks like

$$L_{kin} = \frac{1}{2} \partial_\mu S(x) \partial^\mu S(x) + \frac{1}{4} S^2(x) \mathrm{tr} \partial_\mu U^\dagger \partial^\mu U. \tag{1.21}$$

The effect of the nucleons comes from the Yukawa term (1.15). In the broken-symmetry phase, one has

$$S(x) = s_0 + s(x), \qquad g(N_R^\alpha \bar{N}_L^\beta) = B \mathscr{M}^{\alpha\beta}, \tag{1.22}$$

where $\mathscr{M}$ is a diagonal matrix. Neglecting the effect of the fluctuation $s(x)$ in the kinetic density, one recognizes that the dynamics of the massive $s(x)$ decouples, and one arrives at the nonlinear dynamics of the Goldstone modes:

$$L_\pi = \frac{s_0^2}{4} \mathrm{tr} \partial_\mu U^\dagger \partial^\mu U - B \mathrm{tr} \left(\mathscr{M}^\dagger U + U^\dagger \mathscr{M} \right). \tag{1.23}$$

This is the $SU(2) \times SU(2)$ symmetric nonlinear σ-model with the second term reflecting the explicit symmetry-breaking effect from the condensate of fermions. This model has been analyzed in great detail, also including terms containing higher derivatives of the Goldstone fields [12]. It is one of the most popular effective models of strong interactions, which can be mapped exactly onto the quantum chromodynamic theory at low enough energies.

All these effective models built on the principle of approximate chiral symmetry have been extended to three flavors. In the context of nuclear matter, the most advanced formulation was provided in the framework of the Walecka model [13]. It generalizes the Johnson–Teller model by including the baryon octet and also some members of the decuplet. In addition to the scalar and pseudoscalar meson octets, one also includes the vector and axial-vector resonances.

For applications to particle physics, it is more appropriate to replace the nucleons by u, d, s quarks in the baryon sector of these models. It is the smallness of the Lagrangian mass parameters of these quarks as compared to Λ_{QCD}, the scale parameter of QCD, that clarifies the rather accurate realization of the chiral symmetry. The emerging quark–meson model was introduced in 1973 by Chan and Haymaker [14]:

$$\begin{aligned} L(M) = & \frac{1}{2}\mathrm{tr}(\partial_\mu M^\dagger \partial^\mu M - \mu^2 M^\dagger M) - f_1 \left(\mathrm{tr}(M^\dagger M)\right)^2 - f_2 \mathrm{tr}(M^\dagger M)^2 \\ & - g\left(\det(M) + \det(M^\dagger)\right) + \epsilon_x \sigma_x + \epsilon_y \sigma_y. \end{aligned} \tag{1.24}$$

The first term in the last line is 't Hooft's determinant term [15], which represents in the effective model the $U_A(1)$ axial anomaly. The last two terms correspond to explicit symmetry-breaking. Also, in this version of the effective model, effort is actually invested to include higher meson resonances [16].

Till now, we have followed the order of discovery of the effective models of strong interactions. It is worthwhile to add two remarks on the role played by the effective scalar-spinor models in the electroweak sector of the standard model (SM). At least one major question still remains open after the discovery of the scalar excitation of the symmetry-breaking field. This is the triviality of the Higgs sector, in other words, the presence of a nonintegrable ultraviolet singularity in the momentum-dependence of the self-coupling of the Higgs field. Estimates on the location of the so-called Landau pole are based on nonperturbatively resummed perturbative contributions to the momentum-dependence of this coupling.

An escape from this limitation in the applicability of SM could be the Landau singularity preempted by some substantial deviation in the momentum-dependence of the self-coupling from the behavior suggested by the (resummed) weak coupling perturbation series. A candidate scenario, called *asymptotic safety*, introduces a radical change in the scale-dependence of the couplings by the existence of a fixed point below the location of the would-be singularity, which would attract the flow of the couplings in the ultraviolet. The larger the mass of a field, the stronger its Yukawa coupling to the Higgs field. Therefore, it is a natural first step to investigate

the ultraviolet behavior of the couplings of a reduced Higgs–top–bottom Yukawa model:

$$S = \int_x \Big[\mathrm{tr}(\partial_\mu \Phi^\dagger \partial^\mu \Phi) + U(\mathrm{tr}(\Phi^\dagger \Phi)) + \bar{Q}_L i\gamma_\mu \partial^\mu Q_L + \bar{t}_R i\gamma_\mu \partial^\mu t_R + \bar{b}_R i\gamma_\mu \partial^\mu b_R + i h_b (\bar{Q}_L \Phi b_R + \bar{b}_R \Phi^\dagger Q_L) + i h_t (\bar{t}_L \Phi_C b_R + \bar{t}_R \Phi_C^\dagger Q_L) \Big], \tag{1.25}$$

where

$$Q^a = \begin{pmatrix} t^a \\ b^a \end{pmatrix}, \tag{1.26}$$

where a denotes the color of the quarks. Simpler variants of this model were shown to possess a UV-safe fixed point in space-time dimensions less than 4 [17–19]. At present, intensive search is being conducted on UV-safe fixed points in systems mimicking SM in four dimensions; see [20] and references therein.

Another approach is to question the existence of an intrinsically elementary Higgs particle and assume that a new strong interaction creates scalar bound states with the quantum numbers of the Higgs multiplet that would dissolve at a scale below the Landau pole, in this way erasing any trace of the would-be triviality. This scale refers then to the breakdown of the $SU(2)_L \times U(1)_Y$ symmetry. As a workable mechanism for this scenario, at the end of 1980s several authors rephrased in the electroweak context the idea of Nambu explaining the origin of the pions as a result of nucleon–antinucleon condensation [21–23]. Again, it was natural to consider an effective four-fermion interaction due to an unspecified new interaction in the top–bottom (t, b) family resulting at scale Λ in quark–antiquark condensation, at the same time leaving out the elementary Higgs field from the SM:

$$L_{SM,no-Higgs} = L_{SM,kin} + \frac{g_{new}^2}{\Lambda^2} (\bar{Q}_L^{aI} t_R^a)(\bar{t}_R^b Q_L^{bI}). \tag{1.27}$$

Here a, b refer to the color, and $I = (1/2, -1/2)$ are the weak isospin indices of the quarks. The invariance of the additional term under the global $SU(3)_c \times SU(2)_L \times U(1)_Y$ is obvious. The scale Λ is much higher than in the Nambu–Jona-Lasinio model (not lower than the electroweak scale). The term $L_{SM,kin}$ contains the gauge-invariant kinetic terms of all fermions and nonabelian vector fields, but the Higgs sector is assumed to emerge dynamically. A composite doublet field

$$\Phi^I(x) = -\frac{g_{new}}{\Lambda M_{aux}} \bar{t}_R^a(x) Q_L^{aI}(x) \tag{1.28}$$

is introduced, together with an auxiliary mass that ensures its correct scaling dimension on the addition of an appropriately chosen constraint term to the Lagrangian density:

$$\begin{aligned} L_{SM,no-Higgs} &\to L_{SM} \\ &= L_{SM,kin} - \left[M_{aux}\Phi^{\dagger I} + \frac{g_{new}}{\Lambda}\bar{Q}_L^{aI} t_R^a\right]\left[M_{aux}\Phi^I + \frac{g_{new}}{\Lambda}\bar{t}_R^b Q_L^{bI}\right] \\ &= L_{SM,kin} - M_{aux}\frac{g_{new}}{\Lambda}\left(\bar{Q}_L \Phi t_R + \bar{t}_R \Phi^\dagger Q_L\right] - M_{aux}^2 \Phi^\dagger \Phi. \end{aligned} \tag{1.29}$$

The new strong interaction is taken into account on the level of the loop corrections of the heavy quarks arising from the new piece of the Lagrangian that generate both a gauge-invariant kinetic term and a stabilizing quartic potential in addition to the wrong sign coefficient of the mass term (the result does not depend on M_{aux}). At this point, one can go over to the standard BEH treatment of symmetry-breaking. It turns out that a purely radiatively generated top mass in the right ballpark requires the choice $\Lambda \sim 10^{13}$ GeV. Unfortunately, from this approach a very robust Higgs to top mass relation emerges, $m_H \approx 2m_t$, which in the light of experiments is incompatible with nature. The scheme has been taken over to models giving more freedom for tuning the couplings, where the condensation of techniquarks is responsible for the breakdown of the $SU(2)_L \times U(1)_Y$ symmetry (for comprehensive reviews see [24, 25]).

References

1. E. Fermi, Ric. Sci. **2**, 2 (1933); Z. Phys. **88**, 161 (1934)
2. W. Heisenberg, Z. Phys. **77**, 1 (1932)
3. H. Yukawa, Proc. Phys.-Math. Soc. Jpn. **17**, 48 (1935)
4. N. Kemmer, Proc. R. Soc. Lond. **A166**, 127 (1938)
5. B. Cassen, E.V. Condon, Phys. Rev. **50**, 846 (1936)
6. E.P. Wigner, Phys. Rev. **51**, 106 (1937)
7. M.H. Johnson, E.Teller, Phys. Rev. **98**, 783 (1955)
8. Y. Nambu, Phys. Rev. Lett. **4**, 380 (1960)
9. J. Goldstone, Nuovo Cimento **19**, 154 (1961)
10. M. Gell-Mann, M. Lévy, Nuovo Cimento **16**, 705 (1960)
11. Y. Nambu, G. Jona-Lasinio, Phys. Rev. **122**, 345 (1961); ibid. Phys. Rev. **124**, 246 (1961)
12. J. Gasser, H. Leutwyler, Ann. Phys. **158**, 142 (1984); Nucl. Phys. B **250**, 465 (1985)
13. B.D. Serot, J.D. Walecka, Adv. Nucl. Phys. **16**, 1 (1986)
14. L.H. Chan, R.W. Haymaker. Phys. Rev., D **7**, 402 (1973)
15. G. 't Hooft, Phys. Rev. D **14**, 3432 (1976); ibid. **18**, 2199 (1978)
16. D. Parganlija, P. Kovács, Gy. Wolf, F. Giacosa, D.H. Rischke, Phys. Rev. D **87**, 014011 (2013)
17. B. Rosenstein, D.Warr, S.H. Park, Phys. Rev. Lett. **62**, 1433 (1989)
18. K. Gawedzki, A. Kupiainen, Phys. Rev. Lett. **55**, 363 (1985)
19. C. de Calan, O.A. Faria de Vega, J. Megnen, R. Seneor, Phys. Rev. Lett. **66**, 3233 (1991)
20. H. Gies, R. Sonderheimer, Eur. J. Phys. C **75**, 68 (2015)

21. Y. Nambu, New theories in physics, in *Proceedings of the XI International Symposium on Elementary Particle Physics*, Katimierz, Poland, eds. by Z. Ajduk, S. Pokorski, A. Trautman. (World Scientific, Singapore, 1988), pp. 1–10
22. V.A. Miransky, M. Tanabashi, K. Yamawaki, Mod. Phys. Lett. A **4**, 1043 (1989)
23. W.A. Bardeen, C.T. Hill, M. Lindner, Phys. Rev. D **41**, 1647 (1990)
24. G. Cvetic, Rev. Mod. Phys. **71**, 513 (1999)
25. C.T. Hill, E.H. Simmons, Phys. Rep. **381**, 235 (2003)

Chapter 2
Finite Temperature Field Theories: Review

This introductory section very concisely summarizes the most important features of the process of constructing quantum field theories at zero and nonzero temperatures. There are excellent books and monographs in the literature where the interested reader can find further details. Without trying to be complete, we give here some basic references. For general questions on quantum field theory, one can make use of several books [1–3]. For the more specialized problems of finite-temperature field theory, a very useful review can be found in [4], and two more recent books are also available [5] and [6]. It is often useful to think about a field theory as the continuum limit of a theory defined on a spacetime lattice: an excellent book on this topic was written by Montvay and Münster [7]. Our review of renormalization in the next chapter is largely based on the book of Collins [8]. Beyond these basic works, there are numerous excellent books and papers on more specific subjects that we are going to quote in the text.

Throughout these notes, field variables are defined in spacetime points x of flat d-dimensional Minkowskian or Euclidean spacetime M isomorphic to $\mathbf{R}^d$. It is often useful to have an observer splitting the spacetime into time and space extensions, denoted by $x = (t, \mathbf{x})$; here $\mathbf{x}$ is a $(d-1)$-dimensional vector.

2.1 Review of Classical Field Theory

In classical field theory, the basic object is the field $A : M \to V$, where V is some vector space. The state of the system at time t is characterized by the configuration $A(t, \mathbf{x})$. The dynamics of the system is determined by the action S, which is a real-valued functional of the field configurations: $S : A \mapsto \mathbf{R}$. The classically realizable time evolutions are solutions of the equation of motion (EoM) manifesting themselves as the extrema of the action $\delta S/\delta A = 0$; these solutions are

A. Jakovác, A. Patkós, *Resummation and Renormalization in Effective Theories of Particle Physics*, Lecture Notes in Physics 912,
DOI 10.1007/978-3-319-22620-0_2

also called physical configurations. In local field theories, the action can be written as an integral over the Lagrangian density, $S = \int d^d x \mathscr{L}$. In the fundamental field theories, the Lagrangian density depends only on the field and its first derivatives: $\mathscr{L}(A(x), \partial_\mu A(x))$. In this case, we can introduce the canonically conjugate field $\Pi = \partial\mathscr{L}/\partial\dot{A}$.

We can apply to the configurations transformations represented by bijections $U : A \mapsto A'$. The transformations of the system form a group. We will consider only pointwise transformations, where the transformed new field at a given position depends on the original field at another position, i.e., $A'(x') = U_V(A(x))$, where $x' = U_M(x)$. The transformation is called internal if $U_M = \mathbf{1}$ (identity); otherwise, it is an external transformation. We often encounter transformations determined by continuously varying parameters, i.e., when a certain subgroup of all transformations forms a Lie group. In this case, the transformation U can be characterized by a set of parameters $c \in \mathbf{R}^n$. In the standard representation, the transformation is written as $U(c) = e^{-ic_a T_a}$, where T_a are the generators of the transformation.

The transformation is a symmetry if $S[A'] = S[A]$. This also means that if A is an extremum of S (i.e., realizable motion), then A' is an extremum, too. In several cases, we expect that the system exhibits some abstractly defined symmetry group. In this case, the fields are classified as irreducible representations of the abstract group, and S is built up from the group invariants constructed from the field products.

An important theorem (Noether's theorem) states that if U is a continuous symmetry of the system, then a conserved current associated with it always exists. The proof can be found in all basic field theory textbooks [8], but for the later use of its logic of construction, we present a brief overview. Consider a one-parameter continuous symmetry U_τ, where $U_0 = \mathbf{1}$. The transformed field is $A_\tau = U_\tau(A)$, and the transformed action is $S_\tau[A] = S[A_\tau]$. If the transformation is a symmetry, then $S_\tau = S$. Now let us consider an infinitesimal but position-dependent parameter $\delta\tau(x)$. Then two statements can be made. First, the change of the action can be written as

$$\delta S[A] = S_{\delta\tau}[A] - S[A] = -\int d^d x j^\mu(x) \partial_\mu \delta\tau, \tag{2.1}$$

since at constant $\delta\tau$, it must be identically zero. Then, after partial integration, we obtain

$$\frac{\delta S}{\delta\tau(x)} = \partial_\mu j^\mu(x). \tag{2.2}$$

On the other hand, $A_{\delta\tau}$ is the variation of the original configuration. Therefore, if at $\delta\tau = 0$ we began from the solution of the equations of motion (EoM), we obtain

$$\left.\frac{\delta S}{\delta\tau(x)}\right|_{A_{ph}} = 0. \tag{2.3}$$

These statements together mean that j^μ is a conserved current when evaluated at solutions of EoM.

The conserved current associated with spacetime translations is the energy–momentum tensor

$$\mathscr{T}_{\mu\nu} = \partial_\mu A \frac{\partial \mathscr{L}}{\partial(\partial^\nu A)} - g_{\mu\nu}\mathscr{L}, \tag{2.4}$$

or its symmetrized version [9]. In particular, the energy density and momentum density read as

$$\varepsilon = \dot{A}\Pi - \mathscr{L}, \qquad P_i = \Pi \partial_i A \tag{2.5}$$

(for fields carrying discrete indices, the product of two field variables implies summation over the indices). Another often used example is the current associated with a linear internal symmetry. In this case, the infinitesimal transformations can be written with the help of the generators T_{ij} of the symmetry transformations as $\delta A_i = -iT_{ij}A_j\delta\tau$ (where we have written indices explicitly for a more transparent result). Thus

$$j_{i\mu} = T_{ij}\frac{\partial \mathscr{L}}{\partial(\partial^\mu A_j)}. \tag{2.6}$$

2.2 Quantization and Path Integral

The main difference between a classical and a quantum system is the characterization of each of their states. While in a classical system the state could be fully described by the configuration of the generalized coordinates and the canonically conjugated momenta, in the quantum system we introduce a separate Hilbert space H for the states. The physical states are $\Psi[A] \in H$ of unit norm $|\Psi[A]| = 1$.

The transformations of the quantum system form $U : H \to H$ isomorphisms. These are (anti)linear maps that map a state onto a state, i.e., it conserves the norm; therefore, the transformation must be (anti)unitary, $U^\dagger = U^{-1}$. In the continuous case, $U_c = e^{-ic_aT_a}$, just as in the classical case; if U is unitary, then the generator T is Hermitian, $T^\dagger = T$.

Consider now a one-parameter subgroup $U_\tau = e^{-i\tau T}$ of the linear transformations. The eigenstates of the transformation are eigenstates of the generator, too: if $T\Psi = \lambda\Psi$, then $U\Psi = e^{-i\tau\lambda}\Psi$. The eigenvalues of T are real numbers; those of U lie on the unit circle. We can also describe the transformation of the system by transforming instead of the states, the operators $\hat{O}$ acting on H (Heisenberg picture) requiring unchanged values for the inner products

$$\langle\tilde{\Psi}'|\hat{O}|\Psi'\rangle = \langle\tilde{\Psi}|\hat{O}'|\Psi\rangle \to \hat{O}' = U_\tau^\dagger \hat{O} U_\tau, \tag{2.7}$$

or infinitesimally $\delta O = i[T, \hat{O}]\delta\tau$.

The generator of a transformation does not change under the effect of the same transformation $T' = U^\dagger T U = T$. It makes it possible to identify the generator of a symmetry transformation as the conserved quantity belonging to this transformation: in field theory, this is the conserved quantity coming from Noether's theorem. Therefore, the generators of the space and time translations are the Noether charges coming from the energy–momentum tensor, i.e., the conserved momentum and energy, respectively. After quantization, these become the momentum operator $\hat{P}_i$ and Hamilton operator $\hat{H}$, and so the space and time translations are $e^{-i\hat{P}_i x^i/\hbar}$ and $e^{-i\hat{H}t/\hbar}$, respectively ($\hbar$ is introduced in order to have dimensionless quantities in the exponent).

The infinitesimal transformations of the system are interpreted as measurements. In an eigenstate, we obtain a definite value for the result of the measured quantity; in other cases, the projection of the arising state onto the eigenstates gives the probability amplitude of the possible outcomes of the measurement. Two measurements are not interchangeable if the corresponding generators do not commute.

In particular, in quantum field theories there is an operator that measures the field at spacetime position x, denoted by $\hat{A}(x)$, and another one that measures the canonically conjugated momentum ($\hat{\Pi}(x)$). The generator of the space translations Π_i is defined in any field theory with the help of the energy-momentum tensor as $P_i = T_{0i} = \int dy \Pi(y)\partial_i A(y)$. On the other hand, the fields transform under an infinitesimal space translation as $\delta A(x) = A(x+\delta x) - A(x) = \partial_i A \delta x^i$. When substituted into the relation expressing the action of an infinitesimal translation on the field A as $(i/\hbar)\delta x^i [P_i, A(x)] = \delta x^i \partial_i A(x)$, it leads to the canonical commutation/anticommutation relations

$$[\hat{A}(t,\mathbf{x}), \hat{\Pi}(t,\mathbf{y})]_\alpha = i\hbar\delta(\mathbf{x}-\mathbf{y}), \qquad [\hat{A}(t,\mathbf{x}), \hat{A}(t,\mathbf{y})]_\alpha = 0,$$
$$[\hat{\Pi}(t,\mathbf{x}), \hat{\Pi}(t,\mathbf{y})]_\alpha = 0, \tag{2.8}$$

where $\alpha = \pm 1$ and $[X,Y]_\alpha = XY - \alpha YX$, i.e., commutator for $\alpha = 1$ and anticommutator for $\alpha = -1$. In the following, $\hbar = 1$ units are used. The choice $\alpha = 1$ applies for bosons, and $\alpha = -1$ for fermions.[1]

The eigenvectors of $\hat{A}$ (and also those of $\hat{\Pi}$) form an orthonormal basis. In this basis, we can expand any state, and using the projectors on the eigenstates also any operator. In particular, we can expand the time translation operator $e^{-i\hat{H}t}$.

For bosonic fields (denoted by $\Phi(x)$), because of the commutation relations (2.8), there exists a common eigenstate for all field measurement operators at time t, and also (separately) for all canonical momentum measurement operators:

$$\hat{\Phi}(t,\mathbf{x})\,|\varphi\rangle = \varphi(t,\mathbf{x})|\varphi\rangle, \qquad \hat{\Pi}(t,\mathbf{x})\,|\pi\rangle = \pi(t,\mathbf{x})|\pi\rangle. \tag{2.9}$$

[1] We remark that in $(2+1)$-dimensional field theories, there is a possibility to define particles with any α with unit length. These are called anyons.

Their inner product, using again (2.8), is

$$\langle\varphi|\pi\rangle = e^{i\int d^d\mathbf{x}\,\pi(\mathbf{x})\varphi(\mathbf{x})}. \tag{2.10}$$

Now we can consider a time interval $[0, t]$, which we divide into N equal parts, with each part of length $\Delta t = t/N$. At each division point $r = 0, \ldots, N$ (also at the beginning and at the end), we insert complete sets $\mathbf{1} = \int(\prod_{\mathbf{x}} d\varphi_r(\mathbf{x}))\,|\varphi_r\rangle\,\langle\varphi_r|$ and $\mathbf{1} = \int(\prod_{\mathbf{x}} d\pi_r(\mathbf{x}))\,|\pi_r\rangle\,\langle\pi_r|$ in alternating order. After a bit of algebra, we obtain

$$e^{-i\hat{H}t} = \int \mathscr{D}\varphi\mathscr{D}\pi e^{iS[\varphi,\pi]}\,|\varphi_N\rangle\,\langle\varphi_0|\,, \tag{2.11}$$

where

$$\mathscr{D}\varphi = \prod_{r,\mathbf{x}} d\varphi_r(\mathbf{x}), \quad \mathscr{D}\pi = \prod_{r,\mathbf{x}} d\pi_r(\mathbf{x}), \quad S[\varphi,\pi] = \int dt'\,\left[\pi\dot{\varphi} - H(\varphi,\pi)\right],$$

$$\dot{\varphi}_r\Delta t = \varphi_{r+1} - \varphi_r, \qquad H(\varphi,\pi) = \frac{\langle\varphi|H|\pi\rangle}{\langle\varphi|\pi\rangle}. \tag{2.12}$$

In the case of fermions, the situation is more complicated, because the field measurement operators $\hat{\Psi}(t,\mathbf{x})$ do not commute at a given time. To resolve the problem, one first introduces the Grassmann algebra $\mathscr{G}$. It is a (graded) complex algebra generated by the unity and elements e_i for which the algebraic product is antisymmetric $e_ie_j = -e_je_i$. For the physical applications, one also needs a star operation that connects the generator elements into pairs $* : e \to e^*$. We can define a Hilbert space over the Grassmann algebra $H(\mathscr{G})$, which means that if $|\psi_1\rangle, |\psi_2\rangle \in H(\mathscr{G})$ and $g_1, g_2 \in \mathscr{G}$, then $g_1\,|\psi_1\rangle + g_2\,|\psi_2\rangle \in H(\mathscr{G})$. The scalar product is Grassmann-algebra-valued, $\langle\psi_1|\psi_2\rangle \in \mathscr{G}$. In the physical applications, one introduces two Grassmann algebra generators for each spatial position and for each fermionic component $e_{\alpha,\mathbf{x}}$ and $e^*_{\alpha,\mathbf{x}}$. The field operators $\hat{\Psi}(t,\mathbf{x})$ and $\hat{\Psi}^\dagger(t,\mathbf{x})$ act linearly on $H(\mathscr{G})$, i.e., $\hat{\Psi}(t,\mathbf{x})(g_1\,|\psi_1\rangle + g_2\,|\psi_2\rangle) = g_1\hat{\Psi}(t,\mathbf{x})\,|\psi_1\rangle + g_2\hat{\Psi}(t,\mathbf{x})\,|\psi_2\rangle$, and similarly for $\hat{\Psi}^\dagger(t,\mathbf{x})$.

Let us consider a single degree of freedom, where we have just two field operators $\hat{\Psi}$ and $\hat{\Psi}^\dagger$. We assume, in agreement with most physical applications, that $\hat{\Pi} = i\hat{\Psi}^\dagger$, which implies

$$[\hat{\Psi}, \hat{\Psi}^\dagger]_+ = 1. \tag{2.13}$$

The corresponding Grassmann algebra generators are e and e^*. The complete algebra is four-dimensional; it has the basis 1, e, e^*, and ee^*. We take an element from the Hilbert space $|\psi\rangle \in H(\mathscr{G})$ and apply $\hat{\Psi}$ to it. We obtain

$$|\psi'\rangle = \hat{\Psi}|\psi\rangle, \qquad \hat{\Psi}\,|\psi'\rangle = 0. \tag{2.14}$$

This means that either $|\psi'\rangle = 0$ itself, or $\hat{\Psi}|\psi'\rangle = 0$. Therefore, there exists an element in the Hilbert space that is annihilated by $\hat{\Psi}$: this is the vacuum $|0\rangle$. Applying $\hat{\Psi}^\dagger$ to the vacuum, we obtain

$$|1\rangle = \hat{\Psi}^\dagger|0\rangle, \quad \hat{\Psi}^\dagger|1\rangle = 0, \qquad \hat{\Psi}|1\rangle = \hat{\Psi}\hat{\Psi}^\dagger|0\rangle = (1 + \hat{\Psi}^\dagger\hat{\Psi})|0\rangle = |0\rangle. \tag{2.15}$$

Therefore, the Hilbert space is two-dimensional. The basis elements are $|0\rangle$ and $|1\rangle$.

Now we can define fermionic coherent states: we take a grade-1 Grassmann element, i.e., $\eta = \alpha e + \beta e^*$. It is nilpotent, $\eta^2 = 0$. The product $\eta^*\eta$ formed with the help of the conjugated element $\eta^* = \alpha^* e^* + \beta^* e$ is a commuting element of the algebra. The definition of the coherent state is

$$|\eta\rangle = e^{-\frac{1}{2}\eta^*\eta + \eta\hat{\Psi}^\dagger}|0\rangle = (1 - \frac{1}{2}\eta^*\eta)|0\rangle + \eta|1\rangle. \tag{2.16}$$

This is an eigenstate of $\hat{\Psi}$:

$$\hat{\Psi}|\eta\rangle = \eta|0\rangle = \eta|\eta\rangle, \tag{2.17}$$

because of the nilpotency of η. The norm of $|\eta\rangle$ is unity.

Two linearly independent coherent states would form a basis if there existed an inverse element in the Grassmann algebra. Though this is not the case here, we can introduce a formal integral over the Grassmann elements of grade 1 (Berezin integrals), which does the job for us:

$$\int d\eta = 0, \qquad \int d\eta\eta = 1. \tag{2.18}$$

Then we obtain

$$\int d\eta^* d\eta\, |\eta\rangle\langle\eta| = \mathbf{1}, \tag{2.19}$$

because

$$\int d\eta^* d\eta \left[(1 - \eta^*\eta)|0\rangle\langle 0| + \eta|1\rangle\langle 0| + \eta^*|0\rangle\langle 1| + \eta\eta^*|1\rangle\langle 1| \right] = |0\rangle\langle 0| + |1\rangle\langle 1| = \mathbf{1}. \tag{2.20}$$

Similarly, we obtain

$$\int d\eta^* d\eta \left\langle -\eta|\hat{O}|\eta \right\rangle = \mathrm{Tr}\,\hat{O}, \tag{2.21}$$

because

$$\int d\eta^* d\eta \left[(1-\eta^*\eta)\langle 0|\hat{O}|0\rangle - \eta^*\langle 1|\hat{O}|0\rangle + \eta\langle 0|\hat{O}|1\rangle - \eta^*\eta\langle 1|\hat{O}|1\rangle\right]$$
$$= \langle 0|\hat{O}|0\rangle + \langle 1|\hat{O}|1\rangle. \tag{2.22}$$

Note that for the trace, one has to evaluate an antisymmetric expectation value (2.21).

The case of a single degree of freedom discussed above can be taken over for more fermionic dynamical variables without any problem. The most important finding is the integral formula representing the spectral decomposition of the identity and the trace formula.

Now we can write explicitly the representation of the time evolution operator with the help of the fermionic integrals. Just as in the bosonic case, we split the time interval $[0, t]$ into N parts and insert an identity at each of these division points. Finally, we obtain

$$e^{-i\hat{H}t} = \int \mathscr{D}\psi^\dagger \mathscr{D}\psi \; e^{iS[\psi^*,\psi]} \; |\psi_0\rangle \langle\psi_N| \,, \tag{2.23}$$

where

$$\mathscr{D}\psi^\dagger \mathscr{D}\psi = \prod_{n=1}^{N} d\psi_n^* d\psi_n, \qquad \psi_{r+1} - \psi_r = \partial_t \psi_r \Delta t,$$
$$S[\psi^*,\psi] = \int dt \left(\psi^* \dot{\psi} - H[\psi^*,\psi]\right), \qquad H[\psi^*,\psi] = \langle\psi|H|\psi\rangle \,. \tag{2.24}$$

We have obtained analogous formulas for both the bosonic and fermionic theories. Symbolically, we write in common notation

$$e^{-i\hat{H}t} = \int \mathscr{D}A e^{iS[A]} \, |A_0\rangle \langle A_N| \,. \tag{2.25}$$

Once we have a representation for the time evolution operator, we can work out any n-point correlation function. We are primarily interested in expectation values of the product of Heisenberg-picture operators:

$$\mathrm{Tr}\, \hat{A}_n(t_n) \ldots \hat{A}_1(t_1)\hat{\varrho}, \tag{2.26}$$

where $\hat{\varrho}$ is the initial density operator defined at time t_0. Using the cyclic property of the trace and the time evolution of the field operators $\hat{A}(t) = e^{iH(t-t_0)}\hat{A}e^{-iH(t-t_0)}$, we have

$$\mathrm{Tr}\, e^{-iH(t_i-t_f)} e^{-iH(t_f-t_n)} \hat{A}_n e^{-iH(t_n-t_{n-1})} \ldots e^{-iH(t_2-t_1)} \hat{A}_1 e^{-iH(t_1-t_0)} \hat{\varrho} e^{-iH(t_0-t_i)}, \tag{2.27}$$

where t_i and t_f are two arbitrary moments of time, practically $t_i \to -\infty$ and $t_f \to \infty$.

Now we can substitute the path integral representation of the time evolution operator. Between two time translations, there appear matrix elements of the $\hat{A}$ operators evaluated between states sitting on the first point of the left side and the next point of the right side of the time evolution operator. We can write (also introducing a complete system with $|\pi\rangle$ representation in the bosonic case)

$$\frac{\langle\pi_N|\hat{\Pi}|\varphi_0\rangle}{\langle\pi_N|\varphi_0\rangle} = \pi_N, \quad \frac{\langle\pi_N|\hat{\Phi}|\varphi_0\rangle}{\langle\pi_N|\varphi_0\rangle} = \phi_0,$$
$$\frac{\langle\psi_N|\hat{\Psi}|\psi_0\rangle}{\langle\psi_N|\psi_0\rangle} = \psi_0, \quad \frac{\langle\psi_N|\hat{\Psi}^\dagger|\psi_0\rangle}{\langle\psi_N|\psi_0\rangle} = \psi_N^*. \tag{2.28}$$

We will also encounter the matrix elements of the density matrix

$$\varrho[A_N, A_0] = \frac{\langle A_N|\hat{\varrho}|A_0\rangle}{\langle A_N|A_0\rangle}, \tag{2.29}$$

which can be, of course, a rather complicated functional. In the $\Delta t \to 0$ limit, we will denote the arguments by A and $\dot{A}$. We have finally, in symbolic notation,

$$\mathrm{Tr}\,\hat{A}_n(x_n)\ldots\hat{A}_1(x_1)\hat{\varrho} = \int_{P/A}^{C\,path} \mathscr{D}A\; e^{i\int_C dt\mathscr{L}} A_n(t_n)\ldots A_1(t_1)\varrho[A,\dot{A}]. \tag{2.30}$$

Here P/A means periodic/antiperiodic contours: for bosons we must apply periodic, for fermions antiperiodic, boundary conditions. In this representation, the time flows along a closed time path (CTP) $C : t_i \to t_0 \to t_1 \to \cdots \to t_n \to t_f \to t_i$. To emphasize the order of the time arguments along the contour, we can introduce a parameterization $t(\tau)$. In the "contour time" τ, the contour is monotonic and closed. The representation of the time evolution in fact uses operators that depend on the contour time, and we obtain contour time ordering in a natural way.

In real time, however, if the time arguments appear without any definite order, the contour runs back and forth several times. If for a certain section it is monotonic, those subsections can be merged into a common section; e.g., if $t_1 < t_2 < t_3$, then we can write instead of $t_1 \to t_2 \to t_3$ simply $t_1 \to t_3$. Moreover, we can always plug in a unit operator as $e^{iH(t'-t)}e^{-iH(t'-t)}$, i.e., we can include a bypass anywhere in the time chain: instead of $t_n \to t_{n+1}$, we can write $t_n \to t' \to t_{n+1}$. According to these observations, the time contour can be standardized as $t_i \to t_f \to t_i \to \cdots \to t_f \to t_i$, where a sufficient number of back-and-forth sections must be allowed for it to contain (taking into account the ordering) all the operators. This form depends on the operators only through their number. On the sections where the time flows as $t_i \to t_f$, the contour ordering is time ordering, while along the backward-running contours, the contour ordering is anti-time-ordering.

To simplify the treatment, one usually considers only two time sections (this is the minimal choice, since we always have to return to the same time t_i). The path integral variables are called $A^{(1)}$ for the contour segment $t_i \to t_f$, and $A^{(2)}$ for

the section $t_f \to t_i$. In the contour ordering, segment 2 always follows segment 1, independently of the actual time values. On segment 1, the usual action

$$S = \int_{t_i}^{t_f} dt\, L \tag{2.31}$$

is used. On segment 2, where the orientation of the integration is $t_f \to t_i$, the action $-S$ can be used with the same ordering of the endpoints as on segment 1. With this setup, we can study correlation functions like

$$F = \mathrm{Tr}\left[T^*(\hat{A}_n(x_n)\dots\hat{A}_k(x_k))\, T(\hat{A}_{k-1}(x_{k-1})\dots\hat{A}_1(x_1))\hat{\varrho}\right], \tag{2.32}$$

where T^* is anti-time-ordering, T is time-ordering. In this simplified setup, F has the following path integral representation:

$$F = \int\limits_{P/A} \mathscr{D}A\, e^{iS[A^{(1)}]-iS[A^{(2)}]} A_n^{(2)}(t_n)\dots A_1^{(1)}(t_1)\varrho[A^{(1)}, \dot{A}^{(1)}], \tag{2.33}$$

where $\mathscr{D}A = \mathscr{D}A^{(1)}\mathscr{D}A^{(2)}$. This is the generic path integral representation for arbitrary initial conditions encoded into the density matrix.

The *generating functional* of the n-point functions can be written as

$$Z[J] = \int\limits_{P/A} \mathscr{D}A\, e^{iS[A^{(1)}]-iS[A^{(2)}]+\int JA}\varrho[A^{(1)}, \dot{A}^{(1)}], \tag{2.34}$$

where $J = (J^{(1)}, J^{(2)})$ and $\int JA = \int(J^{(1)}A^{(1)} + J^{(2)}A^{(2)})$. Note that $Z[J = 0] = \mathrm{Tr}\,\hat{\varrho} = 1$. An n-point correlation function can be obtained as

$$F = \left.\frac{\partial^n Z[J]}{\partial J_n^{(2)}(x_n)\dots\partial J_k^{(2)}(x_k)\partial J_{k-1}^{(1)}(x_{k-1})\dots\partial J_1^{(1)}(x_1)}\right|_{J=0}. \tag{2.35}$$

In the case of fermions, all derivations must operate from the left.

2.3 Equilibrium

While for an arbitrary initial density matrix the above path integral is hardly accessible for practical use (but see [10]), we can have more definite yet still simple formulas if we are in equilibrium. There, the form of the density matrix is

$$\hat{\varrho} = \frac{1}{Z_0}\, e^{-\beta\hat{H}}, \qquad Z_0 = \mathrm{Tr}\, e^{-\beta\hat{H}}. \tag{2.36}$$

Note that thermodynamics tells us that $Z_0 = e^{-\beta F}$, where F is the free energy of the system.

Now we can exploit that formally, this density matrix is similar to the time evolution operator with $\beta \to it$, $t \to -i\beta$. There we can use the representation discussed in the previous subsection. Choosing the time arguments (only their difference matters) $t_i \to t_i - i\beta$, we have

$$e^{-\beta \hat{H}} = \int \mathscr{D}A \, e^{i \int_{t_i}^{t_i - i\beta} dt \, L} \, |A_N\rangle \, \langle A_0| \, . \tag{2.37}$$

In the action, we can introduce the integration variable τ with the definition $t = t_i - i\tau$, and define new field variables as $A(t_i - i\tau) = A^{(3)}(\tau)$. Then there appears

$$S_E = -i \int_{t_i}^{t_i - i\beta} dt \, L[A(t), \partial_t A(t)] = - \int_0^{\beta} d\tau \, L[A^{(3)}(\tau), i\partial_\tau A^{(3)}(\tau)]. \tag{2.38}$$

The corresponding contour section continuously joins the end of segment 2, and it is labeled as segment 3. The time contour then goes out to complex time values, as can be seen in Fig. 2.1. For the generating functional, we introduce external currents for all the sections of the contour. Then it has the form

$$Z[J] = Z_0 \left\langle e^{\int JA} \right\rangle = \mathrm{Tr} \, e^{-\beta \hat{H}} e^{\int J \hat{A}} = \int_{P/A} \mathscr{D}A \, e^{iS[A^{(1)}] - iS[A^{(2)}] - S_E[A^{(3)}] + \int JA}, \tag{2.39}$$

where now $J = (J^{(1)}, J^{(2)}, J^{(3)})$. With this definition, in view of the second equality, the contribution to $Z_0 = Z[J = 0] = \mathrm{Tr} \, e^{-\beta \hat{H}}$ comes purely from segment 3. The free energy defined from $Z[J]$ can be considered a free energy in the presence of an external time-dependent field.

The consequence of equilibrium is that we have time translation-invariance in the observables. Therefore, we can put the initial density matrix anywhere in time, even $t_i \to -\infty$. But in this case, all propagation between contour sections $C_{1,2}$ and C_3 is suppressed, since we would need infinitely long propagation. This means that segment 3 factorizes from segments 1 and 2. The formalism that uses exclusively

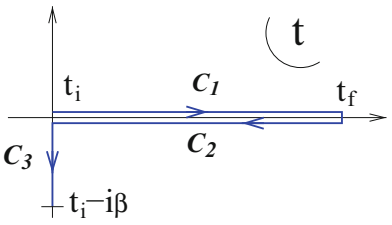

Fig. 2.1 Closed time path contour for equilibrium

segment 3 is called Euclidean, or imaginary, time or the Matsubara formalism. The theory built on contours 1 and 2 is called real time, or the Keldysh formalism.

If there is a conserved quantity in the system, i.e., if there is an operator $\hat{N}$ that commutes with the Hamiltonian $[\hat{H}, \hat{N}] = 0$, then we can associate a chemical potential with this operator. Then the density matrix reads as

$$\hat{\varrho} = \frac{1}{Z_0} e^{-\beta(\hat{H}-\mu\hat{N})}, \qquad Z_0 = \operatorname{Tr} e^{-\beta(\hat{H}-\mu\hat{N})}. \tag{2.40}$$

Formally, the treatment of this system is equivalent to that presented above just involving a modified imaginary time evolution operator $\hat{H}' = \hat{H} - \mu\hat{N}$, or in the path integral formalism with $L' = L + \mu N$.

2.4 Propagators

Let us consider the two-point functions in more detail. Path integration implies contour time ordering in the integrand, so we have several choices for two arbitrary local operators A and B:

$$iG_{AB}^{(ij)}(t) = \langle \mathrm{T}_C A^{(i)}(t) B^{(j)}(0) \rangle \tag{2.41}$$

(here and below, the distinctive sign $\hat{}$ will be omitted from the operators for the sake of notational simplicity). In terms of operator expectation values, we have

$$\begin{aligned}
iG_{AB}^{(12)}(t) &= \alpha \frac{1}{Z_0} \operatorname{Tr}\left[e^{-\beta H} B(0) A(t)\right] \\
iG_{AB}^{(21)}(t) &= \frac{1}{Z_0} \operatorname{Tr}\left[e^{-\beta H} A(t) B(0)\right] \\
iG_{AB}^{(11)}(t) &= \frac{1}{Z_0} \operatorname{Tr}\left[e^{-\beta H} \mathrm{T} A(t) B(0)\right] = \Theta(t)\, iG_{AB}^{21}(t) + \Theta(-t)\, iG_{AB}^{12}(t) \\
iG_{AB}^{(22)}(t) &= \frac{1}{Z_0} \operatorname{Tr}\left[e^{-\beta H} \mathrm{T}^* A(t) B(0)\right] = \Theta(t)\, iG_{AB}^{12}(t) + \Theta(-t)\, iG_{AB}^{21}(t) \\
G_{AB}^{(33)}(t) &= \frac{1}{Z_0} \operatorname{Tr}\left[e^{-\beta H} \mathrm{T}_\tau A(-i\tau) B(0)\right] = \Theta(\tau)\, iG_{AB}^{21}(-i\tau) + \Theta(-\tau)\, iG_{AB}^{12}(-i\tau).
\end{aligned} \tag{2.42}$$

In the case of nonzero chemical potential, we should use the replacement $H \to H'$. Remark: for $G_{AB}^{(33)}$, as is usual, we do not include the imaginary factor i in the definition.

The following identity is always true:

$$G_{AB}^{(11)} + G_{AB}^{(22)} = G_{AB}^{(12)} + G_{AB}^{(21)}. \tag{2.43}$$

To avoid the use of nonindependent quantities, it is sometimes useful to change to another basis, called a retarded/advanced (R/A) basis. We introduce the fields

$$A^{(r)} = \frac{A^{(1)} + A^{(2)}}{2}, \qquad A^{(a)} = A^{(1)} - A^{(2)}. \tag{2.44}$$

The propagators of the ordered products of $A^{(r)}$ and $A^{(a)}$ are expressed in terms of the previously defined contour-ordered quantities as follows:

$$\begin{aligned} iG_{AB}^{(ra)}(t) &= iG_{AB}^{(11)}(t) - iG_{AB}^{(12)}(t) = \Theta(t)(iG_{AB}^{21}(t) - iG_{AB}^{12}(t)) \\ iG_{AB}^{(ar)}(t) &= iG_{AB}^{(11)}(t) - iG_{AB}^{(21)}(t) = -\Theta(-t)(iG_{AB}^{21}(t) - iG_{AB}^{12}(t)) \\ iG_{AB}^{(rr)}(t) &= \frac{iG_{AB}^{21}(t) + iG_{AB}^{12}(t)}{2}, \end{aligned} \tag{2.45}$$

while $G_{AB}^{(aa)} = 0$. The nonzero combinations are called the retarded, advanced, and Keldysh propagators, respectively.

As these equations show, all propagators can be expressed through $G^{(21)}$ and $G^{(12)}$; this is true also out of equilibrium. Moreover, in equilibrium, these two apparently independent propagator are also related through the Kubo–Martin–Schwinger (KMS) relation. Consider the 12 propagator of the A and B operators and use the cyclic property of the trace to obtain

$$iG_{AB}^{(12)}(t) = \alpha \frac{1}{Z_0} \operatorname{Tr}\left[e^{-\beta H'} B(0) A(t)\right] = \alpha \frac{1}{Z_0} \operatorname{Tr}\left[e^{-\beta H'} e^{\beta H'} A(t) e^{-\beta H'} B(0)\right]. \tag{2.46}$$

We assume that the operator A has a definite charge with respect to the symmetry, i.e., $[N, A] = qA$. Then this implies $e^{-\beta\mu N} A e^{\beta\mu N} = e^{-\beta\mu q} A$. We also use the time translation $e^{iHt'} A(t) e^{-iHt'} = A(t + t')$, applicable also to imaginary $t' = -i\beta$ values. Then we have

$$\begin{aligned} e^{\beta H'} A(t) e^{-\beta H'} &= e^{\beta H} e^{-\beta\mu N} A(t) e^{\beta\mu N} e^{-\beta H} \\ &= e^{-\beta\mu q} e^{\beta H} A(t) e^{-\beta H} = e^{-\beta\mu q} A(t - i\beta). \end{aligned} \tag{2.47}$$

Therefore,

$$iG_{AB}^{(12)}(t) = \alpha e^{-\beta\mu q} iG^{(21)}(t - i\beta), \tag{2.48}$$

which leads in Fourier space to the KMS relation:

$$iG^{(12)}_{AB}(\omega) = \alpha e^{-\beta(\omega+\mu q)} iG^{(21)}(\omega). \tag{2.49}$$

Now all operators can be expressed solely through $G^{(12)}$ or $G^{(21)}$.

We can also define the *spectral function* ϱ as

$$\varrho_{AB}(x) = iG^{(21)}_{AB}(x) - iG^{(12)}_{AB}(x). \tag{2.50}$$

The spectral function has many advantageous properties, which we summarize in Appendix A: it satisfies sum rule, and under some conditions, it is a positive definite function of positive frequencies. Therefore, it is advantageous to choose the spectral function for the basic quantity in equilibrium thermodynamics, describing two-point correlations.

From the KMS relation (2.49), we obtain

$$iG^{(12)}_{AB}(k) = \alpha n_\alpha(k_0+\mu q)\varrho(k), \qquad iG^{(21)}_{AB}(k) = (1+\alpha n_\alpha(k_0+\mu q))\varrho(k), \tag{2.51}$$

where

$$n_\alpha(\omega) = \frac{1}{e^{\beta\omega} - \alpha} \tag{2.52}$$

is the Bose–Einstein ($\alpha = 1$) or Fermi–Dirac ($\alpha = -1$) distribution, respectively. We note that although this is a discussion of the full interacting theory, the same distribution function always appears, irrespective of the choice of the operators A and B. The distribution function satisfies the equality

$$n_\alpha(\omega) + n_\alpha(-\omega) + \alpha = 0. \tag{2.53}$$

The dynamical information is exclusively contained in the spectral function. The Keldysh propagator is expressed as

$$iG^{(rr)}_{AB}(k) = \left(\frac{1}{2} + \alpha n_\alpha(k_0 + \mu q)\right) \varrho_{AB}(k). \tag{2.54}$$

The proportionality function $(1/2 + \alpha n_\alpha(\omega))$ is a purely (anti)symmetric function of ω.

The retarded and advanced propagators read as

$$iG^{(ra)}_{AB}(x) = \Theta(t)\varrho_{AB}(x), \qquad iG^{(ar)}_{AB}(x) = -\Theta(-t)\varrho_{AB}(x). \tag{2.55}$$

In Fourier space, using $\Theta(\omega) = i/(\omega + i\varepsilon)|_{\varepsilon\to 0+}$, one derives the convolution

$$iG_{AB}^{(ra)/(ar)}(k) = \int \frac{d\omega}{2\pi} \frac{\varrho_{AB}(\omega, \mathbf{k})}{k_0 - \omega \pm i\varepsilon}, \tag{2.56}$$

which is of the form of a *dispersion relation*, called the Kramers–Kronig relation. The inverse relation is

$$\varrho_{AB}(k) = \operatorname*{Disc}_{k_0} iG_{AB}^{(ra)}(k). \tag{2.57}$$

Note that the discontinuity is equal to -2 times the imaginary part of $G_{AB}^{(ra)}$ only if the spectral function is real, i.e., when $B = A^\dagger$.

Let us examine the imaginary time propagator, too. Since the imaginary contour runs in the interval $[0, \beta]$, the range of the argument of the 33 propagator (which is the difference of two imaginary time values) is $\tau \in [-\beta, \beta]$. For negative τ values, by the definition (2.42), we have

$$G_{AB}^{(33)}(-\tau + \beta) = iG_{AB}^{(21)}(i\tau - i\beta) = \alpha iG_{AB}^{(12)}(i\tau) = \alpha G_{AB}^{(33)}(-\tau). \tag{2.58}$$

With this relation we can extend the definition of the 33 propagator to the complete imaginary axis as an (anti)periodic function.

Since in the $\beta > \tau > 0$ range, we have $G^{(33)}(\tau) = iG^{(21)}(-i\tau)$, it follows that

$$G_{AB}^{(33)}(\tau, \mathbf{k}) = \int \frac{d\omega}{2\pi} e^{-i(-i\tau)\omega}(1 + \alpha n_\alpha(\omega))\varrho_{AB}(\omega, \mathbf{k}) = \int \frac{d\omega}{2\pi} \frac{e^{(\beta-\tau)\omega}}{e^{\beta\omega} - \alpha}\varrho_{AB}(\omega, \mathbf{k}). \tag{2.59}$$

We arrive at a particularly simple form if $B = A$ is a bosonic operator and the spectral function depends only on $k = |\mathbf{k}|$. Then the negative frequency parts can be mapped to the positive frequency part, and

$$G_{AA}^{(33)}(\tau, k) = \int_0^\infty \frac{d\omega}{2\pi} \frac{\cosh\left(\left(\frac{\beta}{2} - \tau\right)\omega\right)}{\sinh\frac{\beta\omega}{2}}\varrho_{AA}(\omega, k). \tag{2.60}$$

In the Fourier space, being periodic, $G^{(33)}$ in general has a discrete spectrum. We use the following definition for the Fourier transformation:

$$f(\omega_n) = \int_0^\beta d\tau\, e^{i\omega_n\tau} f(\tau), \qquad f(\tau) = T\sum_n e^{-i\omega_n\tau} f(\omega_n). \tag{2.61}$$

The (anti)periodicity dictates the possible values of the frequency:

$$\omega_n = \begin{cases} 2\pi nT & \text{bosons} \\ (2\pi + 1)nT & \text{fermions.} \end{cases} \tag{2.62}$$

The actual form of the Fourier transform reads as

$$G^{(33)}_{AB}(\omega_n, \mathbf{k}) = \int_0^\beta d\tau \, e^{i\omega_n \tau} G^{(33)}_{AB}(\tau, \mathbf{k}) = \int \frac{d\omega}{2\pi} \frac{\varrho_{AB}(\omega, \mathbf{k})}{\omega - i\omega_n}. \tag{2.63}$$

If we compare it with the Kramers–Kronig relation obtained for the retarded propagator, we obtain (k stands now for the four-vector of the momentum):

$$-G^{(33)}_{AB}(i\omega_n \to k_0 + i\varepsilon, \mathbf{k}) = G^{ra}_{AB}(k). \tag{2.64}$$

2.5 Free Theories, Propagators, Free Energy

The path integral can be performed if the action is Gaussian. In order to unify the treatment of fermionic and bosonic fields, we write the Lagrangian density as

$$\mathscr{L}(x) = \frac{1}{2} \Psi^T(x) \mathscr{K}(i\partial) \Psi(x). \tag{2.65}$$

Here Ψ can be either a (multicomponent) bosonic field or a (multicomponent) fermionic field in the Nambu representation. The Nambu representation in terms of the original (Dirac) representation can be expressed as

$$\Psi = \begin{pmatrix} \bar{\psi}^T \\ \psi \end{pmatrix}, \qquad \mathscr{K}(i\partial) = \begin{pmatrix} 0 & \mathscr{K}_D(i\partial) \\ -\mathscr{K}_D^T(-i\partial) & 0 \end{pmatrix}. \tag{2.66}$$

If the Ψ field satisfies some self-adjoint property, $\Psi^\dagger = \Psi \Gamma_0$, then the Hermiticity of the action requires $\mathscr{K} = \Gamma_0^\dagger \mathscr{K}^\dagger \Gamma_0^*$. The bosonic/fermionic nature dictates $\mathscr{K}^T(-i\partial) = \alpha \mathscr{K}(i\partial)$.

The operator EoM reads as

$$\mathscr{K}(i\partial)\Psi(x) = 0, \tag{2.67}$$

which implies that the spectral function $\varrho = \varrho_{\Psi\Psi}$ also satisfies the equation

$$\mathscr{K}(i\partial)\varrho(x) = 0. \tag{2.68}$$

In case of general relativistic theories with a single mass shell, there exists a differential operator $D(i\partial)$ (Klein–Gordon divisor [4]), for which

$$\mathscr{K}(i\partial)D(i\partial) = -\partial^2 - m^2, \tag{2.69}$$

the Klein–Gordon operator. Then

$$\varrho(x) = D(i\partial)\varrho_0(x), \qquad \varrho(k) = D(k)\varrho_0(k), \tag{2.70}$$

where $\varrho_0(k)$ is the spectral function of the one-component bosonic field (Klein–Gordon field)

$$(\partial^2 + m^2)\varrho_0(x) = 0, \qquad \varrho_0(t = 0, \mathbf{x}) = 0,\ \partial_t\varrho_0(t = 0, \mathbf{x}) = -i\delta(\mathbf{x}). \tag{2.71}$$

This initial value problem has the following solution in real time:

$$\varrho_0(t, \mathbf{k}) = -i\frac{\sin\omega_k t}{\omega_k}, \qquad \omega_k^2 = \mathbf{k}^2 + m^2; \tag{2.72}$$

in the Fourier space, this implies

$$\varrho_0(k) = 2\pi\ \mathrm{sgn}(k_0)\delta(k^2 - m^2) = \frac{2\pi}{2\omega_k}(\delta(k_0 - \omega) - \delta(k_0 + \omega)). \tag{2.73}$$

As an example we give the Klein–Gordon divisor for the fermion field in the Dirac representation and for the gauge field in R_ξ gauges:

$$D(p) = \not{p} + m, \qquad D^{\mu\nu}(k) = -g^{\mu\nu} + (1 - \xi)\frac{k^\mu k^\nu}{k^2}. \tag{2.74}$$

We can also define the Euclidean version of the Klein–Gordon divisors as

$$D_E(p) = ip_{E\mu}\gamma_\mu + m, \qquad D_{E\mu\nu}(k) = \delta_{\mu\nu} - (1 - \xi)\frac{k_{E\mu}k_{E\nu}}{k_E^2}, \tag{2.75}$$

where $\gamma_{E\mu} = \{\gamma_0, i\gamma\}$ are self-adjoint 4×4 matrices.

Using the generic relations between the spectral functions and propagators, we can write in particular

$$\begin{aligned}
&G^{(ra)}(k) = \frac{D(k)}{k^2 - m^2}\bigg|_{k_0 \to k_0 + i\varepsilon}, \qquad G^{(ar)}(k) = \frac{D(k)}{k^2 - m^2}\bigg|_{k_0 \to k_0 - i\varepsilon},\\
&iG^{(12)}(k) = \alpha n_\alpha(k_0)D(k)\varrho(k), \qquad G^{(21)}(k) = (1 + \alpha n_\alpha(k_0))D(k)\varrho(k),\\
&G^{(33)}(k_E) = \frac{D_E(k_E)}{k_E^2 + m^2} \qquad (k_{E0} = (2n + 1 - \Theta(\alpha))\pi T)
\end{aligned} \tag{2.76}$$

Now let us calculate the path integral in the Gaussian case. By completing the square in the exponent of (2.39), we have schematically (using the Hermiticity of the kernel)

$$\frac{i}{2}\Psi^T\mathscr{K}\Psi + J\Psi = \frac{i}{2}\Psi'^T\mathscr{K}\Psi' + \frac{i}{2}J^T\mathscr{K}^{-1}J, \tag{2.77}$$

where $\Psi' = \Psi - i\mathscr{K}^{-1}J$. Then, by introducing a new integration variable $\Psi \to \Psi'$, we have $Z[J] = Z_0\, e^{\frac{i}{2}J^T\mathscr{K}^{-1}J}$. This form suggests that the generating functional is a Gaussian function of the currents. In the formal derivation, we would have to take into account carefully the boundary conditions when changing over to the new variable. But a shortcut can be taken: we know that the second functional derivative of the generating functional with respect to the currents yields the propagators. Therefore, consistency requires

$$Z[J] = Z_0\, e^{\frac{i}{2}\int \frac{d^4p}{(2\pi)^4} J^T(-p)G(p)J(p)}, \qquad Z_0 = \operatorname{Tr} e^{-\beta H}. \tag{2.78}$$

We can also evaluate Z_0 in the quadratic theory. We should take into account that it comes entirely from the Euclidean part (segment 3) of the time path. The Gaussian integral in the case of bosonic/fermionic variables yields

$$Z_0 = \int \mathscr{D}\Psi e^{-\frac{1}{2}\int \Psi^\dagger \mathscr{K}_E \Psi} = (\det \mathscr{K}_E)^{-\alpha/2}. \tag{2.79}$$

The free energy is therefore

$$F = \frac{\alpha T}{2} \ln\det \mathscr{K}_E = \frac{\alpha V}{2}\int \frac{d^4p}{(2\pi)^4} \ln\det \mathscr{K}_E(p). \tag{2.80}$$

For fermions, up to a constant, the integrand can be expressed through the Euclidean Dirac kernel as $2\ln\det \mathscr{K}_{DE}(p)$ (see Eq. (2.66)).

To evaluate this expression formally, we derive a differential equation for it, by shifting first $\mathscr{K}_E \to \mathscr{K}_E + a$, and then differentiating with respect to a. We have for the free energy density $f = F/V$,

$$\frac{\partial f}{\partial a} = \frac{\alpha}{2}\int \frac{d^4p}{(2\pi)^4} \operatorname{Tr}(\mathscr{K}_E + a)^{-1} = \frac{\alpha}{2}\operatorname{Tr} G_a^{(33)}(x=0), \tag{2.81}$$

where the a subscript in $G_a^{(33)}$ reminds us that here we have to work with the shifted kernel. Using the definition of $G^{(33)}$ through $G^{(12)}$ and $G^{(21)}$ (cf. (2.42)), we can

write the symmetric combination

$$\frac{\partial f}{\partial a} = \frac{\alpha}{2}\,\mathrm{Tr}\, iG_a^{(rr)}(x=0) = \frac{\alpha}{2}\int \frac{d^4p}{(2\pi)^4}\left(\frac{1}{2} + \alpha n_\alpha(p_0-\mu)\right)\varrho_{0a}(p)\,\mathrm{Tr}\, D_{Ea}(p), \tag{2.82}$$

where we also have taken into account chemical potential.

To proceed, it is worth beginning with a brief discussion of the bosonic and fermionic cases separately. In the bosonic case, the Klein–Gordon divisor D_{Ea} is a projector, and the trace simply yields the dimension, i.e., the number of bosonic degrees of freedom N_b. Here a has the meaning of a shift in the squared mass, so we have

$$\frac{\partial f_b}{\partial m^2} = \frac{N_b}{2}\int \frac{d^4p}{(2\pi)^4}\left(\frac{1}{2} + n_+(p_0-\mu)\right)\varrho_0(p), \tag{2.83}$$

where ϱ_0 is the Klein–Gordon spectral function with mass m.

For fermions, we do not have the $1/2$ in passing to the Dirac representation D_{DEa}, but now a has the meaning of a (linear) mass term. The trace of the kernel is $N_f m$. Therefore, the m^2 derivative can be written

$$\frac{\partial f_f}{\partial m^2} = -\frac{N_f}{2}\int \frac{d^4p}{(2\pi)^4}\left(\frac{1}{2} - n_-(p_0-\mu)\right)\varrho_0(p). \tag{2.84}$$

The two cases therefore yield a result that can be uniformly summarized as

$$\begin{aligned}\frac{\partial f}{\partial m^2} &= \frac{\alpha N}{2}\int \frac{d^4p}{(2\pi)^4}\left(\frac{1}{2} + \alpha n_\alpha(p_0-\mu)\right)\varrho_0(p)\\ &= \frac{N}{2}\int \frac{d^3\mathbf{p}}{(2\pi)^3 2\omega_p}\left(n_\alpha(\omega_p-\mu) + n_\alpha(\omega_p+\mu) + \alpha\right),\end{aligned} \tag{2.85}$$

where we used the free Klein–Gordon spectral function. In this expression, the last term is a constant not depending on the temperature. It has no thermodynamic meaning,[2] and so we omit it. The rest can be integrated, and we use the physical condition $f(m^2\to\infty)=0$ to obtain, eventually,

$$f = \frac{N}{2}[f(T,\mu) + f(T,-\mu)], \qquad f(T,\mu) = \alpha T\int \frac{d^3\mathbf{p}}{(2\pi)^3}\,\ln(1-\alpha e^{-\beta(\omega_p-\mu)}). \tag{2.86}$$

[2] This vacuum contribution used to be attributed to the Casimir effect, where we measure the energy difference arising when the volume of the quantization space is changed. It is also worth noting that fermions and bosons contribute with opposite signs, which means that in supersymmetric models, the net zero-point contribution is zero.

The two terms of this formula can be associated with the separate contributions of particles and their antiparticles, respectively. The number of degrees of freedom equals $N/2$ for both. The chemical potential of the antiparticles has opposite sign relative to μ of the particles.

From the thermodynamic potential, one obtains the other thermodynamic quantities, too. The grand canonical potential f is connected to the internal energy density by

$$f = \varepsilon - Ts - \mu n = -p. \tag{2.87}$$

The energy density and number density for one particle degree of freedom have the expressions

$$\varepsilon = \frac{\partial(\beta f)}{\partial \beta} = \int \frac{d^3\mathbf{p}}{(2\pi)^3}\, \omega_p n_\alpha(\omega_p - \mu), \qquad n = -\frac{\partial f}{\partial \mu} = \int \frac{d^3\mathbf{p}}{(2\pi)^3}\, n_\alpha(\omega_p - \mu). \tag{2.88}$$

These expressions are finite unless $\alpha = 1$ and $|\mu| > m$ (the $|\mu| \to m + 0$ case is still finite). In this pathological case, there appears a pole at $p = \sqrt{\mu^2 - m^2}$. Physically, this phenomenon is connected to the Bose–Einstein condensation: in response to trying to increase the number density of particles, the system generates a finite field condensate.

Some limiting cases are the following:

- If $T \ll m$ and $\mu = 0$, one has, for both the fermionic and bosonic cases,

$$p = T\left(\frac{mT}{2\pi}\right)^{3/2} e^{-\beta m}, \qquad \frac{\varepsilon}{p} = \frac{3}{2} + \frac{m}{T}. \tag{2.89}$$

- If $T \gg m, \mu$, one has

$$\frac{p_b}{T^4} = \frac{\pi^2}{90}, \qquad p_f = \frac{7}{8} p_b, \qquad \varepsilon = 3p. \tag{2.90}$$

2.6 Perturbation Theory

If the action contains nonquadratic terms, then we must rely on some approximations for the evaluation of the path integral. Under the assumption that the quadratic (Gaussian) approximation captures the main physical features of the system, only slight nonlinear modifications are expected. Then one can use perturbation theory.

In conformity with this understanding, the action is split into a quadratic and a higher-order part,

$$S[\Psi] = S^{(2)}[A] + S_{int}[A], \tag{2.91}$$

and we write formally

$$S_{int}[A] = \int d^d x\,(-g) A_1(x) \ldots A_v(x) \tag{2.92}$$

for the interaction part. In general, g could contain local operations such as derivations, which we leave hidden in this overview. We recognize next that the generating functional (2.39) can be written as an expectation value of the free theory:

$$Z[J] = Z_{00} \left\langle e^{iS_{int}[A] + \int JA} \right\rangle_0 , \tag{2.93}$$

where Z_{00} is the free partition function at $J = 0$. For perturbation theory, we expand the exponential in a Taylor series:

$$Z[J] = Z_{00} \sum_{m=0}^{\infty} \frac{1}{m!} \left\langle (iS_{int}[A])^m e^{\int JA} \right\rangle_0 . \tag{2.94}$$

Formally, we can also rewrite it as

$$Z[J] = Z_{00} e^{iS_{int}[\frac{\delta}{\delta J}]} \left\langle e^{\int JA} \right\rangle_0 = e^{iS_{int}[\frac{\delta}{\delta J}]} e^{\frac{i}{2} \int J^T G J} . \tag{2.95}$$

For a certain n-point function, we need to apply the required functional derivatives to this expression and eventually put $J = 0$ (cf. (2.35)). This leads to the Feynman rules for the computation of the n-point function $\langle T_c A_{i_1}(p_1) \ldots A_{i_n}(p_n) \rangle$, where $A_i(p)$ are fundamental fields with momentum p and with a generic index (also including the Keldysh indices) i:

- draw a graph with points and links (lines);
- associate the points where only a single link ends (external legs) to the fields $A_{i_k}(p_k)$, $k = 1 \ldots, n$, where n is the number of this type of point;
- associate the points with v links to the piece in the interaction S_{int} containing the product of v field operators. These points are called interaction vertices;
- associate propagators to the links connecting any two points. A number of externally determined propagators enter into each vertex and generate virtual fields propagating along the internal lines of the diagram.

Draw all possible diagrams with n external fields and m vertices, and eventually evaluate them with help of the following rules:

- external legs force the joining propagator to have momentum p_k;
- a link connecting points with indices i and j is represented by $iG^{(ij)}(q)$;
- a vertex having incoming momenta $q_1, \ldots, q_v$ yields a contribution $-ig(2\pi)^d \delta(\sum_{a=1}^{v} q_a)$.

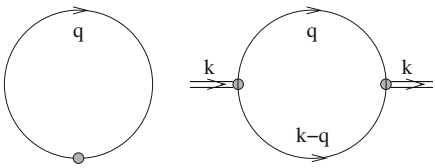

Fig. 2.2 The tadpole and the bubble diagrams

In the last step, one multiplies all these contributions, and an extra factor $1/m!$ is included in the mth order of the perturbation theory. Finally, one evaluates the integrals over the momenta flowing through the internal links: $\Pi_i \int \frac{d^d q_i}{(2\pi)^d}$.

At the one-loop level, there are two diagrams that are the most important: the tadpole and the bubble diagrams; cf. Fig. 2.2. The details of their computation can be found in Appendix B.

2.7 Functional Methods

Perturbation theory can be made more efficient if we realize that the only quantities that need calculation are the loop integrals arising from the rules for setting up Feynman diagrams described in the last section. Therefore, it is worth developing a formalism that concentrates solely on them.

The first step is to introduce $W[J]$, the generator of the connected diagrams:

$$Z[J] = e^{W[J]}. \tag{2.96}$$

Since the generator of the imaginary time diagrams $Z[J_3]$ can be considered the partition function in the presence of an external field, it follows that $-W[J_3]$ is the free energy in the presence of an external field.

The generator W generates the connected diagrams, which can be proved by differentiating Z with respect to the current J_x as follows. The differentiation yields a series of diagrams with one external leg. There is a portion of each diagram connected to the external leg; if we denote by $\bar{W}$ the generator of the connected diagrams, this portion can be computed as $\delta\bar{W}/\delta J_x$. The remainder, on the other hand, is the sum of all zero leg diagrams, i.e., just $Z[J]$. Therefore, we can write down the functional differential equation

$$\frac{\delta Z[J]}{\delta J_x} = \frac{\delta \bar{W}[J]}{\delta J_x} Z[J]. \tag{2.97}$$

Its obvious solution is $Z[J] = e^{\bar{W}[J]}$. Thus we have $W = \bar{W}$.

The connected n-point function is the (left) derivative of W at the zero external field. In particular, the propagator is calculated as

$$iG_{xy} = \frac{\partial^2 W[J]}{\partial J_x \partial J_y}. \tag{2.98}$$

Using (2.93), we find that

$$W[J] = \frac{i}{2} J_x G_{xy} J_y - \frac{\alpha\beta V}{2} \operatorname{Tr} \ln \mathscr{K}_E + \left\langle e^{\int JA} \left(e^{iS_{int}[A]} - 1 \right) \right\rangle_{conn}. \tag{2.99}$$

Then the free energy reads

$$F[J] = \frac{\beta}{2} J_x G_{E,xy} J_y + F_0 + \beta \left\langle e^{\int JA} \left(1 - e^{-S_{E,int}[A]} \right) \right\rangle_{conn}, \tag{2.100}$$

with F_0 denoting the free energy of the free system evaluated in the previous section. Here W (or the free energy F) is a function(al) of the external current. The external current can be set by hand. This is the "tool" for controlling the system from outside; thermodynamically, the currents/sources correspond to the extensive variables. We may, however, want to express the dependence of the free energy on

$$\bar{A}_x[J] \equiv \langle A_x \rangle_J = \frac{\partial W}{\partial J_x}, \tag{2.101}$$

where the subscript J is to emphasize that the expectation value is to be evaluated in the presence of the external current. This is a dynamical quantity, thermodynamically corresponding to the intensive variables. In thermodynamics, this type of change is realized by applying a Legendre transformation, which will be applied here, too.

Technically, the change of W under an infinitesimal change of J reads as $\delta W = \delta J_x \bar{A}_x$ (the ordering is important in the case of fermionic theories). We define the associated potential via a Legendre transformation:

$$i\Gamma[\bar{A}] = W[J] - \int J_x \bar{A}_x. \tag{2.102}$$

In the Euclidean case, we proceed by the replacement $i\Gamma \to -\Gamma_E$. Since $-W_E$ is the free energy expressed through J, Γ_E is the free energy expressed through $\bar{A}$. As can be easily seen, $\delta i\Gamma = -J_x \delta \bar{A}_x$, or

$$\frac{\partial i\Gamma}{\partial \bar{A}_x} = -J_x. \tag{2.103}$$

In the fermionic case, it is a right derivative.

The value of Γ thus defined has many interesting properties. Diagrammatically, $\langle A_x \rangle_J$ is a one-point function. Fixing the value of $\bar{A}$ means fixing the value of the one-point function. Therefore, we must ensure the vanishing of the perturbative corrections to the one-point function. This requirement is equivalent to the omission of all diagrams that contain a part connected to the rest by a single line. Such diagrams are called one-particle reducible diagrams. Those diagrams that remain connected after cutting a line form the class of one-particle irreducible (1PI) diagrams. Therefore, Γ can be interpreted as being the generator of the 1PI diagrams.

The physical expectation values must be computed at zero external current, which means that the physical value of $\bar{A}$ can be determined as a solution of

$$\left.\frac{\partial \Gamma}{\partial \bar{A}_x}\right|_{\bar{A}_{phys}} = 0. \tag{2.104}$$

This is the same EoM as obtained in the classical case, except that one replaces the classical action by Γ. Therefore, the generator of the 1PI diagrams is also called the quantum effective action.

In the functional integral representation, we have

$$e^{i\Gamma[\bar{A}]} = e^{iW[J]-\int J\bar{A}} = \int \mathscr{D}A\, e^{iS[A]+\int J(A-\bar{A})} = \int \mathscr{D}a\, e^{iS[\bar{A}+a]+\int Ja}, \tag{2.105}$$

where in the last equality, the integration variable is shifted to a by $A = \bar{A} + a$, and the full quantum field is split into the sum of the expectation value (mean field, background) $\bar{A}$ and the fluctuations around it, a. This means that $\langle a \rangle = \langle A \rangle - \bar{A} = 0$, i.e., the expectation value of the fluctuations is zero.

In fact, the role of the external current is to ensure that the fluctuations have zero expectation value. This can equivalently be required by an extra condition as

$$e^{i\Gamma[\bar{A}]} = \left.\int \mathscr{D}a\, e^{iS[a+\bar{A}]}\right|_{\langle a \rangle = 0}. \tag{2.106}$$

This is the compact formulation of the background field method.

From this formula, it is also evident that if we require $a = 0$ instead of $\langle a \rangle = 0$, i.e., no fluctuations are allowed at all, then $\Gamma = S$ will be the result. This means that the quantum effective action to leading order is the classical action:

$$\Gamma = S + \text{quantum fluctuations}. \tag{2.107}$$

Together with (2.104), this formula further supports the interpretation of Γ as the quantum effective action.

2.7.1 Two-Point Functions and Self-Energies

Let us investigate, in particular, the second derivative of Γ at the physical value. The 1PI quantum correction to the two-point function is called the self-energy $i\Sigma$:

$$i\Gamma^{(1,1)}_{xy} = \frac{\partial^2 i\Gamma}{\partial\bar{A}_x\partial\bar{A}_y} = i\mathscr{K}_{xy} - i\Sigma_{xy}, \tag{2.108}$$

where $\mathscr{K}_{xy} = \frac{\partial^2 S}{\partial\bar{A}_x\partial\bar{A}_y}$ is the classical kernel. In the case of fermion fields, we have to apply one left and one right derivative here, which is indicated by the upper (double) index of the notation introduced on the left-hand side.

On differentiating (2.103) with respect to J from the left, we obtain

$$\frac{\partial^2 W}{\partial J_x\partial J_z}\frac{\partial^2 i\Gamma}{\partial\bar{A}_z\partial\bar{A}_y} = -\delta_{xy}. \tag{2.109}$$

The second derivatives of W and Γ are therefore the inverse quantities of each other. We can write this expression as

$$G_{xz}(\mathscr{K}_{zy} - \Sigma_{zy}) = (\mathscr{K}_{xz} - \Sigma_{xz})G_{zy} = \delta_{xy}. \tag{2.110}$$

In the Euclidean formalism, we define the self-energy as

$$(\mathscr{K}_E + \Sigma_E(p))G_E(p) = \delta_{xy}. \tag{2.111}$$

Since Σ is the (quantum part of the) 1PI two-point function and G is the inverse of the full two-point function, (2.110) generates the iterative relation that tells how the 1PI diagrams should be resummed in order to give the full result. To leading order we have $\Sigma = 0$, and so $G_0 = \mathscr{K}^{-1}$. With it we obtain formally

$$G = G_0 + G_0\Sigma G = G_0 + G\Sigma G_0 = G_0 + G_0\Sigma G_0 + G_0\Sigma G_0\Sigma G_0 + \cdots. \tag{2.112}$$

This formula is sometimes called the Dyson–Schwinger (DS) series.

From this formula, a simple rule can be read off how to determine the self-energy. The first correction to the two-point function that is $\delta\langle T_C AA\rangle = \langle T_C AA\rangle - iG_0$ can always be written formally as

$$\delta\langle T_C AA\rangle = iG_0\delta\langle T_C AA\rangle_{amp} iG_0 = iG_0\Sigma G_0 + \cdots, \tag{2.113}$$

or in the Euclidean formalism,

$$\delta\langle T_C A^{(3)}A^{(3)}\rangle = G_0\delta\left\langle T_C A^{(3)}A^{(3)}\right\rangle_{amp} G_0 = -G_0\Sigma_E G_0 + \cdots, \tag{2.114}$$

which means

$$\Sigma = i\delta \langle T_C AA \rangle_{amp}\,, \qquad \Sigma_E = -\delta \langle T_C A^{(3)} A^{(3)} \rangle_{amp}. \tag{2.115}$$

The quantity $\delta \langle T_C AA \rangle_{amp}$ is the "amputated" two-point function, where we chop off the propagators belonging to the external lines.

Although it looks quite simple, (2.112) in fact avoids by resummation a series of individually increasingly divergent contributions. Namely, the free propagator exhibits a pole at $p^2 = m^2$ on the mass shell. Near the mass shell, we have $p^2 = m^2 + x$, and the free propagator behaves as $G_0 \sim 1/x$. Therefore, the nth term in the DS series is proportional to $1/x^n$. These terms are therefore more and more divergent at a finite value of the momentum: this is characteristic of an infrared (IR) divergence. The DS series resums the most relevant terms and provides the propagator G free of unphysical divergences. It also may have a pole, but that is already physical: no further diagrams can change it. This logic will be followed later in performing the resummation of IR divergent (IR sensitive) series.

The propagator is in general a matrix expressing the correlation of all possible field components at the same momentum (if we have spacetime translation-invariance). This holds for the self-energy, too. In particular, if we use the real-time formalism, then Σ is a matrix with Keldysh indices $1, 2$. Omitting other components, the DS equation can be written as

$$\mathscr{K}(p) G^{(ij)}(p) = (-1)^{i+1} (\delta^{ij} + \Sigma^{(ik)}(p) G^{(kj)}(p)),, \qquad i,j,k \in \{1,2\}, \tag{2.116}$$

i.e., the sign is $+$ for $i = 1$ and $-$ for $i = 2$. In the R/A formalism, $G^{(aa)} = 0$ implies $\Sigma^{(rr)} = 0$. The previous equation can be rewritten with help of the σ_1 Pauli matrix:

$$\mathscr{K}(p) G^{(ab)}(p) = \sigma_1^{ab'} \left[\delta^{b'b} + \Sigma^{(b'c)}(p) G^{(cb)}(p) \right], \qquad a,b,b',c \in \{r,a\}. \tag{2.117}$$

This relation shows that the retarded propagator is not mixed with the others:

$$\mathscr{K}(p) G^{(ra)}(p) = 1 + \Sigma^{(ar)}(p) G^{(ra)}(p). \tag{2.118}$$

The generic relation between the propagators discussed in Sect. 2.4 implies relations between the self-energies. In particular,

$$\Sigma^{(11)} = \Sigma^{(ar)} - \Sigma^{(12)} = \Sigma^{(ra)} - \Sigma^{(21)}, \qquad \Sigma^{(aa)} = -\frac{\Sigma^{(12)} + \Sigma^{(21)}}{2} \tag{2.119}$$

Moreover,

$$\Sigma_E(\omega_n) = \Sigma^{(ar)}(k_0 \to i\omega_n). \tag{2.120}$$

The causal behavior of the retarded propagator implies that $\Sigma^{(ar)}$ is either local or at least causal itself. Therefore, after separating the local contribution Σ_0, one writes for the remainder ($\Sigma_1^{(ar)}$) a dispersive representation:

$$\Sigma^{(ar)}(k) = \Sigma_0 + \Sigma_1^{(ar)}(k), \qquad \Sigma_1^{(ar)}(k) = \int \frac{d\omega}{2\pi} \frac{\mathrm{Disc}_{k_0}\, i\Sigma^{(ar)}(k_0, \mathbf{k})}{k_0 - \omega + i\varepsilon}. \tag{2.121}$$

The discontinuity can be expressed through other self-energies, too:

$$\mathrm{Disc}\,\Sigma^{(ar)} = \Sigma^{(ar)} - \Sigma^{(ra)} = \Sigma^{(12)} - \Sigma^{(21)} \tag{2.122}$$

Finally, the relation between $G^{(rr)}$ and the retarded propagator implies that

$$\Sigma^{(aa)} = \left(\frac{1}{2} + \alpha n_\alpha(k_0)\right) \mathrm{Disc}\ \ i\Sigma^{(ar)} \tag{2.123}$$

This means that full knowledge of the retarded self-energy (or equivalently, the Matsubara self-energy) is enough to fully reconstruct all the self-energies of the system.

2.7.2 Higher n-Point Functions

Further derivatives of (2.109) exploiting (2.101) provide relations between the 1PI and the connected n-point functions. In particular,

$$\begin{aligned} iW^{(3)}_{ijk} &= iG_{ii'}iG_{jj'}iG_{kk'}i\Gamma^{(3)}_{i'j'k'}, \\ iW^{(4)}_{ijk\ell} &= iG_{ii'}iG_{jj'}i\Gamma^{(3)}_{i'j'k'}iG_{k'a}i\Gamma^{(3)}_{abc}iG_{bk}iG_{c\ell} + \ldots \\ &\quad + iG_{ii'}iG_{jj'}iG_{kk'}iG_{\ell\ell'}i\Gamma^{(4)}_{i'j'k'\ell'}. \end{aligned} \tag{2.124}$$

Here we used the notation

$$\Gamma^{(n)}_{i_1\ldots i_n} = \frac{\partial^n \Gamma[\bar{A}]}{\partial\bar{A}_{i_1}\ldots\partial\bar{A}_{i_n}}, \qquad W^{(n)}_{i_1\ldots i_n} = \frac{\partial^n W[J]}{\partial J_{i_1}\ldots\partial J_{i_n}}. \tag{2.125}$$

In the case of fermions, one has to pay attention to the order of differentiation.

These formulas correspond to the tree-level relations between the n-point functions and the vertices when vertex strengths are derived from the classical action. The derivatives of the effective action therefore play the role of the classical vertices: hence the name *proper vertices*. In contrast to the classical theory, quantum fluctuations produce nonzero values for arbitrary high n-point functions.

2.8 The Two-Particle Irreducible Formalism

In the previous subsection we investigated the generator of the 1PI diagrams, where the system is forced by a choice of appropriate external current distribution to take a predetermined value $\bar{A} = \langle A \rangle$ for the expectation value of the field operator. We can go on with this logic and try to impose other constraints on the path integral. The next step is to fix the value of the two-point functions as well. Technically, what we have to do is to assign an external current to the two-point function and determine its value from the requirement that the exact two-point function coincide with the a priori chosen expression.

Thus we define an extended generator functional containing both an external current J and an external bilocal source term R:

$$Z[J,R] = e^{W[J,R]} = \int \mathscr{D}A e^{iS[A]+J_xA_x+\frac{1}{2}iR_{xy}A_xA_y}, \tag{2.126}$$

where we have suppressed the explicit indication of summation/integration. We want to fix the values of the field expectation value to $\bar{A}$ and the connected two-point function to $\bar{G}$:

$$\begin{aligned} \frac{\partial W[J,R]}{\partial J_x} &= \langle A_x \rangle = \bar{A}_x, \\ 2\frac{\partial W[J,R]}{\partial iR_{xy}} &= \left\langle T_C A_x A_y \right\rangle = i\bar{G}_{xy} + \bar{A}_x\bar{A}_y. \end{aligned} \tag{2.127}$$

From these equations, one can in principle determine J and R.

Just as in the 1PI case, we define the extended effective action as

$$i\Gamma[\bar{A},\bar{G}] = W[J,R] - J_x\bar{A}_x - \frac{1}{2}iR_{xy}(\bar{A}_x\bar{A}_y + i\bar{G}_{xy}). \tag{2.128}$$

After differentiation (right differentiation in the case of fermi fields), this double Legendre transform provides us with the relations

$$\frac{\partial i\Gamma[\bar{A},\bar{G}]}{\partial \bar{A}_x} = -J_x - iR_{yx}\bar{A}_y, \qquad \frac{\partial i\Gamma[\bar{A},\bar{G}]}{\partial i\bar{G}_{xy}} = -\frac{1}{2}iR_{xy}. \tag{2.129}$$

In the physical point we should set the external sources to zero, and therefore, we have

$$\left.\frac{\partial i\Gamma[\bar{A},\bar{G}]}{\partial \bar{A}_x}\right|_{phys} = 0, \qquad \left.\frac{\partial i\Gamma[\bar{A},\bar{G}]}{\partial i\bar{G}_{xy}}\right|_{phys} = 0, \tag{2.130}$$

which suggests that Γ is indeed the quantum analogue of the extended classical action. By substituting back the physical value of $\bar{G}$ obtained with fixed $\bar{A}$ function

from the solution of the second equation, we obtain the (1PI) effective action:

$$\Gamma[\bar{A}] = \Gamma[\bar{A}, \bar{G}_{phys}[\bar{A}]]. \tag{2.131}$$

Since $\bar{A}$ and $\bar{G}$ are the *exact* one- and two-point functions, respectively, there should be no quantum correction to them, and this is true even on the internal lines of the diagrams. In the case of the predetermined one-point function, this has had the consequence that the effective action is the generator of 1PI diagrams. In a similar manner for the case of the exact two-point function, only two-particle-irreducible (2PI) diagrams can appear in the perturbation theory, which do not fall apart when we cut two internal lines of a diagram. In other words, we do not have perturbative self-energy corrections to the propagators representing the lines in the corresponding Feynman diagrams (called also *skeleton* diagrams). If we apply this requirement to the physical value of the propagator, using the fact that on the one hand, $\langle T_C AA \rangle_{conn}$ equals $i\bar{G}_{phys}$, and on the other hand, we can express it by the self-energy, we obtain

$$\bar{G}^{-1}_{phys} = G_0^{-1} - \Sigma_{2PI}[\bar{A}, \bar{G}_{phys}]. \tag{2.132}$$

This is a self-consistent (gap) equation that allows to determine the value of the physical connected propagator.

In special cases, we can determine $\Gamma[\bar{A}, \bar{G}]$. If there is no quantum correction at all, then the path integral substitutes the solution of the classical EoM, which is the same as the first equation of (2.129) with $\Gamma \to S$. Classically, $\bar{G} = 0$, and so the classical 2PI effective action reverts to the classical 1PI case, i.e., $\Gamma = S$.

In the free case, we can solve the system even in the presence of external sources. In bosonic theories, in copying the steps leading to (2.78), one arrives at

$$W[J, R] = \frac{1}{2} J\, i(G_0^{-1} + R)^{-1} J - \frac{1}{2} \operatorname{Tr} \ln(G_0^{-1} + R). \tag{2.133}$$

This implies

$$\begin{aligned} \frac{\partial i W[J,R]}{\partial J} &= i(G_0^{-1} + R)^{-1} J = \bar{A}, \\ 2\frac{\partial i W[J,R]}{\partial iR} &= J\, i(G_0^{-1} + R)^{-2} J + i(G_0^{-1} + R)^{-1} = i\bar{G}_{xy} + \bar{A}_x \bar{A}_y, \end{aligned} \tag{2.134}$$

which means

$$\begin{aligned} & G_0^{-1} + R = \bar{G}^{-1}, \qquad \bar{A} = i\bar{G}J, \\ & i\Gamma[\bar{A}, \bar{G}] = iS[\bar{A}] - \frac{1}{2} \operatorname{Tr} \ln \bar{G}^{-1} - \frac{1}{2} \operatorname{Tr} G_0^{-1} \bar{G}. \end{aligned} \tag{2.135}$$

Motivated by the result of the free theory, in the interacting case we write

$$i\Gamma[\bar{A},\bar{G}] = iS[\bar{A}] - \frac{1}{2}\operatorname{Tr}\ln\bar{G}^{-1} - \frac{1}{2}\operatorname{Tr}G_0^{-1}\bar{G} + i\Gamma_{int}[\bar{A},\bar{G}], \tag{2.136}$$

where in the correction part Γ_{int}, we should use the exact propagator $\bar{G}$ and keep only the 2PI diagrams. The physical value of the propagator, using (2.130), leads to (2.132) with

$$\Sigma_{2PI}[\bar{A},\bar{G}] = 2\frac{\partial i\Gamma_{int}[\bar{A},\bar{G}]}{\partial\bar{G}}. \tag{2.137}$$

A peculiarity of the 2PI formalism is that we can access the same correlation functions in different ways. For example, the self-energy can be expressed from (2.137) as the derivative of the 2PI action with respect to $\bar{G}$, but it is also the second derivative with respect to $\bar{A}$. This ambiguity remains true for all higher point functions. For the exact correlation functions, these definitions yield the same result, but in the perturbative expansion, usually we find deviations. The derivative of the 1PI effective action, for example, always respects the symmetry of the Lagrangian, and so it satisfies Goldstone's theorem in the case of spontaneous symmetry-breaking (SSB) of a continuous symmetry. This is not true for the solution of the 2PI equation (2.132) if we substitute back the physical value of the background. The reason is that Goldstone's theorem is satisfied at each order of perturbation theory as a result of subtle cancellations between the self-energy and the vertex corrections. Therefore, when we resum all the self-energy diagrams up to a certain order using the 2PI formalism and leave the vertex corrections at their tree-level perturbative value, we easily find a mismatch. We will return to this point later, in Sect. 4.7.

This line of thought can be continued, and we can demand that the correlation functions up to n-point functions have predetermined values, denoted by $\bar{A} \equiv V_1, \bar{G} \equiv V_2$ and V_k, $k > 2$; in general, we refer to them as V_k ($k = 1,\dots,n$) (cf. [11]). Similarly as above, we can force the system to provide the required n-point functions by introducing external currents besides J_x, R_{xy}. These will be denoted by $R^{(k)}_{x_1\dots x_n}$ ($k = 1,\dots,n$):

$$iS \to iS + \sum_{k=1}^{n}\frac{1}{k!}R^{(k)}_{x_1,\dots,x_k}A_{x_1}\dots A_{x_k}. \tag{2.138}$$

The derivative of $W[R^{(k)}]$ with respect to these sources will give us the k-point functions. We require that the fully connected part coincide with the predefined values.

We can also perform a Legendre transformation to obtain the free energy $\Gamma[V_k]$, which is the functional of V_k, where we can also express the external sources $R^{(k)}$ through V_k. The physical value of the vertices comes from the requirements $\delta\Gamma[V_k]/\delta V_j = 0$. Since we fixed all the correlation functions up to the n-point

functions, the perturbative expansion should contain only n-particle-irreducible (nPI) diagrams, which remain connected even after cutting n internal lines.

2.9 Transformations of the Path Integral

In this subsection we will perform some changes in the integration variable of the path integral

$$Z[J] = \int \mathscr{D}A e^{iS[A]+JA}. \tag{2.139}$$

Let us consider an infinitesimal transformation $A_i \to A_i' = A_i + \varepsilon_i \Delta A_i[A]$ for which the corresponding Jacobian is unity to linear order in ε_i (no summation is understood for i):

$$\ln \text{ Jacobian} = \ln \det \left(\delta_{ij} + \varepsilon_i \frac{\partial \Delta A_i}{\partial A_j} \right) = \text{Tr}\, \varepsilon_i \frac{\partial \Delta\, A_i}{\partial A_j} + \mathscr{O}(\varepsilon^2) \stackrel{!}{=} 0. \tag{2.140}$$

The change in the path integral up to leading order in ε_i reads as

$$\begin{aligned} Z[J] &= \int \mathscr{D}A' e^{iS[A']+JA'} = \int \mathscr{D}A e^{iS[A+\varepsilon_i \Delta A_i]+J(A+\varepsilon_i \Delta A_i)} \\ &= \int \mathscr{D}A e^{iS[A]+JA} \left(1 + i\varepsilon_i \frac{\partial S}{\partial \varepsilon_i} + J_i \varepsilon_i \Delta A_i \right) \\ &= Z[J] \left(1 + i\varepsilon_i \left\langle \frac{\partial S}{\partial \varepsilon_i} - i J_i \Delta A_i \right\rangle \right). \end{aligned} \tag{2.141}$$

The invariance under this change of variables implies

$$\left\langle \frac{\partial S[A]}{\partial \varepsilon_i} - i J_i \Delta A_i[A] \right\rangle = 0, \tag{2.142}$$

a true set of relations for any transformation.

One way in which we can exploit this equation is to take its nth derivative with respect to $J_{a_1}, \ldots, J_{a_n}$:

$$\left\langle \left(\frac{\delta S}{\delta \varepsilon_i} - i J_i \Delta A_i \right) A_{a1} \ldots A_{a_n} - i \sum_{k=1}^{n} \delta_{ia_k} A_{a1} \ldots A_{a_{k-1}} \Delta A_{a_k} A_{a_{k+1}} \ldots A_{a_n} \right\rangle = 0. \tag{2.143}$$

In the physical vacuum, $J = 0$, and we obtain

$$\left\langle \frac{\delta S}{\delta \varepsilon_i} A_{a1} \dots A_{a_n} \right\rangle_{phys} = i \sum_{k=1}^{n} \delta_{ia_k} \left\langle A_{a1} \dots A_{a_{k-1}} \Delta A_{a_k} A_{a_{k+1}} \dots A_{a_n} \right\rangle_{phys} . \tag{2.144}$$

We can also use (2.142) to find equations for W and Γ, exploiting that

$$\langle f(A) \rangle = \frac{1}{Z[J]} f\left(\frac{\partial}{\partial J}\right) Z[J] = e^{-W} f\left(\frac{\partial}{\partial J}\right) e^{W} = f\left(\frac{\partial}{\partial J} + \frac{\partial W}{\partial J}\right). \tag{2.145}$$

Therefore, we should substitute $A \to \partial_J + \partial W/\partial J$ in (2.142) to obtain its functional expression and set $J = 0$ at the end.

To have an equation for the effective action, we use (2.103) and

$$\frac{\partial}{\partial J_x} = \frac{\partial A_y}{\partial J_x} \frac{\partial}{\partial A_y} = \frac{\partial^2 W}{\partial J_x \partial J_y} \frac{\partial}{\partial A_y} = iG_{xy} \frac{\partial}{\partial A_y} \tag{2.146}$$

(in the fermionic case, left differentiation should be applied here). Since $iJ = \partial \Gamma / \partial A$ (with right differentiation), we have

$$\frac{\partial}{\partial \varepsilon_i} S\left[A + iG\frac{\partial}{\partial A}\right] = \Delta A_i \left[A + iG\frac{\partial}{\partial A}\right] \frac{\partial \Gamma}{\partial A_i}. \tag{2.147}$$

The expressions in the square brackets denote the "variables" of the functionals S and ΔA_i, respectively. We should emphasize that (2.142) and therefore (2.147) are true for every transformation. Specifying the form of the transformation leads to different applications.

2.9.1 Equation of Motion, Dyson–Schwinger Equations

In the simplest application, the transformation is a simple shift of the field value, that is, $A'(x) = A(x) + \varepsilon(x)$. Then $\Delta A = 1$, and the ε derivative is the same as the A derivative. Then we obtain the Dyson–Schwinger equations

$$\left\langle \frac{\partial S}{\partial A_i} - iJ_i \right\rangle = 0 \qquad \text{or} \qquad \frac{\partial S}{\partial A_i}\left[A + iG\frac{\partial}{\partial A}\right] = \frac{\partial \Gamma}{\partial A_i}. \tag{2.148}$$

In particular, for the physical vacuum ($J = 0$), we obtain the EoM

$$\left\langle \frac{\partial S}{\partial A_i} \right\rangle\Big|_{phys} = 0 \qquad \text{or} \qquad \frac{\partial S}{\partial A_i}\left[A + iG\frac{\partial}{\partial A}\right]\Big|_{phys} = 0. \tag{2.149}$$

An illustrative example of the application of these general formulas is presented in the next subsection. Taking the derivative of the previous equation with respect to $J_{a_1}, \ldots, J_{a_n}$ we obtain, in the physical vacuum $J = 0$,

$$\left\langle \frac{\delta S}{\delta A_i} A_{a1} \ldots A_{a_n} \right\rangle = i \sum_{k=1}^{n} \delta_{ia_k} \left\langle A_{a1} \ldots A_{a_{k-1}} A_{a_{k+1}} \ldots A_{a_n} \right\rangle . \tag{2.150}$$

This relation corresponds to (2.144) for the actual transformation.

In the real time formalism we should take into account that the Lagrangian is $\mathscr{L} = \mathscr{L}[A^{(1)}] - \mathscr{L}[A^{(2)}]$, and so

$$\frac{\partial S}{\partial A^{(i)}} = (-1)^{i+1} \left. \frac{\partial S}{\partial A} \right|_{A=A^{(i)}} . \tag{2.151}$$

Therefore,

$$\left\langle \left. \frac{\partial S}{\partial A} \right|_{A=A^{(i)}} A_{a1} \ldots A_{a_n} \right\rangle = i(-1)^{i+1} \sum_{k=1}^{n} \delta_{ia_k} \left\langle A_{a1} \ldots A_{a_{k-1}} A_{a_{k+1}} \ldots A_{a_n} \right\rangle . \tag{2.152}$$

2.9.2 *Ward Identities from a Global Symmetry*

If the transformation $A' = A + \varepsilon \Delta A$ corresponds to a global symmetry of the system, then the derivative is (cf. (2.2))

$$\frac{\partial S}{\partial \varepsilon_i} = \partial_\mu j_i^\mu . \tag{2.153}$$

We remark here that j^μ is the conserved current, which is a functional of the field variables, while J is the current assigned to sustain a certain field configuration. In this way, we obtain

$$\left\langle \partial_\mu j_i^\mu - i J_i \Delta A_i \right\rangle = 0 \qquad \text{or} \qquad \partial_\mu j^\mu \left[A + iG \frac{\partial}{\partial A} \right] = \frac{\partial \Gamma}{\partial A_i} \Delta A_i \left[A + iG \frac{\partial}{\partial A} \right] . \tag{2.154}$$

For the n-point function, we obtain, from (2.144),

$$\partial_\mu \left\langle j_i^\mu A_{a1} \ldots A_{a_n} \right\rangle = i \sum_{k=1}^{n} \delta_{ia_k} \left\langle A_{a1} \ldots A_{a_{k-1}} \Delta A_i A_{a_{k+1}} \ldots A_{a_n} \right\rangle . \tag{2.155}$$

This is the generic form of the Ward identities. These are nothing other than the current conservation equations for the quantum case.

We discuss here three short applications.

1. If we integrate over the variable i (which also contains the spacetime integration), we obtain

$$0 = \sum_{k=1}^{n} \left\langle A_{a1} \dots A_{a_{k-1}} \Delta A_{a_k} A_{a_{k+1}} \dots A_{a_n} \right\rangle . \tag{2.156}$$

The right-hand side is the total change in the expectation value

$$0 = \Delta \left\langle A_{a_1} \dots A_{a_n} \right\rangle . \tag{2.157}$$

This means that the expectation value of every n-point function is invariant under the global symmetry transformation. Note that this is true for the complete n-point function, not just the connected part.

2. In the case of linear continuous transformations, $\Delta A_i = T_{ij} A_j$. Taking the integrated form of the effective action expression with a constant (i.e., zero-momentum) A field, we have

$$0 = \frac{\partial \Gamma}{\partial A_i} T_{ij} A_j, \tag{2.158}$$

where one sums over repeated indices. Taking its functional derivative yields

$$\frac{\partial^2 \Gamma}{\partial A_k \partial A_i} T_{ij} A_j + \frac{\partial \Gamma}{\partial A_i} T_{ik} = 0. \tag{2.159}$$

In the physical point, $\frac{\partial \Gamma}{\partial A_i} = 0$, but the field itself can take a (constant) expectation value in the SSB case. Therefore,

$$\frac{\partial^2 \Gamma}{\partial A_k \partial A_i} T_{ij} A_j = 0, \tag{2.160}$$

which is *Goldstone's theorem*: the inverse propagator has a zero mode at zero momentum in the SSB case.

3. Remaining in the class of linearly represented symmetries, we write down the Ward identity for two fields explicitly, displaying the spacetime indices:

$$\partial_x^\mu \left\langle j_\mu(x) A_i(y) A_j(z) \right\rangle = i\delta(x-y) T_{ik} \left\langle A_k(y) A_j(z) \right\rangle + i\delta(x-z) T_{jk} \left\langle A_i(y) A_k(z) \right\rangle . \tag{2.161}$$

We assume that we are in the symmetric case (the SSB case is only formally more complicated). One introduces for the left-hand side a 1PI proper vertex:

$$\left\langle j_\mu(x) A_i(y) A_j(z) \right\rangle = iG_{ii'}(y-y')\, iG_{jj'}(z-z')\, \Gamma^\mu_{i'j'}(x, y', z'). \tag{2.162}$$

The Ward identity takes the following form after passage to Fourier space:

$$G_{ii'}(p)G_{jj'}(q)(-ik_\mu)\Gamma^\mu_{i'j'}(k,p,q) = T_{ik}G_{jk}(q) + T_{jk}G_{ik}(p), \tag{2.163}$$

where $k + p + q = 0$. Multiplying by the inverse propagators gives us

$$(-ik_\mu)\Gamma^\mu_{ij}(k,p,q) = G^{-1}_{ik}(p)T_{kj} + G^{-1}_{jk}(q)T_{ki}. \tag{2.164}$$

There is a special case, in which the propagation is diagonal ($G_{ij} = G_i\delta_{ij}$ and $T_{ij} = -T_{ji}$. Then

$$(-ik_\mu)\Gamma^\mu_{ij}(k,p,q) = T_{ij}\left(G^{-1}_i(p) - G^{-1}_j(q)\right). \tag{2.165}$$

This is an often used consequence of the Ward identity.

2.10 Example: Φ^4 Theory at Finite Temperature

The simplest example for perturbation theory that is appropriate for demonstrating the mechanisms of finite temperature calculations is the Φ^4 theory of a one-component scalar field. The Lagrangian reads as

$$\mathscr{L} = \frac{1}{2}\Phi(-\partial^2 - m^2)\Phi - \frac{\lambda}{24}\Phi^4. \tag{2.166}$$

This is the basic form of the Lagrangian. However, we should use it in other forms at finite temperature. The free part was discussed in Sect. 2.5; the propagators are listed in (2.76). Here the Klein–Gordon divisor is 1. The Euclidean and Keldysh forms of the interactions are respectively

$$\mathscr{L}_{E,int} = \frac{\lambda}{24}\Phi^4, \qquad \mathscr{L}_{int} = -\frac{\lambda}{24}\left(\Phi_1^4 - \Phi_2^4\right), \tag{2.167}$$

while in the R/A formalism, we obtain

$$\mathscr{L}_{int} = -\frac{\lambda}{6}\Phi_r^3\Phi_a - \frac{\lambda}{24}\Phi_r\Phi_a^3. \tag{2.168}$$

In the perturbation theory, first we calculate the 1PI correction to the 2-point function (the self-energy). This is the amputated connected 2-point function, as can be seen from (2.115). At one loop level in the coordinate space in the Euclidean formalism we obtain

$$\Sigma_E(x) = -\left\langle \mathrm{T}_C\Phi^{(3)}(x)\Phi^{(3)}(0)(-S_{E,int})\right\rangle_{amp} = \frac{\lambda}{2}G^{(33)}(0)\delta(x) = \frac{\lambda}{2}\mathscr{T}\delta(x), \tag{2.169}$$

where $\mathscr{T}$ is the tadpole function defined in Appendix B.1. In momentum space, the self-energy is a constant. Therefore, in the R/A formalism, $\Sigma^{(ar)} = \Sigma^{(ra)} = \Sigma_E$ and $\Sigma^{(aa)} = 0$. Physically, it is a mass correction. Using the results of Appendix B.1 derived with dimensional regularization, at zero temperature we obtain for the second derivative of the effective action

$$\Gamma^{(2)}(p) = p^2 + m^2 + \frac{\lambda m^2}{32\pi^2}\left[-\frac{1}{\varepsilon} + \gamma_E - 1 + \ln\frac{m^2}{4\pi\mu^2}\right], \tag{2.170}$$

while in the high-temperature expansion, we have

$$\Gamma^{(2)}(p) = p^2 + m^2 + \frac{\lambda T^2}{24} - \frac{\lambda m T}{8\pi} + \frac{\lambda m^2}{32\pi^2}\left[-\frac{1}{\varepsilon} + \gamma_E - \ln\frac{4\pi T^2}{\mu^2}\right]. \tag{2.171}$$

In the symmetric phase, the three-point function vanishes; the four-point proper vertex is therefore the amputated four-point function. The first quantum correction is of second order in the coupling constant expansion. In the Euclidean formalism,

$$\Gamma_E^{(4)}(p_1,p_2,p_3,p_4) = -\left\langle \mathrm{T}_C \Phi(p_1)\Phi(p_2)\Phi(p_3)\Phi(p_4)(1 - S_{E,int} + \frac{1}{2}S_{E,int}^2)\right\rangle_{amp}, \tag{2.172}$$

where we should use fields on the Euclidean contour (segment 3). The first term gives a disconnected piece. For the connected part, we have from momentum conservation

$$\Gamma_{E,conn}^{(4)}(p_1,p_2,p_3,p_4) = \bar{\Gamma}_E^{(4)}(p_1,p_2,p_3,p_4)(2\pi)^4\delta(p_1+p_2+p_3+p_4),$$

where

$$\bar{\Gamma}_E^{(4)}(p_1,p_2,p_3,p_4) = \lambda - \frac{\lambda^2}{2}\left[\mathscr{I}_E(p_1+p_2) + \mathscr{I}_E(p_1+p_3) + \mathscr{I}_E(p_1+p_4)\right], \tag{2.173}$$

where $\mathscr{I}_E(k)$ is the contribution from the bubble diagram, defined in Appendix B.2.

We can also give the effective potential to this lowest order. We use the background field method of (2.106), i.e., we shift the field $\Phi \to \varphi + \bar{\Phi}$ and omit linear terms in the fluctuations (and at higher order all contributions to the 1-point function). We obtain for the shifted Lagrangian

$$\mathscr{L} = \mathscr{L}(\bar{\Phi}) + \frac{1}{2}\varphi(-\partial^2 - m^2 - \frac{\lambda}{2}\bar{\Phi}^2)\varphi - \frac{\lambda}{6}\bar{\Phi}\varphi^3 - \frac{\lambda}{24}\bar{\Phi}^4. \tag{2.174}$$

The first term gives the classical effective potential. For the first quantum corrections, we need just the free fluctuation part, which will lead to some quantum correction $\delta\Gamma$. We could use the formula (2.86) with $\mu = 0$, $\alpha = 1$, but here we should keep the regularized form. We can use that for constant fields,

$\frac{\partial\delta\Gamma}{\partial\bar{\Phi}^2} = \frac{1}{2}\Sigma_E(p=0,\bar{\Phi})$. In the self-energy one can take $p=0$, since it is a tadpole, and does not depend on the momentum in any way. In Σ, all the Φ-dependence is through the mass term. Therefore, $\Sigma_E(M) = \lambda\frac{\partial\delta\Gamma}{\partial M^2}$, where $M^2 = m^2 + \frac{\lambda}{2}\bar{\Phi}^2$. Using (2.169), we have

$$\frac{\partial\delta\Gamma}{\partial M^2} = \frac{1}{2}\mathscr{T}(M,T). \tag{2.175}$$

The integration constant is $\delta\Gamma|_{M=0} = \frac{\pi^2T^4}{90}$. Finally, we obtain at zero temperature

$$\delta\Gamma_E(T=0) \equiv V_{\mathit{eff}}(T=0) = \frac{m^2}{2}\bar{\Phi}^2 + \frac{\lambda}{24}\bar{\Phi}^4 + \frac{M^4}{64\pi^2}\left[\mathscr{D}_\varepsilon + \ln\frac{M^2}{4\pi\mu^2}\right], \tag{2.176}$$

and in the high-temperature expansion,

$$V_{\mathit{eff}} = \frac{\pi^2T^4}{90} + \frac{m^2}{2}\bar{\Phi}^2 + \frac{\lambda}{24}\bar{\Phi}^4 + \frac{T^2M^2}{24} - \frac{M^{3/2}T}{12\pi} + \frac{M^4}{64\pi^2}\left[\mathscr{D}_\varepsilon + \frac{3}{2} - \ln\frac{4\pi T^2}{\mu^2}\right], \tag{2.177}$$

where $\mathscr{D}_\varepsilon = -\frac{1}{\varepsilon} + \gamma_E - \frac{3}{2}$ is a divergent constant. We remark here that in the spontaneously broken phase, where $m^2 < 0$, the quantum corrections cannot be interpreted physically for $\bar{\Phi}^2$ values yielding $M^2 < 0$ because of the $M^{3/2}$ term.

We may also illustrate the Dyson–Schwinger equations by means of the example of the Φ^4 model. We begin with the generator of the 1PI DS equations (2.148):

$$\Gamma^{(1)}_x = \mathscr{K}_{xy}\Phi_y - \frac{\lambda}{6}\left(\Phi_x^3 + 3\Phi_x iG_{xx} + iG_{xx'}iG_{xy'}iG_{xz'}\Gamma^{(3)}_{x'y'z'}\right), \tag{2.178}$$

where $\mathscr{K}(p) = p^2 - m^2$. Here the indices of the different quantities refer simply to spacetime points, x is the free argument, and one has summation on the others. After differentiating once more with respect to Φ_y, we obtain

$$\begin{aligned}\Gamma^{(2)}_{xy} &= \mathscr{K}_{xy} - \frac{\lambda}{2}\left(\Phi_x^2 + iG_{xx}\right)\delta_{xy} \\ &-\frac{\lambda}{2}\left(\Phi_x iG_{xa}iG_{xb}i\Gamma^{(3)}_{aby} + iG_{xy'}iG_{xz'}\Gamma^{(3)}_{x'y'z'}iG_{xa}iG_{x'b}i\Gamma^{(3)}_{aby}\right) - \\ &-\frac{\lambda}{6}iG_{xx'}iG_{xy'}iG_{xz'}\Gamma^{(4)}_{x'y'z'y}.\end{aligned} \tag{2.179}$$

As a specific application, we can reproduce the perturbative results: we go to the symmetric phase, where $\Phi = 0$, and we restrict ourselves to the lowest order (i.e., we neglect terms $\mathscr{O}(\lambda^2)$). We obtain in the Fourier space

$$\Gamma^{(2)}(p) = p^2 - m^2 - \frac{\lambda}{2}iG_{xx}. \tag{2.180}$$

This form actually agrees with the 2PI equation (2.132) with the self-energy from (2.169). Therefore, in fact, this equation is a gap equation for the propagator.

References

1. M.E. Peskin, D.V. Schroeder, *An Introduction to QFT* (Westview Press, New York, 1995)
2. C. Itzykson, J.-B. Zuber, *Quantum Field Theory* (McGraw-Hill, New York, 1980)
3. J.D. Bjorken, S.D. Drell, *Relativistic Quantum Fields* (McGraw-Hill, New York, 1965)
4. N.P. Landsmann, Ch.G. van Weert, Real- and imaginary-time field theory at finite temperature and density. Phys. Rep. **145**, 141–249 (1987)
5. M. Le Bellac, *Thermal Field Theory* (Cambridge University Press, Cambridge, 1996)
6. J.I. Kapusta, C. Gale, *Finite-Temperature Field Theory, Principles and Applications* (Cambridge University Press, Cambridge, 2006)
7. I. Montvay, G. Münster, *Quantum Fields on a Lattice* (Cambridge University Press, Cambridge, 1994)
8. J. Collins, *Renormalization*. Cambridge Monographs for Mathematical Physics (Cambridge University Press, Cambridge, 1984)
9. L.D. Landau, E.M. Lifshitz, Course of theoretical physics, in *The Classical Theory of Fields*, vol. 2 (Butterworth-Heinemann, Oxford, 1975)
10. M. Garny, M.M. Muller, Phys. Rev. D **80**, 085011 (2009)
11. J. Berges, Phys. Rev. D **70**, 105010 (2004)

Chapter 3
Divergences in Perturbation Theory

Already in the simplest examples where Feynman diagrams involving loops are calculated, perturbative corrections to the tree-level result turn out to be divergent, or very large in certain cases. Several of these divergences can be identified in the example of the one-loop self-energy of Φ^4 theory. In (2.169), we have seen that $\varepsilon \to 0$ (dimensional regularization) yields a divergence, while in the case of $\lambda T^2 \gg m^2$ or $\lambda |\ln T^2/\mu^2| \gg 1$, the one-loop corrections are much bigger than the tree-level mass. We have also seen that in fact, the series of 1PR corrections to the propagator exhibits divergence on the mass shell; see (2.112).

The physical reason for these divergences is that the system interacts with an infinite (or very large) number of fluctuating modes. The mass shell divergence of the 1PR diagrams emerges because the particle on the mass shell lives infinitely long, and so interactions of arbitrarily low intensity are repeated infinitely many times. In the limit $\varepsilon \to 0$, or for $\Lambda \to \infty$ (cutoff regularization), we include more and more short-wavelength fluctuations into the system. For $T^2 \gg m^2$ or μ^2, the heat bath provides us the large number of interacting modes.

There are also further examples. At zero temperature, quantum corrections carry powers of $\ln m/\mu$, and this is also a source of large corrections when the values of m and μ are vastly different. The value of μ usually refers to the scale where we measure the values of the parameters, while m is the physical mass. If these are very different, then we must include a large number of fluctuation modes in comparing the actual physics to the reference scale. A more complicated example arises when two particles propagate with approximately the same momentum (or in other words, the corresponding plane waves have nearby wave vectors): this again gives the possibility for repeated interactions.

These divergences can be physical. For example, the poles of the exact propagator signal the mass shell of a stable particle, the singularities in the derivatives of the free energy signal phase transitions. The problematic divergences are the perturbative ones emerging in the calculation of per se finite quantities, which

A. Jakovác, A. Patkós, *Resummation and Renormalization in Effective Theories of Particle Physics*, Lecture Notes in Physics 912,
DOI 10.1007/978-3-319-22620-0_3

become worse and worse as we go to higher order in perturbation theory. These kinds of divergences are symptoms of the inappropriate organization of perturbation theory.

3.1 Reorganizations of Perturbation Theory

Let us pause at the concluding sentence of the last paragraph. So far, it has seemed that perturbation theory is a well-defined and unique procedure, based on the Taylor expansion of $e^{iS_{int}}$ in (2.94). The open question is, however, how we define S_{int} and what the expansion parameter is.

If we want to maintain the as much generality as possible, we should allow the unperturbed system, which we denote by S_0, to be not necessarily identical to the quadratic part $S^{(2)}$ (although in practice, S_0 is also taken to be a quadratic expression, since it is the only case we can solve). We require only two features for S_0: it should provide a solvable system, and its predictions should be close to the true physical characterization of the system. If these are fulfilled, then we may hope that the small deviations of the leading-order predictions from the exact characteristic quantities can be gradually taken into account by some perturbative series. In that case the interaction Lagrangian is just $S_{int} = S - S_0$, and not $S - S^{(2)}$, as was expected in naive perturbation theory.

This consideration has far-reaching consequences: in fact, the choice of the unperturbed Lagrangian, and thus the perturbation theory itself, is already an interpretation of the physical system. We must determine the most important part of the system, and this can be very dissimilar in various physical situations. The hadron world and the quark–gluon world are different faces of the strong interactions relevant in different physical circumstances. For more, see Sect. 3.6.

Once we have fixed the unperturbed Lagrangian, we also should fix the expansion parameter. It is not necessarily the coupling constant that characterizes the nonlinear part of the action. We can use an arbitrary polynomial of it, like $\sum_{n=1}^{\infty} c_n \lambda^n$, where we can fix $c_1 = 1$. The coefficients of the polynomial might depend on the scale of the investigated physical phenomena. We can call this expansion parameter the *renormalized coupling* λ_{ren}. The interaction Lagrangian S_{int} is then an (infinite) polynomial in λ_{ren}.

In fact, we also have the freedom to choose the operators in which we want to construct the perturbation series. In the simplest case, we can consider the rescaling of the original operators, which we call *wave function renormalization*. In principle, however, we could introduce completely different operators defined in terms of the original field variables for the perturbation series. Technically, it means that we use an *effective model* that is capable of accounting for the true physical observables. The parameters of this effective model are determined either by direct measurements or by matching certain observables that are equally easy to calculate in the original and effective models.

Finally, we have chosen a splitting of the original action as

$$S = S_0 + S_{int}(\lambda_{ren}), \qquad \lambda_{ren} = \lambda_{ren}(\lambda). \tag{3.1}$$

In order to have a well-defined example in mind, we consider the Φ^4 theory, where the original (or *bare*) Lagrangian has the form (2.166). To realize the ideas discussed above, the simplest, but still rather general, choice is obtained by rescaling the original fields as $\Phi = Z^{1/2}\varphi$ and choosing S_0 quadratic. We write

$$\mathscr{L} = \frac{1}{2}\varphi(-\partial^2 - m^2_{ren})\varphi - \frac{\lambda_{ren}}{24}\varphi^4 + \frac{\delta Z}{2}\varphi(-\partial^2)\varphi - \frac{\delta m^2}{2}\varphi^2 - \frac{\delta\lambda}{24}\varphi^4, \tag{3.2}$$

where the first term on the right-hand side is identified with S_0. Consistency requires

$$1 + \delta Z = Z, \qquad m^2_{ren} + \delta m^2 = Z m^2, \qquad \lambda_{ren} + \delta\lambda = Z^2\lambda, \tag{3.3}$$

but otherwise, δZ, δm^2, and $\delta\lambda$ are arbitrary polynomials in λ_{ren},

$$\delta Z = \sum_{n=1}^{\infty} \delta Z_n \lambda^n_{ren}, \qquad \delta m^2 = \sum_{n=1}^{\infty} \delta m^2_n \lambda^n_{ren}, \qquad \delta\lambda = \sum_{n=2}^{\infty} \delta\lambda_n \lambda^n_{ren}, \tag{3.4}$$

provided (3.3) is satisfied. In this rewriting of the original expression (2.166), m^2_{ren} and λ_{ren} are called the *renormalized parameters*; m^2 and λ are the *bare parameters*. The part of the Lagrangian containing the complementary $\delta m^2, \delta\lambda, \delta Z$ are called *counterterms*, forming the *counterterm Lagrangian*. The way of choosing the coefficients of the counterterms is called *renormalization scheme*. To fix the value of the renormalized parameters, one chooses an appropriate number of physical observables: this is called a *renormalization prescription*. And finally, the whole procedure is called *renormalized perturbation theory*.[1]

All this means that there are several representations for the same bare Lagrangian from the point of view of perturbation series. All choices of the form of (3.2) that satisfy (3.3) are permitted. We can thus define an equivalence relation between the renormalized Lagrangians: two theories are equivalent if they describe the same bare Lagrangian, or equivalently, the same physics. Application of the equivalence relation leads to equivalence classes, which may be called equivalence classes of constant physics (ECCP). If we consider just a one-parameter subclass, we obtain the line of constant physics (LCP), nomenclature that is often used in the context of lattice field theory [1].

[1] We remark that these notions usually are applied to the procedure of getting rid of the UV divergences. But as we have seen, the UV divergences are just specific examples the possible divergences of perturbation series, and the complete terminology is applicable to any reorganization of the perturbation theory.

Although at infinite order, all elements of a given ECCP yield the same physics, the rates of convergence of these series can be rather different. Since the renormalized coupling λ_{ren} is a function of λ, the bare coupling, starting with $\lambda_{ren} = \lambda + \mathcal{O}(\lambda^2)$, it follows that the renormalized perturbation series at order n contains the powers λ^k with $k \leq n$ with the same coefficients, while at higher order, the coefficients are different. Therefore, any two perturbation series are the same at the order of the expansion and different at higher orders. Put another way, any two perturbation series are *resummations* of each other. We should choose that representative of the ECCP for which the observable(s) we want to calculate exhibit the best convergence property. The minimal expectation is the requirement to avoid the perturbative UV or IR divergences systematically.

3.2 On the Convergence of Perturbation Theory

Based on the different convergence properties of the perturbation theories, we can find optimal elements of the ECCP showing the fastest convergence. This is the basic idea behind various popular schemes, such as the renormalization group aided, resummed, or optimized perturbative techniques.

These techniques, albeit usually not explicitly stated that way, use two generic features of perturbation series. The first observation is that on the one hand, the divergences appear at each order in perturbation series, but on the other hand, we have also the freedom to update the counterterms at each order. This gives the opportunity to design the counterterms to cancel the divergences. If divergences come from loop corrections, then at nth order, the necessary counterterms are proportional to at least λ_{ren}^n. The so-defined perturbation theory is then divergence-free.

In fact, the bare parameters of (3.3) must be in accordance with this requirement; otherwise, the nonperturbatively defined theory is inconsistent, i.e., there are some physical quantities that are not finite. Therefore, practically, in perturbation theory one uses the renormalized perturbation series to properly define the theory.

In this context, we make an additional remark: the divergences are usually environment-dependent; for example, they depend on the actual momenta we use in an experiment, the temperature and chemical potential if we are in an equilibrium system. Then the divergence-free perturbation theory itself should also depend on the environmental data. The only exception is the elimination of UV divergences, since the physics at short scales is insensitive to the environmental data set by IR physics.

Another remark is that the above procedure can be performed for as many observables, as many free parameters we have in the nth-order counterterms; in the case of Φ^4 theory, this number is three, related to the wave function, the mass, and the self-coupling renormalization. After we have cleared all the divergences in the appropriately chosen (three) observables, we may hope that it has done the job

for all other observables, too. This consistency requirement is not trivial, in fact it represents, in the strictest sense, the criteria for perturbative renormalizability.

The second generic feature of perturbation series is that we can ensure that a renormalized perturbation theory $\mathscr{P}$ belongs to a given ECCP by choosing the values of the renormalized parameters. This can be done in two ways. Either we use the renormalization scheme to directly determine the values of the parameters from experimental observations. This is sometimes tedious, since the perturbation theory is chosen by the requirement that it should give the best performance under special conditions, which usually differ from the circumstances under which the experiments were done. As a second more practical alternative, therefore one conveniently chooses another perturbation theory $\mathscr{P}_\gamma$ optimal for computing a certain set γ of the experimental observables and determines its renormalized parameters. Then we should find observables that are reliably calculable in both $\mathscr{P}$ and $\mathscr{P}_\gamma$. By comparing the calculations, we can determine the relationship between the desired renormalized parameters of $\mathscr{P}$ and those of P_γ. This procedure is called *matching*, and usually this is used to give the best estimate for the renormalized parameters.

3.3 Renormalization of the UV Divergences

Historically, the renormalization program was first developed to treat the UV divergences that endangered the consistency of the whole perturbation theory. The observation is that at each order, loop corrections yield divergent integrals even to physical observables that are clearly finite. Therefore, if we determine the bare parameters from observables (regularization of the loop integrals is needed for this step), the bare parameters should also be divergent when we want to remove the regularization. Unless we have a physical regulator (such as the lattice spacing in solid-state physics) that ensures that even the bare parameters are small, the perturbative series behave very badly. For example, the first-order correction to the mass parameter is proportional to Λ in Φ^4 theory: if $\Lambda \to \infty$, the perturbative series is not convergent at all.

The program of the renormalized perturbation theory, however, helps. We should not develop any quantity in power series of the divergent bare parameters, but in powers of the finite (and eventually small) renormalized ones. At each order, we encounter regularized UV divergences, which, however, are canceled with systematically chosen counterterms. The part of the counterterms relevant to the cancellation of the regularized UV divergences is uniquely fixed, but the rest (sometimes called the "finite part") can be freely chosen to relate the renormalized couplings in the simplest possible way to the chosen set of observables.

To see how this works, we take the Φ^4 theory at the one-loop level. The coefficients of the first two terms of the effective action were calculated in (2.169) and (2.173) using the bare action. Using the renormalized form of the

Lagrangian (3.2) and setting $T = 0$, we obtain

$$\Gamma^{(2)}(p) = p^2 - m_{ren}^2 - \delta m_1^2 - \frac{\lambda_{ren} m_{ren}^2}{32\pi^2}\left[-\frac{1}{\varepsilon} + \gamma_E - 1 + \ln\frac{m_{ren}^2}{4\pi\mu^2}\right], \tag{3.5}$$

and introduce the factorized form $\Gamma^{(4)}(p_i) = -\bar{\Gamma}^{(4)}(p_i)(2\pi)^4\delta(\sum p_i)$

$$\bar{\Gamma}^{(4)}(p_i) = \lambda_{ren} + \delta\lambda_1 + \frac{\lambda_{ren}^2}{32\pi^2}\left[\frac{3}{\varepsilon} + \bar{\mathscr{I}}_0(p_1+p_2) + \bar{\mathscr{I}}_0(p_1+p_3) + \bar{\mathscr{I}}_0(p_1+p_4)\right], \tag{3.6}$$

where

$$\bar{\mathscr{I}}_0(p) = \gamma_E + \int_0^1 dx \, \ln\frac{m_{ren}^2 - p^2 x(1-x)}{4\pi\mu^2}. \tag{3.7}$$

Here we set $\delta Z_1 = 0$ for simplicity (which is a self-consistent assumption).

In principle, $\Gamma^{(2)}$ and $\bar{\Gamma}^{(4)}$ are measurable, so they must be finite. This is made possible if we choose

$$\delta m_1^2 = \frac{\lambda_{ren} m_{ren}^2}{32\pi^2}\left[\frac{1}{\varepsilon} + C_1\right], \qquad \delta\lambda_1 = \frac{3\lambda_{ren}^2}{32\pi^2}\left[-\frac{1}{\varepsilon} + D_1\right], \tag{3.8}$$

where C_1 and D_1 are constant terms, finite for $\varepsilon \to 0$.

Therefore, $\Gamma^{(2)}$ and $\Gamma^{(4)}$ read

$$\Gamma^{(2)}(p) = p^2 - m_{ren}^2 - \frac{\lambda_{ren} m_{ren}^2}{32\pi^2}\left[C_1 + \gamma_E - 1 + \ln\frac{m_{ren}^2}{4\pi\mu^2}\right], \tag{3.9}$$

$$\bar{\Gamma}^{(4)}(p_i) = \lambda_{ren} + \frac{\lambda_{ren}^2}{32\pi^2}\left[3D_1 + \bar{\mathscr{I}}_0(p_1+p_2) + \bar{\mathscr{I}}_0(p_1+p_3) + \bar{\mathscr{I}}_0(p_1+p_4)\right]. \tag{3.10}$$

These expressions are still not fully determined due to the arbitrary constants C_1 and D_1. More precisely, the way in which they are chosen defines the renormalization scheme. Popular choices are the following:

- The minimal subtraction (MS) scheme: $C_1 = D_1 = 0$.
- The $\overline{\text{MS}}$ scheme: here we optimize for the length of the resulting expression, and choose $C_1 = -\gamma_E + 1 + \ln 4\pi$ and $D_1 = -\gamma_E + \ln 4\pi$. Then we have

$$\Gamma^{(2)}_{\overline{\text{MS}}}(p) = p^2 - m_{ren}^2 - \frac{\lambda_{ren} m_{ren}^2}{32\pi^2}\ln\frac{m_{ren}^2}{\mu^2},$$

$$\bar{\Gamma}^{(4)}_{\overline{\text{MS}}}(p_i) = \lambda_{ren} + \frac{\lambda_{ren}^2}{32\pi^2}\left[\bar{\mathscr{I}}_{\overline{\text{MS}}}(p_1+p_2) + \bar{\mathscr{I}}_{\overline{\text{MS}}}(p_1+p_3) + \bar{\mathscr{I}}_{\overline{\text{MS}}}(p_1+p_4)\right], \tag{3.11}$$

where

$$\bar{\mathscr{I}}_{\overline{\rm MS}}(p) = \int_0^1 dx\, \ln \frac{m_{ren}^2 - p^2 x(1-x)}{\mu^2}. \tag{3.12}$$

In the MS and $\overline{\rm MS}$ schemes, the dimensionless counterterms $(\delta m_1^2/m_{ren}^2, \delta\lambda_1)$ are mass-independent.

- The on mass shell (OMS) scheme: we require that $\Gamma^{(2)}(p^2 = m_{ren}^2) = 0$, which means that $C_1 = -\gamma_E + 1 - \ln \frac{m_{ren}^2}{4\pi\mu^2}$. Often, it is used with the requirement that $\Gamma^{(4)}(p_i = 0) = \lambda_{ren}$, yielding $D_1 = -\gamma_E - \ln \frac{m_{ren}^2}{4\pi\mu^2}$. Here we have

$$\begin{aligned}
\Gamma^{(2)}_{\rm OMS}(p) &= p^2 - m_{ren}^2, \\
\bar{\Gamma}^{(4)}_{\rm OMS}(p) &= \lambda_{ren} + \frac{\lambda_{ren}^2}{32\pi^2}\left[\bar{\mathscr{I}}_{\rm OMS}(p_1+p_2) + \bar{\mathscr{I}}_{\rm OMS}(p_1+p_3)\right. \\
&\quad \left. + \bar{\mathscr{I}}_{\rm OMS}(p_1+p_4)\right],
\end{aligned} \tag{3.13}$$

where

$$\bar{\mathscr{I}}_{\rm OMS}(p) = \int_0^1 dx\, \ln \frac{m_{ren}^2 - p^2 x(1-x)}{m_{ren}^2}. \tag{3.14}$$

These expressions for the 2- and 4-point functions are apparently different, but they belong to the same ECCP if we determine the renormalized parameters correctly. For example, we may prescribe the following renormalization conditions to be satisfied in all schemes:

$$\Gamma^{(2)}(p^2 = m_{phys}^2) = 0, \qquad \Gamma^{(4)}(p_i = 0) = \lambda_{phys}. \tag{3.15}$$

This yields in the different schemes for m_{ren}^2 and λ_{ren} different expressions in terms of the "measured" mass and coupling parameters (the indices below explicitly refer to the corresponding renormalization scheme):

$$\begin{aligned}
m_{\rm MS}^2 &= m_{phys}^2 - \frac{\lambda_{phys} m_{phys}^2}{32\pi^2}\left[\gamma_E - 1 + \ln \frac{m_{phys}^2}{4\pi\mu^2}\right] + \mathscr{O}(\lambda_{phys}^2), \\
\lambda_{\rm MS} &= \lambda_{phys} - \frac{3\lambda_{phys}^2}{32\pi^2} \ln \frac{m_{phys}^2}{4\pi\mu^2} + \mathscr{O}(\lambda_{phys}^3),
\end{aligned} \tag{3.16}$$

and

$$m^2_{\overline{\rm MS}} = m^2_{phys} - \frac{\lambda_{phys} m^2_{phys}}{32\pi^2} \ln \frac{m^2_{phys}}{\mu^2} + \mathcal{O}(\lambda^2_{phys}),$$
$$\lambda_{\overline{\rm MS}} = \lambda_{phys} - \frac{3\lambda^2_{phys}}{32\pi^2} \ln \frac{m^2_{phys}}{\mu^2} + \mathcal{O}(\lambda^3_{phys}). \tag{3.17}$$

Moreover,

$$m^2_{\rm OMS} = m^2_{phys}, \qquad \lambda_{\rm OMS} = \lambda_{phys}. \tag{3.18}$$

After back-substituting these values and using λ_{phys} as expansion parameter, we find that the results are equal only up to the next-to-leading order; the higher orders are different. This leads to the aforementioned consequence: the rate of convergence is different in the different schemes. The best convergence for these two quantities is guaranteed in the OMS scheme, and it can be achieved by the choice $\mu^2 = m^2_{phys}$ in $\overline{\rm MS}$. In fact, with this special choice, the OMS and the $\overline{\rm MS}$ schemes are the same at one loop order. This choice also illustrates how one might get rid of nondivergent but potentially large logarithms.

3.4 Renormalizability: Consistency of UV Renormalization

In the previous section, we demonstrated at one loop order that in the Φ^4 model with appropriate choice of the counterterms, the second and fourth derivatives of the effective action could be made finite for arbitrary momentum values. The question still to answer is whether this will be true for every observable and to every order. In the case of an affirmative answer, we say that the theory is renormalizable.

The proof of renormalizability is not easy, and there are several monographs dealing with this topic more deeply [2]. Here we just briefly go over the main points of the arguments and the conclusions.

First we pin down that only loop integrals produce divergences, and so the divergence structure of 1PR diagrams can be built up from the divergences of 1PI building blocks. Stating this in another way, the Legendre transformation leading to W from Γ does not change the UV divergences. So we will consider the divergences of the 1PI diagrams.

With the method of renormalized perturbation theory, divergences can be made to vanish of only those n-point functions that have counterterms. In Φ^4 theory, therefore, one can arrange only the cancellation of the divergences showing up in 2- and 4-point functions.

Now consider a contribution to the n-point function, and define its overall divergence: this is the behavior of the integral corresponding to a certain Feynman diagram when the momenta on all lines go to infinity at the same rate. The most

singular behavior of a diagram comes from the overall divergence. This necessarily has to be canceled by a counterterm.

The overall divergence of an integral can be determined by simple dimensional analysis. Let us assume that the renormalized coupling constant has mass dimension d_λ. For simplicity, we use cutoff regularization. Then consider an observable at Nth order in perturbation theory, and examine the relative weight of the $(N+1)$th-order contribution to it. Factoring out the value of the Nth-order result shows that the relative contribution is necessarily linear in λ, but in a dimensionless combination. For making it dimensionless, we need $\lambda \#^{-d_\lambda}$, where # is some quantity of mass dimension. Therefore, in general, we must expect the appearance of a contribution $\sim \lambda \Lambda^{-d_\lambda}$ (its coefficient might be zero in some cases). This shows that if $d_\lambda < 0$, then we get a new divergence of $(N+1)$th order. Therefore, above a certain order, all observables will receive divergent contributions. For $d_\lambda > 0$, the divergences will die out after a certain order. If $d_\lambda = 0$, the overall divergence at all orders will be characterized by the same multiplicative expression.

This leads to the conclusion that for $d_\lambda < 0$, we expect overall divergences in all n-point functions. Then for all of these n-point functions, we would need counterterms, which means infinitely many terms in the Lagrangian. In this case, renormalized perturbation theory cannot solve the problem of UV divergences. These are the *perturbatively nonrenormalizable theories*.

If $d_\lambda > 0$, then just a finite number of diagrams are divergent, and only up to a certain order of the perturbation theory. Then the full expression of the counterterms can be determined exactly using perturbation theory. These theories are called *superrenormalizable theories*.

If $d_\lambda = 0$, as in the Φ^4 theory in four dimensions, the n-point functions up to a certain n_{max} can be divergent, but then they are divergent at each order. These are the potentially *perturbatively renormalizable theories*.

The next point that we have to see is that the overall divergent part of the diagram is a polynomial in the external momenta. To see this, one differentiates the expression of the diagram's contribution with respect to one of the external momenta. There must be at least one internal line where the carried momentum contains additively the external momentum. Therefore, differentiation with respect to the external momentum provides a derivative of a propagator, which decreases the degree of the divergence. After some number of differentiations, the diagram will be finite: therefore, the overall divergent part is a polynomial in the chosen external momentum.

This means that an overall divergence can be made to vanish by a local operator counterterm containing a finite number of derivatives.

A diagram can be divergent also in a way that only a finite subset of lines have large momenta, with the rest finite.[2] The finite subset of lines defines a subdiagram, which is perturbatively of lower order than the complete diagram. Therefore, if it is overall divergent, we already have associated a counterterm to it that makes

[2] Actually, they need not be finite; only their ratio must vanish in the limit.

it finite. Since also the counterterm is of lower order perturbatively, it always appears together with the divergent subdiagram in any diagram. Finally, with the earlier determined counterterms, all the subdivergences vanish, and only an overall divergence may remain, which then can be canceled by an appropriate counterterm.

This line of reasoning summarizes the main steps of the demonstration that the renormalized Lagrangian of (3.2) solved with the method of renormalized perturbation theory is an adequate tool for making all the UV divergences vanish from the system in the case of renormalizable theories.

3.5 Scale-Dependence and the Callan–Symanzik Equations

In the renormalization process, the introduction of a scale parameter is unavoidable. It is a direct consequence of the regularization of the logarithmic divergences. Using a cutoff Λ (or a finite lattice spacing a), the divergence is $\sim \ln \Lambda/M$ ($\ln(aM)$), where M is some mass parameter of the theory. When we make the cutoff vanish, we still have $\sim \ln \mu/M$: the parameter μ must be there, since the log needs a dimensionless argument. In the case of dimensional regularization, the μ scale compensates the change in the dimension of the infinitesimal phase-space volume.

The peculiarity of μ in the renormalized perturbation theory is that on the one hand, it is not present in the original bare theory, so it cannot influence the physics; on the other hand, its value is arbitrary. Since it does not influence the physics, any choice of μ yields a theory that is in the same ECCP: therefore, perturbation theories based on different choices of μ can be connected by appropriate relations among the renormalized parameters. This means that if g stands for the renormalized parameters at scale μ (in the case of Φ^4, these are λ_{ren} and m_{ren}), and g' at scale μ', then there exists a relation $g'(g, \mu, \mu')$ emerging from the condition that both belong to the same ECCP. This relation expresses the fact that the renormalized perturbation theory describes the same physical n-point functions as the bare one.

Taking into account that the field is also rescaled as compared to the bare one, we can write

$$\Gamma^{(n)}(p_i, g, \Lambda) = Z^{-n/2}\Gamma^{(n)}_{ren}(p_i, g_{ren}, \mu), \tag{3.19}$$

for every n and for arbitrary momentum set $\{p_i\}$. Clearly, it is enough to consider a finite number of equations of this kind for the determination of Z and g_{ren}. Renormalizability ensures that with these parameters, all n-point functions will satisfy (3.19).

An equivalent approach is to compare two renormalized perturbation theories defined at different scales. A direct consequence of (3.19) is

$$\Gamma^{(n)}_{ren}(p_i, g_{ren}, \mu) = \zeta^{n/2}\Gamma^{(n)}_{ren}(p_i, g'_{ren}, \mu'), \tag{3.20}$$

where $\zeta = Z/Z'$ is a finite wave function renormalization factor. The result of this equation is the curves $g(\mu^2)$ and $\zeta(\mu^2)$ that characterize the scale-dependence of the couplings and the wave function renormalization constant for a given ECCP.

One can use this equation in perturbation theory; for example, we can apply this relation to the four-point function of the Φ^4 model at one loop order at $p = 0$ and at $T = 0$ in the $\overline{\text{MS}}$ scheme (cf. (3.11)). We use the fact that $Z = 1$ (there is no infinite wave function renormalization at one loop order), and therefore,

$$\lambda_{ren} + \frac{3\lambda_{ren}^2}{32\pi^2} \ln \frac{m_{ren}^2}{\mu^2} + \mathcal{O}(\lambda_{ren}^3) = \lambda'_{ren} + \frac{3\lambda'^2_{ren}}{32\pi^2} \ln \frac{m'^2_{ren}}{\mu'^2} + \mathcal{O}(\lambda'^3_{ren}), \tag{3.21}$$

where we have set $\lambda_{ren} = \lambda_{ren}(\mu^2)$ and $\lambda'_{ren} = \lambda_{ren}(\mu'^2)$. Up to the desired accuracy, we obtain

$$\lambda'_{ren} = \lambda_{ren} + \frac{3\lambda_{ren}^2}{32\pi^2} \ln \frac{\mu'^2}{\mu^2} + \mathcal{O}(\lambda_{ren}^3). \tag{3.22}$$

We can follow an even cleverer strategy. As we discussed earlier, the matching of two renormalization schemes should rely on observables that can be computed in both schemes with high precision. In the example above, the direct matching of the two schemes is problematic if the scales μ and μ' differ considerably. But we can always match theories with scales μ and $\mu + d\mu$, and then we can progress to μ' gradually in repeated infinitesimal $d\mu$ steps.

We can implement this strategy by differentiating (3.22) with respect to $\log \mu^2$; since the left-hand side does not depend on μ^2, we have

$$\mu^2 \frac{d\lambda_{ren}(\mu^2)}{\partial \mu^2} = \frac{3\lambda_{ren}^2}{32\pi^2} + \mathcal{O}(\lambda_{ren}^3) \equiv \beta_\lambda. \tag{3.23}$$

The right-hand side is called the *beta function*. It characterizes the scale-dependence of the coupling. We can even solve this differential equation,

$$\lambda_{ren}(\mu^2) = \frac{\lambda_0}{1 - \dfrac{3\lambda_0}{32\pi^2} \log \dfrac{\mu^2}{\mu_0^2}}, \tag{3.24}$$

where λ_0 is the integration constant of the differential equation, $\lambda_{ren}(\mu_0^2) = \lambda_0$. This equation describes the *running* of the renormalized coupling.

This relation is an example of the effect of a partial resummation of perturbation series (performed this time with the help of the renormalization group equation). On expanding the denominator into a power series of λ_0, one sees that its first two terms reproduce (3.22). The rest (with $\lambda_0^n, n > 2$) is the result of the so-called leading-log resummation, corresponding to the infinite nested repetition of the bubble diagram (see the details in Chap. 5 on the N-component scalar model).

The dependence of the other constants on the scale can be obtained when we differentiate (3.19) with respect to $\ln \mu^2$:

$$\begin{aligned} 0 &= \mu^2 \frac{d}{d\mu^2} \Gamma^{(n)}(p_i, \Lambda, \lambda(\Lambda^2), m^2(\Lambda^2)) \\ &= \mu^2 \frac{d}{d\mu^2} \left[Z_\phi^{-n/2} \left(\Lambda^2/\mu^2, \lambda(\Lambda^2) \right) \Gamma_R^{(n)} \left(p_i, \mu, \lambda(\mu^2), m^2(\mu^2) \right) \right] \\ &= Z_\phi^{-n/2} \left[\mu^2 \frac{\partial \Gamma_R^{(n)}}{\partial \mu^2} + \beta_\lambda \frac{\partial \Gamma_R^{(n)}}{\partial \lambda} + \beta_{m^2} \frac{\partial \Gamma_R^{(n)}}{\partial m^2} + \frac{n}{2} \eta_\phi \Gamma_R^{(n)} \right]. \end{aligned} \tag{3.25}$$

Here we introduced another beta function characterizing the scale-dependence of the mass and also the anomalous dimension of the field ϕ, η_ϕ:

$$\beta_{m^2} = \mu^2 \frac{\partial m^2}{\partial \mu^2}, \qquad \eta_\phi = -\mu^2 \frac{\partial \ln Z_\phi}{\partial \mu^2}. \tag{3.26}$$

The set (3.25) represents the *Callan–Symanzik equations* [3, 4], or renormalization group equations (RGE). From the 2-point function (3.11) we can also easily determine the latter coefficient functions at the one-loop level:

$$\beta_{m^2} = \frac{\lambda_{ren} m^2_{ren}}{32\pi^2}, \qquad \eta_\phi = 0. \tag{3.27}$$

Since $3\lambda\beta_{m^2} = m^2 \beta_\lambda$, the combination $(m^2)^3/\lambda$ is μ-independent:

$$m^2(\mu^2) = m_0^2 \left(\frac{\lambda(\mu^2)}{\lambda_0} \right)^{1/3}. \tag{3.28}$$

When these are known, we can use (3.25) to predict the form of all n-point functions. We emphasize that the coefficients $\beta_\lambda, \beta_{m^2}, \eta_\phi$ above are accurate only up to one loop level. Therefore, one cannot continue reliably far away from the weak coupling regime.

It is interesting to note that the Λ-independence of $\Gamma_R^{(n)}$, i.e., the right-hand side of (3.19), allows one to write a similar equation describing the cutoff dependence of the unrenormalized 4-point function. This is more appropriate for lattice field theories where the continuum limit is achieved by tuning the lattice constant $a \sim \Lambda^{-1}$ towards zero.

3.5.1 Choice of Scale

Although the scale parameter is arbitrary, the perturbative series built on different choices of μ^2 may have different convergence properties. According to the generic discussion, we should choose the element of the ECCP, in the present case by choosing the scale, that ensures the fastest convergence.

In practice, this means that we should diminish the effects of the logs in the perturbative formulas. In case of the 4-point function (3.11), we see that for small external momentum and finite mass, the best choice is $\mu^2 = m^2_{ren}$ (one may also fine-tune the optimization and apply an appropriate constant); for $p = 0$, this choice suppresses all perturbative corrections in the $\overline{\text{MS}}$ scheme. On the other hand, if we have, for some reason, a vanishing mass, then to avoid the blowup of the perturbative series, we must choose $\mu^2 \sim p^2$.

A physically typical situation arises when one measures the parameters of the model at low momentum and low temperature, and the task is to discover the behavior of the correlation functions in a physical environment where the modulus of the momentum is much larger than the mass. If the momentum is small, we should adapt the scale to the mass, $\mu_0^2 = m^2_{ren}$. We determine the physical values of λ_{ren} and m^2_{ren} at this scale. These will be the measured λ_{phys} and m^2_{phys} values. In the case of large external momentum, another choice is more convenient: $\mu^2 = p^2$. Then to a good approximation in that kinematic region, we again obtain $\Gamma^{(4)}(p) = \lambda_{ren}(p)$, i.e., formally, there is no quantum correction. In order to obtain simple results at large p^2, we should work with renormalized couplings defined at the scale μ^2. To ensure that the two perturbation theories belong to the same LCP equivalence class, the two couplings are related to each other by the relation

$$\lambda_{ren}(p) = \frac{\lambda_{phys}}{1 - \beta_{\lambda 1}\lambda_{phys} \ln \dfrac{p^2}{m^2_{phys}}}, \tag{3.29}$$

where $\beta_{\lambda 1}$ is the coefficient of the leading (one-loop) term in β_λ:

$$\beta_{\lambda 1} = \frac{3}{32\pi^2}. \tag{3.30}$$

A generic strategy seems to emerge. We should always choose for the computation the relevant scale in the system. By doing so, the quantum corrections will be small, so we can essentially use the classical results, but with μ^2-dependent running values of the couplings.

We should make here a remark concerning the counterterms of the system. We have mentioned that since the overall divergences are polynomial in the external momentum, the counterterms depend polynomially on the momenta. The counterterms depend on λ_{ren} (cf., for example (3.8)). But we see from (3.29) that λ_{ren}

actually depends on the momentum logarithmically. One may ask whether there is a contradiction here.

The answer is that the relations in (3.8) represent counterterms for local operators irrespective of the choice of the renormalized couplings. We may choose the value of μ^2 to be whatever we wish; we may even fix it to the value of the typical external momentum. But any choice of μ^2 just defines a specific scheme for the perturbation series. Therefore, we must not mix momentum dependencies coming from the optimized *choice* of the renormalized parameters with the dependency that originates from the inclusion of nonlocal operators (involving an infinite number of derivatives). This lesson will be recalled when we use temperature-dependent values for the renormalized parameters.

3.5.2 Landau Pole, Triviality, and Stability

Let us briefly elaborate further on the running of the renormalized coupling (3.24). We can rewrite it as

$$\lambda(\mu^2) = \frac{1}{\beta_{\lambda 1} \ln \dfrac{\Lambda^2_{\overline{\rm MS}}}{\mu^2}}, \tag{3.31}$$

where

$$\Lambda^2_{\overline{\rm MS}} = \mu_0^2 e^{\frac{1}{\beta_{\lambda 1}\lambda_0}}. \tag{3.32}$$

This form is very instructive for drawing physical conclusions. First, let us remark that instead of a dimensionless initial value λ_0 at μ_0^2, we have expressed $\lambda(\mu^2)$ with the help of a dimensional parameter $\Lambda_{\overline{\rm MS}}$. This is called *dimensional transmutation*. The value of $\Lambda_{\overline{\rm MS}}$ specifies the ECCP, so it is a renormalization-group-independent quantity.

We can also see that $\lambda(\mu^2)$ is a monotonically increasing function of μ^2. We have seen that the value of μ^2 is the typical energy scale of the system. At very high scale, we resolve the close neighborhood of the (pointlike) source of the Φ-field. If we move from higher scales (shorter distances) to lower scales (larger distances), the strength of the interaction decreases: this is the *screening effect* of the quantum fluctuations.

If we go with the scale to the UV cutoff Λ, then we reach the source of the Φ field as closely as is allowed in the regularized system. There the value of the coupling is the largest; it is the bare coupling $\lambda = \lambda_{ren}(\mu^2 = \Lambda^2)$. At every lower resolution, the value of the coupling is smaller.

Obviously, one cannot choose the maximal value of μ^2 arbitrarily large, because a pole will be hit at $\mu^2 = \Lambda^2_{\overline{\rm MS}}$ with a $\sim (\mu^2 - \Lambda^2_{\overline{\rm MS}})^{-1}$ divergence of the coupling. This singularity differs substantially from the divergences of the perturbation theory.

It is a physical effect, called the *Landau pole*. At the Landau pole, the quartic coupling changes sign. Since this coupling is the coefficient of the highest power in the potential, with this change the potential becomes unstable.

Assigning any finite value to the coupling at some μ^2 always leads to a Landau-pole singularity. The only scalar field theory in which we can choose arbitrary values of the scale is one in which $\Lambda_{\overline{\rm MS}} \to \infty$. This is, however, possible only by choosing $\lambda(\mu^2) = 0$ for every finite μ^2. One arrives at the conclusion that the Φ^4-theory is trivial: the only consistent Φ^4-theory from which the cutoff can be fully eliminated, extending in this way its validity to arbitrarily high momentum, is a free and noninteracting theory.

The perturbative input into the renormalization group equation assumes that λ is small. One might hope that its increase will necessitate the inclusion of further (higher) contributions into its beta function, altering the conclusion based on the leading-log approximation. However, nonperturbative studies in the four-dimensional theory have arrived at unchanged conclusions.

The present leading-order perturbative analysis repeats itself without any conceptual change for every field theory that has a beta function starting with a positive coefficient in front of some power of the coupling. This is the case for quantum electrodynamics but not quantum chromodynamics (QCD). In quantum electrodynamics, the charges are screened, which is consistent with the intuition based on classical arguments. In QCD, however, the screening effect of fermionic degrees of freedom is counterbalanced by the gluonic contribution, leading eventually to antiscreening.

3.5.3 Stability and Renormalization

The influence of the quantum fluctuations on the stability of the effective potential depends critically on the renormalization process. Considerable insight can be gained by studying the effect of the fermionic fluctuations coupled to a scalar with Yukawa coupling on the effective potential of the scalar field [5]. Let us consider the Euclidean model

$$L[\phi, \psi, \bar{\psi}] = \bar{\psi}(x)\partial\!\!\!/\psi(x) + \frac{1}{2}(\partial_m \phi(x))^2 + U(\rho = \phi^2/2) + h\phi(x)\bar{\psi}(x)\psi(x), \tag{3.33}$$

and

$$U(\rho) = m^2\rho + \frac{\lambda}{2}\rho^2. \tag{3.34}$$

Integrating over the Fermi field in a constant $\phi = v$ background, one obtains the following formal expression for the effective potential (one-loop contribution):

$$U_{eff}(\rho_0) = U(\rho_0) - \frac{1}{2V_d} \ln \frac{\det[-\Box + M^2]}{\det[-\Box]} = U(\rho_0) - 2 \int_p \ln \left(1 + \frac{M^2}{p^2}\right), \tag{3.35}$$

where $M^2 = 2h^2\rho_0$ and V_d is the d-dimensional quantization volume.

A sharp four-dimensional cutoff Λ is applied, and the integral can be done analytically:

$$U_{eff}(\rho_0) = U(\rho_0) - \frac{M^2\Lambda^2}{16\pi^2} + \frac{1}{16\pi^2}\left[M^4 \ln\left(1 + \frac{\Lambda^2}{M^2}\right) + \Lambda^4 \ln\left(1 + \frac{M^2}{\Lambda^2}\right)\right]. \tag{3.36}$$

One obtains the divergent pieces of the fermionic contribution by expanding it for large Λ^2/M^2:

$$-\frac{M^2\Lambda^2}{8\pi^2} + \frac{M^4}{16\pi^2} \ln \frac{\Lambda^2}{M^2} + \frac{M^4}{32\pi^2} + \mathcal{O}(M^2/\Lambda^2). \tag{3.37}$$

The conventional renormalization consists in canceling the divergent terms by separating appropriate divergent pieces from the bare parameters as follows:

$$m^2 = m_R^2 + \frac{h^2\Lambda^2}{4\pi^2}, \qquad \lambda = \lambda_R - \frac{h^4}{2\pi^2} \ln \frac{\Lambda^2}{\mu^2}. \tag{3.38}$$

Here in the argument of the logarithm, the squared mass m^2 is changed to the square of an arbitrary renormalization scale μ. After cancellation of the divergences, one obtains

$$U_{eff}(\rho_0, \mu) = m_R^2\rho_0 + \frac{\lambda_R}{2}\rho_0^2 - \frac{h^4}{16\pi^2}\rho_0^2 \ln \frac{2e^{-1/2}h^2\rho_0}{\mu^2} \tag{3.39}$$

for the finite and Λ-independent effective potential. It is obvious that for a sufficiently large value of ρ_0, the fermionic contribution destabilizes the renormalized potential.

However, if one keeps an arbitrary finite cutoff Λ, then using $\lambda = \lambda(\Lambda^2)$, but performing the mass renormalization as before, one writes, without expanding in powers of M^2/Λ^2,

$$U_{eff} = m_R^2\rho_0 + \frac{\lambda}{2}\rho_0^2 + \frac{1}{16\pi^2}\left[M^4 \ln\left(1 + \frac{\Lambda^2}{M^2}\right) + \Lambda^4\left(\frac{M^2}{\Lambda^2} - \ln\left(1 + \frac{M^2}{\Lambda^2}\right)\right)\right]. \tag{3.40}$$

The effect of the fermionic fluctuations is now positive definite without any sign of instability. The lesson is that no instability occurs by keeping the cutoff finite though arbitrarily high: if one uses positive values of $\lambda(\Lambda^2)$, one cannot cross over to the unstable regime.

We can also interpret this scenario in a different way: the instability of the potential reflects the fact that the one-loop correction to the coupling λ is larger than its tree-level value. This, in fact, signals a nonconvergent behavior of the perturbation theory. This situation begs for some resummation; up to the present order, one can envisage several possibilities. For example, we may assume that the asymptotics of the potential change from ρ_0^2 to $\kappa^\eta \rho_0^{2-\eta}$, where κ is some constant with mass-squared dimension. The value of η can be read off the requirement to reproduce (3.39) in an expansion in the powers of the small parameter η. Using $\kappa^\eta \rho_0^{2-\eta} \approx \rho_0^2 - \eta \rho_0^2 \ln \rho_0/\kappa$, we obtain

$$\eta = \frac{h^4}{8\pi^2 \lambda_R}, \qquad \kappa = \frac{\mu^2}{2e^{-1/2}h^2}, \tag{3.41}$$

where both quantities are finite positive numbers. Then we have

$$U_{eff}(\rho_0, \mu) = m_R^2 \rho_0 + \frac{\lambda_R}{2} \kappa^\eta \rho_0^{2-\eta}, \tag{3.42}$$

which is a stable potential. The consistency of this resummation can and should be checked against higher-order perturbative and nonperturbative calculations.

The two solutions of the stability problem are different, and they yield different potentials, too. However, both lead to stable potentials, and they differ from each other only at high values of ρ_0, where the perturbation theory is no longer reliable.

3.6 The Wilsonian Concept of Renormalization

The exploration of the universal scaling features at large distances of continuous phase transitions led L. Kadanoff to propose coarse graining of statistical models defined on regular lattices by applying block-spin transformations [6]. Wilson's generalization [7] of mapping a system with characteristic upper momentum scale Λ onto a system of lower maximal momentum k to continuum field theories is easiest to formulate in terms of Feynman's path integral:

$$\begin{aligned} Z[J] &= \mathcal{N} \int [\Pi_{q<\Lambda} d\phi(q)] e^{-S_E^\Lambda[\phi] + \int^\Lambda J_q \phi_q} \\ &= \mathcal{N} \int [\Pi_{q<k} d\phi(q)] \left\{ \int [\Pi_{k<q<\Lambda} d\phi(q)] e^{-S_E^\Lambda[\phi] + \int^\Lambda J_q \phi_q} \right\} \Big|_{J(q)=0, k<q<\Lambda} \\ &\equiv \mathcal{N}' \int [\Pi_{q<k} d\phi(q)] e^{-S_E^k[\phi] + \int^k J_q \phi_q}. \end{aligned} \tag{3.43}$$

Here S_E^k denotes the classical action of a Euclidean field theory depending on Fourier components with maximal wave number k. No restriction is put on the highest power of the fields allowed to appear in this action. All terms obeying the symmetry of the model can be present. Information concerning the microscopic action, valid at the highest momentum Λ, just provide the initial conditions for the gradual integration over the field components of lower and lower momenta.

The evolution of a local potential given initially as $U^\Lambda = \sum_{n=1}^{M} g_n^\Lambda \phi^n$ can be characterized by the mapping $g_n^k = g_n^k(\{g^\Lambda\})$, usually called a *renormalization group (RG) transformation*. Pictorially, it is represented as a trajectory in the coupling space, where each point corresponds to a theory potentially reachable via the subsequent scale transformations. Important points are the sinks and the sources, the fixed points where the theory is scale-invariant. If an initial theory is located near a fixed point, it might be attracted to it when the momentum scale is lowered. Such fixed points are called IR (infrared) points. If the theory is repelled away from the fixed point, then such a fixed point is of UV (ultraviolet) type. The direction(s) in the operator space along which the theory is repelled from a fixed point are called *relevant*; those along which it is attracted to the fixed point are classified as *irrelevant*. The Lagrangian for which one keeps only the relevant operators can be understood as an effective theory valid in a neighborhood of the fixed point.

A particularly important fixed point is the origin of the coupling space, which corresponds to a free massless theory. Perturbation theory deals with the dynamics of models defined in a neighborhood of this point. The coupling $\lambda(k^2)$ of the one-component scalar theory approaches this point with decreasing k. It moves away when one increases the maximum momentum scale, but it cannot be extended ad infinitum, because it reaches the Landau pole. On the other hand, with increasing momentum, QCD moves toward the origin (and moves away toward the infrared), which is a feature called asymptotic freedom.

The above brief characterization of the RG transformation is illustrated in Fig. 3.1, where a conjectured RG structure of quantum gravity is displayed in a two-

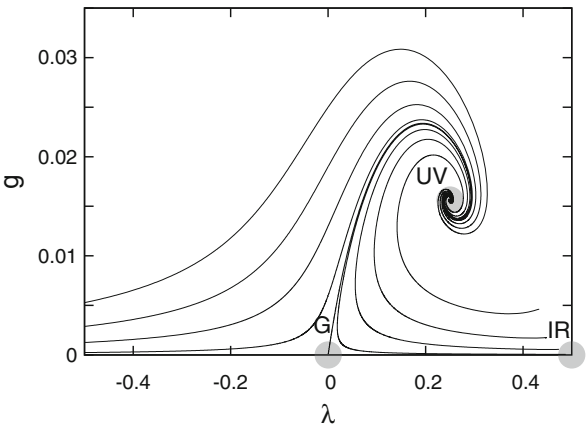

Fig. 3.1 Conjectured renormalization group trajectories of quantum gravity in the two-dimensional coupling space consisting of Newton's gravitational constant (g) and Einstein's cosmological constant (λ) (from [10])

dimensional coupling space, where in addition to Newton's gravitational constant (g), a scale-dependent cosmological constant (λ) is also included. It is well known that toward the ultraviolet, g is increasing, which is displayed by the (renormalized) trajectory starting from the origin and conjecturally ending in an ultraviolet stable fixed point (signaled by the inscription "UV"). Trajectories starting with nonzero λ are attracted to this trajectory. There is a third fixed point in the figure, which is IR-attractive and corresponds to the dominance of the cosmological constant term of the gravitational action at the largest distance scales.

The original scheme of the gradual integration, which used a sharp value for the maximal momentum, has been generalized by several authors. The most popular is the so-called Wetterich–Morris equation [8, 9], which is the easiest to implement for finding the $k = 0$ effective action dressed with the effect of quantum fluctuations at all wavelengths. A recent detailed pedagogical introduction can be consulted in [10].

The functional integration is restricted to the momentum range above some scale k by modifying the propagator of the field $\phi(k)$:

$$S_{free}[\phi] = \frac{1}{2}\int_q \phi(-q)\left(q^2 + m^2\right)\phi(q) \to \frac{1}{2}\int_q \phi(-q)\left(q^2 + m^2 + R_k(q)\right)\phi(q), \tag{3.44}$$

where the *infrared regulator* function $R_k(q)$ obeys the limiting behaviors

$$\lim_{q^2/k^2\to 0} R_k(q) > 0, \qquad \lim_{k^2/q^2\to 0} R_k(q) = 0. \tag{3.45}$$

The first feature "freezes" the IR fluctuations by increasing the inertia of the modes below the actual value of k. There is no change in the ultraviolet, and therefore, one effectively integrates layer by layer near the moving scale k. The most popular choice is the so-called linear regulator:

$$R_k(q) = (k^2 - q^2)\Theta(k^2 - q^2), \tag{3.46}$$

which for $k \to \Lambda$ blocks all quantum fluctuations. Different functional choices of R_k correspond to the freedom of choosing different renormalization schemes in perturbation theory.

The rate of change of the generating functional of the 1PI Feynman diagrams is solely due to the IR regulator function and is easily shown to obey the following equation ($t = \ln(k/\Lambda)$) [11]:

$$\partial_t W_k[J] = -\frac{1}{2}\int_x\int_y \partial_t R_k(x-y)\left(\frac{\delta^2 W[J]}{\delta J(x)\delta J(y)} + \frac{\delta W_k[J]}{\delta J(x)}\frac{\delta W_k[J]}{\delta J(y)}\right). \tag{3.47}$$

By the conventional Legendre transform of W_k, one obtains the functional equation describing the scale-dependence of the effective action Γ_k. The simplest form is

obtained for a slightly modified effective action defined as

$$\Gamma_k[\phi] = -W_k[J_\phi] + \int_q J_\phi(-q)\phi(q) - \frac{1}{2}\int_q \phi(-q)R_k(q)\phi(q), \tag{3.48}$$

which goes over to the conventional effective action when $k \to 0$. (The index ϕ associated with the source J reminds one that the specific J_ϕ appearing in this relation is just the source distribution needed to sustain the field configuration $\phi(x)$.) This effective action functional obeys the following equation:

$$\partial_t \Gamma_k[\phi] = \frac{1}{2}\mathrm{Tr}\left\{(\partial_t R_k)\left[\Gamma_k^{(2)} + R_k\right]^{-1}\right\}, \tag{3.49}$$

with the second functional derivative of $\Gamma_k[\Phi]$ appearing on the right-hand side. In integrating this equation from $k = \Lambda$ down to $k = 0$, the effective action picks up the effect of all quantum fluctuations and fully determines the infrared physics of the model. A similar, but less explicit, functional equation was proposed earlier by Polchinski [12].

The renormalization procedure in terms of the functional renormalization group (FRG) is equivalent to including gradually the effect of all quantum fluctuations into the effective action. Therefore, if one starts at $k = \Lambda$ with a stable theory, its stability is maintained toward the infrared. There is no question of "sending" Λ to infinity, and therefore no Landau singularity will arise. The procedure can be applied to any theory, even those that are not renormalizable perturbatively near the Gaussian fixed point. The only valid question is the sensitivity of the infrared physics to the initial value of the momentum Λ. In other words, one might question whether the value of the maximal momentum scale Λ belongs to the physical data set of the model.

References

1. I. Montvay, G. Münster, *Quantum Fields on a Lattice* (Cambridge University Press, Cambridge, 1994)
2. J.C. Collins, *Renormalization: An Introduction to Renormalization, the Renormalization Group and the Operator-Product Expansion* (Cambridge University Press, Cambridge, 1984)
3. C.G. Callan, Phys. Rev. D **12**, 1541 (1970)
4. K. Symanzik, Commun. Math. Phys. **18**, 27 (1970)
5. H. Gies, C. Gneiting, R. Sondenheimer, Phys. Rev. D **89**, 045012 (2014)
6. L.P. Kadanoff, Physics (N.Y.) **2**, 263 (1966)
7. K.G. Wilson, Rev. Mod. Phys. **55**, 583 (1983)
8. C. Wetterich, Phys. Lett. B **352**, 90 (1993)
9. T.R. Morris, Int. J. Mod. Phys. A **9**, 2411 (1994)
10. S. Nagy, Ann. Phys. **350**, 310 (2014)
11. J. Berges, N. Tetradis, C. Wetterich, Phys. Rep. **363**, 223 (2002)
12. J. Polchinski, Nucl. Phys. B **231**, 269 (1984)

Chapter 4
Optimized Perturbation Theory

In Chap. 3, we discussed how the different schemes belonging to the equivalence class of the same physics help us to resum the ultraviolet (UV) divergences coming from loop corrections, thus making it possible to define a consistent perturbation theory. The aim of this chapter is to present methods for improving the convergence properties of the perturbation theory. In particular, the influence of new energy scales appearing when one embeds a field theory into a specific environment might require critical analysis of the formal perturbation series, since infrared (IR) divergences might be generated by the new scale.

For speeding up the convergence of perturbation theory of specific observables, in particular avoiding IR sensitivity of the perturbation series, an adequate method is a rearrangement of the series, as suggested first by Stevenson [1]. Since then, it has been exploited abundantly in calculating cross sections, mass spectra, etc., in various models. The optimization of the renormalization group equations to incorporate environmental effects was first mentioned in [2].

The chapter begis with a discussion of the origin of IR singularities. It is followed by the presentation of the general optimization strategy and the question of the renormalizability of optimized series following the logic outlined in papers by Chiku and Hatsuda [3, 4]. At this stage, a *static* rearrangement of the perturbation series is realized, which means redefining the renormalized mass parameters and couplings in a momentum-independent manner. It will be introduced here through the example of the three-flavor linear sigma model of Chan and Haymaker [5]. Next, the detailed implementation of the strategy will be illustrated with the example of the one-component ϕ^4-theory. The version used for actual phenomenological investigations of the three-flavor quark–meson effective theory will be worked out at the level of the one-loop approximation. In the second half of the chapter, an enlarged perturbative framework will be introduced for situations in which a static resummation is not satisfactory, and a momentum-dependent resummation is

A. Jakovác, A. Patkós, *Resummation and Renormalization in Effective Theories of Particle Physics*, Lecture Notes in Physics 912,
DOI 10.1007/978-3-319-22620-0_4

needed. This is accomplished by the two-particle-irreducible (2PI) approximation, which is understood in our interpretation also as a specific example of resummation.

4.1 Infrared Divergences and Their Resummation

IR divergences, or IR sensitivity,[1] appear under the influence of new characteristic energy scales, determined usually by some external (environmental) effect such as the transferred momentum in a scattering process, the temperature in a finite temperature medium, or an external field. This implies that IR divergences are not universal, and therefore, the way they are treated cannot be universal either. Moreover, IR singularities might reflect a physical phenomenon such as the diverging correlation length at a second-order phase transition or the on-mass-shell singularity of a propagator.

There are two approaches to dealing with IR divergences. The first uses a fixed renormalization scheme such as $\overline{\text{MS}}$ and "discovers" within this scheme the occurrence of IR sensitive contributions. Then one attempts the identification of the source of the divergences at each order of perturbation theory, and eventually resums the sensitive terms. One must proceed carefully, however, in this case, since in order to maintain UV consistency, the corresponding counterterm diagrams should also be summed.

In the other approach, one makes use of the freedom of choosing an optimally selected representative of the perturbation theories belonging to the same equivalence class of constant physics, which is free of IR divergences. In practice, one first identifies the IR divergence occurring at some level of perturbation theory. Then one chooses an appropriate counterterm to cancel this IR divergent part, just as one does in the case of UV divergences. Finally, one should make sure that the perturbation theory defined with this extra subtraction belongs to the desired equivalence class by choosing the renormalized parameters appropriately. This can be achieved by fulfilling the renormalization prescriptions (as in the case of UV divergences) or comparing the expressions to some reference renormalization scheme or directly to the bare theory. It is important to emphasize that the countercouplings canceling the IR-sensitive effects will depend on the environmental parameters, since the perturbatively computed IR-sensitive terms themselves depend on external parameters.

Let us discuss the question of consistency of the described second procedure here in this introduction. One might ask whether by choosing an environmentally (temperature, external field, external momentum) dependent mass term, we spoil the consistency of perturbation theory. The criticism can be stated simply that one loses the universal nature of the UV renormalization by making use of a

[1] Often, IR problems appear only as enhanced contributions and not actual divergences. Nevertheless, we will call them "IR divergences."

counterterm $\sim m^2 \log \Lambda$, defined with m depending on the temperature. The answer is that the consistency of the perturbation theory does allow a choice among the representatives of the equivalence class of constant physics characterized by temperature (environment) dependence of the renormalized parameters. This does not mean that the divergences generated in perturbation theory (expressed through the bare parameters) are temperature-dependent, just as by choosing an external momentum (scale-)dependent coupling $g(p)$ we do not generate momentum-dependent counterterms. If the counterterms are proportional to the parameters of the renormalized Lagrangian, then the renormalized perturbation theory works consistently, irrespective of the chosen value of the renormalized parameters. The perturbation theory is truly inconsistent if terms like $\frac{1}{\varepsilon}\log p$ and $\frac{1}{\varepsilon}T$ are produced directly (independent of the renormalized couplings), but this is not the case for the renormalizable theories.

4.2 The Optimization Strategy and the Renormalizability of the Optimized Series

The general strategy of the optimized perturbation theory (OPT) will be described by means of the phenomenologically relevant example of the three-flavor linear sigma model (cf. Eq. (1.24)):

$$L(M) = \frac{1}{2}\mathrm{tr}(\partial_\mu M^\dagger \partial^\mu M - \mu^2 M^\dagger M) + f_1\left(\mathrm{tr}(M^\dagger M)\right)^2 + f_2 \mathrm{tr}(M^\dagger M)^2 + g\left(\det(M) + \det(M^\dagger)\right) + \epsilon_x \sigma_x + \epsilon_y \sigma_y + L_{ct}(\mu^2, f_1, f_2, g), \tag{4.1}$$

where the 3×3 matrix M is defined with the Gell-Mann matrices λ_i, $i = 1, \ldots, 8$ completed with a ninth generator normalized in the same way: $\mathrm{tr}\lambda^a\lambda^b = 2\delta^{ab}$. The ninth matrix is denoted by λ_0. Note the "wrong" sign of the mass parameter $-\mu^2$, which implies already at tree level the existence of a symmetry-breaking ground state. It is physically more transparent to perform a rotation in the "0-8"-plane and work with the nonstrange component $\sigma_x + i\pi_x$ and the strange component $\sigma_y + i\pi_y$ instead of $\sigma_8 + i\pi_8$ and $\sigma_0 + i\pi_0$. In terms of its components, the matrix M is expressed as

$$M = \frac{1}{\sqrt{2}}\sum_{i=1}^{7}(\sigma_i + i\pi_i)\lambda_i + \frac{1}{\sqrt{2}}\mathrm{diag}(\sigma_x + i\pi_x, \sigma_x + i\pi_x, \sqrt{2}(\sigma_y + i\pi_y)). \tag{4.2}$$

The Lagrangian density depends on μ^2, f_1, f_2, g, which are the renormalized coupling parameters, and ϵ_1, ϵ_2, which characterize the strength of the explicit symmetry-breaking. The counterterm Lagrangian L_{ct} depends on the

renormalized couplings and ensures the order-by-order finiteness of the perturbative computations.

The N-point functions on a scalar background $M_0 = \mathrm{diag}(x, x, \sqrt{2}y)$ can be derived from the effective quantum action defined symbolically as

$$\Gamma[M_0] = \delta \ln \int \mathscr{D}M \exp\Big\{-\frac{1}{\delta}\int d^4x \Big[L(M + M_0, \mu^2, f_1, f_2, g) + \epsilon_x(\sigma_x + x) + \epsilon_y(\sigma_y + y)\Big]\Big\}. \tag{4.3}$$

The parameter δ is introduced for bookkeeping the number of loops in the perturbative expansion. Therefore, it is considered a small parameter in the course of the loop expansion. On completing the computation at some finite m-loop level, one sets $\delta = 1$.

The general strategy of optimization begins with the splitting of the original renormalized couplings in an arbitrary way,

$$-\mu^2 = m^2 - \Delta m^2, \qquad f_i = \lambda_i - \Delta\lambda_i \quad (i = 1, 2), \qquad g = \gamma - \Delta\gamma, \tag{4.4}$$

and we assume that the difference between the original and the arbitrary new parameters is of higher loop order:

$$\Delta\lambda_i,\ \Delta\gamma, \Delta m^2 \sim \delta. \tag{4.5}$$

This means that the contributions proportional to these quantities appear at higher loop order than the contributions involving only m^2, λ_i, γ.

Since the splitting is arbitrary, no observable can depend on any of the newly introduced parameters in the exact solution of the theory:

$$\frac{\partial \mathscr{O}}{\partial m^2} = \frac{\partial \mathscr{O}}{\partial \lambda_i} = \frac{\partial \mathscr{O}}{\partial \gamma} = 0. \tag{4.6}$$

At any finite order, however, there might still appear a nontrivial dependence on these parameters. Then the preceding equations are understood as nontrivial optimization conditions. Actually, one is free to optimize the perturbative computation for each coupling with a different observable ($\mathscr{O}.$) and at a different level ($N.$) of the loop expansion:

$$\frac{\partial \mathscr{O}_m^{(N_m)}}{\partial m^2} = \frac{\partial \mathscr{O}_{\lambda_i}^{(N_{\lambda_i})}}{\partial \lambda_i} = \frac{\partial \mathscr{O}_\gamma^{(N_\gamma)}}{\partial \gamma} = 0. \tag{4.7}$$

These conditions represent the *principle of minimal sensitivity (PMS)*, which (if a solution exists) self-consistently determine the newly introduced parameters. Another version is the requirement not to produce any further correction at some

order $n.$ of the perturbation series (the principle of *fastest apparent convergence (FAC)*):

$$\mathscr{O}_{m,n_m} = \mathscr{O}_{\lambda_i,n_{\lambda_i}} = \mathscr{O}_{\gamma,n_\gamma} = 0. \tag{4.8}$$

In practical applications, one has at one's disposal only a limited perturbation series (mostly only the first quantum corrections to the tree-level expressions of the different observables). Below, the FAC conditions will be worked out for the 3-flavor linear sigma model. Before we proceed to it, a simple formal argument will be given for the renormalizability of the OPT valid for any model that is assumed to possess renormalizable series for the observables in terms of the conventional perturbation theory.

Let us consider the renormalized effective action determined in the conventional perturbation theory at coupling order n. It is the sum of contributions from several m-loop diagrams, up to the maximal n-loop contribution:

$$\Gamma_{R,n} = \sum_{m=0}^{n} \Gamma_R^{(m)}. \tag{4.9}$$

The renormalized m-loop contribution is the sum of a (divergent) term $\Gamma^{(m)}$ not containing any contribution from the counter-Lagrangian and a compensating term $C^{(m)}$ that makes it finite. Both of them can be expanded in terms of the renormalized couplings:

$$\Gamma_R^{(m)} = \sum_{l=0}^{\infty} (\mu^2)^l \sum_{t_i}^{t_1+t_2+t_3=n} f_1^{t_1} f_2^{t_2} g^{t_3} \left(\Gamma_{l,t_i}^{(m)} + C_{l,t_i}^{(m)} \right). \tag{4.10}$$

This equality expresses the renormalizability of the model in the framework of the conventional perturbation theory by stating that the sum of the two terms in the last bracket on the right-hand side is finite. The presence of infinite powers in the expansion in μ^2 is easy to accept when we take into account the way μ^2 appears in the propagators of various fields.

Now we substitute (4.4) and rearrange the sum (4.9), taking into account that each extra factor of Δm^2, $\Delta\lambda_i$, $\Delta\gamma$ increases the loop order. One can write, with the help of the binomial coefficients C_q^t, the following expression for the s-loop contribution to the nth-order effective action:

$$\begin{aligned} \Gamma_R^{(s)} = \sum_{l=0}^{\infty} \sum_{t_i}^{t_1+t_2+t_3=n} \sum_{q_i=0}^{t_i} \sum_{p=0}^{l} & C_{q_1}^{t_1} C_{q_2}^{t_2} C_{q_3}^{t_3} C_p^l (m^2)^{l-p} \lambda_1^{t_1-q_1} \lambda_2^{t_2-q_2} \gamma^{t_3-q_3} \\ & \times (-\Delta m^2)^p (-\Delta\lambda_1)^{q_1} (-\Delta\lambda_2)^{q_2} (-\delta\gamma)^{q_3} \left(\Gamma_{l,t_i}^{(s)} + C_{l,t_i}^{(s)} \right). \end{aligned} \tag{4.11}$$

If we count powers of δ, this expression contains terms of $s, s+1, s+2, \ldots$ loop order. If $s < l$, a subsum will contribute to the $(l < n)$-loop contribution of $\Gamma_{R,n}$. One has to choose from each $\Gamma_R^{(s)}$, $s = 0, 1, \ldots, n$, those terms for which the equality $s + p + q_1 + q_2 + q_3 = l$ is satisfied. Denoting the sum of these contributions by $\Gamma_R^{(s)}(\delta^l)$, one obtains the contributions to Γ_{R,δ^n}, which represents the series rearranged in powers of δ and complete up to power δ^n:

$$\Gamma_{R,\delta^n} = \sum_{s=0}^{n} \sum_{l=s}^{n} \Gamma_R^{(s)}(\delta^l). \tag{4.12}$$

Since the original expression was finite, this remains true also after the series has been rearranged, which proves the renormalizability of the optimized perturbation series.

If we think about all of this less formally, this statement is intuitively obvious, since the original procedure of the renormalization is completed before the optimization conditions are imposed. These conditions do not change by reshuffling the series and imposing the optimization conditions. Of course, there is no guarantee that one will find a physically reasonable solution for the corresponding self-consistent equations.

It should be emphasized also that if one has several renormalized parameters, which are usually fitted to some phenomenological information, then the number of observables for which optimization conditions are prescribed could be higher than the exact number of the couplings involved in the optimization (but less than the number of renormalized parameters to be fitted). Once the values of the couplings are determined with the help of this modified set of conditions, the phenomenological ("measured") values of the observables replaced in the fit by the extra optimization conditions can now be confronted with the "predictions" based on values found with the help of a larger number of optimization conditions. This attitude was taken in the phenomenologically motivated investigations of the three-flavor linear sigma model [6].

The above cumbersome expression for the terms of the optimized series becomes much more transparent if one applies only a partial procedure, for instance if only the mass parameter is optimized. Then for the rest of the couplings, one computes the expansion in terms of the original renormalized quantities. The introduction of an improved (optimized) mass parameter is almost unavoidable when models with spontaneous symmetry-breaking are investigated. In these models, the renormalized squared mass becomes negative, and in the perturbative treatment of the quantum fluctuations, tachyonic modes will show up, presenting an obstacle to the evaluation of some loop integrals. By optimizing the mass parameter, one can put aside this difficulty. The example of the ϕ^4-theory serves as a detailed illustration for the mass optimization; it will be discussed in the next section.

4.3 OPT for the ϕ^4-Theory

The OPT strategy will be illustrated using the example of mass-parameter optimization [7]. The reorganization of the perturbation series is based on the following rearrangement of the Lagrangian density:

$$\begin{aligned} L[\phi_B, m_B^2, \lambda_B] &= \frac{1+\delta Z}{2}(\partial_m \phi_B)^2 + \frac{m^2+\delta m^2}{2}\phi_B^2 + \frac{\lambda+\delta\lambda}{24}\phi_B^4 \\ &= \frac{1+\delta Z}{2}(\partial_m \phi_B)^2 + \frac{m^2+\Delta M^2}{2}\phi_B^2 + \frac{\lambda+\delta\lambda}{24}\phi_B^4 \\ &+ \left(\frac{-\Delta M^2+\delta m^2+\delta M^2}{2}\phi_B^2\right) + \left(-\frac{\delta M^2}{2}\phi_B^2\right). \end{aligned} \tag{4.13}$$

In the spirit of the discussion in the previous section, one assumes that the countercouplings $\delta m^2, \delta\lambda$ are known as Taylor series in the renormalized couplings (m^2, λ) to all orders from the condition of canceling the divergences showing up in subsequent orders of the conventional perturbation theory. In an OPT computation, the mass parameter $M^2 = m^2 + \Delta M^2$ is used in the perturbative propagators. The effective counterterm is written in the last line of the equation. In the first set of brackets, in addition to the combination $-\Delta M^2 + \delta m^2$, a third term, also δM^2, appears. It will be determined by requiring the finiteness of the one-loop contribution calculated with optimized mass parameter. The last term has to be taken into account only at the two-loop level.

The one-loop expression of the self-energy reads as

$$\Sigma_{1-loop} = M^2 + \frac{\lambda}{2}\mathscr{T}(M^2) - \Delta M^2 + \delta m_1^2 + \delta M_1^2, \tag{4.14}$$

where the lower index "1" refers to the loop level of the actual calculation. The expressions of the $T = 0$ tadpole integral and of the conventional 1-loop countermass calculated with the help of an ϵ-expansion in dimension $d = 4 - \epsilon$ are the following (see Eq. (B.6) in the appendix):

$$\begin{aligned} (tadpole) = \mathscr{T}(M^2) &= \frac{M^2}{16\pi^2}\left[-\frac{1}{\epsilon} + \gamma_E - 1 + \ln\frac{M^2}{4\pi\mu^2}\right], \\ \delta m_1^2 &= -m^2\frac{\lambda}{32\pi^2}\left[-\frac{1}{\epsilon} + \gamma_E - 1 - \ln(4\pi)\right]. \end{aligned} \tag{4.15}$$

Clearly, the divergences of these two terms would cancel each other if there were no mass optimization. Now it is the "duty" of the intermediate 1-loop counterterm

δM_1^2 to eliminate the mismatch:

$$\delta M_1^2 = -\Delta M^2 \frac{\lambda}{32\pi^2}\left[-\frac{1}{\epsilon} + \gamma_E - 1 - \ln(4\pi)\right]. \tag{4.16}$$

If ΔM^2 (note that its value is not fixed, since no optimization requirement yet applies) depended on the environment (it would be proportional to T^2 in case of the thermal mass), then the result after its subtraction would change arbitrarily with changing environment (temperature), which would endanger the comparability of results obtained, for instance, at different temperatures. This danger can be eliminated if the renormalized couplings and also the counterterms are related to quantities defined in a unique environment-independent renormalization scheme (more explicit discussion follows below).

Now the question is whether this conveniently chosen counterterm (the last term of the rearranged Lagrangian (4.13)) cancels in the next loop order. The Feynman diagrams contributing at two-loop order appear in Fig. 4.1. Denoting the contributions by names with direct reference to the corresponding Feynman diagrams, one can write

$$\begin{aligned}\Sigma_{2-loop} = &\frac{\lambda^2}{4} \times (double - scoop) + \frac{\lambda^2}{6} \times (setsun) \\ &+ \frac{\lambda}{2} \times (mass - insertion) + \frac{\delta\lambda_1}{2} \times (tadpole) \\ &- \delta Z_2 p^2 + \delta m_2^2 - \delta M_1^2 + \delta M_2^2.\end{aligned} \tag{4.17}$$

In the first line, one writes the unrenormalized two-loop contributions. In the second line, the contribution arising from inserting the effective one-loop mass counterterm on a tadpole appears together with the one-loop self-coupling counterterm contribution. In the third line, the first two terms are known from the conventional perturbation series. The third one was determined at one loop of the perturbation theory with shifted mass, and now has to be compensated. The last term is again determined by the requirement of canceling fully any remaining mass divergence at the two-loop level.

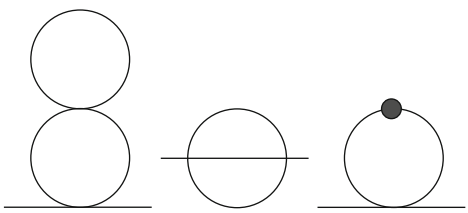

Fig. 4.1 Feynman diagrams contributing to the self-energy at the two-loop level, called "doublescoop," "setsun," and "mass-insertion," respectively

The contributions from the new diagrams are calculated with the dimensional regularization in $d = 4 - \varepsilon$ and have the following expressions:

$$
\begin{aligned}
(mass - insertion) &= \left(\Delta M^2 + \delta m_1^2 + \Delta M_1^2\right) \\
&\quad \times \left[\frac{1}{16\pi^2}\left(-\frac{1}{\epsilon} + \gamma_E + \ln\frac{M^2}{4\pi\mu^2}\right) + I^F_{mass-ins}\right] \\
(sunset) &= \frac{3M^2}{(4\pi)^4}\left[\frac{1}{2\epsilon^2} - \frac{1}{\epsilon}\left(\gamma_E - \frac{3}{2} + \ln\frac{M^2}{4\pi\mu^2}\right)\right] \\
&\quad - \frac{p^2}{4(4\pi)^4}\frac{1}{\epsilon} - \frac{3}{16\pi^2}\mathscr{T}(M^2)\frac{1}{\epsilon} + I^F_{sunset}, \\
(double - scoop) &= \frac{M^2}{(4\pi)^4}\left[\frac{1}{\epsilon^2} - \frac{1}{\epsilon}\left(2\gamma_E - 1 + 2\ln\frac{M^2}{4\pi\mu^2}\right)\right] \\
&\quad - \frac{1}{16\pi^2}\frac{1}{\epsilon}\left(\mathscr{T}^F(M) + M^2 I^F_{mass-ins}\right) + I^F_{double-scoop}.
\end{aligned}
\tag{4.18}
$$

Only the divergent parts are needed in explicit form; the finite parts are denoted below by $I^F_{mass-ins}, I^F_{setsun}, I^F_{double-scoop}$, respectively. The conventional two-loop level counterterm contributions to the countercouplings are the following:

$$
\begin{aligned}
\delta m_2^2 &= m^2\frac{\lambda^2}{2(4\pi)^4}\left(\frac{1}{\epsilon^2} - \frac{1}{\epsilon}\left(1 - \ln(4\pi)\right)\right) + \text{finite} \\
\delta\lambda_1 &= -\frac{3\lambda^2}{32\pi^2}\left(-\frac{1}{\epsilon} + \gamma_E - \ln(4\pi)\right), \qquad \delta Z_2 = \frac{1}{4(4\pi)^4}\frac{1}{\epsilon}.
\end{aligned}
\tag{4.19}
$$

Substitution into (4.17) leads to the following remainder in the divergent contributions:

$$
\Sigma_{2,div} = -\Delta M^2\frac{\lambda^2}{2(4\pi)^4}\left(\frac{1}{\epsilon^2} - \frac{1}{\epsilon}\left(1 - \ln(4\pi)\right)\right) + \delta M_2^2. \tag{4.20}
$$

The cancellation of this remainder leads to the determination of δM_2^2:

$$
\delta M_2^2 = \Delta M^2\frac{\lambda^2}{2(4\pi)^4}\left(\frac{1}{\epsilon^2} - \frac{1}{\epsilon}\left(1 - \ln(4\pi)\right)\right) + \text{finite}. \tag{4.21}
$$

Comparing with the expression of δm_2^2, one recognizes that it is the same expression except that the substitution $m^2 \to \Delta M^2$ was made (the arbitrary finite piece is conveniently added to ensure the coincidence). This remark was first made in [8].

The results of the first two loop orders is generalized with the following conjecture: *The series expansion of the complementary counterterm δM^2 coincides*

with the series of $\delta m^2 = z_m m^2$ computed in the conventional perturbation series. The only change is the replacement $m^2 \to \Delta M^2$, resulting in $\delta M^2 = z_m \Delta M^2$.

The conjecture can be verified based on the following arguments. At some loop order l, any diagram $\mathscr{D}(M^2)$ whose subdivergences were already renormalized will contribute an overall divergence proportional to M^2 whose coefficient is $\partial_{M^2}\mathscr{D}_{div}$. This quantity itself does not depend on M^2; it is the same divergence that would be produced if the diagram were computed with the original mass parameter m^2. These divergences add together into $-z_m^{(l)} M^2$, the negative of the original mass renormalization factor. In the modified perturbation theory, at this loop order one has by the above conjecture the shifted mass counterterm: $\delta m_l^2 + \delta M_l^2 = z_m^{(l)} M^2$, canceling the sum of the overall divergences.

Another type of divergence appears from the diagrams of the previous perturbative order, on one of the internal lines of which a new mass insertion is applied. If the coupling $-\Delta M^2$ is put on any internal propagator D, it introduces into the contribution of the corresponding diagram the replacement $D \to -\Delta M^2 \times D^2$. But this is just the result of the action of ∂_{M^2} on the diagram multiplied this time by $-\Delta M^2$. The sum equals $-\Delta M^2 z_m^{(l)}$, and this is what will be canceled at l-loop order by the supplementary counterterm δM_l^2.

No optimization condition was imposed at this stage in order to make it clear that the order-by-order renormalizability of the theory in terms of the rearranged perturbation series is a feature independent of this requirement. Therefore, the feature of renormalizability is valid for any choice of ΔM^2. Now one can return to the 1-loop term of the renormalized self-energy computed with shifted mass term and require that it remain at its tree-level value:

$$\Sigma_{1-loop} = M^2 + \frac{\lambda}{2}\mathscr{T}^F(M^2) - \Delta M^2 = M^2. \tag{4.22}$$

This FAC condition produces the gap equation determining the optimal ΔM^2.

4.4 Optimization and Renormalization Schemes

After this carefully detailed analysis, it is instructive to see in a most direct way an algorithm for designing optimized estimates at one-loop order for both the 2-point and the 4-point couplings: m^2, λ.

The one-loop expression of the effective potential computed with $M^2 = m^2 + \lambda v^2/2$ (the squared mass on the background v) is the following:

$$V = \frac{1}{2}m^2 v^2 + \frac{\lambda}{24}v^4 + \Delta V_{1-loop}(M^2) + \frac{1}{2}\delta m^2 v^2 + \frac{\delta\lambda}{24}v^4, \tag{4.23}$$

where ΔV_{1-loop} comes from (2.176) at zero and from (2.177) at high temperature. It gives for the second and fourth derivatives the following expressions:

$$\frac{d^2V}{dv^2} = M^2 + \delta m^2 + \frac{\delta\lambda}{2}v^2 + \lambda\Delta V'_{1-loop}(M^2) + \lambda^2 v^2 \Delta V''_{1-loop}(M^2),$$
$$\frac{d^4V}{dv^4} = \lambda + \delta\lambda + 3\lambda^2\Delta V''_{1-loop}(M^2) + \mathcal{O}(\lambda^3 v^2). \tag{4.24}$$

The FAC condition for λ requires the $\mathcal{O}(\lambda^2)$ quantum correction to vanish (the correction to the tree-level value is pulled down to $\mathcal{O}(\lambda^3)$),

$$\frac{d^4V}{dv^4} = \lambda + \mathcal{O}(\lambda^3 v^2) \quad \leftrightarrow \quad \delta\lambda = -3\lambda^2\Delta V''(M^2), \tag{4.25}$$

which is used in turn in the optimization condition of M^2:

$$\frac{d^2V}{dv^2} = M^2 \quad \leftrightarrow \quad \delta m^2 = -\lambda\Delta V'_{1-loop}(M^2) + \frac{1}{2}\lambda^2 v^2 \Delta V''_{1-loop}(M^2). \tag{4.26}$$

What was done here was to choose specific finite parts of the counterterms; i.e., we have chosen the renormalization scheme. Since both countercouplings depend on the background, we have a specific optimized scheme for each background value. We have still to ensure that all these schemes belong to the same equivalence class of constant physics. Here we solve this problem by comparison to a common "reference" renormalization scheme, for instance the $\overline{\rm MS}$ scheme, where the renormalized 2- and 4-point couplings are obtained by simply subtracting the divergent parts of the respectively contributing quantum expressions:

$$\delta\lambda_{\overline{MS}} = -3\lambda^2\Delta V''_{1-loop}(M^2)\big|_{div},$$
$$\delta m^2_{\overline{MS}} = -\lambda\Delta V'_{1-loop}(M^2)\big|_{div} + \frac{1}{2}\lambda^2 v^2 \Delta V''_{1-loop}(M^2)\big|_{div}. \tag{4.27}$$

Since the bare couplings are the same, ($m^2 + \delta m^2 = m^2_{\overline{MS}} + \delta m^2_{\overline{MS}}$), and the same kind of invariance is valid also for λ_B, one obtains

$$\lambda - \lambda_{\overline{MS}} = 3\lambda^2\Delta V''_{\overline{MS}}(M^2), \qquad m^2 - m^2_{\overline{MS}} = \lambda\Delta V'_{\overline{MS}}(M^2) - \frac{1}{2}\lambda^2 v^2 \Delta V''_{\overline{MS}}(M^2), \tag{4.28}$$

where $\Delta V_{\overline{\rm MS}} = \Delta V_{1-loop} - \Delta V_{1-loop}|_{div}$.

We see that the renormalized parameters of the optimized scheme belonging to the same equivalence class of constant physics depend on the background, and they contain all powers of couplings defined in the reference $\overline{\rm MS}$ scheme. Therefore, from the point of view of the reference scheme, the result is nonperturbative. It can be obtained only after the resummation of an infinite set of Feynman diagrams.

For this reason, one can baptize these particular renormalization schemes *RS, or resummation schemes*.

So far, we have done "full optimization," i.e., we required that no corrections whatsoever come to certain quantities. With a somewhat more moderate attitude, one can perform only a partial optimization. A typical example for that is to take into account only the leading temperature effect in the one-loop mass correction (see Chap. 6). This leads to the following definition of the optimized mass:

$$M^2 = m^2_{\overline{\rm MS}} + \frac{\lambda}{24} T^2, \tag{4.29}$$

while the coupling λ is the same as in $\overline{\rm MS}$. This is the thermal mass approximation, and it nicely catches several important physical effects, such as the continuous restoration of symmetry with increasing temperature from a low-temperature spontaneous symmetry-breaking ground state.

In fact, if $m^2_{\overline{\rm MS}} < 0$, then the classical $T = 0$ effective potential exhibits a minimum at a finite value of v:

$$V'(v_0) = 0 \quad \Rightarrow \quad v_0 = -\frac{6 m^2_{\overline{\rm MS}}}{\lambda}. \tag{4.30}$$

With the mass optimization of (4.29), $m^2_{\overline{\rm MS}}$ is replaced by M^2, and we obtain that at

$$T_c^2 = \frac{-24 m^2_{\overline{\rm MS}}}{\lambda}, \tag{4.31}$$

the optimized mass is zero, signaling a second-order phase transition. For $T > T_c$, the value of the squared mass turns into the positive range, and one recovers the symmetric phase.

Let us remark that one can arrive at the thermal mass using the $\overline{\rm MS}$ scheme without optimization, directly resumming an infinite series of diagrams. It turns out (see Chap. 6) that the relevant diagrams are the *daisy diagrams*, where each propagator line is decorated by a sequence of tadpole diagrams following each other like petals of a daisy and the leading-temperature contribution from each tadpole corrects multiplicatively the expression of the propagator.

The compensation of the $T = 0$ wrong sign mass by a perturbatively first-order mass correction $\sim \lambda T^2$ is of dubious validity. The implementation of the full optimization relation (4.28) might ensure the optimal convergence of the perturbation series and at the same time also revise the false conclusion of first-order symmetry-restoring transition drawn from the daisy resummation (see (6.41)). The application of this step is equivalent to the so-called super-daisy resummation.

Let us return therefore to (4.28). It is easier to solve these equations using the high-temperature expansion of the integrals contributing to the derivatives of the potential. Moreover, we substitute on the right-hand side of the first (λ) equation by

$\lambda\lambda_{\overline{\rm MS}} + \mathcal{O}(\lambda^3)$, and omit the corrections. Then we find at high temperatures,

$$\lambda = \frac{\lambda_{\overline{\rm MS}}}{1 - \frac{3\lambda_{\overline{\rm MS}}}{32\pi^2}\log\frac{c_+^2 T^2}{4\pi\mu^2} + \frac{\lambda_{\overline{\rm MS}} T}{16\pi M}}, \qquad m^2 = \sqrt{U^2 + W^2} - W, \tag{4.32}$$

where

$$U = \frac{1}{\kappa}\left[m^2_{\overline{\rm MS}} + \frac{\lambda_{\overline{\rm MS}} T^2}{24} + \frac{\lambda^2_{\overline{\rm MS}} v^2}{64\pi^2}\right], \qquad W = \frac{\lambda_{\overline{\rm MS}} T}{16\pi\kappa}, \tag{4.33}$$

and $\kappa = 1 - \frac{\lambda_{\overline{\rm MS}}}{32\pi^2}\log\frac{c_+^2 T^2}{4\pi\mu^2}$. Here c_+ is a constant defined in (B.24). For the scale-dependence of these equations, we can recover the solution of the renormalization group equations, cf. (3.24), but the complete expressions have additional terms. Near T_c given in (4.31) and at $v = 0$, the mass will satisfy $M^2 = m^2 \approx 0$, and then other types of behavior will be dominant. In this regime, we obtain the following (tri)critical behavior:

$$m = \frac{2\pi}{3}(T - T_c), \qquad \lambda = \frac{16\pi m}{T_c}. \tag{4.34}$$

This means that the second and fourth derivatives change sign simultaneously. We have to admit that this is still not the correct Wilson–Fisher critical point of the one-component real field. in this approximation, we rather obtain the $O(N)$ critical exponents valid for $N \to \infty$.

Several variants of the OPT have been proposed and used in computing the thermodynamic characterization of various model field theories (for a recent rediscovery, see [9]). In the next section, the lowest-order mass parameter optimization is worked out in a model that was successfully applied to the study of the phase structure of strongly interacting matter.

4.5 Optimized Perturbation Theory for the $SU(3)_L \times SU(3)_R$ Symmetric Meson Model

The propagators of the scalar and pseudoscalar mesons are computed at the one-loop level for the model (4.1) [6, 10]. Only the squared mass parameter $-\mu^2$ is replaced by m^2, to be found from the FAC condition imposed on the pion and kaon propagators. Additional equations will be invoked to determine all seven free parameters of the model. The mass of the heavier pseudoscalar mesons in the η-sector and all scalar mesons are predicted once these parameters are fixed.

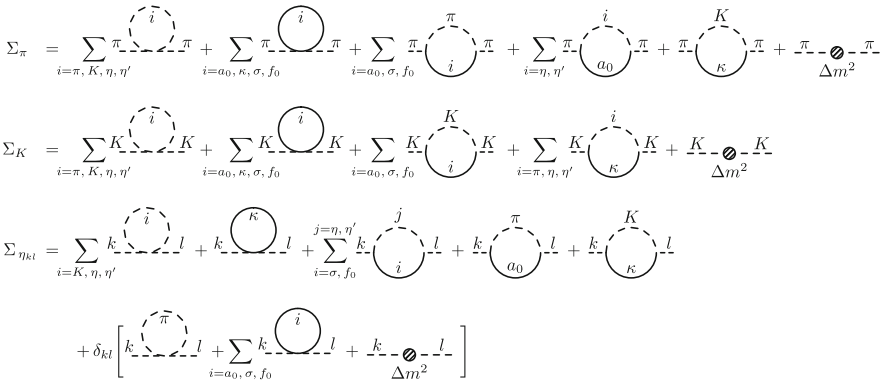

Fig. 4.2 Diagrams contributing to the self-energies of the π, K, η fields at one-loop. The fields propagating on the internal *lines* have tree-level masses. The last diagram in each *line* corresponds to taking into account the "optimizing counterterm" Δm^2 (from [6])

The propagators of the pion and the kaon are parameterized as

$$D_\pi(p)^{-1} = Z_\pi(p^2 + m_\pi^2 + \Sigma_\pi^F(p^2, m_i, \kappa)),$$
$$D_K(p)^{-1} = Z_K(p^2 + m_K^2 + \Sigma_K^F(p^2, m_i, \kappa)), \tag{4.35}$$

where m_π^2 and m_K^2 are the tree-level masses computed with the optimally chosen mass parameter m^2:

$$m_\pi^2 = m^2 + 2(2f_1 + f_2)x^2 + 4f_1y^2 + 2gy,$$
$$m_K^2 = m^2 + 2(2f_1 + f_2)(x^2 + y^2) + 2f_2y^2 - \sqrt{2}x(2f_2y - g). \tag{4.36}$$

The self-energies contain the loop contributions depicted in Fig. 4.2 (κ is the renormalization momentum scale, m_i is the set of masses of the fields π_i, σ_i, which couple via the three-point vertex to either π or K in the bubble integral). The self-energies are renormalized by including appropriate tree-level contributions from the counterterm Lagrangian:

$$L_{ct}(M) = -\frac{1}{2}\delta\mu^2 \mathrm{tr}(M^\dagger M) + \delta f_1 \left(\mathrm{tr}(M^\dagger M)\right)^2 + \delta f_2 \mathrm{tr}(M^\dagger M)^2$$
$$+ \delta g \left(\det(M) + \det(M^\dagger)\right), \tag{4.37}$$

with

$$\delta\mu^2 = \tfrac{1}{\pi^2}(5f_1 + 3f_2)\left(\Lambda^2 + m^2 \ln\tfrac{\Lambda^2}{\kappa^2}\right) - \tfrac{g^2}{\pi^2}\ln\tfrac{\Lambda^2}{\kappa^2},$$
$$\delta f_1 = -\tfrac{1}{2\pi^2}(13f_1^2 + 12f_1f_2 + 3f_2^2)\ln\tfrac{\Lambda^2}{\kappa^2}, \qquad \delta f_2 = -\tfrac{1}{\pi^2}(3f_1f_2 + 3f_2^2)\ln\tfrac{\Lambda^2}{\kappa^2},$$
$$\delta g = \tfrac{1}{2\pi^2}3g(f_2 - f_1)\ln\tfrac{\Lambda^2}{\kappa^2}. \tag{4.38}$$

The replacement $-\mu^2 \to m^2$ is reflected only in the divergence of the tadpole. This counter-Lagrangian cancels the divergences of the tadpoles and the bubble integrals.

The FAC conditions reduce the form (4.35) of the pion and kaon propagators to their optimized tree-level form:

$$D_\pi(p) = \frac{1}{p^2 + m_\pi^2}, \qquad D_K(p) = \frac{1}{p^2 + m_K^2}, \tag{4.39}$$

which is ensured partly by an appropriate choice of Z_π and Z_K. Both the pion and the kaon self-energies are expanded up to terms linear in $p^2 + m_{pole}^2$ around the respective squared pole masses:

$$\begin{aligned}
\Sigma_\pi^F(p^2, m_i, \kappa) &\approx \Sigma_\pi^F(-m_\pi^2, m_i, \kappa) + \frac{\partial \Sigma_\pi^F}{\partial p^2}\Big|_{-m_\pi^2}(p^2 + m_\pi^2), \\
\Sigma_K^F(p^2, m_i, \kappa) &\approx \Sigma_K^F(-m_K^2, m_i, \kappa) + \frac{\partial \Sigma_K^F}{\partial p^2}\Big|_{-m_K^2}(p^2 + m_K^2).
\end{aligned} \tag{4.40}$$

Choosing the finite wave function renormalisation coefficients as

$$Z_\pi^{-1} = 1 + \frac{\partial \Sigma_\pi^F}{\partial p^2}\Big|_{-m_\pi^2}, \qquad Z_K^{-1} = 1 + \frac{\partial \Sigma_K^F}{\partial p^2}\Big|_{-m_K^2}. \tag{4.41}$$

The expressions of the inverse propagators corresponding to Fig. 4.2 change to

$$\begin{aligned}
D_\pi(p)^{-1} &= p^2 + m_\pi^2 + Z_\pi \Sigma_\pi^F(-m_\pi^2, m_i, \kappa), \\
D_K(p)^{-1} &= p^2 + m_K^2 + Z_K \Sigma_K^F(-m_K^2, m_i, \kappa).
\end{aligned} \tag{4.42}$$

The second step in imposing the optimization conditions is to require the vanishing of the one-loop contribution to the masses of the pion and the kaon, which leads to the following two equations:

$$0 = Z_\pi \Sigma_\pi^F(-m_\pi^2, m_i, \kappa) = Z_K \Sigma_K^F(-m_K^2, m_i, \kappa). \tag{4.43}$$

These equations are written more explicitly by separating the true one-loop contributions and the result of the optimizing mass shift:

$$\begin{aligned}
Z_\pi \Sigma_\pi^F(-m_\pi^2, m_i, \kappa) &= Z_\pi \Sigma_\pi^{(1-loop)F}(-m_\pi^2, m_i, \kappa) - m^2 - \mu^2 = 0, \\
Z_K \Sigma_K^F(-m_K^2, m_i, \kappa) &= Z_K \Sigma_K^{(1-loop)F}(-m_K^2, m_i, \kappa) - m^2 - \mu^2 = 0.
\end{aligned} \tag{4.44}$$

The optimization conditions take explicitly the form of self-consistent equations for the pion/kaon masses when one uses the tree-level mass expressions of the pion and the kaon to express m^2 and substitute the respective expressions into the FAC

condition (4.44):

$$\begin{aligned} m_K^2 &= -\mu^2 + 2(2f_1 + f_2)(x^2 + y^2) + 2f_2 y^2 - \sqrt{2}x(2f_2 y - g) \\ &\quad + Z_K \Sigma_K^{(1-loop)F}(-m_K^2, m_i(m_K), \kappa), \\ m_\pi^2 &= -\mu^2 + 2(2f_1 + f_2)x^2 + 4f_1 y^2 + 2gy \\ &\quad + Z_\pi \Sigma_\pi^{(1-loop)F}(-m_\pi^2, m_i(m_\pi), \kappa). \end{aligned} \tag{4.45}$$

The masses of all other mesons appearing in the one-loop contributions to the self-energies are computed at tree level with m^2. (The explicit expression for the remaining pseudoscalars will be given below; the masses of the scalar excitations are not listed here.) However, m^2 should be expressed everywhere with the help of either the pion or the kaon mass from (4.36), depending on which of the self-consistent equations is under consideration.

These one-loop level self-consistent equations display very much the same structure as the leading-order large-N gap equation of the $O(N)$-model, which determines the mass of the Goldstone excitation.

The determination of the coupling parameters $\mu^2, f_1, f_2, g, \epsilon_x, \epsilon_y, m^2$ and the values of the condensates x, y needs five more equations beyond the four equations expressing the FAC condition for the pion and the kaon propagators. In the meson mass spectra, one has reliable information in the pseudoscalar $\eta - \eta'$ sector. At the one-loop level, the 2×2 matrix describing the mixing spectra (choosing the x, y coordinates in place of the 0, 8-components) is the following:

$$\mathscr{D}_\eta^{-1}(k) = \begin{pmatrix} p^2 + m_{\eta_{xx}}^2 + \Sigma_{\eta_{xx}}^F(k, m_i, \kappa) & m_{\eta_{xy}}^2 + \Sigma_{\eta_{xy}}^F(k, m_i, \kappa) \\ m_{\eta_{xy}}^2 + \Sigma_{\eta_{xy}}^F(k, m_i, \kappa) & p^2 + m_{\eta_{yy}}^2 + \Sigma_{\eta_{yy}}^F(k, m_i, \kappa) \end{pmatrix}, \tag{4.46}$$

with the tree-level entries

$$\begin{aligned} m_{\eta_{xx}}^2 &= m^2 + 2(2f_1 + f_2)x^2 + 4f_1 y^2 - 2gy, \\ m_{\eta_{yy}}^2 &= m^2 + 4f_1 x^2 + 4(f_1 + f_2)y^2, \\ m_{\eta_{xy}}^2 &= -2gx, \end{aligned} \tag{4.47}$$

and the one-loop self-energy components calculable by the Feynman diagrams of Fig. 4.2. The roots $-p^2 = M_\eta^2, M_{\eta'}^2$ of the determinant of this matrix can be used in the fit. Actually, one selects only the lighter one of them.

In addition to the pseudoscalar mass spectra, one can exploit the Ward identities of the model, which relate the condensates to specific combinations of the inverse

propagators at vanishing momentum:

$$\epsilon_x = Z_\pi^{-1} D_\pi^{-1}(0) x, \qquad \epsilon_y = Z_K^{-1} D_K^{-1}(0) \left(\frac{x}{\sqrt{2}} + y \right) - Z_\pi^{-1} D_\pi^{-1}(0) \frac{x}{\sqrt{2}}. \tag{4.48}$$

As an external source of information, one also invokes the PCAC relations, which relate the strength of explicit symmetry-breaking to the weak decay amplitudes f_π, f_K of the pion and the kaon:

$$\epsilon_x = Z_\pi^{-1/2} f_\pi M_\pi^2, \qquad \epsilon_y = \sqrt{2} Z_K^{-1/2} f_K M_K^2 - \frac{1}{\sqrt{2}} Z_\pi^{-1/2} f_\pi M_\pi^2. \tag{4.49}$$

Here the capital letters M_K, M_π are used for the physical mass values of the pion and kaon. These values are substituted everywhere in the above equations for m_π, m_K.

The fitting procedure begins by expressing μ^2 from the gap equation of the pion (the second equation of (4.45)) and g from the tree-level mass expression of the kaon rewritten with the help of the pion mass:

$$m_K^2 = m_\pi^2 - \sqrt{2}\,(g - 2 f_2 y)\,(\sqrt{2} y - x). \tag{4.50}$$

These expressions are used for finding the values of f_1, f_2, x, y by solving numerically the set of nonlinear equations consisting of the gap equation of the kaon (the first equation of (4.45)), the mass formula for the smaller mass in the η–η'-sector, and the combined Ward identities (4.48) and PCAC-relations (4.49) from which ϵ_x, ϵ_y was eliminated. Finally, the external fields ϵ_x, ϵ_y are extracted from the PCAC relations after the finite wave-function renormalization factors have been evaluated.

The couplings and also the masses are actually functions of the renormalization scale κ. The sensitivity of the renormalized couplings to κ is natural, since they do not represent physical observables. The sensitivity to κ is a consequence of the finite perturbative order of the calculation. One can plot the dependence of the order parameters of the chiral symmetry-breaking and of the one-loop estimate for the heavier eigenvalue in the $\eta - \eta'$ sector, and choose a range of κ values where this dependence is minimal.

It is important to note that the procedure described above does not rely on any data from the scalar meson sector, contrary to a typical feature of the tree-level or other perturbative determinations of the meson spectra. In this way, one avoids a major source of systematic inaccuracy because of the uncertain experimental situation in the scalar sector. The common experience is that the fully predicted scalar spectrum is rather insensitive to κ.

A detailed presentation of the $T \neq 0$ phenomenology based on this model can be found in Chap. 7.

4.6 OPT for the Three-Flavor Quark–Meson Model

The completion of (4.1) by a density accounting for the interaction of the constituent quarks with the mesons is achieved by adding to it

$$\begin{aligned} L_Q &= \bar{q}^a(x)(\gamma_m \partial_m \delta^{ab} - g_F M_5^{ab}(x))q^b(x), \\ M_5^{ab}(x) &= \frac{1}{\sqrt{2}} \sum_{l=1}^{7} (\sigma_l(x) + i\gamma_5 \pi_l(x))\lambda_l^{ab} \\ &\quad + \frac{1}{2}\big[(\delta^{a1}\delta^{b1} + \delta^{a2}\delta^{b2})(\sigma_x(x) + i\gamma_5 \pi_x(x)) \\ &\quad + \delta^{a3}\delta^{b3}\sqrt{2}(\sigma_y(x) + i\gamma_5 \pi_y(x))\big]. \end{aligned} \tag{4.51}$$

Here λ_l, $l = 1, \ldots, 7$ stand for the standard Gell-Mann matrices of the $SU(3)$ group, while the diagonal part corresponds to the pure nonstrange–strange parameterization arising from redefining the contributions proportional to λ_8^{ab} and $\sqrt{2/3}\delta^{ab}$.

With the new coupling g_F one has to determine the values of nine physical parameters and one optimization mass. In order to simplify the presentation, the finite wave-function renormalization constants are not included in the discussion that follows [10] and is outlined below. The ten equations one needs include, with one exception, all those used in the pure meson model in [6].

If we assume a homogeneous condensate in $\sigma_x(x) = x$ and $\sigma_y(x) = y$, the constituent quark masses are generated as

$$M_u = M_d = \frac{g_F}{2}x, \qquad M_s = \frac{g_F}{2}y. \tag{4.52}$$

In the parameter fitting, one makes use of the estimates for the constituent masses arising in the additive quark model:

$$M_u = M_d = \frac{M_N}{3}, \qquad M_s = \frac{1}{2}(M_\Lambda + M_\Sigma) - 2M_u. \tag{4.53}$$

In this way, one has two relations among three parameters (x, y, g_F). These are used in the parameter fitting together with the PCAC relation $x = f_\pi$ (the equation for f_K can be left out, since the quark sector provides two equations at the expense of only one new parameter).

The one-loop equations of state are used to determine the strengths of the explicit symmetry-breaking:

$$\begin{aligned} \epsilon_x &= x(-\mu^2 + 2gy + 2(2f_1 + f_2)x^2 + 4f_1 y^2) \\ &\quad + \sum_{\alpha_i \alpha_j} t^x_{\alpha_i \alpha_j} \mathscr{T}_b^F(ij) + \frac{g_F}{2}(\mathscr{T}_f^F(u) + \mathscr{T}_f^F(d)), \end{aligned}$$

$$\epsilon_y = y(-\mu^2 + 4f_1 xy + 4(f_1 + f_2)y^2 + 4f_1 x^2) + gx^2 + \sum_{\alpha_i\alpha_j} t^y_{\alpha_i\alpha_j} \mathscr{T}_b^F(ij) + \frac{g_F}{\sqrt{2}} \mathscr{T}_f^F(s). \tag{4.54}$$

The renormalized bosonic tadpole contribution of the $\alpha = \sigma, \pi$ sector (allowing for mixing between the mesons of types i and j) is given as $\mathscr{T}_b^F(\alpha_i\alpha_j)$ with the algebraic coefficients $t^z_{\alpha_i\alpha_j}$ (of mass dimension) in the $z = x, y$ directions. Similar contributions describing the quark tadpoles $\mathscr{T}_f^F(q) = -4M_q \mathscr{T}_b^F(M_q)$ are now added with simple algebraic coefficients.

The five additional equations included in the determination of the couplings and condensates are the formulas for the π, K, η masses and the two optimization constraints. The masses of the kaon and the η are the pole masses calculated in the same way as in the pure meson theory, just including the contribution of the fermion loops to the self-energy of these fields. The pion mass is given by the tree-level expression calculated with the optimal mass, and it provides also one FAC condition:

$$m_\pi^2 = m^2 + 2(2f_1 + f_2)x^2 + 4f_1 y^2 + 2gy, \qquad m^2 + \mu^2 = \Sigma_\pi(p = 0, m_i(m_\pi), M_u). \tag{4.55}$$

Here instead of its pole mass, the pion mass is estimated by evaluating the self-energy contribution at vanishing momentum. The reason is that the optimization equation defined with the pole mass turned out not to have a solution for the interesting range of the parameters. The self-energy has the previous contribution from the mesons and also a u-quark contribution, which at $p = 0$ can be reduced to an expression proportional to the quark tadpole (expressed here with a bosonic tadpole integral calculated with the quark mass):

$$\Sigma^F_{\pi(f)}(p = 0) = -2g_F^2 \mathscr{T}_b^F(M_u). \tag{4.56}$$

Similar equations are obtained for the kaon, which can be used at the pole:

$$\begin{aligned} m_K^2 &= m^2 + 2(2f_1 + f_2)(x^2 + y^2)(x^2 + y^2) + 2f_2 y^2 - \sqrt{2}x(2f_2 y - g), \\ m^2 + \mu^2 &= \Sigma_K(p^2 = -M_K^2, m_i(m_\pi), M_u, M_s). \end{aligned} \tag{4.57}$$

The fermionic contribution comes from a bubble integral composed with a u and an s-quark propagator:

$$\Sigma^F_{K(f)}(p^2 = -m_K^2) = -g_F^2 \Big[\mathscr{T}_b^F(M_u) + \mathscr{T}_b^F(M_s) + (m_K^2 + (M_u - M_s)^2) \mathscr{B}_b^F(p^2 = -m_K^2, M_u, M_s) \Big]. \tag{4.58}$$

The fifth equation is the mass formula for the lighter excitation in the $\eta - \eta'$ sector, to be calculated from the mixing mass matrix of (4.46). Here again, the fermionic contribution to the matrix elements has to be given:

$$\Sigma^F_{\eta_{xx}(f)}(p) = -g_F^2\left[2\mathscr{T}_b^F(M_u) - p^2\mathscr{B}_b^F(p, M_u, M_u)\right], \qquad \Sigma^F_{\eta_{xy}(f)} = 0,$$
$$\Sigma^F_{\eta_{yy}(f)}(p) = -g_F^2\left[2\mathscr{T}_b^F(M_s) - p^2\mathscr{B}_b^F(p, M_s, M_s)\right]. \tag{4.59}$$

The values of the input parameters for finding the couplings of the model were chosen as

$$m_\pi[MeV] = 138, \qquad m_K[MeV] = 495.01, \qquad m_\eta[MeV] = 947.8,$$
$$f_\pi[MeV] = 93, \qquad M_u[MeV] = 313, \qquad M_s[MeV] = 530. \tag{4.60}$$

The parameterization to be used for phenomenology was found by minimizing the deviation of the predicted masses for η' and in the scalar sector (a_0, f_0, σ) from their observed values. This can be tuned with two free parameters: M_{0b}, the bosonic, and M_{0f}, the fermionic renormalization mass scales. The best fit obtained numerically in [10] led to the choice

$$M_{0b}[MeV] = 520, \qquad M_{0s}[MeV] = 1210.9. \tag{4.61}$$

With this input, one "predicts" the following physical data:

$$m_\sigma[MeV] = 614.2, \qquad M_{f_0}[MeV] = 1210.9, \qquad f_K[MeV] = 125.23. \tag{4.62}$$

This parameterization is used in Chap. 7 for studying the phase diagram of the quark–meson model at finite temperature and finite baryonic density.

4.7 The 2PI Formalism as Resummation and Its Renormalization

We have seen earlier, in Sect. 2.8, that the 2PI formalism is appropriate for solving a field theory by beginning with a prescribed propagator of the theory. The value of the prescription is demonstrated by (2.132): there, the right-hand side is the exact propagator calculated in the theory, while the left-hand side is the predefined propagator. The theory is consistent if the two definitions are the same.

We can approach the 2PI formalism also from another viewpoint, as a resummation of a certain subset of Feynman diagrams. In fact, the 1PI formalism has already provided a resummation: (2.112) demonstrates that the iterative evolution of the self-energy is equivalent to a summation of an infinite series of diagrams. In the case of the 2-point functions, the self-energy-diagrams (the Dyson–Schwinger

series) are summed. For higher-order diagrams, the 1PI formalism in general sums all diagrams with one-particle-reducible skeleton structure.

The algorithm of the 2PI formalism can be interpreted also as a resummation: it sums all the self-energy diagrams including that of the internal lines. In fact, (2.132) requires that the propagator representing a line contributing to Σ_{2PI} be already the exact one. There is no need to include further self-energy corrections. It is exactly this property that allows one to take into account only two-particle irreducible diagrams in $\Gamma_{int}[\bar{\Phi}, \bar{G}]$ of (2.130). This aspect will be discussed in Sect. 4.7.1

However, the formal definition of the 2PI resummation is not enough. We should define a theory that shows good convergence properties against the potential UV divergences, i.e., it should renormalized. The renormalization issue is far from trivial in the 2PI case, exactly because a 2PI skeleton in fact resums an infinite number of diagrams in the original perturbation theory. For consistency, the counterterm diagrams should also have been included. In the literature, there are thoroughly detailed accounts on the renormalizability of the 2PI resummation, providing useful recipes on how to perform practically the resummation [11–19]. The main conceptual points will be reviewed in Sect. 4.7.2.

4.7.1 2PI Resummation as Optimized Perturbation Theory

A peculiarity of the 2PI resummation is the fact that it represents a *momentum-dependent reorganization of the perturbation series*, since the full propagator should reproduce the exact one, not just a single value taken for a fixed value of the momentum. We have seen that momentum-independent reorganizations (optimization) are obtained by appropriately choosing a momentum-independent finite part of the counterterms, eventually ensuring that we remain in the same equivalence class of constant physics. Momentum-dependent resummation means that (the finite part of) the counterterms must be momentum-dependent, and the new kind of terms (and counterterms) in the 2PI effective action simply reflect this new kind of optimization.

Let us illustrate this line of thought by the example of the Φ^4 model. We generalize the renormalized form of the Lagrangian (3.2) as

$$\mathscr{L} = \frac{1}{2}\varphi\, \mathscr{K}(i\partial)\varphi - \frac{\lambda_{ren}}{24}\varphi^4 + \frac{1}{2}\varphi\delta\mathscr{K}(i\partial)\varphi - \frac{\delta\lambda}{24}\varphi^4, \tag{4.63}$$

where we allow rather general momentum-dependence in $\mathscr{K}$ and $\delta\mathscr{K}$.

As we will demonstrate in the next subsection, the 2PI renormalization is possible because the overall divergences are local independently of the propagators used on the internal lines, at least within a certain limit (for example, we must not change the scaling dimension of the propagator in the far UV). This means that (4.63) will provide us a theory that can be renormalized in exactly the same way as we did for the choice of the free kernel $\mathscr{K}_0 = -\partial^2 - m^2$. This means that we obtain δZ, δm^2,

and $\delta\lambda$ in the same way as before, but of course, the values of the divergent terms may be rather different. In particular, at the one-loop level,

$$\delta\lambda = -\frac{\lambda_{ren}^2}{2}\left(\int \frac{d^4p}{(2\pi)^4} G^2(p)\right)_{div}, \tag{4.64}$$

where $G = \mathscr{K}^{-1}$. We should remark here that this $\delta\lambda$, in accordance with the usual expectations based on perturbation theory, is just the (overall) divergent part of the bubble diagram.

In this way, we see that for every choice of $\mathscr{K}$ and $\delta\mathscr{K}$, provided that this latter contains the appropriate local terms that cancel the UV divergences, we obtain a well-defined renormalized perturbation theory.

We have still to ensure that we are in a fixed equivalence class of constant physics. Since the physics is fully determined by the bare action, it is enough to reproduce it. In particular, we have

$$\mathscr{K}(p) + \delta\mathscr{K}(p) = Zp^2 - m_B^2. \tag{4.65}$$

Since $\mathscr{K}$ is finite, this equation tells us that $\delta\mathscr{K}$ must have a divergence structure of $\delta Zp^2 - \delta m^2$, where δZ and δm^2 are determined by consistency. Therefore, we can write

$$\mathscr{K}(p) + \delta\mathscr{K}_{fin}(p) = \zeta p^2 - m_{ren}^2, \qquad \delta\mathscr{K}_{div} = \delta Zp^2 - \delta m^2. \tag{4.66}$$

There are still some free parameters, ζ, m_{ren}^2, and λ_{ren}. These must be determined by the usual renormalization scheme prescriptions, for example requiring that $\Gamma^{(2)}(p^2 \approx m_{ren}^2, T = 0) = p^2 - m_{ren}^2$ and $\Gamma^{(4)}(p_i = 0, T = 0) = \lambda_{ren}$.

The above analysis is valid for *any* (reasonable) choice of the kernel. The possibility that we can work consistently with any tree-level propagator widens the potential of the optimization. In particular, in (4.22), the FAC could be achieved by ensuring that the mass counterterm and the self-energy correction cancel each other. This is impossible if Σ is explicitly momentum-dependent, as in (4.44), where we must choose a specific momentum, e.g., $p^2 = m^2$, and require the self-energy to vanish at this point. But in a 2PI framework, when we can choose $\delta\mathscr{K}$ freely, we can require that the complete self-energy vanish *for all momenta*:

$$\Sigma(\mathscr{K}, p) = \Sigma_{diagram}(\mathscr{K}, p) - \delta\mathscr{K}(p) \overset{!}{=} 0, \tag{4.67}$$

which means that $\delta\mathscr{K} = \Sigma_{diagram}(\mathscr{K}, p)$, where $\Sigma_{diag} = \Sigma_{div} + \Sigma_{fin}$ is the self-energy expression coming from the diagrams. On substituting it into the consistency equation (4.66), we obtain

$$\mathscr{K}(p) + \Sigma_{fin}(\mathscr{K}, p) = \zeta p^2 - m_{ren}^2 \tag{4.68}$$

and $\Sigma_{div}(\mathscr{K}, p) = \delta Zp^2 - \delta m^2$, which is, in fact, just the definition of δZ and δm^2.

We see that the momentum-dependent optimization condition (4.67) leads to the 2PI equation (2.132). It is also true that all diagrams that contain self-energy insertions (i.e., the 2PR diagrams) are canceled by the counterterm diagram containing $\delta\mathscr{K}$. So this optimization process is equivalent to the 2PI resummation.

Then the strategy for a finite-temperature 2PI calculation can be the following: we start from some initial choice for the kernel and determine the counterterms order by order at zero temperature, just as in an ordinary perturbation theory, applying some renormalization prescription: for example, we choose the finite parts of the subtracted divergences for which (4.68) is satisfied with $\zeta = 1$ and a given m_{ren}. Then with the same counterterms, we determine the finite-temperature self-energy: this will be finite, since the counterterms do not depend on temperature. Finally, we use (4.68) to update the kernel until the recursion is closed.

4.7.2 Perturbative Renormalization of the 2PI Equations

A separate discussion of the perturbative renormalization of the 2PI formalism is necessary, since the coefficients in front of various terms of the 2PI effective action are not measurable quantities. These terms contain integrals to be performed, and therefore also counterterms are needed that render the result of the integration finite when performed with the physical propagators. The 2PI action is in some sense halfway between the original action and the fully physical 1PI action, in which the coefficients are measurable n-point functions.

The most important feature that makes renormalization possible at all is that the overall UV divergences of the 2PI skeleton diagrams, after subtracting subdivergences, are local. The reason is that the only property of the propagator needed for the demonstration of the relevant theorem (Weinberg's theorem) within perturbation theory is that differentiation with respect to its momentum lowers the polynomial power of its asymptotic behavior. This is in fact true for every smooth enough function. Then from Weinberg's theorem, it directly follows that the degree of the overall divergence decreases when we differentiate with respect to any momentum external to some diagram; therefore, the overall divergences are all local. And so after we have subtracted the subdivergences, the remainder can be made finite with local counterterms. Because of the generality of Weinberg's theorem, all these statements remain true when we evaluate a diagram with a generic propagator instead of the tree-level (perturbative) one.

This means that the counterterm renormalization works also in the case of the 2PI resummation. These counterterms are, however, necessarily different from the operators renormalizing the 1PI perturbation theory. After this conceptual clarification, the remaining problem is to determine the counterterms.

Let us examine in detail why the logic of the determination of counterterms is different from the conventional perturbative procedure. The basic reason is that the operators in the 2PI action (2.132) themselves represent an iterative structure, not just the couplings that determine the respective strengths of the contributions to

Σ_{2PI}. Since the same counterterms should appear, the counteroperators are also summed iteratively. To see the problem more clearly, we discuss here the 2PI equations at vanishing classical field. The 2PI action reads (cf. (2.136))

$$i\Gamma_{2PI}[G] = \frac{1}{2}\operatorname{Tr}\ln G - \frac{1}{2}\operatorname{Tr} G_0^{-1}G + i\Gamma_{int}[G], \tag{4.69}$$

with G_0 given by the free theory. Then the corresponding 2PI equations can be written as

$$G^{-1} = G_0^{-1} - \Sigma_{2PI}[G], \qquad \Sigma_{2PI}[G] = 2i\frac{\delta\Gamma_{int}[G]}{\delta G}. \tag{4.70}$$

The parameters of G_0 are the bare parameters: these are responsible for the cancellation of the overall divergences of the self-energy. This means that the Σ_{2PI} self-energy must be free of subdivergences, at least when evaluated at the solution of (4.70). In fact, this condition is enough to determine the counterterm structure of Γ_{int} [20].

The condition for the cancellation of the subdivergences can be made explicit with the help of a trick. We exploit that if we change the free propagator by an amount δG_0 that does not affect the UV behavior, then the overall divergences of the Feynman diagrams are not affected. But the finite parts of the variation are multiplied by the possible subdivergences. Therefore, if the Σ_{2PI} determined from the theory is free from subdivergences, the change due to the variation remains finite.

Therefore, one assumes at the start that a propagator G has been found that solves (4.70) with a fixed G_0 and that the emerging solution is well renormalized. Now let us change $G_0 \to G_0 + \delta G_0$, where δG_0 is sufficiently (at least exponentially) suppressed in the UV. Expanding the 2PI equation (4.70) around G, we obtain the modified solution $G + \delta G$. It is important to note that asymptotically, to leading order, $G \sim p^{-2}$ and $\delta G \sim p^{-4}$ up to logarithmic terms. Now let us examine the change of Σ_{2PI}:

$$\Sigma_{2PI}[G + \delta G] = \Sigma_{2PI}[G] + \Sigma^{(0)} + \Sigma^{(r)}, \tag{4.71}$$

where

$$\Sigma^{(0)} = \frac{1}{2}\int \Lambda\delta G, \qquad \Lambda = 2\frac{\delta\Sigma_{2PI}[G]}{\delta G} \tag{4.72}$$

and $\Sigma^{(r)}$ functionally depends at least quadratically on δG. By the starting assumptions, the modified theory should also be correctly renormalized, which implies that $\Sigma^{(0)}$ and $\Sigma^{(r)}$ are finite.

Here $\Sigma^{(r)}$ is explicitly finite: due to the 2PI nature, every subdiagram contains at least three legs, which by dimensional analysis asymptotically behaves as $\sim p^{-2}$. Therefore, integrating it by two factors of $\delta G \sim p^{-4}$ results in a convergent integral.

The critical term is $\Sigma^{(0)}$, which can contain extra subdivergences, even when Λ contains only overall divergences. This is because $\delta G \sim p^{-4}$, while $\Lambda \sim p^0$ (up to logarithmic corrections). Therefore, there is a source of divergences in the integral $\int \Lambda \delta G$ itself. To localize the subdivergences, we use the splitting $\delta G = \delta G^{(0)} + \delta G^{(r)}$, where $\delta G^{(0)}$ is proportional to p^{-4} at large momenta, while $\delta G^{(r)}$ is at most p^{-6}. The crucial observation here is that $\delta G^{(0)}$ must come from the self-energy $\Sigma^{(0)}$:

$$\delta G^{(0)} = G\Sigma^{(0)}G. \tag{4.73}$$

Otherwise, we do not get $\sim p^{-4}$ corrections, when one subtracts eq. (4.70) written down for G from the same equation written for $G+\delta G$. Substituting back into (4.72), we obtain

$$\Sigma^{(0)} = \frac{1}{2}\int \Lambda \left(G\Sigma^{(0)}G + \delta G^{(r)}\right). \tag{4.74}$$

This defines a self-similar structure, similar to the Bethe–Salpeter equations. Its solution reads

$$\Sigma^{(0)} = \frac{1}{2}\int V\delta G^{(r)}, \tag{4.75}$$

where

$$V = \Lambda + \frac{1}{2}\int \Lambda GVG. \tag{4.76}$$

To prove this statement, we substitute back the desired form:

$$\frac{1}{2}\int V\delta G^{(r)} \stackrel{!}{=} \frac{1}{2}\int \Lambda \left(G\Sigma^{(0)}G + \delta G^{(r)}\right) = \frac{1}{2}\int \left(\Lambda + \frac{1}{2}\int \Lambda GVG\right)\delta G^{(r)}, \tag{4.77}$$

where in the last term, we changed the order of the two integrations. Factoring out $\delta G^{(r)}$, we see that we indeed have the desired equation.

The main point in (4.75) is that it is finite if V is finite. The reason is that V remains $\sim p^0$, but $\delta G^{(r)} \sim p^{-6}$, so the integral does not produce extra divergences. Therefore, we have arrived at the main result: the 2PI effective action is free of subdivergences if V defined in (4.76) is finite.

The above proof in fact is appropriate for proving that it is enough to make V finite at zero temperature; the self-energy remains free of subdivergences also at finite temperatures. Namely, the change at finite temperature is only in the free propagator $G_0 \to G_0 + \delta G_T$, where δG_T is exponentially suppressed at large momenta. Therefore, what was said above can be repeated exactly to conclude that the finite temperature corrections remain finite.

Finally, we demonstrate how counterterms can be used to make V finite. We separate the first nontrivial term from Γ_{int}:

$$i\Gamma_{2PI}[G] = \frac{1}{2}\operatorname{Tr}\ln G - \frac{1}{2}\operatorname{Tr} G_0^{-1}G + \frac{\lambda_0}{8}(\operatorname{Tr} G)^2 + i\Gamma'_{2PI}[G]. \tag{4.78}$$

(Truncating at this term constitutes the Hartree approximation.) Then

$$\Lambda = \lambda_0 + \Lambda', \qquad \Lambda' = 2\frac{\delta\Sigma'_{2PI}[G]}{\delta G}. \tag{4.79}$$

Substituting back into the equation of V (4.76), we obtain

$$V = \lambda_0 + \Lambda' + \frac{1}{2}\int (\lambda_0 + \Lambda')GVG. \tag{4.80}$$

The above equation can be made finite only if Λ' is only overall divergent; this will lead to additional conditions for the couplings in Γ'_{2PI}. The overall divergence of Λ' is momentum-independent, and so we can make it finite by defining the divergent part of the coupling λ_0 at any specific momentum. Practically, one chooses the momentum q^* where the renormalization of the coupling is defined (subtraction point). There we can demand $V(q^*) = \lambda_{ren}$, and so we have formally

$$\lambda_0 = \frac{\lambda_{ren} - \Lambda' - \frac{1}{2}\int \Lambda' GVG}{1 + \frac{1}{2}\int GVG}. \tag{4.81}$$

We emphasize here again that λ_0 is not only responsible for making the Λ' contribution finite; it also accounts for the extra divergences caused by the explicit integrals in the formula.

In particular, if $\Lambda' = 0$, then $V = \lambda_{ren}$, and we obtain

$$\frac{1}{\lambda_0} = \frac{1}{\lambda_{ren}} + \frac{1}{2}\int G^2, \tag{4.82}$$

which is the same equation as (4.64).

This line of thought can be generalized to systems in which we take into account the background field as well. We will not discuss it here; the interested reader will find details in [19]. The result is that we have another Bethe–Salpeter-like equation for

$$\tilde{\Lambda} = \frac{\partial^2 \Sigma[G, \Phi]}{\partial \Phi^2}, \tag{4.83}$$

namely

$$\tilde{V} = \tilde{\Lambda} + \frac{1}{2}\int \tilde{\Lambda} G V G. \tag{4.84}$$

Attention! There is no mistake on the right-hand side: there it is V that appears, not $\tilde{V}$. If one can make both V and $\tilde{V}$ finite, the theory will be free of subdivergences.

In certain truncations, one has $V = \tilde{V}$, but in a generic truncation, this is not the case. This is closely related to the fact that in a given truncation,

$$\frac{1}{2}\frac{\delta^3 \Gamma_{2PI}}{\delta \Phi^2 \delta G} \neq \frac{\delta^2 \Gamma_{2PI}}{\delta G \delta G}. \tag{4.85}$$

As a consequence, different counterterms are needed for different diagram topologies, in particular, the leading terms in Γ_{2PI}:

$$i\Gamma_{2PI}[\Phi, G] = \frac{\lambda_0}{8}(\mathrm{Tr}\, G)^2 + \frac{\lambda_2}{4}\Phi^2 \,\mathrm{Tr}\, G + i\Gamma'_{int}[\Phi, G]. \tag{4.86}$$

Here λ_0 comes from (4.81), and λ_2 from an analogous equation with the change $\Lambda \to \tilde{\Lambda}$. Thus for a generic truncation, $\lambda_0 \neq \lambda_2$.

References

1. P.M. Stevenson, Phys. Rev. D **23**, 2916 (1981)
2. D. O'Connor, C.R. Stephens, Int. J. Mod. Phys. A **9**, 2805 (1994)
3. S. Chiku, T. Hatsuda, Phys. Rev. D **58**, 076001 (1998)
4. S. Chiku, Prog. Theor. Phys. **104**, 1129 (2000)
5. L.H. Chan, R.W. Haymaker, Phys. Rev. D **7**, 402 (1973)
6. T. Herpay, Zs. Szép, Phys. Rev. D **74**, 025008 (2006)
7. A. Jakovác, Zs. Szép, Phys. Rev. D **71**, 105001 (2005)
8. P. Petreczky, F. Karsch, A. Patkós, Phys. Lett. B **401**, 69 (1997)
9. J.-P. Blaizot, N. Wschebor, Phys. Lett. B741, 310 (2014)
10. P. Kovács, Zs. Szép, Phys. Rev. D **75**, 025015 (2007)
11. H.v. Hees, J. Knoll, Phys. Rev. D **65**, 025010 (2002)
12. H.v. Hees, J. Knoll, Phys. Rev. D **65**, 105005 (2002)
13. H.v. Hees and J. Knoll, Phys. Rev. D **66**, 025028 (2002)
14. J.P. Blaizot, E. Iancu, U. Reinosa, Phys. Lett. B **568**, 160 (2003)
15. J.P. Blaizot, E. Iancu, U. Reinosa, Nucl. Phys. A **736**, 149 (2004)
16. F. Cooper, B. Mihaila, J.F. Dawson, Phys. Rev. D **70**, 105008 (2004)
17. E. Calzetta, B.L. Hu, Phys. Rev. D **35**, 495 (1987)
18. A. Arrizabalaga, J. Smit, Phys. Rev. D **66**, 065014 (2002)
19. J. Berges, S. Borsányi, U. Reinosa, J. Serreau, Ann. Phys. **320**, 344 (2005)
20. A. Patkós, Zs. Szép, Nucl. Phys. A **811**, 329 (2008)

Chapter 5
The Large-N Expansion

In conventional perturbation theory, one computes physical observables in power series of some coupling strengths, which in effective theories of strong interactions leads to large higher-order corrections. This situation begs for alternative nonperturbative methods. One of the most efficient propositions is an expansion in the inverse powers of the number of degrees of freedom representing the dynamical variables. In connection with the chiral symmetry-breaking, the inverse of the number of light (nearly massless) quarks and correspondingly the inverse of the number of light (pseudo-Goldstone) mesons provide examples of such acceptably small parameters. In the first case, the solution of $U_L(2) \times U_R(2)$ or $U_L(3) \times U_R(3)$ symmetric theories is attempted by departing from the large-n solution of the $U_L(n) \times U_R(n)$ symmetric theory. In the second, the solution of an $O(N)$ symmetric effective Gell-Mann–Lévy meson theory is continued down to $N = 4$ with the help of a power series in $1/N$.

In this chapter, we shall first give a technically detailed account of constructing the renormalized leading-order (LO) and next-to-leading-order (NLO) solutions of a scalar field with N components supplied with $O(N)$-symmetric dynamics. Our discussion is largely self-contained, although several aspects, in particular applications to critical phenomena, are exhaustively covered by recent reviews and monographs [1–3]. A less comprehensive analysis of the application of the saddle-point approximation to the solution of $U_L(n) \times U_R(n)$ symmetric scalar field theories will also be presented. The chapter closes with a review of the large-N behavior of the quark–meson model, where the $O(N)$-symmetric meson theory is supplemented with quark degrees of freedom interacting with meson fields via Yukawa coupling. The renormalization process described in this chapter will serve as the basis of the phenomenological applications to be presented in Chap. 7.

A. Jakovác, A. Patkós, *Resummation and Renormalization in Effective Theories of Particle Physics*, Lecture Notes in Physics 912,
DOI 10.1007/978-3-319-22620-0_5

5.1 The Dyson–Schwinger Equation of the N-Component Scalar Theory

The classical Euclidean action of the perturbatively renormalizable $O(N)$-symmetric theory of the N-component scalar field $\phi_j, j = 1, 2, \ldots, N$ has the following expression:

$$S_{cl}[\phi_j] = \int dx \left[\frac{1}{2}\phi_j(x)(-\Box + m^2)\phi_j(x) + \frac{\lambda}{24N}\left(\phi_j(x)\phi_j(x)\right)^2 \right]. \tag{5.1}$$

We shall investigate the question of the emergence of a symmetry-breaking minimum that is taken into account in the following parameterization of the ϕ_j-field:

$$\phi_j(x) \to (\sqrt{N}v + \sigma(x), \pi_\alpha(x)). \tag{5.2}$$

The scaling of the quartic term in the original action and here in the shifted part of ϕ_1 corresponds to the extensive nature of the effective action, that is, the fact that the potential energy density in the large-volume (thermodynamic) limit is proportional to the number of the degrees of freedom of the system. After this shift, one obtains

$$\begin{aligned} S_{cl}[\sigma, \pi_\alpha] = \int dx \Big[& \frac{1}{2}\sigma(x)(-\Box + m^2)\sigma(x) \\ & + \frac{1}{2}\pi_\alpha(x)(-\Box + m^2)\pi_\alpha(x) + \frac{1}{2}m^2\left(Nv^2 + 2\sqrt{N}v\sigma\right) \\ & + \frac{\lambda}{24N}\left(Nv^2 + 2\sqrt{N}v\sigma + \sigma(x)^2 + \pi_\alpha^2(x)\right)^2 \Big]. \end{aligned} \tag{5.3}$$

The classical field equations of σ and π_α are found by taking the appropriate functional derivatives:

$$\begin{aligned} \frac{\delta S_{cl}}{\delta\sigma(x)} = & \left(-\Box + m^2 + \frac{\lambda}{2}v^2\right)\sigma(x) + \sqrt{N}v\left(m^2 + \frac{\lambda}{6}v^2\right) + \frac{\lambda v}{6\sqrt{N}}\left(3\sigma^2 + \pi_\alpha^2\right) \\ & + \frac{\lambda}{6N}\left(\sigma^3 + \sigma\pi_\beta^2\right), \end{aligned} \tag{5.4}$$

$$\frac{\delta S_{cl}}{\delta\pi_\alpha(x)} = \left(-\Box + m^2 + \frac{\lambda}{2}v^2\right)\pi_\alpha(x) + \frac{\lambda v}{3\sqrt{N}}\sigma\pi_\alpha + \frac{\lambda}{6N}\left(\sigma^2\pi_\alpha + \pi_\beta^2\pi_\alpha\right). \tag{5.5}$$

The derivative of the quantum action Γ with respect the field variables (the quantum equations of motion) can be obtained from these two equations by applying the

construction rule (2.148) for generating the n-point functions of some generic field theory in the one-particle-irreducible formalism:

$$\frac{\delta\Gamma}{\delta\Phi_U} = \frac{\delta S_{cl}}{\delta\Phi_U}\left[\Phi_A + G_{\Phi_A\Phi_B}\frac{\delta}{\delta\Phi_B}\right], \tag{5.6}$$

where Φ_U stands for the field variables, and U includes all discrete and continuous (space-time) indices of the field. The quantity

$$G_{\Phi_A\Phi_B} = \left[\frac{\delta^2\Gamma}{\delta\Phi_U\delta\Phi_V}\right]^{-1}\Big|_{\Phi_A\Phi_B} \equiv \left[\Gamma^{(2)}\right]^{-1}_{\Phi_A\Phi_B} \tag{5.7}$$

is the $\Phi_A\Phi_B$ element of the inverse of the second functional derivative "matrix" of the effective action. Repeated appearance of an index means summation/integration over it. The use of this rule for the present model is illustrated by working out the transmutation of a specific classical product into an expression of the quantum field theory:

$$\begin{aligned}\sigma(x)\pi_\alpha(y) &\to \left(\sigma(x) + G_{\sigma\phi_j}(x,z)\frac{\delta}{\delta\phi_j(z)}\right)\left(\pi_\alpha(y) + G_{\pi_\alpha\phi_k}(y,w)\frac{\delta}{\delta\phi_k(w)}\right)\mathbf{1}\\ &= \left(\sigma(x) + G_{\sigma\phi_j}(x,z)\frac{\delta}{\delta\phi_j(z)}\right)\pi_\alpha(y) = \sigma(x)\pi_\alpha(y) + G_{\sigma\pi_\alpha}(x,y),\end{aligned} \tag{5.8}$$

where $\mathbf{1}$ denotes the identity element of the functional space. An important relation, repeatedly used below, gives the functional derivative of a propagator:

$$\begin{aligned}\frac{\delta G_{\phi_i\phi_l}(x,y)}{\delta\phi_k(z)} &= -G_{\phi_i\phi_{j_1}}(x,z_1)\frac{\delta\Gamma^{(2)}_{\phi_{j_1}\phi_{j_2}}(z_1,z_2)}{\delta\phi_k(z)}G_{\phi_{j_2}\phi_l}(z_2,y)\\ &= -G_{\phi_i\phi_{j_1}}(x,z_1)\Gamma_{\phi_{j_1}\phi_{j_2}\phi_k}(z_1,z_2,z)G_{\phi_{j_2}\phi_l}(z_2,y),\end{aligned} \tag{5.9}$$

where

$$\Gamma_{\phi_{j_1}\phi_{j_2}\phi_k}(z_1,z_2,z) = \frac{\delta^3\Gamma}{\delta\phi_{j_1}(z_1)\delta\phi_{j_2}(z_2)\delta\phi_k(z)}. \tag{5.10}$$

With these remarks, one obtains the two fundamental quantum equations of the model (with the simplified notation $G_{\pi_\alpha\phi_j} = G_{\alpha\phi_j}$):

$$\begin{aligned}\frac{\delta\Gamma}{\delta\sigma(x)} &= \left(-\Box + m^2 + \frac{\lambda}{2}v^2\right)\sigma + \sqrt{N}v\left(m^2 + \frac{\lambda}{6}v^2\right)\\ &+ \frac{\lambda v}{6\sqrt{N}}\left(3\sigma^2 + 3G_{\sigma\sigma}(x,x) + \pi_\alpha^2 + G_{\alpha\alpha}(x,x)\right)\end{aligned}$$

$$+\frac{\lambda}{6N}\left(\sigma^3+3\sigma G_{\sigma\sigma}(x,x)-G_{\sigma\phi_k}(x,z_1)G_{\sigma\phi_j}(x,z_2)\Gamma_{\phi_j\phi_l\phi_k}(z_2,z_3,z_1)G_{\phi_l\sigma}(z_3,x)\right)$$

$$+\frac{\lambda}{6N}\Big(\pi_\alpha^2\sigma+2\pi_\alpha G_{\alpha\sigma}(x,x)+\sigma G_{\alpha\alpha}(x,x)$$

$$-G_{\alpha\phi_k}(x,z_1)G_{\alpha\phi_j}(x,z_2)\Gamma_{\phi_j\phi_l\phi_k}(z_2,z_3,z_1)G_{\phi_l\sigma}(z_3,x)\Big). \tag{5.11}$$

$$\frac{\delta\Gamma}{\delta\pi_\alpha(x)}=\left(-\Box+m^2+\frac{\lambda}{6}v^2\right)\pi_\alpha+\frac{\lambda v}{3\sqrt{N}}\left(\sigma\pi_\alpha+G_{\sigma\alpha}(x,x)\right)$$

$$+\frac{\lambda}{6N}\big(\sigma^2\pi_\alpha+\pi_\alpha G_{\sigma\sigma}+2\sigma G_{\sigma\pi_\alpha}$$

$$-G_{\sigma\phi_k}(x,z_1)G_{\sigma\phi_j}(x,z_2)\Gamma_{\phi_j\phi_l\phi_k}(z_2,z_3,z_1)G_{\phi_l\alpha}(z_3,x)\big)$$

$$+\frac{\lambda}{6N}\Big(\pi_\alpha\pi_\beta^2+\pi_\alpha G_{\beta\beta}(x,x)+2\pi_\beta G_{\beta\alpha}(x,x)$$

$$-G_{\beta\phi_k}(x,z_1)G_{\beta\phi_j}(x,z_2)\Gamma_{\phi_j\phi_l\phi_k}(z_2,z_3,z_1)G_{\phi_l\alpha}(z_3,x)\Big). \tag{5.12}$$

The equation that determines the vacuum expectation value of the variable σ is obtained by equating (5.11) to zero, at the same time setting all fields and nondiagonal propagator components ($G_{\pi_\alpha,\sigma}$) on the right side equal to zero:

$$0=\sqrt{N}v\left(m^2+\frac{\lambda}{6}v^2\right)+\frac{\lambda v}{6\sqrt{N}}\left(3G_\sigma(x,x)+(N-1)G_\pi(x,x)\right)$$

$$-\frac{\lambda}{6N}\Big(G_\sigma(x,z_1)G_\sigma(x,z_2)\Gamma_{\sigma\sigma\sigma}(z_2,z_3,z_1)G_\sigma(z_3,x)$$

$$+G_\pi(x,z_1)G_\pi(x,z_2)\Gamma_{\alpha\sigma\alpha}(z_2,z_3,z_1)G_\sigma(z_3,x)\Big). \tag{5.13}$$

Here further simplified notation is introduced for the diagonal propagator elements, $G_{\alpha\beta}=G_\pi\delta^{\alpha\beta}, G_{\sigma\sigma}=G_\sigma$, and the discrete summation is performed using $\delta^{\alpha\alpha}=N-1$.

The Dyson–Schwinger equations for higher n-point functions of the theory are obtained by taking appropriate further functional derivatives of (5.11) and (5.12). The final result of a lengthy but straightforward sequence of calculational steps also involves the fourth functional derivatives of Γ. For these higher n-point functions, one assumes the tensorial structure dictated by the corresponding functional derivatives of the classical action S_{cl}.

In particular, for the two-point functions, it will be shown that the leading order (LO) of the $1/N$ hierarchy self-consistently required for the 3- and 4-point functions naturally truncates the infinite set of coupled n-point equations within the subset of the two-point functions and one three-point function. For this, one needs the large-N scaling of the related 3- and 4-point functions, which can be naturally

assumed to coincide with the leading N-dependence of their classical (tree-level) expressions:

$$\Gamma^{class}_{\sigma\sigma\sigma}(x,y,z) = \frac{\lambda v}{3\sqrt{N}}\delta(x-y)\delta(x-z),$$

$$\Gamma^{class}_{\alpha\beta\sigma}(x,y,z) = \frac{\lambda v}{3\sqrt{N}}\delta(x-y)\delta(x-z)\delta^{\alpha\beta},$$

$$\Gamma^{class}_{\sigma\sigma\sigma\sigma}(x,y,z,w) = \frac{\lambda}{N}\delta(x-y)\delta(x-z)\delta(x-w),$$

$$\Gamma^{class}_{\alpha\beta\gamma\epsilon}(x,y,z,w) = \frac{\lambda}{3N}\delta(x-y)\delta(x-z)\delta(x-w)(\delta^{\alpha\beta}\delta^{\gamma\epsilon} + \delta^{\alpha\gamma}\delta^{\beta\epsilon} + \delta^{\alpha\epsilon}\delta^{\beta\gamma}),$$

$$\Gamma^{class}_{\sigma\sigma\alpha\beta}(x,y,z,w) = \frac{\lambda}{3N}\delta(x-y)\delta(x-z)\delta(x-w)\delta^{\alpha\beta}. \tag{5.14}$$

The 3- and 4-point functions with any other index set consistently vanish. In view of this, we introduce the following scaled 3- and 4-point functions, which are assumed to be independent of N at LO:

$$\Gamma_{\sigma\sigma\sigma}(x,y,z) = \frac{v}{\sqrt{N}}\Gamma_{sss}(x,y,z), \qquad \Gamma_{\alpha\beta\sigma}(x,y,z) = \frac{v}{\sqrt{N}}\delta^{\alpha\beta}\Gamma_{\pi\pi s}(x,y,z)$$

$$\Gamma_{\sigma\sigma\sigma\sigma}(x,y,z,w) = \frac{1}{N}\Gamma_{ssss}(x,y,z,w),$$

$$\Gamma_{\sigma\sigma\alpha\beta}(x,y,z,w) = \frac{1}{N}\Gamma_{ss\pi\pi}\delta^{\alpha\beta}(x,y,z,w),$$

$$\Gamma_{\alpha\beta\gamma\epsilon}(x,y,z,w) = \frac{1}{N}\Gamma_{\pi\pi\pi\pi}(x,y,z,w)(\delta^{\alpha\beta}\delta^{\gamma\epsilon} + \delta^{\alpha\gamma}\delta^{\beta\epsilon} + \delta^{\alpha\epsilon}\delta^{\beta\gamma}). \tag{5.15}$$

One obtains, for the elements of the inverse propagator matrix,

$$\begin{aligned}
G^{-1}_{\alpha\gamma}(x,y) = G^{-1}_{\pi}(x,y)\delta^{\alpha\gamma} &= \left(-\Box + m^2 + \frac{\lambda}{6}v^2\right)\delta(x-y)\delta^{\alpha\gamma} \\
&-\frac{\lambda v}{3\sqrt{N}}G_\sigma(x,z_1)\Gamma_{\sigma\alpha\gamma}(z_1,z_2,y)G_\pi(z_2,x) \\
&+\frac{\lambda}{6N}\Big[\delta^{\alpha\gamma}\delta(x-y)G_\sigma(x,x) \\
&-G_\sigma(x,z_1)G_\sigma(x,z_3)\Gamma_{\sigma\alpha\sigma\gamma}(z_1,z_2,z_3,y)G_\pi(z_2,x) \\
&+G_\sigma(x,v_1)G_\sigma(x,v_2)\Gamma_{\sigma\sigma\sigma}(v_1,v_2,v_3)G_\sigma(v_3,z_1)\Gamma_{\sigma\alpha\gamma}(z_1,z_2,y)G_\pi(z_2,x) \\
&+2G_\sigma(x,z_1)\Gamma_{\sigma\epsilon\gamma}(z_1,z_2,y)G_\pi(v_3,z_2)G_\sigma(v_1,x)\Gamma_{\sigma\alpha\epsilon}(v_1,v_2,v_3)G_\pi(v_2,x)\Big]
\end{aligned}$$

$$
\begin{aligned}
&+\frac{\lambda}{6N}\Big[\delta^{\alpha\gamma}(N+1)\delta(x-y)G_\pi(x,x)\\
&-G_\pi(x,z_1)G_\pi(x,z_2)\Gamma_{\beta\alpha\beta\gamma}(z_1,z_2,z_3,y)G_\pi(z_3,x)\\
&+G_\pi(x,v_1)G_\pi(x,v_3)\Gamma_{\beta\sigma\beta}(v_1,v_2,v_3)G_\sigma(v_2,z_1)\Gamma_{\sigma\alpha\gamma}(z_1,z_2,y)G_\pi(z_2,x)\\
&+2G_\pi(x,z_1)\Gamma_{\beta\sigma\gamma}(z_1,z_2,y)G_\sigma(v_3,z_2)G_\pi(x,v_1)\Gamma_{\beta\alpha\sigma}(v_1,v_2,v_3)G_\pi(v_2,x)\Big].
\end{aligned}
\tag{5.16}
$$

$$
\begin{aligned}
G_\sigma^{-1}(x,y) &= \left(-\Box+m^2+\frac{\lambda}{2}v^2\right)\delta(x-y)\\
&-\frac{\lambda v}{6\sqrt{N}}\left(3G_\sigma(x,z_1)\Gamma_{\sigma\sigma\sigma}(z_1,z_2,y)G_\sigma(z_2,x)\right.\\
&\left.+G_\pi(x,z_1)\Gamma_{\alpha\alpha\sigma}(z_1,z_2,y)G_\pi(z_2,x)\right)\\
&+\frac{\lambda}{6N}\Big[3G_\sigma(x,x)\delta(x-y)-G_\sigma(x,z_1)G_\sigma(x,z_2)\Gamma_{\sigma\sigma\sigma\sigma}(z_1,z_2,z_3,y)G_\sigma(z_3,x)\\
&+3G_\sigma(x,z_1)G_\sigma(z_2,v_1)\Gamma_{\sigma\sigma\sigma}(z_1,z_2,y)G_\sigma(x,v_2)\Gamma_{\sigma\sigma\sigma}(v_1,v_2,v_3)G_\sigma(v_3,x)\Big]\\
&+\frac{\lambda}{6N}\Big[(N-1)G_\pi(x,x)\delta(x-y)\\
&-G_\pi(x,z_3)G_\pi(x,z_1)\Gamma_{\alpha\sigma\alpha\sigma}(z_1,z_2,z_3,y)G_\sigma(z_2,x)\\
&+G_\pi(x,v_3)G_\pi(x,v_1)\Gamma_{\alpha\sigma\alpha}(v_1,v_2,v_3)G_\sigma(v_2,z_1)\Gamma_{\sigma\sigma\sigma}(z_1,z_2,y)G_\sigma(z_2,x)\\
&+2G_\pi(x,z_1)\Gamma_{\alpha\beta\sigma}(z_1,z_2,y)G_\pi(z_2,v_3)G_\pi(x,v_1)\Gamma_{\alpha\sigma\beta}(v_1,v_2,v_3)G_\sigma(v_2,x)\Big].
\end{aligned}
\tag{5.17}
$$

5.2 The Large-N Closure and Its Recursive Renormalization

Using the scaled quantities, one can find in the large-N limit the LO form for (5.13), (5.16), and (5.17) determining the 1- and 2-point functions:

$$
\begin{aligned}
0 &= \sqrt{N}v\left(m^2+\frac{\lambda}{6}(v^2+G_\pi(x,x))\right),\\
G_\sigma^{-1}(x,y) &= \left(-\Box+m^2+\frac{\lambda}{6}(3v^2+G_\pi(x,x))\right)\delta(x-y)
\end{aligned}
$$

$$- \frac{\lambda v^2}{6} G_\pi(x,z_1)\Gamma_{\pi\pi s}(z_1,z_2,y)G_\pi(z_2,x),$$

$$G_\pi^{-1}(x,y) = \left(-\Box + m^2 + \frac{\lambda}{6}(v^2 + G_\pi(x,x))\right)\delta(x-y). \tag{5.18}$$

An important feature of the large-N approximation is that it satisfies Goldstone's theorem [4], which can be seen by comparing the equation of state with

$$m_\pi^2 = m^2 + \frac{\lambda}{6}(v^2 + G_\pi(x,x)), \tag{5.19}$$

the mass term in the pion propagator. In the presence of an explicit symmetry-breaking term in the Lagrangian density, $(\sqrt{N}v + \sigma)h\sqrt{N}$, the squared pion mass is given as h/v. The same relation reappears also in the quark–meson model of Sect. 5.7 in Eq. (5.158). (The N-scaling of the symmetry-breaking term is again determined by its extensive nature.)

The other observation is that despite considerable simplifications, this large-N set is not yet closed; one still needs an equation providing the large-N expression of $\Gamma_{\pi\pi s}$. The equation for $\Gamma_{\alpha\gamma\sigma}$ can be obtained by returning to an intermediate stage in deriving (5.16) for $G^{-1}_{\alpha\gamma}$, where all terms of the corresponding second functional derivative of Γ are still kept. One has to take the additional functional derivative of this expression with respect to $\sigma(z)$ and extract its large-N asymptotic form. After scaling out the factor $v/\sqrt{N}\delta^{\alpha\gamma}$ on both sides, as required by the second scaling rule in (5.15), one arrives at the following LO equation:

$$\Gamma_{\pi\pi s}(x,y,z) = \frac{\lambda}{3}\delta(x-y)\delta(x-z) - \frac{\lambda}{6}G_\pi(x,z_1)\Gamma_{\pi\pi s}(z_1,z_2,z)G_\pi(z_2,x)\delta(x-y). \tag{5.20}$$

This is a self-consistent equation for the $\pi\pi\sigma$ 3-point function, which means that at LO in the large-N approximation, the set of equations consisting of (5.18) and (5.20) closes in a natural way.

By the translational invariance of the theory, $\Gamma_{\pi\pi s}$ depends only on the coordinate differences $x-y$ and $x-z$, which implies momentum conservation. Moreover, the proportionality of the right-hand side of (5.20) to $\delta(x-y)$ implies also

$$\Gamma_{\pi\pi s}(x-y,x-z) = \tilde{\Gamma}_{\pi\pi s}(x-z)\delta(x-y), \tag{5.21}$$

which leads after Fourier transformation and the separation of the delta function, expressing momentum conservation, to the simple equation

$$\tilde{\Gamma}_{\pi\pi s}(q) = \frac{\lambda}{3} - \frac{\lambda}{6}\tilde{\Gamma}_{\pi\pi s}(q)\int_p G_\pi(p)G_\pi(p+q). \tag{5.22}$$

The determination of the finite 3-point function as a solution of this equation is a simple and transparent application of the iterative renormalization procedure [5]. A perturbation series in powers of λ is generated for $\tilde{\Gamma}_{\pi\pi s}$ by the iterative solution of (5.22). Since one recognizes the logarithmic divergence of the "bubble" integral formed with the pion propagators at each step of the iteration, one has to renormalize the coupling λ in order to keep $\tilde{\Gamma}_{\pi\pi s}$ finite. Separating the finite ($\mathscr{B}_\pi^F$) and the divergent parts ($\mathscr{B}_d^{(0)}$) of the bubble integral and splitting the coupling into renormalized (λ_R) and counterterm ($\delta\lambda$) piece yields the equation in the following form:

$$\tilde{\Gamma}_{\pi\pi s}(q) = \frac{\lambda_R + \delta\lambda}{3}\left(1 - \frac{1}{2}\tilde{\Gamma}_{\pi\pi s}(q)(\mathscr{B}_\pi^F + \mathscr{B}_d^{(0)})\right),$$
$$\mathscr{B}(q) = \int_p G_\pi(p)G_\pi(p+q) = \mathscr{B}_\pi^F(q) + \mathscr{B}_d^{(0)}. \tag{5.23}$$

The goal of the perturbation theory is to determine both $\tilde{\Gamma}_{\pi\pi s}(q)$ and $\delta\lambda$ in power series of λ_R:

$$\tilde{\Gamma}_{\pi\pi s}(q) = \sum_{n=1}^{\infty} \lambda_R^n \tilde{\Gamma}_{\pi\pi s}^{(n)}(q), \qquad \delta\lambda = \sum_{n=1}^{\infty} c_d^{(n)} \lambda_R^{n+1}. \tag{5.24}$$

The iteration begins with the classical value

$$\tilde{\Gamma}_{\pi\pi s}^{(1)}(q) = \frac{1}{3}. \tag{5.25}$$

The first iteration consists in substituting this value into the second term of the right-hand side and comparing the two sides at the level of λ_R^2,

$$\lambda_R^2 \tilde{\Gamma}_{\pi\pi s}^{(2)}(q) = c_d^{(1)} \frac{\lambda_R^2}{3} - \frac{\lambda_R^2}{18}(\mathscr{B}_\pi^F + \mathscr{B}_d^{(0)}), \tag{5.26}$$

which gives

$$\tilde{\Gamma}_{\pi\pi s}^{(2)}(q) = -\frac{1}{18}\mathscr{B}_\pi^F(q), \qquad c_d^{(1)} = \frac{1}{6}\mathscr{B}_d^{(0)}. \tag{5.27}$$

It is worthwhile following in detail the second iteration, since it provides insight into the cancellation of the so-called subdivergences. The equality at level λ_R^3 takes the form

$$\tilde{\Gamma}^{(3)}(q) = \frac{1}{2}c_d^{(2)} - \frac{1}{6}(\mathscr{B}_\pi^F + \mathscr{B}_d^{(0)})(\tilde{\Gamma}^{(2)}(q) + c_d^{(1)}\tilde{\Gamma}^{(1)}(q))$$
$$= \frac{1}{2}c_d^{(2)} - \frac{1}{108}(\mathscr{B}_d^{(0)2} - \mathscr{B}_\pi^{F2}). \tag{5.28}$$

The absence of the mixed product term $\mathscr{B}_\pi^F \mathscr{B}_d^{(0)}$ exemplifies the cancellation of subdivergences, and one easily identifies

$$\tilde{\Gamma}^{(3)}_{\pi\pi s}(q) = \frac{1}{3}\left(-\frac{1}{6}\mathscr{B}_\pi^F\right)^2, \qquad c_d^{(2)} = \left(\frac{1}{6}\mathscr{B}_d^{(0)}\right)^2. \tag{5.29}$$

Further, one guesses and proves by complete induction the following recurrence relations:

$$\tilde{\Gamma}^{(n)}_{\pi\pi s}(q) = -\frac{1}{6}\mathscr{B}_\pi^F \tilde{\Gamma}^{(n-1)}_{\pi\pi s}(q), \qquad c_d^{(n)} = \frac{1}{6}\mathscr{B}_d^{(0)} c_d^{(n-1)}. \tag{5.30}$$

Since these geometric series can be summed, one ends up with the *resummed and renormalized nonperturbative result*

$$\tilde{\Gamma}_{\pi\pi s}(q) = \frac{\lambda_R}{3}\frac{1}{1+\frac{\lambda_R}{6}\mathscr{B}_\pi^F(q)}, \qquad \delta\lambda = \frac{\lambda_R}{6}\mathscr{B}_d^{(0)}\frac{1}{1-\frac{\lambda_R}{6}\mathscr{B}_d^{(0)}}. \tag{5.31}$$

The term "resummation" is rightly used, since the result is the sum of the infinite pion bubble series (see Fig. 5.1) contribution to the 3-point function emerging from the original quartic Lagrangian density by the shift (5.2).

The same results can be obtained also by a more formal (more intuitive?) procedure when one directly solves (5.22) as

$$\begin{aligned}\tilde{\Gamma}_{\pi\pi s}(q) &= \frac{\lambda}{3}\frac{1}{1+\frac{\lambda}{6}(\mathscr{B}_\pi^F(q)+\mathscr{B}_d^{(0)})} \\ &= \frac{1}{3}\frac{1}{\left(\frac{1}{\lambda}+\frac{1}{6}\mathscr{B}_d^{(0)}\right)+\frac{1}{6}\mathscr{B}_\pi^F(q)} = \frac{1}{3}\frac{1}{\frac{1}{\lambda_R}+\frac{1}{6}\mathscr{B}_\pi^F(q)},\end{aligned} \tag{5.32}$$

$$\frac{1}{\lambda_R} = \frac{1}{\lambda} + \frac{1}{6}\mathscr{B}_d^{(0)}. \tag{5.33}$$

The LO solution is completed by finding the explicitly finite equation for G_σ^{-1} starting with the formal expression in (5.18). Using the first equation of (5.18) together with (5.20), one obtains

$$G_\sigma^{-1}(x,y) = -\Box\delta(x-y) + v^2\tilde{\Gamma}_{\pi\pi s}(x-y). \tag{5.34}$$

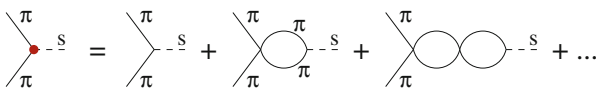

Fig. 5.1 The resummed bubble series contributing to the $s-\pi-\pi$ vertex in the large-N limit

When we apply (5.21) and (5.31), this propagator assumes a rather simple finite expression in Fourier space without any need for further renormalization:

$$G_\sigma^{-1}(q) = q^2 + v^2 \tilde{\Gamma}_{\pi\pi s}(q) = q^2 + \frac{\lambda_R v^2}{3} \frac{1}{1 + \frac{\lambda_R}{6} \mathscr{B}_\pi^F(q)}. \tag{5.35}$$

The last step is to renormalize the equation of state. The tadpole integral of a zero-mass pion propagator is a pure quadratically divergent quantity:

$$G_\pi(x,x) = \int_p G_\pi(p) = \mathscr{T}_d^{(2)}. \tag{5.36}$$

With the help of this representation, one can easily write the following for the equation of state:

$$0 = \sqrt{N} v \left(\frac{6}{\lambda} m^2 + v^2 + \mathscr{T}_d^{(2)} \right) = \sqrt{N} v \left(\frac{6}{\lambda_R} m_R^2 + v^2 \right), \tag{5.37}$$

which requires the counterterm relation

$$\delta \left(\frac{m^2}{\lambda} \right) + \mathscr{T}_d^{(2)} = 0. \tag{5.38}$$

5.3 Landau Singularity and Triviality

The formally perfect analysis of the renormalization reveals its limitation when one analyzes (5.33), employing the explicit expression of $\mathscr{B}_d^{(0)}$ obtained with cutoff regularization:

$$\mathscr{B}_d^{(0)} = \frac{1}{16\pi^2} \ln \frac{\Lambda^2}{M_0^2}, \tag{5.39}$$

where Λ is the maximal momentum at which the integral defining $\mathscr{B}(q)$ in Eq. (5.23) is cut off, and M_0 is the normalization scale. One recognizes $\lambda_R(\Lambda) = \lambda$ by choosing $M_0 = \Lambda$. Using this, the relation defining the renormalized coupling can be considered a function describing the Λ-dependence of $\lambda_R(M_0)$:

$$\lambda_R(M_0) = \frac{\lambda_R(\Lambda)}{1 + \frac{\lambda_R(\Lambda)}{96\pi^2} \ln \frac{\Lambda^2}{M_0^2}}. \tag{5.40}$$

Renormalizability in the strict sense means finding results independent of the regularization, which requires sending Λ to infinity. But then one obtains (keeping $\lambda_R(\Lambda)$ fixed)

$$\lim_{\Lambda\to\infty} \lambda_R(M_0) = 0, \tag{5.41}$$

which means that the coupling characterizing the pointlike source is completely screened at every finite scale. The feature revealed by this analysis is called *triviality*. The same phenomenon was found in the one-loop analysis of the one-component scalar theory in Sect. 3.5.2. Here, however, it is an exact statement in the $N \to \infty$ limit. Only asymptotically free theories escape this consequence of the scale-dependence of couplings. Quantum electrodynamics and the Higgs sector of the standard model share this feature, and these sectors can be used only as effective theories up to some maximal momentum (cutoff) value. In such theories, renormalization turns into a weaker statement: one expects that physical results are not sensitive to a sufficiently high choice of Λ. However, the fulfillment of such an expectation can be checked only numerically by choosing at physically relevant scales phenomenologically "dictated" values for the couplings.

The presence of a maximal allowed momentum in the theory is signaled by a singularity: the *Landau pole*. It shows up in the momentum-dependence of the $\pi - \pi - \sigma$ coupling when one continues the theory from the Euclidean to the Minkowski metrics with the help of the following rules:

$$q_E^2 \to -q_M^2, \qquad \mathscr{B}_E^F(q_E) \to -\mathscr{B}_M^F(q_M), \qquad G_{\sigma\sigma}^{-1(E)} \to -iG_{\sigma\sigma}^{-1(M)}, \tag{5.42}$$

resulting in

$$\tilde{\Gamma}^{(M)}_{\pi\pi s}(q_M) = \frac{\lambda_R}{3} \frac{1}{1 - \frac{\lambda_R}{96\pi^2} \ln \frac{-q_M^2}{M_0^2}}. \tag{5.43}$$

This expression obviously has a pole located at the imaginary momentum

$$-q_M^2 = M_0^2 e^{96\pi^2/\lambda_R}, \tag{5.44}$$

which by analyticity in the complex q_M-plane puts a limit on the range of convergence in momentum. The larger the value of $\lambda_R(M_0)$, the lower this upper limit.

The singularity shows up also in the physical (Minkowskian) spectra of the σ-channel. It leads to the existence of a purely imaginary (tachyonic) zero of the equation

$$iG_{\sigma\sigma}^{-1(M)} = q_M^2 - \frac{\lambda_R}{3} v^2 \frac{1}{1 - \frac{\lambda_R}{96\pi^2} \ln \frac{-q_M^2}{M_0^2}} = 0, \tag{5.45}$$

which should be separated (to lie much higher in absolute value) from the domain of physical momenta described by the effective theory. In this sense, the energy scale of the Landau pole represents an upper bound on the masses of the physically meaningful excitations. If one identifies the $O(N)$ model with the Higgs sector of the standard model, one obtains an upper bound on the mass of the Higgs boson [6]. In the case of the strong interaction, a similar bound is produced for the mass of the σ-meson. This issue will be discussed in applications of the linear σ-model to the phenomenology of strong interactions.

5.4 Auxiliary Field Formulation of the $O(N)$ Model

An alternative formulation of the model (5.1) is sometimes more convenient for developing the large-N expansion. It transforms formally the term depending quartically on σ and π_α into a quadratic dependence with the help of the so-called Hubbard–Stratonovich transformation. The price to pay is the introduction of a new field ($\bar{\rho}(x)$), which is a quadratic composite of the original variables and can be thought of as describing in a pointlike approximation some two-particle (bound) state of them. The extended classical action has the following form after the shift (5.2):

$$\begin{aligned} S[\sigma,\pi_\alpha,\bar{\rho},v] = \int d^4x \Big[& \frac{1}{2}\big(\partial_m\sigma(x)\big)^2 + \frac{1}{2}\big(\partial_m\pi_\alpha(x)\big)^2 \\ & + \frac{m^2}{2}\Big(\sigma^2(x)+\pi_\alpha^2(x)+2\sqrt{N}v\sigma(x)+Nv^2\Big) - \sqrt{N}h(\sqrt{N}v+\sigma) \\ & - \frac{1}{2}\bar{\rho}^2(x) + \frac{1}{2}\sqrt{\frac{\lambda}{3N}}\bar{\rho}(x)\Big(\sigma^2(x)+\pi_\alpha^2(x)+2\sqrt{N}v\sigma(x)+Nv^2\Big)\Big]. \end{aligned} \tag{5.46}$$

The variable $\bar{\rho}(y)$ has no dynamics; the variation of S with respect to $\bar{\rho}$ leads to a local algebraic expression for it, which, after being substituted back, reproduces the original action. Applying the rule (5.6) to the extended action, one arrives at the corresponding set of 1- and 2-point equations. The 1-point equations for σ and $\bar{\rho}$ can be written as follows (setting in the final result the nonzero background for the auxiliary field $\rho = \bar{\rho}\sqrt{\lambda/3N}$):

$$\begin{aligned} & Nv\left(-h+m^2+\rho\right) + \sqrt{\frac{\lambda}{3}}vG_{\rho\sigma}(x,x) = 0, \\ & -\frac{3N}{\lambda}\rho + \frac{1}{2}\left[Nv^2 + (N-1)G_\pi(x,x) + G_{\sigma\sigma}(x,x)\right] = 0. \end{aligned} \tag{5.47}$$

A second functional derivation gives the equations that determine the 2-point functions:

$$
\begin{aligned}
G^{-1}_{\sigma\sigma}(x,y) &= D^{-1}_{\sigma\sigma}(x,y) - \sqrt{\frac{\lambda}{3N}} G_{\rho A}(x,z) G_{B\sigma}(w,x) \Gamma_{AB\sigma}(z,w,y), \\
G^{-1}_{\sigma\rho}(x,y) &= D^{-1}_{\sigma\rho}(x,y) - \sqrt{\frac{\lambda}{3N}} G_{\rho A}(x,z) G_{B\sigma}(w,x) \Gamma_{AB\rho}(z,w,y), \\
G^{-1}_{\rho\rho}(x,y) &= D^{-1}_{\rho\rho}(x,y) \\
&\quad -\frac{1}{2}\sqrt{\frac{\lambda}{3N}} \Big[G_{\sigma A}(x,z) G_{B\sigma}(w,x) + G_{\alpha A}(x,z) G_{B\alpha}(w,x) \Big] \Gamma_{AB\rho}(z,w,y), \\
G^{-1}_{\alpha\beta}(x,y) &= \delta^{\alpha\beta} D^{-1}_{\pi}(x,y) - \sqrt{\frac{\lambda}{3N}} G_{\rho A}(x,z) G_{B\alpha}(w,x) \Gamma_{AB\beta}(z,w,y).
\end{aligned}
\tag{5.48}
$$

The indices A, B run through the set σ, π_α, ρ, and one has to integrate/sum over all repeated space coordinates/indices. The tree-level propagators appearing here have the following expressions in Fourier space:

$$
D^{-1}_{\sigma\sigma}(k) = D^{-1}_{\pi}(k) = k^2 + M^2, \qquad D^{-1}_{\rho\rho}(k) = -1, \qquad D^{-1}_{\rho\sigma}(k) = \sqrt{\frac{\lambda}{3}} v. \tag{5.49}
$$

Here we introduced an abbreviated notation for the permanent combination

$$
m^2 + \rho = M^2. \tag{5.50}
$$

From (5.46), one finds that only $\Gamma_{\rho\sigma\sigma}$ and $\Gamma_{\rho\pi\pi}$ assume nonzero tree-level values,

$$
\begin{aligned}
\Gamma_{\rho\sigma\sigma}(x,y,z) = \sqrt{\frac{\lambda}{3N}} \delta(x-y)\delta(x-z), \quad \Gamma_{\rho\alpha\beta}(x,y,z) = \delta^{\alpha\beta} \Gamma_{\rho\pi\pi}(x,y,z), \\
\Gamma_{\rho\pi\pi} = \Gamma_{\rho\sigma\sigma}.
\end{aligned}
\tag{5.51}
$$

Since all other 3-point functions vanish at this level, in an iterative sense their exact value is also compatible with zero. On the other hand, for the nonzero vertices, one can argue that in (5.48) it is sufficient to use the above tree-level expressions if one is interested in the determination of the propagators with $\mathcal{O}(1/N)$ accuracy.

The argument goes as follows. A first type of typical quantum contribution to $\Gamma_{\sigma\sigma\rho}$ has the following structure:

$$
\sqrt{\frac{\lambda}{3N}} G_{\rho C} G_{DA} \Gamma_{CD\rho} G_{B\sigma} \Gamma_{AB\sigma}, \tag{5.52}
$$

which iteratively contributes at level $\mathcal{O}(N^{-3/2})$, and is therefore negligible at the required accuracy. The other typical contribution is of the form

$$\sqrt{\frac{\lambda}{3N}} G_{\rho A} G_{B\sigma} \Gamma_{AB\sigma\rho}. \tag{5.53}$$

The iterative determination of the 4-point function begins with the contribution of terms that contain exclusively lower n-point functions (that is, propagators and 3-point functions). As one can trace by further derivations of (5.48), the iterative determination of any 4-point function then contains at least the functional product of three 3-point functions plus the explicit $1/\sqrt{N}$ factor. Therefore, the N-dependence of this contribution can be estimated as $\sim N^{-2}$. This makes the second type of contribution also negligible.

This argument allows us to write the Dyson–Schwinger equations completely explicitly with $\mathcal{O}(1/N)$ relative accuracy using (5.51):

$$\begin{aligned}
G^{-1}_{\sigma\sigma}(x,y) &= (-\Box + M^2)\delta(x-y) \\
&\quad -\frac{\lambda}{3N}\left[G_{\rho\rho}(x,y)G_{\sigma\sigma}(y,x) + G_{\rho\sigma}(x,y)G_{\sigma\rho}(y,x)\right], \\
G^{-1}_{\sigma\rho}(x,y) &= \sqrt{\frac{\lambda}{3}} v\delta(x-y) - \frac{\lambda}{3N} G_{\rho\sigma}(x,y)G_{\sigma\sigma}(y,x), \\
G^{-1}_{\rho\rho}(x,y) &= -\delta(x-y) - \frac{\lambda}{6N}\left[G_{\sigma\sigma}(x,y)G_{\sigma\sigma}(y,x)\right. \\
&\quad \left. +(N-1)G_{\pi}(x,y)G_{\pi}(y,x)\right], \\
G^{-1}_{\pi}(x,y) &= (-\Box + M^2)\delta(x-y) - \frac{\lambda}{3N} G_{\rho\rho}(x,y)G_{\pi}(y,x).
\end{aligned} \tag{5.54}$$

These equations form a closed set together with the two equations of (5.47), which demonstrates that the $1/N$ expansion provides a natural closure also at the NLO.

Before proceeding to a discussion of the renormalization of these equations, we remark that one can construct an effective action from which these equations follow by considering v, ρ, $G_{\sigma\sigma}$, $G_{\sigma\rho}$, $G_{\rho\rho}$, and G_{π} to be independent variational variables:

$$\begin{aligned}
\Gamma_{\mathit{eff}}[v,\rho,\mathscr{G},G_\pi] &= \frac{1}{2}NM^2v^2 - \frac{3N}{2\lambda_R}\rho^2 - Nhv \\
&+\frac{1}{2}\int_k \left[(N-1)(\ln G_\pi^{-1}(k) + D_\pi^{-1}(k)G_\pi(k)) + \operatorname{Tr}\ln\mathscr{G}^{-1}(k) + \operatorname{Tr}\left(\mathscr{D}^{-1}(k)\mathscr{G}(k)\right)\right] \\
&-\frac{\lambda_R}{12N}\int_k\int_p \left[G_{\sigma\sigma}(k)G_{\sigma\sigma}(k+p)G_{\rho\rho}(p) + (N-1)G_\pi(k)G_\pi(k+p)G_{\rho\rho}(p)\right. \\
&\qquad \left. + 2G_{\sigma\rho}(k)G_{\sigma\rho}(p)G_{\sigma\sigma}(p+k)\right] + \Delta\Gamma[v,\rho,G_\pi,\mathscr{G}].
\end{aligned} \tag{5.55}$$

Here the matrices

$$\mathscr{D}^{-1}(k) = \begin{pmatrix} D^{-1}_{\rho\rho}(k) & D^{-1}_{\rho\sigma}(k) \\ D^{-1}_{\sigma\rho}(k) & D^{-1}_{\sigma\sigma}(k) \end{pmatrix} = \begin{pmatrix} -1 & \sqrt{\frac{\lambda_R}{3}}v \\ \sqrt{\frac{\lambda_R}{3}}v & k^2 + M^2 \end{pmatrix},$$
$$\mathscr{G} = \begin{pmatrix} G_{\rho\rho}(k) & G_{\rho\sigma}(k) \\ G_{\sigma\rho}(k) & G_{\sigma\sigma}(k) \end{pmatrix} \tag{5.56}$$

are introduced. The second represents the components of the exact propagator matrix in the $\rho - \sigma$ sector; the first is just the tree-level expression of its inverse matrix. Here the part of the action depending on the renormalized coupling is separated from the counteraction $\Delta\Gamma$ depending on the countercouplings. The countercouplings themselves have to be determined as functions of the renormalized parameters. This action coincides with the NLO part of the two-particle irreducible (2PI) action obtained by introducing explicit bilocal sources conjugated to the quadratic combinations of the field variables in addition to the source terms linear in the fields and constructing the functional Legendre transform with respect to both (see Sects. 2.8 and 4.7). The effective action was obtained in this way in [7].

5.5 Renormalization of the $O(N)$-Model in the Auxiliary Formulation

In this section, the counterterm $\Delta\Gamma[v, \rho, G_\pi, \mathscr{G}]$ displayed in the effective action (5.55) will be constructed, which provides on variational differentiation the appropriate subtractions renormalizing (5.47) and (5.54) of the 1- and 2-point functions. The task will be solved in two steps. One starts at LO, and using its results, one can proceed to the determination of the NLO piece of $\Delta\Gamma$. The treatment follows the constructive strategy of [8, 9]. For notational simplicity below, the index "R" is omitted from the symbols of the renormalized coupling and the mass parameter appearing in (5.55).

5.5.1 Leading-Order Counterterm Action Functional

The respective LO parts of the equations of (5.47) in momentum representation are reproduced by taking the derivative of (5.55) with respect to v and ρ

and keeping only terms proportional to N. It will be sufficient to assume that $\Delta\Gamma^{(LO)}[v,\rho,G_\pi,\mathscr{G}] = \Delta\Gamma_\rho^{(LO)}[\rho]$:

$$\frac{\delta\Gamma_{eff}}{\delta v} = N(vM^2 - h) = 0,$$
$$\frac{\delta\Gamma_{eff}}{\delta\rho} = -\frac{3N}{\lambda}\rho + \frac{N}{2}\left(v^2 + \int_k G_\pi(k)\right) + \frac{\delta\Delta\Gamma_\rho^{(LO)}}{\delta\rho} = 0. \tag{5.57}$$

Only the second equation requires a counterterm contribution, since it has the divergent piece originating from the pion tadpole. It is a modified expression of (5.36), valid for nonzero pion mass. From here on, a unified notation of the divergent (strongly cutoff-dependent) quantities will be used throughout the chapter. The quadratically divergent expression $\mathscr{T}_d^{(2)}$ is denoted by $\mathscr{I}_d^{(0,1)}$, and the logarithmically divergent $\mathscr{B}_d^{(0)}$ by $\mathscr{I}_d^{(0,2)}$. The complete set of divergent quantities relevant for the renormalization will be listed in Eq. (5.75). With the new notation, the finite part of the pion tadpole is defined after subtracting the quadratic and the logarithmic divergences:

$$\int_k G_\pi(k) = \mathscr{T}_\pi^F + \mathscr{I}_d^{(0,1)} + (M_0^2 - M^2)\mathscr{I}_d^{(0,2)}. \tag{5.58}$$

The divergence due to the pion tadpole is compensated by the following contribution to the counterterm action,

$$\Delta\Gamma_\rho^{(LO)}[\rho] = -\frac{N}{2}\rho\left[\mathscr{I}_d^{(0,1)} - \left(m^2 - M_0^2 + \frac{\rho}{2}\right)\mathscr{I}_d^{(0,2)}\right], \tag{5.59}$$

resulting in a finite equation that determines ρ (called a *saddle-point equation*):

$$-\frac{3}{\lambda}\rho + \frac{1}{2}\left(v^2 + \mathscr{T}_\pi^F\right) = 0. \tag{5.60}$$

The meaning of M^2 is determined by the LO expression of the pion propagator:

$$\frac{\delta\Gamma_{eff}}{\delta G_\pi(k)} = N\frac{1}{2}\left(-G_\pi^{-1}(k) + D_\pi^{-1}(k)\right) = 0, \qquad M_\pi^2 = M^2 = \frac{h}{v}. \tag{5.61}$$

The last equality, which exploits the equation of state, expresses Goldstone's theorem in the presence of the explicit symmetry-breaking source h.

The leading-order propagators in the coupled $\rho - \sigma$ sector are determined by the NLO piece of (5.55) using the above LO solution of the model in the auxiliary formulation. Since its result for $G_{\sigma\sigma}$ is necessary for the com-

plete comparison with the LO solution obtained with the approach based on the directly derived Dyson–Schwinger equations, we discuss this sector in this subsection.

The inverse propagator matrix to leading order can be read off from (5.54) keeping only $\mathcal{O}(N^0)$ terms on the right-hand side:

$$\mathcal{G}_{LO}^{-1}(k) = \begin{pmatrix} -1 - \frac{\lambda}{6}(\mathcal{B}_\pi^F(k) + \mathcal{I}_d^{(0,2)}) & \sqrt{\frac{\lambda}{3}}v \\ \sqrt{\frac{\lambda}{3}}v & k^2 + M^2 \end{pmatrix}. \tag{5.62}$$

Clearly, the cancellation of the logarithmic divergence in $G_{\rho\rho}^{-1}$ requires the following additional piece into the counteraction functional:

$$\Delta\Gamma_{\rho\rho}[G_{\rho\rho}] = \frac{\lambda}{12}\mathcal{I}_d^{(0,2)} \int G_{\rho\rho}(k). \tag{5.63}$$

Then the renormalized propagator matrix is given as

$$\mathcal{G}_{LO}(k) = -\left((k^2 + M^2)\left(1 + \frac{\lambda}{6}\mathcal{B}_\pi^F(k)\right) + \frac{\lambda}{3}v^2\right)^{-1} \begin{pmatrix} k^2 + M^2 & -\sqrt{\frac{\lambda}{3}}v \\ -\sqrt{\frac{\lambda}{3}}v & -1 - \frac{\lambda}{6}\mathcal{B}_\pi^F(k) \end{pmatrix}, \tag{5.64}$$

which leads for $G_{\sigma\sigma}$ to the same expression as (5.35), generalized to nonzero pion mass. The common denominator signals that the σ and the composite $\rho \sim \sigma^2 + \pi^2$ fields have degenerate spectra (in the broken symmetry phase), a phenomenon sometimes called *hybridization*.

Some further insight can be gained into the working of the large-N expansion by rederiving the inverse propagator matrix of the $\rho - \sigma$ sector in an alternative way. Let us return to (5.46). Recognizing that it is formally quadratic in $\pi_\alpha(x)$, one is allowed to perform the functional integral over this multiplet in an inhomogeneous $\bar{\rho}(x)$ background. In this integration, however, one has to include the part of the counteraction depending on the pion fields. Therefore, in this part of the action one has to make use of the bare couplings. In order to avoid confusion, we append to them explicitly the lower index B. From the auxiliary field, the constant piece is transferred into the effective pion mass term

$$\bar{\rho} \to \bar{\rho}_0 + \bar{\rho}, \qquad M_B^2 = m_B^2 + \sqrt{\frac{\lambda_B}{3}}\bar{\rho}_0, \tag{5.65}$$

yielding in this way the effective theory of the $\rho - \sigma$ sector:

$$S_{eff}[\sigma, \bar{\rho}, v] = \int d^4x \Bigg[\frac{1}{2}(\partial_m \sigma(x))^2 - \sqrt{N} h(\sqrt{N} v + \sigma(x)) + \frac{1}{2}\left(M_B^2 + \sqrt{\frac{\lambda_B}{3N}}\bar{\rho}(x) \right)\left(\sigma^2(x) + 2\sqrt{N} v \sigma(x) + N v^2 \right) - \frac{(\bar{\rho}_0 + \bar{\rho}(x))^2}{2} \Bigg] + \frac{N-1}{2} \mathrm{Tr}_x \log\left(-\Box + M_B^2 + \sqrt{\frac{\lambda_B}{3N}}\bar{\rho}(x) \right). \tag{5.66}$$

If we take the derivative of this effective action with respect to v, the equation of state tells us that the combination M_B^2 is finite: $M_B^2 = M^2$. This is reflected already in the notation if we rewrite the last term, relying on the basic features of the logarithm, as

$$\frac{N-1}{2} \mathrm{Tr}_x \log\left(-\Box + M^2 + \sqrt{\frac{\lambda_B}{3N}}\bar{\rho}(x) \right) = \frac{N-1}{2} \mathrm{Tr}_x \left[\log\left(-\Box + M^2 \right) + \sum_{n=1}^{\infty} \frac{(-1)^{n+1}}{n} \left(D_\pi(x, z) \sqrt{\frac{\lambda_B}{3N}} \bar{\rho}(z) \right)^n \right]. \tag{5.67}$$

The elements of the inverse $\rho - \sigma$ propagator matrix are constructed by computing the second functional derivative of (5.66) with respect to the appropriate pairs of the field variables. Not surprisingly, we arrive at the matrix $\mathscr{G}_{LO}^{-1}$ as given in (5.62) with the replacement $\lambda \to \lambda_B$, which makes the $\rho\rho$ element finite. It automatically contains the additional $\mathscr{O}(N^0)$ contribution to the propagator matrix in the $\rho - \sigma$-sector relative to its tree-level expression. This rederivation of (5.64) reveals an important advantage of using the auxiliary field: the contribution of a single pion-loop integral to the self-energy of the auxiliary field modifies the σ-propagator in the same way as does an infinite set of iterated pion bubbles. Also, (5.67) explicitly displays the large-N hierarchy of the different n-point functions of the composite field $\bar{\rho}$, which was important in the argument of the previous section for the natural truncation of the Dyson–Schwinger equations at $\mathscr{O}(1/N)$ order.

5.5.2 *Next-to-Leading-Order Counterterm Action Functional: Effects of the Landau Pole*

The NLO part of the counterfunctional $\Delta\Gamma^{(NLO)}$ will be determined as the sum of three terms:

$$\Delta\Gamma^{(NLO)}[G_\pi, v, \rho] = \Delta\Gamma_\pi[G_\pi, v, \rho] + \Delta\Gamma_v[v, \rho] + \Delta\Gamma_\rho^{(NLO)}[\rho]. \tag{5.68}$$

The piece $\Delta\Gamma_\pi$ cancels the divergence of the NLO part of the pion propagator. It contributes also to the expressions of $\delta\Delta\Gamma^{(NLO)}/\delta v$ and $\delta\Delta\Gamma^{(NLO)}/\delta\rho$. The next piece is determined by the requirement of suppressing the divergences of the equation of state. It contributes to $\delta\Delta\Gamma^{(NLO)}/\delta\rho$, but has no feedback on $\delta\Delta\Gamma^{(NLO)}/\delta G_\pi$. Finally, $\Delta\Gamma_\rho^{(NLO)}$ depends only on ρ. Therefore, it plays no role in canceling divergences in the other two equations. The three additive contributions are determined in this sequence.

5.5.2.1 Determination of $\delta\Gamma_\pi[G_\pi, v, \rho]$

The only 2-point function that has to be renormalized at the $\mathcal{O}(1/N)$ level for the determination of $\Delta\Gamma^{(NLO)}$ is the equation of G_π. The Fourier transform of its expression in (5.54) reads

$$G_\pi^{-1}(k) = D_\pi^{-1}(k) - \frac{\lambda}{3N}\int_p G_{\rho\rho}(p)G_\pi(p+k) + \frac{2}{N}\frac{\delta\Delta\Gamma_\pi}{\delta G_\pi(k)}. \tag{5.69}$$

Here in the last term, $\Delta\Gamma_\pi$ is the only piece of the full counterterm action that contributes to the pion propagator. It will be found by "integrating" the divergent $\mathcal{O}(1/N)$ contribution with respect to $G_\pi(k)$. In the integrand of the second term on the right-hand side, one is allowed to replace both propagators by their $\sim N^0$ accurate expressions:

$$\begin{aligned} D_\pi(q) &= \frac{1}{q^2+M^2}, \\ \lambda D_{\rho\rho}(q) &= -\frac{\lambda}{1+\frac{\lambda}{6}\mathcal{B}_\pi^F(q)+\frac{\lambda}{3}v^2 D_\pi(q)} \equiv -\frac{\lambda(p)}{1+\frac{v^2}{3}\lambda(p)D_\pi(p)}. \end{aligned} \tag{5.70}$$

Note that $\lambda(p)$ is defined here. After substitution, one can expand the integrand in powers of $\lambda(p)D_\pi$:

$$G_\pi^{-1}(k) = D_\pi^{-1}(k) + \frac{1}{3N}\int_p \lambda(p)D_\pi(p+k)\sum_{n=0}^{\infty}\left(-\frac{\lambda(p)}{3}v^2 D_\pi(p)\right)^n + \frac{2}{N}\frac{\delta\Delta\Gamma_\pi}{\delta G_\pi(k)}. \tag{5.71}$$

Since among the terms of the expansion, arbitrarily high powers of $\lambda(p)$ appear, it is clear that one is not allowed to send the upper limit of the momentum integral to infinity. The cutoff value should be chosen below the location (5.44) of the Landau singularity. The sensitivity of the different terms is illustrated by Fig. 5.2, which displays the cutoff dependence of several integrals from the set

$$\mathcal{I}^{(n,m)} = \int_p \lambda^n(p)D_\pi^m(p) \tag{5.72}$$

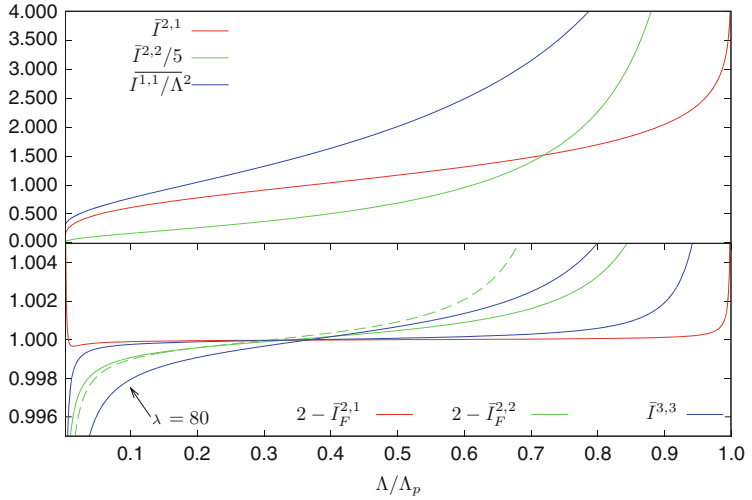

Fig. 5.2 The dependence of the "divergent" integrals (*upper part*) and subtracted or convergent integrals (*lower part*) on the cutoff Λ measured in proportion to the estimated location of the Landau pole (Λ_p). The integrals are defined in (5.72). One applies $\Lambda \to \infty$ in the finite bubble integrals $\mathscr{B}_\pi^F(p)$ and $\mathscr{B}_0^F(p)$, with the exception of the *dashed curve* corresponding to $j = k = 2$, for which a cutoff regularization is applied. The *bar* on $\mathscr{I}^{j,k}$ indicates that the integrals are scaled by the value taken at the inflection point (inflection of $\mathscr{I}^{1,1}/\Lambda^2$ when $j = k = 1$) and, for the sake of the presentation, also by an additional factor in the case of $j = k = 2$. We set $M = 1$, $M_0/M = 2$, and used $\lambda = 65$ for the coupling, except where indicated (from [9])

up to the Landau pole for various choices of n, m for a pion mass much below the cutoff ($M^2 \ll \Lambda^2$).

From Fig. 5.2, it is obvious that the integrals that are termed "convergent" by a simple power counting ($m > 2$) become insensitive to the cutoff well below the Landau pole, while the integrals with $m = 1, 2$ display clear numerical evidence for divergence. The graphs in the lower part demonstrate that with appropriate subtractions, these integrals are made cutoff-insensitive. Such subtractions are applied in the consistent renormalization procedure described below. For this reason, the conventional classification of the integrals into "divergent" and "convergent" classes will be employed below, although one is not allowed to send the cutoff beyond the Landau singularity. One expects that the NLO correction to the pion propagator will become insensitive to the actual value of the cutoff momentum below the Landau pole if one subtracts appropriate expressions from the integrals of the $n = 0, 1$ terms of (5.71). This is a mathematically less strict but pragmatic understanding of the renormalization [9], which represents an intuitive attempt to carry over the results of perturbative renormalization theory to this cutoff theory.

Before proceeding to the construction of the counterterms, one has to investigate whether there is any prospective dependence of the divergences on the external momentum of the pion propagator. Consider first the difference

$$\int_p \lambda(p)(D_\pi(p+k) - D_\pi(p)) = \int_p \lambda(p) \frac{1}{p^2+M^2} \sum_{n=1}^{\infty} \left(-\frac{k^2+2pk}{p^2+M^2} \right)^n . \tag{5.73}$$

Any contribution to the possible wave function renormalization should show up in terms proportional to k^2. These contributions are contained in the $n = 1, 2$ terms of the above expansion. Terms of the integral proportional to k^2 are

$$\int_p \lambda(p) \frac{1}{(p^2+M^2)^3} [4(pk)^2 - k^2(p^2+M^2)], \tag{5.74}$$

from which the term in the integrand proportional to k^2M^2 is convergent, while by the $O(4)$ invariance of the Euclidean integrand, one is allowed to make the replacement $4(pk)^2 \to k^2p^2$. This proves that the expression of the pion propagator displays only momentum-independent divergence.

The subtractions will be made independent of the dynamical variables of the system (recall that $M^2 \sim \rho$) by subtracting a combination of the following divergent integrals, each depending on a single mass scale, the renormalization scale M_0:

$$\begin{aligned} &\mathscr{I}_d^{(0,1)} = \int_p D_0(p), \qquad \mathscr{I}_d^{(0,2)} = \int_p D_0^2(p), \qquad \mathscr{I}_a^{(1,1)} = \int_p \lambda_0(p) D_0(p) \\ &\mathscr{I}_a^{(2,2)} = \int_p \lambda_0^2(p) D_0^2(p), \qquad \mathscr{I}_a^{(2,I)} = \int_p \lambda_0^2(p) D_0^2(p) \mathscr{B}_0^F(p), \end{aligned} \tag{5.75}$$

where

$$\begin{aligned} D_0(p) &= \frac{1}{p^2+M_0^2}, \quad \mathscr{B}_0^F(p) = \int_q D_0(q) D_0(p+q) - \mathscr{I}_d^{(0,2)}, \\ \lambda_0(p) &= \frac{\lambda}{1 + \frac{\lambda}{6} \mathscr{B}_0^F(p)}. \end{aligned} \tag{5.76}$$

The divergence of the $n = 1$ term of (5.71) is trivially seen to be given by the same integral with the index π replaced everywhere by 0. One promptly identifies the divergent integral with one of the divergent expressions listed in (5.75):

$$-\frac{v^2}{9N} \int_p \lambda^2(p) D_\pi^2(p)\big|_{div} = -\frac{v^2}{9N} \int_p \lambda_0^2(p) D_0^2(p) = -\frac{v^2}{9N} \mathscr{I}_a^{(2,2)}. \tag{5.77}$$

The divergence analysis of the $n = 0$ terms makes use of the following iterative series of D_π and $\lambda(p)$ in terms of D_0 and $\lambda_0(p)$:

$$D_\pi(p) = D_0(p) + (M_0^2 - M^2)D_0(p)D_\pi(p),$$
$$\lambda(p) = \lambda_0(p) + \frac{1}{6}\lambda_0(p)\lambda(p)(\mathscr{B}_0^F(p) - \mathscr{B}_\pi^F(p)). \tag{5.78}$$

Direct analytic integration allows one to determine the difference $\mathscr{B}_0^F(p) - \mathscr{B}_\pi^F(p)$, which one needs here with $\mathscr{O}(1/p^2)$ accuracy:

$$\mathscr{B}_0^F(p) - \mathscr{B}_\pi^F(p)$$
$$= \left[\frac{1}{8\pi^2}\left(3(M^2 - M_0^2) - M^2\ln\frac{M^2}{M_0^2}\right) - 2(M^2 - M_0^2)\mathscr{B}_0^F(p)\right]D_0(p). \tag{5.79}$$

It is obvious that the iteratively produced difference between the quantities defined with different mass scales are $\mathscr{O}(p^{-2})$ in both cases. For finding the divergent piece to be subtracted from the $n = 0$ term of the expansion, it is sufficient to approximate the differences with the first terms of the respective iterations and write

$$\frac{1}{3N}\int_p \lambda(p)D_\pi(p)\big|_{div} = \frac{1}{3N}\int_p \left(\lambda_0(p) + \frac{1}{6}\lambda_0^2(p)(\mathscr{B}_0^F(p) - \mathscr{B}_\pi^F(p))\right)$$
$$\times \left(D_0(p) + (M_0^2 - M^2)D_0^2(p))\right)\big|_{div}. \tag{5.80}$$

In the product, one keeps only the divergent terms

$$\frac{1}{3N}\int_p \lambda(p)D_\pi(p)\big|_{div} = \frac{1}{3N}\int_p \Bigg\{\lambda_0(p)D_0(p) + (M_0^2 - M^2)\lambda_0(p)D_0^2(p)$$
$$+\frac{1}{6}\lambda_0^2(p)D_0^2(p)\left[\left(\frac{3}{8\pi^2} - 2\mathscr{B}_0^F(p)\right)(M^2 - M_0^2) - \frac{1}{8\pi^2}M^2\ln\frac{M^2}{M_0^2}\right]\Bigg\}. \tag{5.81}$$

Since the counterterm should be a polynomial of the variables, one reexpresses the last term in the square brackets with the help of the explicit expression for the finite part of the tadpole integral:

$$\frac{1}{16\pi^2}M^2\ln\frac{M^2}{M_0^2} = \mathscr{T}_\pi^F - \frac{1}{16\pi^2}(M_0^2 - M^2)$$
$$= \int_p G_\pi(p) - \mathscr{I}_d^{(0,1)} - (M_0^2 - M^2)\mathscr{I}_d^{(0,2)} - \frac{1}{16\pi^2}(M_0^2 - M^2), \tag{5.82}$$

which is nothing but the relation (5.58). The final form to be used in the determination of $\Delta\Gamma_\pi$ is the following:

$$\begin{aligned}
&\frac{1}{3N}\int_p \lambda(p)D_\pi(p)\big|_{div} \\
&= \frac{1}{3N}\Bigg[\mathscr{I}_a^{(1,1)} + \frac{1}{2}(M_0^2 - M^2)\mathscr{I}_a^{(2,I)} + \mathscr{I}_a^{(2,2)}(M_0^2 - M^2)\left(\frac{1}{\lambda} - \frac{1}{24\pi^2}\right) \\
&\quad - \frac{1}{3}\mathscr{I}_a^{(2,2)}\left(\int_p G_\pi(p) - \mathscr{I}_d^{(0,1)} - (M_0^2 - M^2)\mathscr{I}_d^{(0,2)}\right)\Bigg].
\end{aligned} \tag{5.83}$$

The sum of the two contributions (5.77) and (5.83) determines the necessary counterterm

$$\begin{aligned}
&\Delta\Gamma_\pi[G_\pi, v, \rho] \\
&= -\frac{1}{6}\int_q G_\pi(q)\Bigg\{\mathscr{I}_a^{(1,1)} + \frac{1}{2}(M_0^2 - M^2)\mathscr{I}_a^{(2,I)} \\
&\quad + \mathscr{I}_a^{(2,2)}\left[-\frac{v^2}{3} + (M_0^2 - M^2)\left(\frac{1}{\lambda} - \frac{1}{24\pi^2}\right)\right] \\
&\quad - \frac{1}{3}\mathscr{I}_a^{(2,2)}\left(\frac{1}{2}\int_q G_\pi(q) - \mathscr{I}_d^{(0,1)} - (M_0^2 - M^2)\mathscr{I}_d^{(0,2)}\right)\Bigg\}.
\end{aligned} \tag{5.84}$$

5.5.2.2 Determination of $\Delta\Gamma_v[v, \rho]$

One can proceed further with the equation of state:

$$\frac{\delta\Gamma}{\delta v} = N(M^2 v - h) + \sqrt{\frac{\lambda}{3}}\int_p D_{\rho\sigma}(p) + \frac{\delta\Delta\Gamma_v}{\delta v} + \frac{\delta\Delta\Gamma_\pi}{\delta v} = 0. \tag{5.85}$$

Using the explicitly known expressions for $D_{\rho\sigma}$ and $\Delta\Gamma_\pi$, one has to determine a new piece of the counterterm action, $\Delta\Gamma_v$, not allowing any feedback on the pion propagator equation, that does not depend on $\mathscr{T}_\pi \equiv \int_q D_\pi(q)$. The equation to be integrated is the following:

$$0 = \frac{1}{3}\int_p \lambda(p)D_\pi(p)\sum_{n=1}^{\infty}\left(-\frac{\lambda(p)}{3}v^2 D_\pi(p)\right)^n\Big|_{div} + 2\frac{\delta\Delta\Gamma_v}{\delta v} + \frac{1}{9}\mathscr{T}_\pi\mathscr{I}_a^{(2,2)}. \tag{5.86}$$

The cancellation condition of the divergences can be written down instantly, since the first term on the right-hand side exactly coincides with the expression already analyzed in connection with the pion propagator:

$$0 = \frac{2\delta\Delta\Gamma_v}{\delta v^2} + \frac{1}{9}\mathscr{T}_\pi \mathscr{I}_a^{(2,2)} + \frac{1}{3}\Bigg\{ -\frac{v^2}{3}\mathscr{I}_a^{(2,2)} + \mathscr{I}_a^{(1,1)} + \frac{1}{2}(M_0^2 - M^2)\mathscr{I}_a^{(2,I)} + \mathscr{I}_a^{(2,2)}\Big[(M_0^2 - M^2)\left(\frac{1}{\lambda} - \frac{1}{24\pi^2}\right) - \frac{1}{3}\left(\mathscr{T}_\pi - \mathscr{I}_d^{(0,1)} - (M_0^2 - M^2)\mathscr{I}_d^{(0,2)}\right)\Big]\Bigg\}. \tag{5.87}$$

The mutual cancellation of the two terms proportional to $\mathscr{T}_\pi$ is important from two aspects. First, it ensures the independence of $\Delta\Gamma_v$ on G_π. Second, it demonstrates the cancellation of a subdivergence $\sim \mathscr{T}_\pi^F \mathscr{I}_a^{(2,2)}$, the presence of which would be dangerous, since $\mathscr{T}_\pi^F$ is environment- (temperature- and/or density-) dependent. The integration of the resulting form of the condition is very simple; it gives

$$\Delta\Gamma_v[v,\rho] = \frac{v^4}{36}\mathscr{I}_a^{(2,2)} - \frac{v^2}{6}\Bigg[\mathscr{I}_a^{(1,1)} + \frac{1}{2}(M_0^2 - M^2)\mathscr{I}_a^{(2,I)} + \mathscr{I}_a^{(2,2)}\left(\frac{1}{\lambda} - \frac{1}{24\pi^2} + \frac{1}{3}\left(\mathscr{I}_d^{(0,1)} + (M_0^2 - M^2)\mathscr{I}_d^{(0,2)}\right)\right)\Bigg]. \tag{5.88}$$

It is interesting to note that a counterterm $\sim v^4$ is also generated, although the (renormalized) coefficient of this term in the auxiliary formulation of the model is fixed to zero. This is not forbidden, since this piece is fully compatible with the symmetry of the system.

5.5.2.3 Determination of $\Delta\Gamma_\rho^{(NLO)}[\rho]$

The final task is the renormalization of the saddle point equation that determines the actual value of the composite field ρ. Both previously determined counterterms contribute to the divergence cancellation condition to be satisfied for the NLO-renormalization of $\delta\Delta\Gamma/\delta\rho$:

$$0 = \frac{1}{2}\int_k G_\pi^{(NLO)}(k)\Big|_{div} + \frac{1}{2}\int_k (D_{\sigma\sigma}(k) - D_\pi(k))\Big|_{div} + \frac{\delta[\Delta\Gamma_\pi + \Delta\Gamma_v]}{\delta\rho} + \frac{\delta\Delta\Gamma_\rho^{(NLO)}}{\delta\rho}. \tag{5.89}$$

From (5.84) and (5.88), one directly obtains

$$\frac{\delta[\Delta\Gamma_\pi + \Delta\Gamma_v]}{\delta\rho} = \frac{1}{6}\left(v^2 + \mathscr{T}_\pi\right)\left[\frac{1}{2}\mathscr{I}_a^{(2,I)} + \mathscr{I}_a^{(2,2)}\left(\frac{1}{\lambda} - \frac{1}{24\pi^2} + \frac{1}{3}\mathscr{I}_d^{(0,2)}\right)\right], \tag{5.90}$$

which has to be canceled by the divergences of the first two terms for a self-consistent determination of $\Delta\Gamma_\rho$, since this functional can depend on neither on v^2 nor $\mathscr{T}_\pi$.

The divergence of the second term on the right-hand side of (5.89) is found rather easily by exploiting the explicit expression of $D_{\sigma\sigma}$ from (5.64):

$$\begin{aligned}\frac{1}{2}\int_k \left(D_{\sigma\sigma}(k) - D_\pi(k)\right)\Big|_{div} &= \frac{1}{2}\sum_{n=1}^{\infty}\int_k D_\pi(k)\left(-\frac{\lambda(k)}{3}v^2 D_\pi(k)\right)^n\Big|_{div} \\ &= -\frac{v^2}{6}\int_k D_\pi^2(k)\lambda(k)\Big|_{div} = -\frac{v^2}{6}\left(\frac{1}{\lambda}\mathscr{I}_a^{(2,2)} + \frac{1}{6}\mathscr{I}_a^{(2,I)}\right).\end{aligned} \tag{5.91}$$

The divergence analysis of the first term on the right-hand side of (5.89) begins by finding a more explicit representation for the NLO correction of the tadpole integral of the pion, to be calculated from the definition of the renormalized NLO self-energy:

$$\begin{aligned}G_\pi^{(NLO)-1}(p) &= D_\pi^{-1}(p) + \frac{1}{N}\Sigma_\pi^{(NLO)}(p), \\ \Sigma_\pi^{(NLO)}(p) &= \frac{1}{3}\left[\int_k \lambda G_{\rho\rho}(k) D_\pi(p+k) - t_{div} + \frac{1}{3}\mathscr{I}_a^{(2,2)}(v^2 + \mathscr{T}_\pi)\right].\end{aligned} \tag{5.92}$$

The expression completing the integral in the square brackets ensures the finiteness of $\Sigma_\pi^{(NLO)}$. Here t_{div} is a shorthand notation for the part of the divergence of $\int_k \lambda G_{\rho\rho}(k) D_\pi(k)$ that is independent of both v^2 and $\mathscr{T}_\pi$:

$$\begin{aligned}t_{div} &= \mathscr{I}_a^{(1,1)} + \frac{1}{2}(M_0^2 - M^2)\mathscr{I}_a^{(2,I)} \\ &\quad + \mathscr{I}_a^{(2,2)}\left[(M^2 - M_0^2)\left(\frac{1}{\lambda} - \frac{1}{24\pi^2} + \frac{1}{3}\mathscr{I}_d^{(0,2)}\right) + \frac{1}{3}\mathscr{I}_d^{(0,1)}\right].\end{aligned} \tag{5.93}$$

Calculating the reciprocal of the expression of $G_\pi^{(NLO)-1}$ with $\mathscr{O}(1/N)$ accuracy gives

$$\frac{1}{2}\int_k G_\pi^{(NLO)}(k) = -\frac{1}{2}\int_k D_\pi^2(k)\Sigma_\pi^{(NLO)}(k)$$

$$= -\frac{1}{6}\int_k D_\pi^2(k)\int_p \lambda D_{\rho\rho}(p) D_\pi(p+k) + \frac{1}{6}\mathscr{B}_\pi(0)\left(t_{div} - \frac{1}{3}\mathscr{I}_a^{(2,2)}(v^2 + \mathscr{T}_\pi)\right). \tag{5.94}$$

One obtains the complete divergence by analyzing the divergence of its first term (the second belongs fully to the divergent part). One can interchange the k- and p-integrations and use the analytic expression of the internal integral:

$$\int_k D_\pi^2(k) D_\pi(p+k) = -\frac{1}{p^2+4M^2}\left(\mathscr{B}_\pi^F(p) - \mathscr{B}_\pi^F(0) - \frac{1}{8\pi^2}\right) \tag{5.95}$$

with

$$\mathscr{B}_\pi^F(0) = -\frac{1}{16\pi^2}\ln\frac{M^2}{M_0^2}. \tag{5.96}$$

For the relevant integral, one arrives at a representation very convenient for the divergence analysis:

$$\begin{aligned}
&\frac{1}{6}\int_p \lambda D_{\rho\rho}(p)\frac{1}{p^2+4M^2}\left(\mathscr{B}_\pi^F(p) - \mathscr{B}_\pi^F(0) - \frac{1}{8\pi^2}\right)\Big|_{div} \\
&= \frac{1}{6}\int_p \lambda D_{\rho\rho}(p) D_\pi(p)\mathscr{B}_\pi^F(p)\Big|_{div} - \frac{1}{6}\int_p \lambda D_{\rho\rho}(p) D_\pi(p)\left(\mathscr{B}_\pi^F(0) + \frac{1}{8\pi^2}\right)\Big|_{div} \\
&\quad - \frac{1}{6}\int_p \lambda(p)\frac{3M^2}{(p^2+M_0^2)^2}\left(\mathscr{B}_0^F(p) - \mathscr{B}_\pi^F(0) - \frac{1}{8\pi^2}\right)\Big|_{div}.
\end{aligned} \tag{5.97}$$

In the first integral, one has to expand $D_{\rho\rho}$ up to the term linear in v^2 to obtain

$$\frac{1}{6}\int_p \lambda D_{\rho\rho}(p) D_\pi(p)\mathscr{B}_\pi^F(p)\Big|_{div} = -\frac{1}{18}v^2\mathscr{I}_a^{(2,I)} + \mathscr{I}_d^{(0,1)} + (M_0^2 - M^2)\mathscr{I}_d^{(0,2)} - \frac{1}{\lambda}t_{div} + \frac{1}{3\lambda}\mathscr{I}_a^{(2,2)}\mathscr{T}_\pi. \tag{5.98}$$

The second integral of (5.97) is dangerous, since it is proportional to $-\mathscr{B}_\pi^F(0)$, which depends logarithmically on M^2. However, it is multiplied just by the integral giving the divergence of $\Sigma^{(NLO)}$. Therefore, it is canceled by a part of the last term of (5.94). We obtain in this way

$$-\frac{1}{6}\int_p \lambda D_{\rho\rho}(p) D_\pi(p)\left(\mathscr{B}_\pi^F(0) + \frac{1}{8\pi^2}\right)\Big|_{div}$$

$$+\frac{1}{6}\mathscr{B}_\pi(0)\left(t_{div}-\frac{1}{3}\mathscr{I}_a^{(2,2)}(v^2+\mathscr{T}_\pi)\right)$$
$$=\frac{1}{6}\left(\mathscr{I}_d^{(0,2)}-\frac{1}{8\pi^2}\right)\left(t_{div}-\frac{1}{3}\mathscr{I}_a^{(2,2)}(v^2+\mathscr{T}_\pi)\right). \tag{5.99}$$

In the third integral of (5.97), again the dangerous factor $\mathscr{B}_\pi^F(0)$ appears. However, it is now multiplied by M^2 and can be replaced using its relationship to the tadpole integral:

$$M^2\mathscr{B}_\pi^F(0)=-\mathscr{T}_\pi+\mathscr{I}_d^{(0,1)}+(M_0^2-M^2)\mathscr{I}_d^{(0,2)}+\frac{1}{16\pi^2}(M^2-M_0^2). \tag{5.100}$$

Using this, the last integral produces the following divergent pieces:

$$-\frac{1}{6}\int_p\lambda(p)\frac{3M^2}{(p^2+M_0^2)^2}\left(\mathscr{B}_0^F(k)-\mathscr{B}_\pi^F(0)-\frac{1}{8\pi^2}\right)\Big|_{div}$$
$$=-3M^2\left(\mathscr{I}_d^{(0,2)}-\frac{1}{\lambda^2}\mathscr{I}_a^{(2,2)}-\frac{1}{6\lambda}\mathscr{I}_a^{(2,I)}\right)$$
$$+\frac{1}{2}\left(\frac{1}{\lambda}\mathscr{I}_a^{(2,2)}+\frac{1}{6}\mathscr{I}_a^{(2,I)}\right)$$
$$\times\left(\frac{M^2}{8\pi^2}-\mathscr{T}_\pi+\mathscr{I}_d^{(0,1)}+(M_0^2-M^2)\mathscr{I}_d^{(0,2)}+\frac{1}{16\pi^2}(M^2-M_0^2)\right). \tag{5.101}$$

One now adds together the contributions to the divergence of the two integrals appearing in the saddle-point equation that are proportional to v^2+T_π, and which can be extracted from Eqs. (5.91), (5.98), (5.99), and (5.101). One finds that the sum exactly cancels the contributions arising from the ρ-derivatives of $\Delta\Gamma_\pi+\Delta\Gamma_v$ in (5.90). This means that the realization of the renormalization program consistently ends with $\Delta\Gamma_\rho^{(NLO)}$:

$$\frac{\delta\Delta\Gamma_\rho^{(NLO)}}{\delta\rho}=-\mathscr{I}_d^{(0,1)}-(M_0^2-4M^2)\mathscr{I}_d^{(0,2)}-\frac{1}{6}\left(\mathscr{I}_d^{(0,2)}-\frac{1}{8\pi^2}-\frac{6}{\lambda}\right)t_{div}$$
$$-\frac{1}{2}\left(\frac{1}{\lambda}\mathscr{I}_a^{(2,2)}+\frac{1}{6}\mathscr{I}_a^{(2,I)}\right)$$
$$\times\left(\mathscr{I}_d^{(0,1)}+(M_0^2-M^2)\mathscr{I}_d^{(0,2)}+\frac{1}{16\pi^2}(3M^2-M_0^2)+\frac{6M^2}{\lambda}\right). \tag{5.102}$$

It is easy to see that $\Delta\Gamma_\rho^{(NLO)}$ is also a quadratic polynomial in M^2, as was the case for $\Delta\Gamma_\rho^{(LO)}$.

5.5.2.4 Summary and Discussion

The LO+NLO counterterm functional that has to be added to (5.55) has a rather simple functional form:

$$\Delta\Gamma[G_\pi, G_{\rho\rho}, v, \rho] = \left(\frac{1}{6}(v^2 + \mathscr{T}_\pi)\right)^2 \mathscr{I}_a^{(2,2)} - \frac{1}{6}(v^2 + \mathscr{T}_\pi)t_{div} + (Nc_1^{(N)} + c_1^{(0)})\rho + (Nc_2^{(N)} + c_2^{(0)})\rho^2, \quad (5.103)$$

where t_{div} was defined in (5.93), and the somewhat complicated divergent coefficients $c_i^{(N)}$ and $c_i^{(0)}$ can be found from $\Delta\Gamma_\rho^{(LO)} + \Delta\Gamma_\rho^{(NLO)}$. When one combines this expression with the renormalized couplings multiplying the corresponding functionals in (5.55), one obtains an expression with the bare couplings for the renormalized effective action. There are several couplings with vanishing renormalized value, still receiving a nonzero counterterm. An important example is given by the first term of (5.103), $\sim (v^2 + \mathscr{T}_\pi)^2$.

One can eliminate easily the auxiliary field ρ from the effective action by completing its quadratic action into a perfect square and substituting for the propagators $G_{\rho\rho}, G_{\rho\sigma}$ their expressions through $G_{\sigma\sigma}$. In this way, one arrives at a form that coincides with the 2PI action of the $O(N)$ model in the original variables [10].

Even though the renormalized action is given in its 2PI appearance, one has to understand that the renormalized action constructed above is not renormalized as an approximate 2PI solution. In the strict $1/N$ expansion, the subsequent terms are determined hierarchically, while in the 2PI approach, even in the large-N limit, the propagators are determined *self-consistently* [11].

An important consequence of the fact that the counteraction functional depends only on the sum $v^2 + \mathscr{T}_\pi$ is that the same subtraction is applied to the equation of $G_\pi^{-1}(p)$ and v. It ensures that Goldstone's theorem is also obeyed in the theory renormalized at the NLO level, since it is obviously satisfied in the unrenormalized expression.

5.6 Large-n Approximation in $U(n)$ Symmetric Models

The linear sigma model is formulated in terms of the matrix M with complex scalar field elements

$$M(x) = (s^a(x) + i\pi^a(x))\frac{\lambda_a}{2}, \quad (5.104)$$

where s^a (π^a) represents the (pseudo)scalar meson multiplet. The matrices $\lambda_a/2$, $a = 0, 1, \ldots, n^2 - 1$, are the generators of the $U(n)$ unitary group (λ^0 being proportional to the identity) satisfying the relations

$$\lambda^a \lambda^b = 2(d^{abc} + if^{abc})\lambda^c, \qquad \mathrm{tr}\lambda^a \lambda^b = 2\delta^{ab}. \tag{5.105}$$

A theory invariant under the global chiral transformation defined with the unitary transformations $U_{L/R}$,

$$M(x) \to U_L(n) M(x) U_R(n), \tag{5.106}$$

can be constructed with the help of the independent local chiral invariants

$$I_l = \mathrm{tr}(M^\dagger(x)M(x))^l, \qquad l = 1, 2, \ldots n-1. \tag{5.107}$$

In view of the requirement of perturbative renormalization in the weak coupling regime, one truncates the invariants to be included into the Lagrangian density at $l = 2$. The following Lagrangian density displaying explicitly the dependence on the bare couplings will be investigated below at large n in Euclidean space-time:

$$\begin{aligned} L = &\frac{1}{2}\left(\mathrm{tr}(\partial_m M^\dagger(x)\partial_m M(x)) + m_B^2 \mathrm{tr} M^\dagger(x) M(x)\right) \\ &+ \frac{g_{1B}}{n^2}\left(\mathrm{tr}M^\dagger(x)M(x)\right)^2 + \frac{g_{2B}}{n}\mathrm{tr}(M^\dagger(x)M(x))^2. \end{aligned} \tag{5.108}$$

The determinant term standing for the $U_A(1)$ anomaly in the case $n = 3$ (see (4.1)) becomes irrelevant for $n \to \infty$. One can therefore discard it. It is convenient for the discussion below to write this Lagrangian explicitly in terms of the component fields:

$$\begin{aligned} L = &\frac{1}{2}[s^a(x)(-\Box + m_B^2)s^a(x) + \pi^a(x)(-\Box + m_B^2)\pi^a(x) - \sqrt{2n^2}hs^0] \\ &+ \frac{g_{1B}}{4n^2}\left[(s^a(x))^2 + (\pi^a(x))^2\right]^2 + \frac{g_{2B}}{2n}(U^a(x))^2, \end{aligned} \tag{5.109}$$

where

$$U^a(x) = \frac{1}{2}d^{abc}(s^b(x)s^c(x) + \pi^b(x)\pi^c) - f^{abc}s^b(x)\pi^c(x). \tag{5.110}$$

5.6.1 Auxiliary Fields and Integration over Large Multiplicity Fields

The nonlinearity in the meson fields can be bypassed by introducing two auxiliary fields:

$$\Delta L = -\frac{1}{2}\left[X - \sqrt{\frac{g_{1B}}{2n^2}}\left((s^a)^2 + (\pi^a)^2\right)\right]^2 - \frac{1}{2}\left[Y^a - \sqrt{\frac{g_{2B}}{n}}U^a\right]^2. \tag{5.111}$$

At the same time, one applies a symmetry-breaking shift

$$s^0 \to s^0 + \sqrt{2n^2}v, \qquad U^a \to U^a + 2\sqrt{n}vs^a + n\sqrt{2n}v^2\delta^{a0}. \tag{5.112}$$

This shift corresponds to the expected spontaneous chiral symmetry-breaking pattern of the $U_L(n) \times U_R(n)$ symmetry.

The resulting shifted Lagrangian is the starting point for integrating over the $\mathcal{O}(n^2)$ multiplicity fields π^a, s^a, Y^a, which will produce the LO effective potential of the theory:

$$\begin{aligned} L = \frac{1}{2}\Bigg[& s^a(x)\left(-\Box + m_B^2 + X\sqrt{\frac{g_{1B}}{2n^2}}\right)s^a(x) \\ & + \pi^a(x)\left(-\Box + m_B^2 + X\sqrt{\frac{g_{1B}}{2n^2}}\right)\pi^a(x)\Bigg] + m_B^2 n^2 v^2 + m_B^2\sqrt{2n^2}s^0 v \\ & - \frac{1}{2}(X^2 + (Y^a)^2) + Y^a\sqrt{\frac{g_{2B}}{n}}U^a + 2\sqrt{g_{2B}}Y^a s^a v + Y^0\sqrt{2g_{2B}}nv^2 \\ & + 2s^0 X\sqrt{g_{1B}}v + X\sqrt{2n^2 g_{1B}}v^2 - \sqrt{2n^2}hs^0 - 2n^2 hv. \end{aligned} \tag{5.113}$$

The saddle-point approximation applied to the $O(N)$ model can be attempted here as well, but as we shall see shortly, the nonlinear interaction induced in the Y^a multiplet places an obstacle in the way of finding the exact LO effective potential.

Since this action contains also a term linear in the pion fields in addition to the quadratic piece,

$$\begin{aligned} & \frac{1}{2}\pi^b(x)\left\{\left[\left(-\Box + m_B^2 + X\frac{\sqrt{2g_{1B}}}{n}\right)\delta^{bc} + \sqrt{\frac{g_{2B}}{n}}Y^a d^{abc}\right]\delta(x-y)\right\}\pi^c(y) \\ & \quad - \sqrt{\frac{g_{2B}}{n}}Y^a f^{abc}s^b(x)\pi^c(x), \end{aligned} \tag{5.114}$$

one can apply the formal rules for the Gaussian functional integration by completing this expression into a perfect square. As a result, one obtains the following contributions to the effective action:

$$\frac{1}{2}\mathrm{Tr}\log(D_\pi^{-1})^{bc}(x-y) - \frac{g_{2B}}{2n}\int_x\int_y s^n(x)\left[f^{mnb}Y^m(x)D_\pi^{bc}(x-y)f^{pqc}Y^p(y)\right]s^q(y), \tag{5.115}$$

where

$$(D_\pi^{-1})^{bc}(x-y) = \left[\left(-\Box + m_B^2 + X\frac{\sqrt{2g_{1B}}}{n}\right)\delta^{bc} + \sqrt{\frac{g_{2B}}{n}}Y^a d^{abc}\right]\delta(x-y). \tag{5.116}$$

The next step is the s^a-integration ($a \neq 0$), in which the last term of (5.115) should also be included. Here one notes again that (5.113) contains a linear piece ($2\sqrt{g_{2B}}vY^a s^a$). Therefore, the structure of the result is similar to the result of the π-integration:

$$\frac{1}{2}\left[\mathrm{Tr}\log(D_s^{-1})^{bc}(x-y) - 4g_{2B}v^2\int_x\int_y Y^n(x)D_s^{nq}(x-y)Y^q(y)\right], \tag{5.117}$$

with

$$(D_s^{-1})^{nq}(x-y) = (D_\pi^{-1})^{nq}(x-y) - \frac{g_{2B}}{2n}\left[f^{mnb}Y^m(x)D_\pi^{bc}(x-y)f^{pqc}Y^p(y)\right]. \tag{5.118}$$

The last step, the integration over the auxiliary multiplet Y^a, cannot be performed exactly, since the π^a- and s^a-integrations induce essential nonlinearities into its effective action. This is why no exact solution can be derived for this model in the large-n limit. The best one can do is to expand the effective action up to quadratic terms in Y^a and take the corresponding one-loop result as an approximation.

Before proceeding with the expansion, we separate from X and Y^0 a homogeneous constant piece and form with them a universal basic propagator:

$$D_M^{-1}(x-y) = \left(-\Box + m_B^2 + \frac{\sqrt{2g_{1B}}}{n}X + \frac{\sqrt{2g_{2B}}}{n}Y^0\right)\delta(x-y) \equiv \left(-\Box + M^2\right)\delta(x-y). \tag{5.119}$$

Expanding the expressions of the "tracelogs" around this massive inverse propagator, one obtains the following contributions:

$$\frac{\delta^2}{\delta Y^e(y)Y^f(z')}\mathrm{Tr}\log(D_\pi^{-1}) = -\frac{g_{2B}}{2}D_M(z-z')D_M(z'-z)\delta^{ef}, \tag{5.120}$$

where one has to exploit the algebraic relation

$$\sum_0^{n^2-1} d^{fbc}d^{ecb} = n(1+\delta^{e0})\delta^{ef}. \tag{5.121}$$

Similarly, one obtains

$$\begin{aligned}
&\frac{\delta^2}{\delta Y^e(y)Y^f(z')}\mathrm{Tr}\log(D_s^{-1}))\\
&\quad = -\frac{g_{2B}}{2n}D_M(z-z')D_M(z'-z)\left(d^{fbc}d^{ecb}+2f^{ebc}f^{fbc}\right)\\
&\quad = -\frac{3g_{2B}}{2}D_M(z-z')D_M(z'-z)\delta^{ef},
\end{aligned} \tag{5.122}$$

where one exploits

$$\sum_1^{n^2-1} d^{fbc}d^{ecb} = n\left(1+\left(1-\frac{2}{n^2}\right)\delta^{e0}\right)\delta^{ef}, \qquad \sum_1^{n^2-1} f^{ebc}f^{fbc} = n(1-\delta^{e0})\delta^{ef}. \tag{5.123}$$

The resulting quadratic action is of the following form:

$$\begin{aligned}
-\frac{1}{2}\int_x\int_y\sum_{a=1}^{n^2-1} Y^a(x)\,&[\delta(x-y)+2g_{2B}D_M(x-y)D_M(y-x)\\
&+4g_{2B}v^2D_M(x-y)\big]\,Y^a(y).
\end{aligned} \tag{5.124}$$

After the approximate (Gaussian) Y^a-integral is performed, one obtains the following estimate for the $\sim n^2$ part of the effective potential per unit four-dimensional volume $V^{(LO)} = \Gamma^{(LO)}/(V_4n^2)$:

$$\begin{aligned}
V^{(LO)}[v,x,y_0] \approx\ & M^2v^2 - 2hv - \frac{1}{4g_{1B}}x^2 - \frac{1}{4g_{2B}}y_0^2\\
&+\frac{1}{2}\int_k\Bigg[\log\frac{k^2+M^2}{k^2+M_0^2}\\
&\quad+\log\frac{(k^2+M^2)(1+2g_{2B}\mathscr{B}_M(k))+4g_{2B}v^2}{(k^2+M_0^2)(1+2g_{2B}\mathscr{B}_0(k))}\Bigg],
\end{aligned} \tag{5.125}$$

where one has introduced the rescaled quantities

$$x = \frac{\sqrt{2g_{1B}}}{n} X, \qquad y_0 = \frac{\sqrt{2g_{2B}}}{n} Y^0, \tag{5.126}$$

and also

$$\mathscr{B}_M(k) = \int_p D_M(p) D_M(p+k). \qquad \mathscr{B}_0(k) = \int_p D_0(p) D_0(p+k), \tag{5.127}$$

with $D_M(k) = (k^2 + M^2)^{-1}$. Using the rescaled mean field condensates, one arrives at the following simple expression for the common effective mass scale:

$$M^2 = m_B^2 + x + y_0. \tag{5.128}$$

The introduction of the arbitrary constant denominators in the arguments of logarithms realizes the subtraction of the quartic divergences. It achieves that only quadratic and logarithmic divergences remain in the expression of the unrenormalized potential. The separation and subtraction of the remaining divergences will be presented in the next subsection after an elaborate discussion of the approximate nature of the proposed approximate large-n solution with the help of the exact large-n leading-order Dyson–Schwinger equations of the system.

5.6.2 *Interpretation and Renormalization of $V^{(LO)}(v, x, y_0)$*

The leading-order effective potential of the homogeneous background condensates displayed in (5.125) can be interpreted with the help of the Dyson–Schwinger equations obtained at leading order in the large-n expansion following the standard procedure. The full set has been derived in [12] on the assumption that the necessary 3-point functions are given by the tree-level expressions obtained from (5.113). It is sufficient here to consider the coupled set of the 2-point equations governing the fields π^a, Y^a, s^a, $a \neq 0$. The propagators are diagonal in the flavor index:

$$\begin{aligned} &G_{\pi^a\pi^b}(x-y) = G_\pi(x-y)\delta^{ab}, \quad G_{Y^aY^b}(x-y) = G_Y(x-y)\delta^{ab}, \\ &G_{Y^as^b}(x-y) = G_{Ys}(x-y)\delta^{ab}, \quad G_{s^as^b}(x-y) = G_s(x-y)\delta^{ab}, \end{aligned} \tag{5.129}$$

and their equations read as follows:

$$\begin{aligned} G_\pi^{-1}(x-y) = G_s^{-1}(x-y) &= (-\Box + M^2)\delta(x-y) \\ &-g_{2B}\left[G_Y(x-y)\left(G_\pi(y-x) + G_s(y-x)\right)\right. \\ &\left.+G_{Ys}(y-x)G_{Ys}(x-y)\right], \end{aligned}$$

$$
\begin{aligned}
G_Y^{-1}(x-y) &= -\delta(x-y) - g_{2B} G_s(y-x) G_\pi(x-y) \\
&\quad -\frac{g_{2B}}{2}\left[G_\pi(x-y)G_\pi(y-x)\right. \\
&\quad \left. +G_s(x-y)G_s(y-x)\right], \\
G_{Ys}^{-1}(x-y) &= 2\sqrt{g_{2B}}v\delta(x-y) \\
&\quad -g_{2B}G_{Ys}(x-y)\left[G_s(y-x) - G_\pi(y-x)\right]. \qquad (5.130)
\end{aligned}
$$

The sequence of functional integrations presented in the previous subsection corresponds to a particular *approximate solution* of the set of DS equations:

$$
\begin{aligned}
G_\pi^{-1}(x-y) &= G_s^{-1}(x-y) = (-\Box + M^2)\delta(x-y) \equiv D_M^{-1}(x-y), \\
G_Y^{-1}(x-y) &= -\delta(x-y) - 2g_{2B}D_M(y-x)D_M(x-y), \\
G_{Ys}^{-1}(x-y) &= 2\sqrt{g_{2B}}v\delta(x-y). \qquad (5.131)
\end{aligned}
$$

Comparing the exact and the approximate equations, it is clear that the approximate nature of the latter equations comes from neglecting the "back-reaction" of the Y^a field on the scalar and pseudoscalar propagators and also on themselves.

One can build a 2PI-like theory in which the 2-point functions of the $\pi^a, Y^a, s^a, a \neq 0$ fields appear as dynamical variables in addition to v, x, y_0, and this leads to the set (5.131):

$$
\begin{aligned}
\frac{1}{n^2}V_{n^2}^{2PI} &= m^2v^2 - 2hv + \frac{1}{4}\left(\frac{x^2}{g_1} + \frac{y_0^2}{g_2}\right) + (x+y_0)v^2 \\
&\quad + \frac{1}{2}\left[\mathrm{Tr}\left(\log G_\pi^{-1} + D_M^{-1}G_\pi\right) + \mathrm{Tr}\left(\log \mathscr{G}_{(s,Y)}^{-1} + \mathscr{D}_{(s,Y)}^{-1}\mathscr{G}_{(s,Y)}\right)\right] \\
&\quad + \frac{1}{n^2}V_{ct}^{2PI}[x, y_0, G_\pi, \mathscr{G}_{(s,Y)}]. \qquad (5.132)
\end{aligned}
$$

Here we use the renormalized couplings and collect the contributions containing the countercouplings in V_{ct}^{2PI}. The counterterm potential should compensate the quadratic and logarithmic divergences showing up when the expressions in the second line are evaluated.

After taking the variation of this potential functional with respect to G_π and the propagator matrix of the (s, Y)-sector $\mathscr{G}_{(s,Y)}$, one obtains

$$
\begin{aligned}
G_\pi^{-1}(k) &= D_M^{-1}(k), \\
\mathscr{G}_{(s,Y)}^{-1}(k) &= \mathscr{D}_{(s,Y)}^{-1}(k) = \begin{pmatrix} -1 - 2g_2(\mathscr{B}_M^F(k) + \mathscr{I}_d^{(0,2)}) & 2\sqrt{g_2}v \\ 2\sqrt{g_2}v & k^2 + M^2 \end{pmatrix}. \qquad (5.133)
\end{aligned}
$$

On substituting these expressions back into $V_{n^2}^{2PI}$, one recovers the integral contributions to (5.125).

The cancellation of all divergences of the effective potential with the help of appropriate counterterms automatically ensures the finiteness of the equation of state and of the saddle point equations (their formal expressions above should be complemented with the corresponding derivatives of the counterterm potential).

The only nontrivial task in (5.125) is to separate the divergences of the term

$$\begin{aligned}
&\frac{1}{2}\int_k \log\frac{(k^2+M^2)(1+2g_{2B}\mathscr{B}_M(k))+4g_{2B}v^2}{(k^2+M_0^2)(1+2g_{2B}\mathscr{B}_0(k))}\\
&=\frac{1}{2}\int_k \log\Bigg(1+\frac{M^2-M_0^2}{k^2+M_0^2}+\frac{2g_{2B}(\mathscr{B}_M(k)-\mathscr{B}_0(k))}{1+2g_{2B}\mathscr{B}_0(k)}\\
&+\frac{4g_{2B}v^2}{(k^2+M_0^2)(1+2g_{2B}\mathscr{B}_0(k))}+\frac{2g_{2B}(\mathscr{B}_M(k)-\mathscr{B}_0(k))(M^2-M_0^2)}{(k^2+M_0^2)(1+2g_{2B}\mathscr{B}_0(k))}\Bigg). \qquad (5.134)
\end{aligned}$$

The expansion of the logarithm up to quadratic terms contributes to the divergences of the integral. The relevant terms are the following, after some minor algebraic simplification:

$$\begin{aligned}
&\frac{1}{2}\int_k\Bigg\{\frac{M^2-M_0^2}{k^2+M_0^2}+\frac{2g_{2B}(\mathscr{B}_M(k)-\mathscr{B}_0(k))}{1+2g_{2B}\mathscr{B}_0(k)}+\frac{4g_{2B}v^2}{(k^2+M_0^2)(1+2g_{2B}\mathscr{B}_0(k))}\\
&-\frac{1}{2}\Bigg[\left(\frac{M^2-M_0^2}{k^2+M_0^2}\right)^2+\left(\frac{2g_{2B}(\mathscr{B}_M(k)-\mathscr{B}_0(k))}{1+2g_{2B}\mathscr{B}_0(k)}\right)^2\\
&+\left(\frac{4g_{2B}v^2}{(k^2+M_0^2)(1+2g_{2B}\mathscr{B}_0(k))}\right)^2\\
&+\frac{8g_{2B}v^2(M^2-M_0^2)}{(k^2+m_0^2)^2(1+2g_{2B}\mathscr{B}_0(k))}+\frac{16g_{2B}^2v^2(\mathscr{B}_M(k)-\mathscr{B}_0(k))}{(k^2+M_0^2)(1+2g_{2B}\mathscr{B}_0(k))^2}\Bigg]\Bigg\}. \qquad (5.135)
\end{aligned}$$

In order to find the divergent contributions explicitly, one has to expand $\Delta\mathscr{B}(k)\equiv\mathscr{B}_M(k)-\mathscr{B}_0(k)$ with k^{-4} accuracy:

$$\begin{aligned}
\Delta\mathscr{B}(k)&=2(M^2-M_0^2)D_0\mathscr{B}_0^F(k)\\
&+\left[\mathscr{T}_\pi-\mathscr{I}_d^{(0,1)}+(M^2-M_0^2)\mathscr{I}_d^{(0,2)}-\frac{1}{4\pi^2}(M^2-M_0^2)\right]D_0\\
&-2(M^2-M_0^2)\left[\mathscr{T}_\pi-\mathscr{I}_d^{(0,1)}+(M^2-M_0^2)\mathscr{I}_d^{(0,2)}+\frac{1}{32\pi^2}(M^2+11M_0^2)\right]D_0^2\\
&-2(M^4+M^2M_0^2-2M_0^4)D_0^2\mathscr{B}_0^F(k). \qquad (5.136)
\end{aligned}$$

The divergent pieces of all integrals appearing in (5.135) can be obtained with some straightforward but somewhat tedious algebra. Divergent terms appearing in some integrands can be absorbed into $\bar{g}_2$, defined with the relation

$$\lambda_g(k) = \frac{2g_{2B}}{1 + 2g_{2B}\mathscr{B}_0(k)} = \frac{2\bar{g}_2}{1 + 2\bar{g}_2\mathscr{B}_0^F(k)}. \tag{5.137}$$

Note that $\bar{g}_2$ is not necessarily finite; it just helps to define the divergent functions occurring in the subtractions in full analogy with the $O(N)$ case. Below, it follows the list of the divergent integrals expressed with the help of the standard functions (5.75), in which the replacement $\lambda/6 \to 2\bar{g}_2$ has to be done:

$$\int_k \frac{M^2 - M_0^2}{k^2 + M_0^2}\Big|_{div} = (M^2 - M_0^2)\mathscr{I}_d^{(0,1)}, \quad 2v^2 \int \lambda_g(k) D_0(k)\Big|_{div} = 2v^2 \mathscr{I}_d^{(1,1)}, \tag{5.138}$$

$$\begin{aligned}
&\int_k \lambda_g(k)(\mathscr{B}_M(k) - \mathscr{B}_0(k))\Big|_{div} = 2(M^2 - M_0^2)\left(\mathscr{I}_d^{(0,1)} - \frac{1}{2\bar{g}_2}\mathscr{I}_d^{(1,1)}\right) \\
&-2(M^2 - M_0^2)\left(\mathscr{I}_a^{(2,I)} + \frac{1}{2\bar{g}_2}\mathscr{I}_a^{(2,2)}\right) \\
&\quad\times\left[\mathscr{T}_\pi - \mathscr{I}_d^{(0,1)} + (M^2 - M_0^2)\mathscr{I}_d^{(0,2)} + \frac{1}{32\pi^2}(M^2 + 11M_0^2)\right] \\
&\quad - 2(M^4 + M^2M_0^2 - 2M_0^4)\left(\mathscr{I}_d^{(0,2)} - \frac{1}{2\bar{g}_2}\mathscr{I}_a^{(2,I)} - \frac{1}{(2\bar{g}_2)^2}\mathscr{I}_a^{(2,2)}\right) \\
&\quad + \left[\mathscr{T}_\pi - \mathscr{I}_d^{(0,1)} + (M^2 - M_0^2)\mathscr{I}_d^{(0,2)} - \frac{1}{4\pi^2}(M^2 - M_0^2)\right]\mathscr{I}_a^{(1,1)},
\end{aligned} \tag{5.139}$$

$$\begin{aligned}
-\frac{1}{2}\int_k \frac{(M^2 - M_0^2)^2}{(k^2 + M_0^2)^2}\Big|_{div} &= -\frac{1}{2}(M^2 - M_0^2)^2\mathscr{I}_d^{(0,2)}, \\
-2v^4 \int \lambda_g^2(k) D_0^2(k)\Big|_{div} &= -2v^4\mathscr{I}_a^{(2,2)},
\end{aligned} \tag{5.140}$$

$$\begin{aligned}
&-\frac{1}{2}\int_k \lambda_g^2(k)(\mathscr{B}_M(k) - \mathscr{B}_0(k))^2\Big|_{div} \\
&\quad = -2(M^2 - M_0^2)\left(\mathscr{I}_d^{(0,2)} - \frac{1}{\bar{g}_2}\mathscr{I}_a^{(2,I)} - \frac{1}{(2\bar{g}_2)^2}\mathscr{I}_a^{(2,2)}\right) \\
&\qquad - 2(M^2 - M_0^2)\left[\mathscr{T}_\pi - \mathscr{I}_d^{(0,1)} + (M^2 - M_0^2)\mathscr{I}_d^{(0,2)} - \frac{1}{4\pi^2}(M^2 - M_0^2)\right]\mathscr{I}_a^{(2,I)}
\end{aligned}$$

$$-\frac{1}{2}\left[\mathscr{T}_\pi - \mathscr{I}_d^{(0,1)} + (M^2 - M_0^2)\mathscr{I}_d^{(0,2)} - \frac{1}{4\pi^2}(M^2 - M_0^2)\right]^2 \mathscr{I}_a^{(2,2)}, \quad (5.141)$$

$$-2v^2(M^2 - M_0^2)\int_k \lambda_g(k) D_0^2(k)\Big|_{div} = -2v^2(M^2 - M_0^2)\left(\mathscr{I}_a^{(2,I)} + \frac{1}{2\bar{g}_2}\mathscr{I}_a^{(2,2)}\right), \quad (5.142)$$

$$-2v^2\int_k \lambda_g^2(k) D_0(k)(\mathscr{B}_M(k) - \mathscr{B}_0(k))\Big|_{div} = -4v^2(M^2 - M_0^2)\mathscr{I}_a^{(2,I)},$$

$$-2v^2\left[\mathscr{T}_\pi - \mathscr{I}_d^{(0,1)} + (M^2 - M_0^2)\mathscr{I}_d^{(0,2)} - \frac{1}{4\pi^2}(M^2 - M_0^2)\right]\mathscr{I}_a^{(2,2)}. \quad (5.143)$$

On collecting the various combinations of the dynamical variables occurring in the above singular integrals, one obtains for the counterterm potential a parameterization with the following nonzero countercouplings:

$$V_{ct}^{2PI}/n^2 = \delta m_0^2 v^2 + \frac{1}{4}\left(\delta_x x^2 + \delta_y y_0^2\right) + \delta_{xy} x y_0 + v^2(\delta_{yv} y_0 + \delta_{xv} x + \delta_{v^4} v^4)$$
$$+ (\delta m_\pi^2 + \delta_{x\pi} x + \delta_{y\pi} y_0) T_\pi + \delta_8 T_\pi^2. \quad (5.144)$$

It is worth remarking that in this expression, there are other counterterm contributions besides those that have nonzero renormalized coefficients. For instance, one obtains a counterterm proportional to the "figure-8" Feynman diagram, the squared pion tadpole. The divergent coefficients of x^2 and y_0^2 determine the bare couplings corresponding to $1/g_1$ and $1/g_2$, respectively.

The corresponding approximate solution for v, x, y_0 is simply given by the extremal point of V^{2PI}. All equations are made automatically finite by the contribution of the derivatives of the counterpotential:

$$\frac{1}{n^2}\frac{dV_{n^2}^{2PI}}{dv} = 0 = 2(M^2 v - h) + 4\bar{g}_2 v\int_k \frac{D_M(k)}{1 + 2\bar{g}_2\mathscr{B}_M^F(k) + 4\bar{g}_2 v^2 D_M(k)} + \frac{1}{n^2}\frac{dV_{ct}^{2PI}}{dv}, \quad (5.145)$$

$$\frac{1}{n^2}\frac{dV_{n^2}^{2PI}}{dx} = 0 = -\frac{1}{2g_1}x + v^2 + \int_k \frac{1}{k^2 + M^2}$$
$$+ \int_k \frac{1}{1 + 2\bar{g}_2\mathscr{B}_M^F(k) + 4\bar{g}_2 v^2 D_M(k)}\left[-4\bar{g}_2 v^2 D_M^2(k) + 2\bar{g}_2\frac{d\mathscr{B}_M(k)}{dM^2}\right] + \frac{1}{n^2}\frac{dV_{ct}^{2PI}}{dx}, \quad (5.146)$$

$$\frac{1}{n^2}\frac{dV_{n^2}^{2PI}}{dy_0} = 0 = -\frac{1}{2g_2}y_0 + v^2 + \int_k \frac{1}{k^2+M^2} + \int_k \frac{1}{1+2\bar{g}_2\mathscr{B}_M^F(k)+4\bar{g}_2v^2D_M(k)}\left[-4\bar{g}_2v^2D_M^2(k) + 2\bar{g}_2\frac{d\mathscr{B}_M(k)}{dM^2}\right] + \frac{1}{n^2}\frac{dV_{ct}^{2PI}}{dy}. \tag{5.147}$$

By the structure of the counterterm contributions, one recognizes that

$$g_2 x = g_1 y_0. \tag{5.148}$$

5.6.3 *Summary Conclusions of the Analysis*

The lengthy, rather technical analysis of this section followed the steps of the successful large-N solution of the $O(N)$ symmetric meson model. The key difference is that in addition to the scalar auxiliary field X, one has an auxiliary multiplet Y^a. Although one can perform the s^a and π^a integrations, the resulting effective action for the Y^a field is not quadratic. Therefore, a Gaussian integration over it does not represent the exact solution in the $n \to \infty$ limit. It is just an approximate solution. A nonzero X-background would lead only to the breakdown of the $O(2n^2)$ symmetry [13]. Therefore, it is tempting to search for other possible symmetry-breaking patterns. An analysis performed in the above approximation revealed several apparently new minima, which, however, turned out to be related by unitary transformations to the pure X-background [14].

5.7 The Quark–Meson Theory at Large N_f

The effective theory approach introduces independent fields for every excitation of the ground state that can be considered stable at the characteristic time scale of the investigated phenomena. Certainly, with the change of the energy scale, the weight of the presence of different excitations changes. In QCD, at short distances the quark degrees of freedom dominate, while at large spatial scales, only meson excitations are observable. The study of the dynamical change in the relative weight is an interesting research direction that can be realized, for instance, using functional renormalization group equations [15].

In particular, at finite temperature, the entities contributing independently to the thermodynamic potential should be considered independent thermodynamic degrees of freedom. At those scales where both quarks and their mesonic composites are active, it is fully legitimate to introduce an effective model in which quarks and

mesons are treated on an equal footing. This question will be further elaborated in Chap. 7.

In the present section, the large-N renormalization features of the combined quark–meson model are investigated, which is a necessary precondition for the consistent treatment at finite temperature/density. The quark–meson theory is a completion of the $O(N)$ model (5.1) with a Yukawa interaction describing the interaction of N_f quark flavors with the meson fields. The meson fields originally are components of the matrix field M transforming in the fundamental representation of the $U_L(N_f) \times U_R(N_f)$ group. For the study of the quark–meson dynamics, only the $N_f^2 - 1$ light pion fields (π^a) and the scalar order parameter field (σ) are kept, which together form a vector of dimension $N = N_f^2$. The $O(N)$-invariant dynamics of the meson fields after a symmetry-breaking shift along the σ-direction has the form (5.3). It is completed by the quark–meson Yukawa interaction:

$$L_Y = \bar{q}_i(x)\left[\partial\!\!\!/\,\delta_{ij} + \frac{g}{\sqrt{N}}\left(\sigma(x)\delta_{ij} + i\gamma_5\sqrt{2N_f}T^a_{ij}\pi^a(x)\right)\right]q_j(x), \quad i,j = 1,\ldots,N_f. \tag{5.149}$$

The notation T^a, $a = 1,\ldots,N_f^2 - 1$, is introduced for the generators of the $SU_V(N_f)$ group. The resulting model is a generalization of the $N_f = 2$ pion-nucleon theory of Gell-Mann and Lévy, except that the proton and the neutron are replaced by quarks. One has to emphasize that this hybrid construction violates both the $O(N)$ and the original $U_L(N_f) \times U_R(N_f)$ symmetry of the model, which will be reflected in the counterterm structure generated in the renormalization process.

The factor $1/\sqrt{N}$ is introduced into (5.149) in such a way that the quark mass generated by the symmetry-breaking shift (5.2) remains finite ($\mathcal{O}(N^0)$):

$$m_q = gv. \tag{5.150}$$

In phenomenological applications, this mass is identified with the constituent mass of the additive quark model, nearly equal to one-third of the nucleon mass. Since the value of the mass parameter of the light quarks in the QCD Lagrangian is ~ 5 MeV, one can convincingly argue for an approximation in which the constituent quark mass is fully generated by the chiral symmetry-breaking. This would not be the case for the pion–nucleon effective model.

The integration over the quark fields can be performed, and the following additional term is generated to the mesonic action from the quantum fluctuations of the quarks:

$$\Delta S_M = -N_c \mathrm{Tr}\log\left[\left(\partial\!\!\!/ + m_q\right)\delta_{ij} + g\left(\sigma(x)\delta_{ij} + i\gamma_5\sqrt{2N_f}T^a_{ij}\pi^a(x)\right)\right]. \tag{5.151}$$

Here the factor N_c reflects the color degeneracy of the quarks and the "color blindness" of the quark–meson interaction.

With one functional derivation with respect to $\sigma(x)$, one obtains the additional correction to the equation of state (5.18):

$$0 = \sqrt{N}v\left(m^2 + \frac{\lambda}{6}(v^2 + G_\pi(x,x)) - \frac{h}{v}\right) - \frac{gN_cN_f}{\sqrt{N}}\mathrm{Tr}(\not{\partial} + m_q)^{-1}. \tag{5.152}$$

The factor N_f in the numerator appears from the trace over the quark flavor indices. The fermion correction is $\mathcal{O}(N^0)$. It is suppressed by a factor $1/\sqrt{N}$ relative to the LO mesonic part, but it dominates over the next order in the mesonic contribution. Therefore, the combination of the LO mesonic and quark contributions is a consistent treatment of the large-N hierarchy of the quark–meson model.

The fermionic tadpole appearing here can be expressed through the tadpole integral introduced above for the bosonic fields:

$$\mathrm{Tr}(\not{\partial} + m_q)^{-1} = 4m_q\mathscr{T}(m_q) = 4m_q(\mathscr{T}^F(m_q) + \mathscr{I}_d^{(0,1)} - (m_q^2 - M_0^2)\mathscr{I}_d^{(0,2)}), \tag{5.153}$$

which requires the following additional pieces in the counterterms:

$$\delta\Delta L_M = \frac{1}{2}\delta m_{1/2}^2 v^2 + \frac{\delta\lambda_{v^4}^{(1/2)}}{24}v^4$$
$$\delta m_{1/2}^2 = \frac{4g^2N_fN_c}{N}(\mathscr{I}_d^{(0,1)} + M_0^2\mathscr{I}_d^{(0,2)}), \quad \delta\lambda_{v^4}^{(1/2)} = -\frac{24g^4N_cN_f}{N}\mathscr{I}_d^{(0,2)}. \tag{5.154}$$

The index $1/2$ refers explicitly to the order of the large-N expansion in which these terms are included.

For the pion propagator, a nontrivial wave function renormalization has to be assumed. The propagator equation completed with the quark-loop contribution looks like

$$G_\pi^{-1}(k) = Z_\pi k^2 + m^2 + \frac{\lambda}{6}\left(v^2 + \mathscr{T}(M_\pi)\right) - \frac{g^2N_cN_f}{N}\int_q \mathrm{tr}_D\left(D_F(q)\gamma_5 D_F(q+k)\gamma_5\right). \tag{5.155}$$

In order to arrive at the present form, one performs the trace on the unitary indices with the help of the normalization of the $SU(N_f)$ generators, $\mathrm{tr}T^aT^b = \delta^{ab}/2$, while the Dirac trace tr_D is still to be done. For this one uses the explicit representation

$$D_F(q) = \frac{-i\gamma_m q_m + m_q}{q^2 + m_q^2}. \tag{5.156}$$

After working out the Dirac trace, one has

$$G_\pi^{-1}(k) = Z_\pi k^2 + m^2 + \frac{\lambda}{6}\left(v^2 + \mathscr{T}(M_\pi)\right) - \frac{4g^2 N_c N_f}{N}\left[\mathscr{T}(m_q) - \frac{k^2}{2}\mathscr{B}(m_q, k)\right], \tag{5.157}$$

where $\mathscr{T}(m_q)$ and $\mathscr{B}(m_q, k)$ are bosonic tadpole and bubble integrals evaluated with the quark mass m_q. The comparison of the equation of state (5.152) with $G_\pi(k = 0)$ demonstrates the validity of Goldstone's theorem also at this order:

$$G_\pi^{-1}(k = 0) \equiv M_\pi^2 = \frac{h}{v}. \tag{5.158}$$

This leads to the finite pion-propagator equation

$$G_\pi^{-1}(k) = k^2\left(1 + \frac{2g^2 N_c N_f}{N}\mathscr{B}^F(k, m_q)\right) + M_\pi^2, \tag{5.159}$$

where the finite self-consistent equation determining M_π follows from (5.157) evaluated at $k^2 = 0$:

$$M_\pi^2 = m_R^2 + \frac{\lambda}{6}\left(v^2 + \mathscr{T}^F(M_\pi)\right) - \frac{4g^2 N_c N_f}{N}\mathscr{T}^F(m_q). \tag{5.160}$$

The leading large-N behavior of the σ-propagator was found in the auxiliary variable formulation of the model. Now after renormalization, the $\sigma\sigma$ matrix element of the inverse propagator matrix of the $\rho - \sigma$ sector receives an additional contribution:

$$\begin{aligned} G_{\sigma\sigma}^{-1}(k) &= D_\pi^{-1}(k) - \frac{4g^2 N_f N_c}{N}\left[\mathscr{T}(m_q) - \frac{k^2}{2}\mathscr{B}^F(k, m_q) - 2m_q^2\mathscr{B}^F(k, m_q)\right] \\ &= G_\pi^{-1}(k) + \frac{8g^4 N_c N_f}{N} v^2 \mathscr{B}^F(k, m_q). \end{aligned} \tag{5.161}$$

The counterterm couplings of the Lagrangian ensuring the finiteness of the inverse propagators are given as

$$\delta Z_{\pi,1/2} = \delta Z_{\sigma,1/2} = -\frac{2g^2 N_c N_f}{N}\mathscr{I}_d^{(0,2)}, \qquad \delta\lambda_{v^2\pi\pi} = \delta\lambda_{v^4}, \qquad \delta\lambda_{v^2\sigma\sigma} = 3\delta\lambda_{v^4}. \tag{5.162}$$

The spectra of the excitations in the $\rho - \sigma$ sector are determined by the determinant of the 2×2 matrix of the inverse propagators, evaluated with the modified expression of $G^{-1}_{\sigma\sigma}$ given above:

$$0 = \left(\frac{3}{\lambda} + \frac{1}{2}\mathscr{B}^F_\pi(k)\right)\left(G^{-1}_\pi(k) + \frac{8g^4 N_c N_f}{N} v^2 \mathscr{B}^F(k, m_q)\right) + v^2. \tag{5.163}$$

Phenomenological finite temperature and finite density applications of this model will be discussed in Chap. 7.

References

1. S.-K. Ma, *Modern Theory of Critical Phenomena* (Benjamin, Reading, 1976)
2. J. Zinn-Justin, *Quantum Field Theory and Critical Phenomena*, 4th edn. (Clarendon Press, Oxford, 2004)
3. M. Moshe, J. Zinn-Justin, Quantum field theory in the large N limit: a review. Phys. Rep. **385**, 69 (2003)
4. J. Goldstone, Nuovo Cimento **19**, 154 (1961)
5. J.-P. Blaizot, E. Iancu, U. Reinosa, Nucl. Phys. A **736**, 149 (2004)
6. M. Lüscher, P. Weisz, Nucl. Phys. B **318**, 705 (1989)
7. G. Aarts, D. Ahrensmeier, R. Baier, J. Berges, J. Serreau, Phys. Rev. D **66**, 045008 (2002)
8. G. Fejős, A. Patkós, Zs. Szép, Phys. Rev. D **80**, 025015 (2010)
9. G. Fejős, A. Patkós, Zs. Szép, Phys. Rev. D **90**, 016014 (2014)
10. D. Dominici, U.M.B. Marconi, Phys. Lett. B **319**, 171 (1993)
11. J. Berges, Sz. Borsányi, U. Reinosa, J. Serreau, Ann. Phys. **320**, 344 (2005)
12. G. Fejős, A. Patkós, Phys. Rev. D **82**, 045011 (2010)
13. H. Meyer-Ortmanns, B.J. Schaefer, Phys. Rev. D **53**, 6586 (1996)
14. G. Fejős, Phys. Rev. D **87**, 056006 (2013)
15. D.U. Jungnickel, C. Wetterich, Phys. Rev. D **53**, 5142 (1996)

Chapter 6
Dimensional Reduction and Infrared Improved Treatment of Finite-Temperature Phase Transitions

The thermal energy $\sim k_B T$ introduces a new energy scale into field theories. In thermal field theories, a specific series of Feynman diagrams of increasing loop order can be found that reveals the presence of increasing powers of the ratio $k_B T/mc^2$ in the self-energy, dangerous at high temperature in the infrared domain ($T \gg m$). Resummation is invoked to avoid the emerging singularity from this class. Application of the method of dimensional reduction is motivated by the observation that it automatically realizes the resummation leading to the replacement of the renormalized mass by an infrared safe thermal mass of $\sim T$.

The main content of this chapter is a detailed presentation of the procedure and features of dimensional reduction. We begin here with a short reminder of the so-called daisy diagram resummation in thermal perturbation theory so that in the bulk of this chapter we can compare to it the results of dimensional reduction. The presentation as it appears in the classical paper of Dolan and Jackiw [1] is followed.

The lowest (one-loop tadpole) contribution to the self-energy of the one-component self-interacting massive Φ^4 theory is given by

$$\Sigma_T^{(1)} = \frac{\lambda}{2} T \sum_n \int_p \frac{1}{\omega_n^2 + \omega_p^2}, \qquad \omega_n = 2\pi T n, \qquad \omega_p = (m^2 + \mathbf{p}^2)^{1/2}, \tag{6.1}$$

where m is the renormalized mass of the field, and λ is the strength of the self-coupling (precise notation will be introduced in the next subsection; the units $k_B = c = \hbar = 1$ are used). After normalizing this expression, one finds the following expression for it in terms of an expansion in m/T:

$$\Sigma_T^{(1R)} = \frac{\lambda}{2}\left(\frac{T^2}{12} - \frac{mT}{4\pi} + \mathcal{O}(m^2 \ln(m^2/T^2))\right). \tag{6.2}$$

A. Jakovác, A. Patkós, *Resummation and Renormalization in Effective Theories of Particle Physics*, Lecture Notes in Physics 912,
DOI 10.1007/978-3-319-22620-0_6

The two-loop (double tadpole or "double-scoop") correction contains the same quantity multiplied by the vertex strength $-\lambda/2$ and an integral over the product of two Euclidean propagators:

$$\begin{aligned}\Sigma_T^{(2)} &= \frac{\lambda}{2} T \sum_n \int_p \frac{1}{\omega_n^2+\omega_p^2} \times \left(-\frac{\lambda}{2}\right) T \sum_{n'} \int_p \frac{1}{(\omega_{n'}^2+\omega_p^2)^2} \\ &= \frac{\lambda}{2} T \sum_n \int_p \frac{1}{\omega_n^2+\omega_p^2} \frac{\lambda}{2} \frac{d}{dm^2} \left(T \sum_{n'} \int_p \frac{1}{\omega_{n'}^2+\omega_p^2} \right) \\ &= \Sigma_T^{(1)} \times \left(-\frac{\lambda}{2}\right) \left(\frac{T}{8\pi m}\right). \end{aligned} \tag{6.3}$$

The large ratio multiplying $\Sigma_T^{(1)}$ challenges the validity of the thermal perturbation theory.

One can continue to put an increasing number of tadpoles along the basic loop (this class of diagrams is called "daisy") and find increasingly dangerous contributions, containing increasingly high powers of T/m. The contribution of the daisy diagram with l petals is written as

$$\begin{aligned}\Sigma_T^{(l)} &= \frac{\lambda}{2} \left(-\frac{\lambda}{2} T \sum_n \int_p \frac{1}{\omega_n^2+\omega_p^2} \right)^l \times T \sum_{n'} \int_p \frac{1}{(\omega_{n'}^2+\omega_p^2)^{l+1}} \\ &= \frac{\lambda}{2} \left(\frac{\lambda}{6} T \sum_n \int_p \frac{1}{\omega_n^2+\omega_p^2} \right)^l \frac{1}{l!} \frac{d^l}{d(m^2)^l} T \sum_{n'} \int_p \frac{1}{\omega_{n'}^2+\omega_p^2}. \end{aligned} \tag{6.4}$$

However, the sum of this series represents a translation in the m^2 variable:

$$\Sigma_T = \exp\left[\frac{\lambda}{2} T \sum_n \int_p \frac{1}{\omega_n^2+\omega_p^2} \frac{d}{dm^2} \right] \left(\frac{\lambda}{2} T \sum_{n'} \int_{p'} \frac{1}{\omega_{n'}^2+\omega_{p'}^2} \right). \tag{6.5}$$

In the exponent of the "translation" operator, one can keep the leading contribution at high T in (6.2), while in the expression on which the m^2-translation acts, both of the first two terms are retained. In this way, one obtains for the temperature-dependent resummed mass an expression free of any infrared singular behavior:

$$m^2 + \Sigma_T \approx m^2 + \frac{\lambda}{24} T^2 - \frac{\lambda T}{8\pi} \left(m^2 + \frac{\lambda T^2}{24} \right)^{1/2} \equiv m_T^2 - \frac{\lambda T}{8\pi} m_T. \tag{6.6}$$

This expression is the same as the one-loop expression (6.2), with m_T replacing m. At large temperature, $\sqrt{\lambda} T$ defines the infrared-safe effective mass scale. In this way, the resummation proves essential for avoiding accumulation of infrared-sensitive self-energy contributions. The "daisy" summation will be shown below

to arise automatically from the infrared safe integration over the nonzero Matsubara frequency modes and will serve as the mass parameter of the effective theory of the static Matsubara fields.

The Matsubara decomposition of the imaginary temporal ("thermal time") dependence of finite-temperature quantum fields defined in d spatial dimensions naturally leads to a separation of the infrared-sensitive light modes of $E \sim p$ and heavy modes $E \sim k_B T$ at sufficiently high temperatures ($p \ll T$). The Wilsonian interpretation of the infrared behavior of field theories suggests a strategy of gradual functional integration for the evaluation of the partition function defining the thermodynamics of the theory [2]. The primary integration over the heavy modes in the background of an arbitrary light configuration results in an effective theory of these modes. The most important feature of this effective theory is a thermal mass generation for most of the light modes, essentially improving the infrared convergence features.

At high temperatures, where $k_B T$ is much larger than the original characteristic masses of the theory, this effective theory containing in principle an infinite number of operators can be constructed perturbatively, for instance in a loop expansion of increasing loop number. The coupling strength in front of most operators will be inversely proportional to powers of $k_B T$, as dictated by simple dimensional considerations. For practical purposes, one keeps those contributions to the coupling strengths that do not vanish with infinitely growing T (these coincide with the "perturbatively renormalizable" operators). In a second stage, one applies various techniques to performing the remaining functional integrations.

In the first part of this chapter, the example of the one-component Φ^4 theory will be used for learning the techniques of the determination of the effective reduced theory [3]. The integration over the heavy modes will be presented with two-loop accuracy. The main emphasis will be put on presenting how the renormalization program applied to the cutoff regularized $(d+1)$-dimensional theory generates the cutoff-dependent counterterms for the d-dimensional effective theory. A discussion of the finite-temperature phase transition occurring in this model will be based on solving the effective dimensionally reduced model. This treatment goes beyond the conventional Landau-type mean field approximation.

In the second part, another technique is presented for the determination of the effective reduced theory. The so-called *matching strategy* is based on determining the relationship among the couplings of the original and the effective theories by requiring coinciding results for a set of n-point functions as obtained from the $(d+1)$-dimensional (full) and the d-dimensional (reduced) theories [4].

In the third part, we shall apply the technique of integrating over the hard Matsubara modes to the thermodynamics of the soft bosonic sector of the $U(1)$-invariant scalar electrodynamics with one-loop accuracy [7]. The corresponding discussion of the cosmological electroweak phase transition based on the $SU(2)$ local symmetry group will be presented in Chap. 8. We close the chapter with a short discussion of the order of the finite-temperature phase transition in a generic dimensionally reduced theory.

6.1 The Φ^4 Theory at Finite Temperature

The thermodynamics of the Φ^4 theory is defined by the Euclidean path integral

$$Z \equiv e^{-\beta \mathscr{F}} = \int_{\Phi_{per}} \mathscr{D}\Phi(\mathbf{x}, \tau) e^{-S_E[\Phi]}, \tag{6.7}$$

where the field $\Phi(\mathbf{x}, \tau)$ is defined in the direct product space of a three-dimensional spatial cube of volume V and the thermal dimension of extension $\beta = (k_B T)^{-1}$. Only fields that are periodic along the thermal extension

$$\Phi(\mathbf{x}, \tau) = \Phi(\mathbf{x}, \tau + \beta) \tag{6.8}$$

are included in the path integral. The Euclidean action is given as

$$S_E[\Phi] = \int_0^\beta d\tau \int d^3x \left[\frac{1}{2} \left(\frac{\partial \Phi}{\partial \tau} \right)^2 + \frac{1}{2} (\nabla \Phi)^2 + \frac{1}{2}(m^2 + \delta m^2)\Phi^2 + \frac{\lambda + \delta\lambda}{24} \Phi^4 \right]. \tag{6.9}$$

Here the bare mass and self-interaction parameters are written as the sum of the renormalized couplings and the countercouplings. The wave function renormalization is neglected for simplicity. The Fourier expansion along the compact thermal dimension is called Matsubara expansion:

$$\Phi(\mathbf{x}, \tau) = \sum_{n=-\infty}^{\infty} \Phi_n(\mathbf{x}) e^{i\omega_n \tau}, \qquad \omega_n = \frac{2\pi}{\beta} n. \tag{6.10}$$

It will be clear soon that these are the static ($\omega_0 = 0$) modes, which are most sensitive to the infrared fluctuations. Therefore, it is convenient to divide the functional integration into two stages using the notation

$$\Phi(\mathbf{x}, \tau) = \Phi_0(\mathbf{x}) + \varphi(\mathbf{x}, \tau), \quad \int_0^\beta d\tau \varphi(\mathbf{x}, \tau) = 0, \quad \varphi(\mathbf{x}, \tau) = \sqrt{\beta} \sum_{n \neq 0} \varphi_n(\mathbf{x}) e^{i\omega_n \tau}. \tag{6.11}$$

Here a special convention is used for the Fourier expansion in the variable τ. With this, one can rewrite (6.7) as

$$Z = \int \mathscr{D}\Phi_0(\mathbf{x}) e^{-S_0[\Phi_0]} \left\{ \int \mathscr{D}\varphi(\mathbf{x}, \tau) e^{-S^{(2)}[\varphi] - S_I[\Phi_0, \varphi_0]} \right\}. \tag{6.12}$$

The original Euclidean action splits into a sum of the three terms indicated above:

$$S_0[\Phi_0] = \beta \int d^3x \left[\frac{1}{2}(m^2 + \delta m^2)\Phi_0^2 + \frac{1}{2}(\nabla \Phi_0)^2 + \frac{\lambda + \delta\lambda}{24}\Phi_0^4 \right], \tag{6.13}$$

$$S^{(2)}[\varphi] = \frac{1}{2}\beta^2 \sum_{n\neq 0} \int d^3x \varphi_n^*(x) \left[-\triangle + m^2 + \frac{\lambda}{2}\Phi_0^2(\mathbf{x}) + \omega_n^2 \right] \varphi_n(x) \tag{6.14}$$

and

$$\begin{aligned} S_I[\Phi_0, \varphi] &= \frac{1}{2}\beta^2 \int d^3x \left(\delta m^2 + \frac{\delta\lambda}{24}\Phi_0^2(\mathbf{x}) \right) \varphi_n^*(\mathbf{x})\varphi_n(\mathbf{x}) \\ &+ \beta^3 \frac{\lambda + \delta\lambda}{24} \int d^3x \sum_{n_1,n_2,n_3,n_4\neq 0} \delta(n_1 + n_2 + n_3 + n_4)\varphi_{n_1}(\mathbf{x})\varphi_{n_2}(\mathbf{x})\varphi_{n_3}(\mathbf{x})\varphi_{n_4}(\mathbf{x}) \\ &+ \beta^{5/2} \frac{\lambda + \delta\lambda}{6} \int d^3x \Phi_0(x) \sum_{n_1,n_2,n_3\neq 0} \delta(n_1 + n_2 + n_3)\varphi_{n_1}(\mathbf{x})\varphi_{n_2}(\mathbf{x})\varphi_{n_3}(\mathbf{x}). \end{aligned} \tag{6.15}$$

In this representation of the canonical partition function, the thermal dimension "disappears," and in its place, infinitely many three-dimensional fields ($\varphi_n(\mathbf{x})$) emerge. Those with index $n \neq 0$ have in the kernel of the quadratic part of the action the term ω_n^2, which dominates m^2 at high temperatures. This "squared thermal mass" contribution is missing for Φ_0, which makes these static configurations the most vulnerable in the infrared. For this reason, one performs the path integration first in the curly brackets of (6.12) with an arbitrary background $\Phi_0(\mathbf{x})$.

For the perturbative integration, one needs the propagator of the nonstatic modes, which is the functional inverse of the kernel defining $S^{(2)}$:

$$D_n(\mathbf{x} - \mathbf{y}) = \left[\beta^2 \left(-\triangle_x + m^2 + \omega_n^2 + \frac{\lambda}{2}\Phi_0^2(\mathbf{x}) \right) \delta(\mathbf{x} - \mathbf{y}) \right]^{-1}, \tag{6.16}$$

which will be expanded into a power series of $\beta^2(m^2 + \lambda/2\Phi_0^2) \equiv \beta^2 M^2(x)$:

$$\begin{aligned} D_n(\mathbf{x} - \mathbf{y}) = D_n^{(0)}(\mathbf{x} - \mathbf{z_1}) \Big[& \delta(\mathbf{z_1} - \mathbf{y}) - D_n^{(0)}(\mathbf{z_1} - \mathbf{y}) \left(\beta^2(m^2 + \lambda/2\Phi_0^2(\mathbf{y})) \right) \\ & + D_n^{(0)}(\mathbf{z_1} - \mathbf{z_2}) \left(\beta^2(m^2 + \lambda/2\Phi_0^2(\mathbf{z_2})) \right) \\ & D_n^{(0)}(\mathbf{z_2} - \mathbf{y}) \left(\beta^2(m^2 + \lambda/2\Phi_0^2(\mathbf{y})) \right) + \ldots \Big], \\ D_n^{(0)}(\mathbf{x} - \mathbf{y}) = \int_p e^{i\mathbf{p}(\mathbf{x}-\mathbf{y})} D_n^{(0)}(\mathbf{p}), \; & D_n^{(0)}(\mathbf{p}) = \frac{1}{\beta^2(\omega_n^2 + p^2)}. \end{aligned} \tag{6.17}$$

6.2 Two-Loop Integration Over the Nonstatic Fields

The perturbative evaluation of the functional integral over the nonstatic modes is done by expanding $\exp(-S_I)$ into a Taylor series and performing the integrals over each term weighted by the Gaussian $\exp(-S^{(2)})$. The exponent of the partition function, e.g., the free energy of the system, is perturbatively determined by the contributions from the one-particle-irreducible diagrams (see Sect. 2.7!). To two-loop order, one has

$$
\begin{aligned}
-\beta\mathscr{F} &= \ln\int \mathscr{D}\Phi e^{-S_E} = -S_0 - \frac{1}{2}\sum_{n\neq 0}\mathrm{Tr}_x \log D_n^{-1}(\mathbf{x},\mathbf{x}) \\
&-\frac{1}{2}\beta^2\int d^3x \sum_{n\neq 0}\langle\varphi_n^*(\mathbf{x})\varphi_n(\mathbf{x})\rangle\left(\delta m^2 + \frac{\delta\lambda}{24}\Phi_0^2(\mathbf{x})\right) \\
&-\beta^3\frac{\lambda}{8}\int d^3x \sum_{n_1,n_2,n_3,n_4\neq 0}\delta(n_1+n_2+n_3+n_4)\langle\varphi_{n_1}(\mathbf{x})\varphi_{n_2}(\mathbf{x})\rangle\langle\varphi_{n_3}(\mathbf{x})\varphi_{n_4}(\mathbf{x})\rangle \\
&+\beta^5\frac{\lambda^2}{12}\int d^3x\int d^3y\Phi_0(\mathbf{x})\Phi_0(\mathbf{y})\sum_{n_i\neq 0}\sum_{m_i\neq 0}\delta(n_1+n_2+n_3)\delta(m_1+m_2+m_3) \\
&\qquad\times\langle\varphi_{n_1}(\mathbf{x})\varphi_{m_1}(\mathbf{y})\rangle\langle\varphi_{n_2}(\mathbf{x})\varphi_{m_2}(\mathbf{y})\rangle\langle\varphi_{n_3}(\mathbf{x})\varphi_{m_3}(\mathbf{y})\rangle. \qquad (6.18)
\end{aligned}
$$

Here the propagators defined with the help of $S^{(2)}$ are defined as

$$
\langle\varphi_n(\mathbf{x})\varphi_m(\mathbf{y})\rangle = \frac{1}{Z^{(2)}}\int e^{-S^{(2)}}\varphi_n(\mathbf{x})\varphi_m(\mathbf{y}) = D_n(\mathbf{x}-\mathbf{y})\delta_{nm}. \qquad (6.19)
$$

Recognizing that the propagators are diagonal in the Matsubara index, one obtains the following simplified expression:

$$
\begin{aligned}
\mathscr{F} &= \beta^{-1}S_0 + \frac{1}{2\beta}\sum_{n\neq 0}\mathrm{Tr}_x\log D_n^{-1}(\mathbf{x},\mathbf{x}) \\
&+\frac{1}{2}\beta\int d^3x\sum_{n\neq 0}D_n(\mathbf{x},\mathbf{x})\left(\delta m^2 + \frac{\delta\lambda}{24}\Phi_0^2(\mathbf{x})\right) \\
&+\beta^2\frac{\lambda}{8}\int d^3x\sum_{n_1,n_2\neq 0}D_{n_1}(\mathbf{x},\mathbf{x})D_{n_2}(\mathbf{x},\mathbf{x}) \\
&-\beta^4\frac{\lambda^2}{12}\int d^3x\int d^3y\Phi_0(\mathbf{x})\Phi_0(\mathbf{y}) \\
&\quad\times\sum_{n_1,n_2,n_3\neq 0}\delta(n_1+n_2+n_3)D_{n_1}(\mathbf{x}-\mathbf{y})D_{n_2}(\mathbf{x}-\mathbf{y})D_{n_3}(\mathbf{x}-\mathbf{y}). \qquad (6.20)
\end{aligned}
$$

One can reproduce the conventional perturbation theory in a $\Phi_0(\mathbf{x})$ background by applying in (6.20) the expansion (6.17). Then the "tracelog" is rewritten in an infinite series of momentum integrals:

$$\frac{1}{2\beta}\sum_{n\neq 0}\mathrm{Tr}_x \log D_n^{-1}(\mathbf{x},\mathbf{x}) = \frac{T}{2}\sum_{n\neq 0}\Bigg\{ V\int_p \log(\beta^2\omega_n^2+\beta^2 p^2)$$

$$\text{`}+\sum_{l=1}^{\infty}\frac{(-1)^{l+1}}{l}\int \Pi_{j=1}^{l}\left[\frac{Vd^3p_j}{(2\pi)^3}\frac{\beta^2\tilde{M}^2(p_j-p_{j+1})}{\beta^2(\omega_n^2+p_j^2)}\right]\Bigg\}\Bigg|_{p_{l+1}=p_1},$$

$$\tilde{M}^2(p) = \frac{1}{V}\int d^3x e^{-i\mathbf{px}}M^2(x). \tag{6.21}$$

The $l=1$ term is simply proportional to $\int d^3x\Phi_0^2(x)$. Therefore, it contributes to the mass term of the reduced theory. Below, we shall discuss the interest of the nonlocal features of the $l=2$ term, but for the moment, this expression plus the other terms appearing in $\mathscr{F}$ will be discussed assuming a constant-Φ_0 background. Then the free energy accounts exclusively for the potential energy density of constant fields.

When Φ_0 is a constant, the contributions of (6.20) can be expressed in terms of the following fundamental sums and integrals:

$$I(M) = T\sum_{n\neq 0}\int_p \log\left(\beta^2(\omega_n^2+p^2+M^2)\right)$$

$$K(M,M,M) = \beta^4\int d\xi \sum_{n_1,n_2,n_3\neq 0}\delta(n_1+n_2+n_3)D_{n_1}(\xi)D_{n_2}(\xi)D_{n_3}(\xi)$$

$$= T^2\sum_{n_1,n_2,n_3\neq 0}\delta(n_1+n_2+n_3)$$

$$\times\int_{p_1}\int_{p_2}\int_{p_3}\frac{(2\pi)^3\delta^{(3)}(p_1+p_2+p_3)}{(\omega_{n_1}^2+p_1^2+M^2)(\omega_{n_2}^2+p_2^2+M^2)(\omega_{n_3}^2+p_3^2+M^2)}. \tag{6.22}$$

With these abbreviations, (6.20) is expressed as

$$\mathscr{F} = V\Big[\frac{1}{2}(m^2+\delta m^2)\Phi_0^2+\frac{\lambda+\delta\lambda}{24}\Phi_0^4+\frac{1}{2}I(M)+\frac{1}{2}\left(\delta m^2+\frac{\delta\lambda}{24}\Phi_0^2\right)I'(M)$$

$$+\frac{\lambda}{8}\left(I'(M)\right)^2-\frac{\lambda^2}{12}\Phi_0^2K(M,M,M)\Big], \tag{6.23}$$

($I'(M) = dI/dM^2$). The integrals can be expanded in powers of M^2 (which is equivalent to an expansion in Φ_0^2), since the heavy modes make the Matsubara summation finite. For the analysis of the effective potential of the reduced theory

up to terms $\sim \Phi_0^4$ below, we need the expansion of $I(M)$ up to $\mathcal{O}(M^6)$:

$$
\begin{aligned}
I(M) &= I_0 + I_1 M^2 + I_2 M^4 + I_3 M^6 + \ldots, \\
I_1 &= I_1^{(2)} \Lambda^2 + I_1^{(1)} \Lambda T + I_1^{(0)} T^2, \qquad I_2 = I_2^{(ln)} \ln \frac{\Lambda}{T} + I_2^{(0)}, \\
I_3 &= \frac{I_3^{(0)}}{T^2},
\end{aligned}
\tag{6.24}
$$

with the coefficients explicitly given in Eq. (C.2) of Appendix C. The coefficient I_0 is an unimportant constant. Therefore, one can get rid of it by redefining the zero point of the effective potential of the reduced theory appropriately. A similar expansion of $K(M, M, M)$ is needed to $\mathcal{O}(M^2)$, and one has by dimensional analysis the following terms:

$$
\begin{aligned}
K(M, M, M) &= K_0 + K_1 M^2 + \ldots, \\
K_0 &= K_0^{(2)} \Lambda^2 + K_0^{(1)} \Lambda T + K_0^{(ln)} T^2 \ln \frac{\Lambda}{T} + K_0^{(0)} T^2, \\
K_1 &= K_1^{(2ln)} \left(\ln \frac{\Lambda}{T} \right)^2 + K_1^{(ln)} \ln \frac{\Lambda}{T} + K_1^{(0)}.
\end{aligned}
\tag{6.25}
$$

The values of the expansion coefficients are given in Eq. (C.6) of Appendix C. In order to separate the dependence of the potential on the cutoff and the temperature, one introduces the renormalization scale μ. The renormalized potential is obtained by fixing its value at the origin to zero (simply throwing away all Φ_0-independent terms) and fixing the first two nonzero derivatives with respect to Φ_0:

$$
\left. \frac{d^2 \mathcal{F}}{d\Phi_0^2} \right|_{T=\Phi_0=0} = V m^2, \qquad \left. \frac{d^4 \mathcal{F}}{d\Phi_0^4} \right|_{T=\Phi_0=0} = V \lambda. \tag{6.26}
$$

These conditions determine the countercouplings, which might contain specific finite terms beyond the cutoff-dependent parts. The finite pieces that correspond to the choice of a specific renormalization scheme are denoted below by $\Delta m_{(l)}^2$, $\Delta \lambda_{(l)}$, where the index l refers to the loop order at which the corresponding quantity is defined. Their explicit expressions will not be given, since they do not give any further insight. The countercouplings ensuring the ultraviolet finiteness of the effective potential at $T = 0$ are found with one- and two-loop accurate reduction and are written here separately:

$$
\begin{aligned}
\delta m_{(1)}^2 &= \Delta m_{(1)}^2 - \lambda \left(\frac{1}{2} I_1^{(2)} \Lambda^2 + m^2 I_2^{(ln)} \ln \frac{\Lambda}{\mu} \right), \\
\delta m_{(2)}^2 &= \Delta m_{(2)}^2 - \Lambda^2 \left(\frac{1}{2} \Delta_{(1)} \lambda I_1^{(2)} - \frac{1}{6} K_0^{(2)} \lambda^2 - I_1^{(2)} I_2^{(ln)} \lambda^2 \ln \frac{\Lambda}{\mu} \right)
\end{aligned}
$$

$$- \left(\Delta m_{(1)}^2 I_2^{(ln)} \lambda + \Delta\lambda_{(1)} I_2^{(ln)} m^2 - 2 I_2^{(ln)} I_2^{(0)} \lambda^2 m^2 - \frac{1}{6} K_1^{(ln)} \lambda^2 m^2 \right) \ln \frac{\Lambda}{\mu}$$
$$+ 2 (I_2^{(ln)})^2 \lambda^2 m^2 \left(\ln \frac{\Lambda}{\mu} \right)^2 , \tag{6.27}$$

$$\delta\lambda_{(1)} = \Delta\lambda_{(1)} - 3\lambda^2 I_2^{(ln)} \ln \frac{\Lambda}{\mu},$$
$$\delta\lambda_{(2)} = \Delta\lambda_{(2)} + 9 (I_2^{(ln)})^2 \lambda^3 \left(\frac{\Lambda}{\mu} \right)^2$$
$$- \left(6\Delta\lambda_{(1)} I_2^{(ln)} \lambda - 12 I_2^{(ln)} I_2^{(0)} \lambda^3 - K_1^{(ln)} \lambda^3 \right) \ln \left(\frac{\Lambda}{\mu} \right). \tag{6.28}$$

The resulting temperature-dependent pieces still contain cutoff-dependent terms whose coefficients vanish for $T = 0$. These are the *induced counterterms* of the reduced three-dimensional effective theory. In order to simplify the expression, it is convenient to choose the normalization scale as $\mu = T$. This choice, however, does not mean that the counterterm operators will depend on the temperature (see the discussion in Sect. 3.5.1). This leads to

$$\frac{1}{V} \mathscr{F} = \frac{1}{24} \lambda \Phi_0^4$$
$$+ \frac{1}{2} \Phi_0^2 \Big(m^2 + T^2 \left\{ \frac{1}{2} \lambda I_1^{(0)} - \lambda^2 \left[I_1^{(0)} I_2^{(0)} + \frac{1}{6} K_0^{(0)} + \left(I_1^{(0)} I_2^{(ln)} + \frac{1}{6} K_0^{(ln)} \right) \ln \frac{\Lambda}{T} \right] \right\}$$
$$+ \Lambda T \left\{ \frac{1}{2} \lambda I_1^{(1)} - \lambda^2 \left[I_1^{(1)} I_2^{(0)} + \frac{1}{6} K_0^{(1)} + I_1^{(1)} I_2^{(ln)} \ln \frac{\Lambda}{T} \right] \right\} \Big). \tag{6.29}$$

The superrenormalizable nature of the effective theory in the present approximation is manifested by the fact that counterterms were induced only to the Φ_0^2 term of the potential.

Let us return to the $l = 2$ term of (6.21), which defines a momentum-dependent contribution the Lagrangian density of the reduced theory containing four powers of Φ_0. The nonlocal part of this term is absent in the original formulation of the three-dimensional theory, which follows the same pattern as the four-dimensional one. We shall discuss in the next section to what extent it is nonnegligible for the consistency of the reduced effective model.

The full quartic contribution is written with the help of the nonstatic part of the bubble integral $\mathscr{B}$ in terms of the Fourier transform of $\Phi_0^2(x)$ as

$$- \frac{\lambda^2}{16} \int_q \tilde{\Phi}_0^2(\mathbf{q}) \tilde{\Phi}_0^2(-\mathbf{q}) \mathscr{B}_{ns}(\mathbf{q}), \quad \mathscr{B}_{ns}(\mathbf{q}) = T \sum_{n \neq 0} \int_p \frac{1}{(\omega_n^2 + \mathbf{p}^2)(\omega_n^2 + (\mathbf{p}+\mathbf{q})^2)}. \tag{6.30}$$

The $\mathbf{q} = 0$ finite part of $\mathscr{B}$ is already included in the local reduced quartic term as $2I_2^{(0)}$. For dimensional reasons, the remaining $\mathbf{q}$-dependent part depends only on the ratios $\kappa = q/T$, $x = q/\Lambda$ ($q = |\mathbf{q}|$). When performing (partially) the sum-integrations, one arrives, for the kernel of the strictly nonlocal (q-dependent) part, through (C.3), at

$$\Omega(q) \equiv \mathscr{B}_{ns}(q) - 2I_2^{(0)}. \tag{6.31}$$

6.3 The Effective Three-Dimensional Theory and Its Two-Loop-Accurate Effective Potential

The effective theory of the static $\Phi_0(x)$ modes can be formulated in terms of the appropriately rescaled fields and couplings:

$$\Phi_3(x) = \sqrt{\beta}\Phi(x), \qquad \lambda_3 = T\lambda, \qquad \Omega_3(q) = \frac{1}{T}\Omega(q). \tag{6.32}$$

After combining (6.29) and (6.31) and adding to it a three-dimensional kinetic density, one has for the effective three-dimensional action,

$$\begin{aligned} S_{3D} = &\int d^3x \left[\frac{1}{2}\left((\nabla\Phi_3)^2 + (m_T^2 + \delta_3 m^2)\Phi_3^2\right) + \frac{\lambda_3}{24}\Phi_3^4\right] \\ &- \frac{1}{16}\lambda_3^2 \int_q \tilde{\Phi}_3^2(q)\Omega_3(q)\tilde{\Phi}_3^2(-q), \end{aligned} \tag{6.33}$$

where the thermal mass and the mass counterterm of the three-dimensional theory are given as

$$\begin{aligned} m_T^2 &= m^2 + T^2\left[\frac{1}{2}\lambda I_1^{(0)} - \lambda^2\left(I_1^{(0)}I_2^{(0)} + \frac{1}{6}K_0^{(0)}\right)\right], \\ \delta_3 m^2 &= T^2 \ln\frac{\Lambda}{T}\left(I_1^{(0)}I_2^{(ln)} + \frac{1}{6}K_0^{(ln)}\right) \\ &\quad + \Lambda T\left[\frac{1}{2}\lambda I_1^{(1)} - \lambda^2\left(I_1^{(1)}I_2^{(0)} + \frac{1}{6}K_0^{(1)} + I_1^{(1)}I_2^{(ln)}\ln\frac{\Lambda}{T}\right)\right]. \end{aligned} \tag{6.34}$$

A computation of the effective potential $U_{3D}(\Phi_{30})$ for a constant three-dimensional background Φ_{30} that fully contains all two-loop contributions of the four-dimensional theory has three types of contributions (involving, however, infrared safe propagators for the static modes). The "classical" potential

$$U_{3D}(\Phi_{30})_{class} = \frac{1}{2}m_T^2\Phi_{30}^2 + \frac{\lambda_3}{24}\Phi_{30}^4 \tag{6.35}$$

includes the effect of one- and two-loop diagrams in which all lines correspond to nonstatic (heavy) modes. The (resummed) two-loop-accurate contributions originating from diagrams containing exclusively static propagators have the same topology as their 4D counterparts (6.23), except that here, the couplings and the phase space of the momentum integrations are three-dimensional:

$$U_{3D}(\Phi_{30})_{static} = \frac{1}{2} I_3(m_T) + \frac{\lambda_3}{8} \left(I_3'(m_T)\right)^2 - \frac{\lambda_3^2}{12} \Phi_0^2 K_3(m_T, m_T, m_T). \tag{6.36}$$

Finally, the contribution from the nonlocal part of L_{3D} should be taken into account only at the one-loop level in order to account for the mixed static–nonstatic two-loop diagrams of the four-dimensional model. In order to find its one-loop contribution, one has to introduce the appropriate splitting of $\Phi_3(x) = \Phi_{30} + \varphi_3(x)$ and keep only the quadratic part in $\varphi_3(x)$. One has to calculate the tracelog of the quadratic part of the action, which looks like

$$S_{3D}^{(2)}[\varphi_3] = \frac{1}{2} \int_q \varphi_3(-q) \left[\left(q^2 + m_T^2 + \frac{\lambda_3}{2} \Phi_{30}^2 \right) - \frac{\lambda_3^2 \Phi_{30}^2}{2} \Omega_3(q) \right] \varphi_3(q). \tag{6.37}$$

The resulting tracelog can be expanded in powers of the nonlocal part:

$$\begin{aligned} U_{3D}(\Phi_{30})_{static-nonstatic} = {} & \frac{1}{2} \int_q \ln \left(q^2 + m_T^2 + \frac{\lambda_3}{2} \Phi_{30}^2 \right) \\ & + \sum_{l=1}^{\infty} \frac{(-1)^{l+1}}{2^{l+1} l} \int_q \left(- \frac{\lambda_3^2 \Phi_{30}^2 \Omega_3(q)}{q^2 + m_T^2 + \frac{\lambda}{2} \Phi_{30}^2} \right)^l . \end{aligned} \tag{6.38}$$

The first term is already included in the static one-loop contribution ($= I_3(m_T)/2$), and therefore, only the infinite sum should be added to the sum of the three different types of contributions in order to avoid double counting. In the nonlocal contribution, all terms are finite but the first one, which contributes to the three-dimensional mass divergence:

$$- \frac{\lambda_3^2 \Phi_{30}^2}{4} \int_q \frac{\Omega_3(q)}{q^2 + m_T^2 + \frac{\lambda}{2} \Phi_{30}^2} = - \frac{\lambda_3^2 \Phi_{30}^2}{64 \pi^4} \left[\frac{\Lambda}{T} \ln \frac{\Lambda}{T} + \pi^2 \ln \frac{\Lambda}{T} - C \frac{\Lambda}{T} + f\left(\frac{m_T^2}{T^2} \right) \right]. \tag{6.39}$$

The constant C as well as the finite function $f(m_T^2/T^2)$ can be determined numerically.

The integrals figuring in (6.36) can be evaluated analytically:

$$\begin{aligned} I_3(m_T) &= 2J^{(1)} \Lambda \left(m_T^2 + \frac{\lambda_3}{2} \Phi_{30}^2 \right) + 2J^{(0)} \left(m_T^2 + \frac{\lambda_3}{2} \Phi_{30}^2 \right)^{3/2}, \\ K_3(m_T, m_T, m_T) &= L^{(ln)} \ln \frac{\Lambda^2}{\mu^2} + L^{(0)} - L^{(ln)} \ln \frac{9(m_T^2 + \lambda_3 \Phi_{30}^2/2)}{\mu^2}, \end{aligned} \tag{6.40}$$

with the coefficients $L^{(i)}$, $J^{(i)}$ taken from Sect. C.2.

The sum of the three-dimensional divergences emerging from the static and the nonlocal contributions exactly cancel the divergences induced by the integration over the nonstatic modes. This shows that it is compulsory to include also the nonlocal piece in the effective three-dimensional action at the two-loop level. One has again the freedom to conveniently choose also a finite counterterm $\Delta_3 m^2$, thereby simplifying the local contributions to the potential. One can arrange the following form:

$$\begin{aligned} U_{3D}(\Phi_{30}) = & \frac{1}{2} m_T^2 \Phi_{30}^2 + \frac{\lambda_3}{24} \Phi_{30}^4 \\ & + J^{(0)} \left(m_T^2 + \frac{\lambda_3}{2} \Phi_{30}^2 \right)^{3/2} + \frac{\lambda_3^2}{12} \Phi_{30}^2 L^{(ln)} \ln \frac{9(m_T^2 + \lambda_3 \Phi_{30}^2/2)}{\mu^2} \\ & + U_{3D}(\Phi_{30})_{nonlocal,ren}. \end{aligned} \tag{6.41}$$

The last term emerges from (6.38) after subtraction of the divergent terms plus the first term on the right-hand side, which is already present in the first term of the second line.

Before developing further the formalism, one can relate the one-loop part of the potential to the "daisy" resummation of the self-energy reviewed in the introduction of this chapter. One expands the potential near $\Phi_{30} = 0$ to quadratic order to find the mass of the static field. Scaling back to four-dimensional quantities and using $J^{(0)} = -(12\pi)^{-1}$, one obtains for $U_{3D} = \beta U_{4D}$

$$\frac{1}{2} m_T^2 \Phi_{30}^2 + J^{(0)} \left(m_T^2 + \frac{\lambda_3}{2} \Phi_{30}^2 \right)^{3/2} \approx \text{const.} + \beta \frac{1}{2} \left(m_T^2 - \frac{\lambda T}{8\pi} m_T \right) \Phi_0^2 + \ldots, \tag{6.42}$$

which exactly reproduces the resummed mass (6.6). Clearly, the higher loop corrections in the nonstatic integration go beyond the simple "daisy" approximation.

The natural question is whether one could choose the couplings of a local 3D theory to reproduce the result obtained by including the nonlocal piece. The method to find an answer to this question is called the *matching procedure*, and its two versions will be outlined in the next section.

6.4 Local Coarse-Grained Effective Theory via Matching

Matching of two theories means to require coincidence of a number of n-point functions for fixed values of their variables when computed simultaneously in both theories (recall Sect. 3.5). The conditions should be imposed in a region where one expects both theories to be valid. Since the scale of nonlocality is $\sim T$, one puts into the matching conditions momentum values much below this scale. The number of matching conditions is chosen to provide the necessary number of equations

for the determination of the relations between the two coupling sets. The local three-dimensional theory that will be matched to the nonlocal theory (6.33) has the following Lagrangian density:

$$L_{3D}^{loc} = \frac{1}{2}\left[(\nabla\varphi_3)^2 + (m_{3loc}^2 + \delta_{3loc}m^2)\varphi_3^2\right] + \frac{\lambda_{3loc}}{24}\varphi_3^4. \tag{6.43}$$

Here $m_{3loc}^2, \lambda_{3loc}$ are couplings to be determined in terms of m_T^2, λ_3, and also there is a finite rescaling relating the field variables:

$$\Phi_3(\mathbf{x}) = \zeta^{-1/2}\varphi_3(\mathbf{x}). \tag{6.44}$$

The mass counterterm of the local superrenormalizable theory at the two-loop level can be extracted from the divergences of the local two-loop contributions to U_{3D} computed in the previous point, just replacing the couplings by those of the local theory:

$$\delta_{3loc}m^2 = -J^{(1)}\lambda_{3loc}\Lambda_{loc} + \frac{\lambda_{3loc}^2}{6}L^{(ln)}\ln\frac{\Lambda_{loc}^2}{\mu^2}. \tag{6.45}$$

The cutoff Λ_{loc} has to be chosen below the scale T.

The most obvious choice for the matching conditions is to require the coincidence of the 2- and 4-point functions of the two theories at vanishing momentum. One also imposes a condition relating the kinetic terms:

$$\begin{aligned}
&\Gamma_2^{nonloc}(m_T,\lambda_3,T,p=0) = \zeta\Gamma_2^{loc}(m_{3loc},\lambda_{3loc},T,p=0),\\
&\Gamma_4^{nonloc}(m_T,\lambda_3,T,p=0) = \zeta^2\Gamma_4^{loc}(m_{3loc},\lambda_{3loc},T,p=0),\\
&\frac{\partial}{\partial p^2}\Gamma_2^{nonloc}(m_T,\lambda_3,T,p=0) = \zeta\frac{\partial}{\partial p^2}\Gamma_2^{loc}(m_{3loc},\lambda_{3loc},T,p=0).
\end{aligned} \tag{6.46}$$

Since the nonlocality of (6.33) is additive, one can decompose the n-point functions of the nonlocal theory into the sum of a local and an intrinsically nonlocal contribution:

$$\begin{aligned}
&\Gamma_2^{nonloc}(m_T,\lambda_3,T,p=0) = \Gamma_2^{loc}(m_T,\lambda_3,T,p=0) + \Delta\Gamma_2^{nonloc}(m_T,\lambda_3,T,0),\\
&\Gamma_4^{nonloc}(m_T,\lambda_3,T,p=0) = \Gamma_4^{loc}(m_T,\lambda_3,T,p=0) + \Delta\Gamma_4^{nonloc}(m_T,\lambda_3,T,0),\\
&\frac{\partial}{\partial p^2}\Gamma_2^{nonloc}(m_T,\lambda_3,T,p=0) = \frac{\partial}{\partial p^2}\Gamma_2^{loc}(m_T,\lambda_3,T,p=0)\\
&\qquad\qquad + \frac{\partial}{\partial p^2}\Delta\Gamma_2^{nonloc}(m_T,\lambda_3,T,0),
\end{aligned} \tag{6.47}$$

where $\Delta\Gamma^{nonloc}$ denotes the one-loop contribution involving one nonlocal vertex to the corresponding n-point function. The obtained expressions should be substituted into the left-hand sides of the previous set of conditions.

This additivity suggests that one looks for linearized relations

$$\zeta = 1 + \lambda_3^2 \Delta_\zeta, \qquad m_{3loc}^2 = m_T^2 + \lambda_3^2 \Delta_m, \qquad \lambda_{3loc} = \lambda_3 + \lambda_3^3 \Delta_\lambda. \tag{6.48}$$

After substituting these ansatzes on the right-hand side of (6.46), one expands to linear order in Δ_i and solves the resulting set of linear equations.

It is suggestive to apply the matching strategy directly between the original four-dimensional model and the dimensionally reduced local model [4]. Naturally, one then applies on the left-hand side of the matching conditions (6.46) derivatives of $\Gamma^{(4d)}$. The two-point function computed perturbatively in the four-dimensional theory to two-loop order can be written in a form whereby the contribution of the purely light (static) modes is separated explicitly:

$$\Gamma_2^{(4d)}(m, \lambda, T, p) = p^2 + m^2 + \Sigma_T(p^2) = p^2 + m^2 + \Sigma_T^{nonstatic} + \Sigma_T^{static}. \tag{6.49}$$

In the nonstatic self-energy contribution one includes also mixed diagrams containing at least two nonstatic propagators. Since these contributions are infrared safe, one is free to expand the nonstatic self-energy in powers of k^2:

$$\Sigma^{nonstatic}(k^2) = \Sigma^{nonstatic}(0) + \frac{d}{dk^2}\Sigma^{nonstatic}(k^2)\Big|_{k^2=0} k^2 + \mathcal{O}(k^4/T^2). \tag{6.50}$$

The renormalized self-energy is calculated with two-loop ($\mathcal{O}(\lambda^2)$) accuracy, its derivatives with one loop. The validity of the reduced model is restricted to momenta $k < \sqrt{\lambda}T$. Then the order of magnitude of the omitted terms of the expansion is estimated as $\lambda^3 T^2$. The effective coupling of the static model is λT. Therefore, the two-loop-accurate static self-energy is $\mathcal{O}(\lambda^2 T^2)$. Taking all these order-of-magnitude estimates into account, one can approximately rearrange the two-point function as

$$\begin{aligned}\Gamma_2^{(4d)}(m, \lambda, T, p) &= \left(1 + \frac{d}{dp^2}\Sigma^{nonstatic}(0)\right) \\ &\times \left[p^2 + (m^2 + \Sigma^{nonstatic}(0))\left(1 - \frac{d}{dp^2}\Sigma^{nonstatic}(0)\right) + \Sigma^{static}(p^2)\right].\end{aligned} \tag{6.51}$$

The expansion leading to this form assumes $d\Sigma^{nonstatic}/dp^2 \sim \mathcal{O}(\lambda^2)$, $\Sigma^{nonstatic} \sim \mathcal{O}(\lambda)$ and it allows the following $4d \leftrightarrow 3d$ identifications:

$$\begin{aligned}\Phi_3^2 &= \beta\left(1 + \frac{d}{dp^2}\Sigma^{nonstatic}(0)\right)\Phi_4^2, \\ m_T^2 &= (m^2 + \Sigma^{nonstatic}(0))\left(1 - \frac{d}{dp^2}\Sigma^{nonstatic}(0)\right).\end{aligned} \tag{6.52}$$

A similar calculation of the four-point function at the origin in both models fixes the self-coupling λ_3:

$$\Gamma_4^{(4d)}(m,\lambda,T,p=0)=\left[\beta\left(1+\frac{d}{dp^2}\Sigma^{nonstatic}(0)\right)\right]^2\Gamma_4^{loc}(m_T,\lambda_3,T,p=0). \tag{6.53}$$

The explicit expressions for Δ_i in the case of the (3D nonlocal) $\leftrightarrow$ (3D local) matching were calculated for the Φ^4 theory with cutoff regularization in an optimally chosen renormalization scheme [3]. The rules of the (4D local) $\leftrightarrow$ (3D local) matching were computed for a rather general class of models using dimensional regularization and $\overline{\text{MS}}$ renormalization [4].

The general constructional rule of the nonlocal three-dimensional theory is to include in the reduced theory all nonlocal vertex operators that are necessary to reproduce, within the renormalized perturbation theory of the reduced model, the contribution of all Feynman diagrams containing mixed (static and nonstatic) propagators in the full theory. The induced counterterms automatically ensure the finiteness of the result obtained in the reduced perturbation theory. Clearly, the number of necessary nonlocal vertices is increasing with the order of the perturbation theory without any limit.

The matching of two theories both containing a fixed number of local perturbatively renormalizable operators can be done by just imposing equality of some lower n-point functions (and their derivatives) at as many appropriately chosen values of their argument(s) as there are couplings that appear in the reduced model. The renormalization procedure is independently implemented in both theories, the matching results in relating the renormalized couplings. This procedure is easier to realize and its outcome is more transparent, but there is no guarantee of the coincidence of any of the n-point functions in an extended range of the arguments even in the lowest orders of the perturbation theory. Parallel applications to specific physical problems of the full and the reduced theories give one a chance to evaluate the accuracy of the matching for physically relevant observables. A nice research program of outstanding physical interest offering the opportunity for this kind of comparative study was the investigation of the electroweak symmetry-restoring phase transition in the 1990s (see Chap. 8).

6.5 Dimensional Reduction of a Gauge Theory at the One-Loop Level

The origin of the matter–antimatter asymmetry of our cosmic neighborhood is one of the most intriguing questions in the focus of both high-energy and astrophysical research. The famous Sakharov conditions [5] for the dynamical generation of this asymmetry include the necessity of far-from-equilibrium evolutionary period(s) during the history of the universe. Since the standard model possesses the other two

features (existence of baryon-number-changing processes and CP-violation), it was an important research direction in the mid-1990s to clarify whether the evolution based on a joint solution of the equations of the gravitational and quantum field theories could lead to substantial deviations from thermal equilibrium in the era of the hot universe.

The most common phenomenon in which thermal equilibrium is temporarily suppressed is a discontinuous (first-order) phase transition. For this reason, it was natural to ask whether the Brout–Englert–Higgs symmetry-breaking phenomenon occurred in the early universe via first-order phase transition. A most economical way to answer this question was the Monte Carlo investigation of the change in the ground state of the standard model in the framework of the dimensionally reduced finite-temperature theory, as initiated by K. Kajantie and collaborators [6].

As preparation for the discussion of the electroweak phase transition in Chap. 8, we shall present the steps and the peculiarities requiring the special attention of dimensional reduction in the case of gauge theories. The example to be used here will be the simplest gauge theory, namely the scalar electrodynamics or the $U(1)$ symmetric Higgs model.

The model is defined with the Euclidean action

$$S_{U(1)} = \int_0^\beta d\tau \int d^3x \left[\frac{1}{4} F_{mn} F_{mn} + \frac{1}{2} |(\partial_m + igA_m)\Phi(\mathbf{x}, \tau)|^2 + \frac{1}{2} m^2 |\Phi|^2 + \frac{\lambda}{24} |\Phi|^4 \right] + S_{U(1),ct}. \tag{6.54}$$

The Euclidean continuation of the field-strength tensor F_{mn} is defined as the antisymmetric derivative of the vector potential: $F_{mn} = \partial_m A_n - \partial_n A_m$. The electric charge of the complex field $\Phi(\mathbf{x}, \tau)$ is g. All couplings are renormalized and $S_{c.t.}$ stands for the counterterms necessary for the cancellation of the four-dimensional UV-divergences of the renormalized perturbation theory.

The one-loop integration over the nonstatic gauge and scalar modes will be done in a static real $\Phi_0(\mathbf{x})$ and $A_0(\mathbf{x})$ background. For the integration, the most convenient approach is to use the so-called thermal axial gauge, whereby the nonstatic part of the $m = 0$ component of the vector potential is set to zero. Therefore, denoting the nonstatic modes by lowercase symbols, one has the following decomposition of the fields:

$$\begin{aligned} &\Phi(\mathbf{x}, \tau) = \Phi_0(\mathbf{x}) + \varphi(\mathbf{x}, \tau), \quad A_i(\mathbf{x}, \tau) = a_i(\mathbf{x}, \tau), \qquad A_0(\mathbf{x}, \tau) = A_0(\mathbf{x}), \\ &\varphi(\mathbf{x}, \tau) = \sum_{n \neq 0} \varphi_n(\mathbf{x}) e^{i\omega_n \tau}, \qquad a_i(\mathbf{x}, \tau) = \sum_{n \neq 0} a_{in}(\mathbf{x}) e^{i\omega_n \tau}. \end{aligned} \tag{6.55}$$

In this gauge and with the present background gauge field, the three-dimensional $U(1)$ local symmetry is preserved. Therefore, the gradient piece of the reduced theory will contain the three-dimensional covariant derivative. Therefore, it is sufficient to find the renormalized kinetic piece for the scalar field. Also, it is

unnecessary to introduce a nonzero $A_i(\mathbf{x})$, since every nonzero mass or higher-power term is forbidden by the reduced gauge invariance.

One-loop integration requires that one finds the part of the action quadratic in the nonstatic fields. The relevant pieces of the Lagrangian density for the one-loop computation are $L^{(0)}+L^{(2)}$, which are easily found:

$$\frac{1}{4}F_{mn}F_{mn} = \frac{1}{2}(\partial_i A_0(\mathbf{x}))^2 + \frac{1}{2}(\partial_i a_0(\mathbf{x}))^2 + \frac{1}{2}\left((\partial_i a_j)^2 - (\partial_i a_i)^2\right), \tag{6.56}$$

$$\begin{aligned}
&\frac{1}{2}D_m\Phi^* D_m\Phi \rightarrow \\
&\rightarrow \frac{1}{2}\left[(\partial_i\Phi_0(\mathbf{x}))^2 + g^2A_0(\mathbf{x})^2\Phi_0^2 + (\partial_m\varphi_1)^2 + (\partial_m\varphi_2)^2 + g^2A_0^2(\varphi_1^2+\varphi_2^2)\right] \\
&\quad + \frac{1}{2}\left[2gA_0(\varphi_2\dot{\varphi}_1 - \varphi_1\dot{\varphi}_2) - 2ga_i\left(\Phi_0\partial_i\varphi_2 - \Phi_0\partial\varphi_1\right) + g^2a_i^2\Phi_0^2\right], \\
&\frac{1}{2}m^2\Phi^*\Phi + \frac{\lambda}{24}(\Phi^*\Phi)^2 \rightarrow \\
&\rightarrow \frac{1}{2}m^2\Phi_0^2 + \frac{\lambda}{24}\Phi_0^4 + \frac{1}{2}m^2(\varphi_1^2+\varphi_2^2) + \frac{\lambda}{12}\Phi_0^2\left(3\varphi_1^2+\varphi_2^2\right).
\end{aligned} \tag{6.57}$$

Here the dot on the top of a symbol denotes the τ-derivative.

On a strictly homogeneous background, one finds the contributions to the potential energy density, though no information is obtained on any change (rescaling) of the kinetic term. In this case, the quadratic piece in Fourier space has the expression

$$\begin{aligned}
L^{(2)} = \frac{1}{2}\varphi_{\alpha n}(k)^*\Bigg[&\left(\omega_n^2 + k^2 + g^2A_0^2 + m^2 + \frac{\lambda}{6}\Phi_0^2\right)\delta_{\alpha\beta} \\
&-2\epsilon_{\alpha\beta}i\omega_n gA_0 + \frac{\lambda}{3}\Phi_0^2\delta_{\alpha 1}\delta_{\beta 1}\Bigg]\varphi_{\beta n}(k) \\
&+\frac{1}{2}a_n^{i*}\left[(\omega_n^2+k^2)\delta_{ij} - k_ik_j + g^2\Phi_0^2\delta_{ij}\right]a_n^j(k) \\
&+ig\phi_0k_ia_n^{i*}(k)\varphi_2(k).
\end{aligned} \tag{6.58}$$

It is obvious that the two scalar components (φ_α, $\alpha = 1, 2$) are coupled to the longitudinal gauge mode $\sim \partial_i a_n^i$. The two transversal gauge modes are eigenmodes of the harmonic expansion around the background. Using the identity "Trlog = logDet" a little algebra allows us to find the contribution of the (3×3)-dimensional coupled

sector to the action of the effective potential of the three-dimensional action:

$$U_{3D} = \frac{1}{2}g^2 A_0(\mathbf{x})^2 \Phi_0^2 + \frac{1}{2}m^2\Phi_0^2 + \frac{\lambda}{24}\Phi_0^4 + \frac{1}{2}\sum_{n\neq 0}\int \frac{d^3k}{(2\pi)^3}\Bigg[\ln\Big[(\omega_n^2 + M_A^2)\left((K^2 + g^2A_0^2 + M_H^2)(K^2 + g^2A_0^2 + M_G^2)\right. \\ \left. -4\omega_n^2 g^2 A_0^2\right) - k^2 M_A^2 (K^2 + g^2A_0^2 + M_H^2)\Big] + 2\ln(K^2 + M_A^2)\Bigg]. \tag{6.59}$$

The following quantities are abbreviated in this formula:

$$M_A = g\Phi_0, \quad M_G^2 = m^2 + \frac{\lambda}{6}\Phi_0^2, \quad M_H^2 = m^2 + \frac{\lambda}{2}\Phi_0^2, \quad K^2 = \omega_n^2 + k^2 \tag{6.60}$$

The Taylor expansion of the logarithms in powers of the masses can be applied to the above expression without any risk, since in the denominators of the different terms of the expansion, expressions of the form $(\omega_n^2)^{l_1}(K^2)^{l_2}$, $n \neq 0$ will figure. After performing the corresponding Matsubara sum-integrals, one proceeds to the determination of the leading-order countercouplings $\delta m_1^2, \delta\lambda_1, \delta g_1$. The divergences occurring in the coefficients of the pure Φ_0 powers are of the same character as in the Φ^4 theory, except there will also be contributions proportional to $g^2, \lambda g$. Since in this calculation the field renormalization is neglected, one cannot determine correctly the charge countercoupling δg_1 from the divergent coefficient of $A_0^2\Phi_0^2$. At this approximation, therefore, δg_1 is also kept at zero. Finally, the coefficients of the pure A_0 powers should turn out free of four-dimensional divergences, since there are no counterterms to these operators.

Let us see in some detail the emerging thermal mass of A_0. Collecting all terms proportional to $g^2A_0^2$, one obtains

$$g^2A_0^2\sum_{n\neq 0}\int_q \left(2\frac{1}{\mathbf{q}^2 + \omega_n^2} - 4\frac{\omega_n^2}{(\mathbf{q}^2 + \omega_n^2)^2}\right). \tag{6.61}$$

For the relevant Matsubara sums we have the following results:

$$\sum_{n\neq 0}\frac{1}{\beta^2(\mathbf{q}^2 + \omega_n^2)} = \frac{1}{4y}\left(1 + \frac{2}{e^{2y} - 1} - \frac{1}{4y^2}\right), \qquad y = \frac{\beta q}{2}$$
$$-\sum_{n\neq 0}\frac{4\beta^2\omega_n^2}{\beta^4(\mathbf{q}^2 + \omega_n^2)^2} = -\frac{1}{2y}\left(1 + 2\frac{1}{e^{2y} - 1}\right) + 2e^{2y}\frac{1}{(e^{2y} - 1)^2}. \tag{6.62}$$

The momentum integral cutoff at $|\mathbf{q}|_{\max} = \Lambda$ over the sum can be performed exactly:

$$\beta V \times \frac{1}{2} A_0^2 \left(\frac{g^2 T^2}{3} - \frac{g^2 \Lambda T}{2\pi^2} \right). \tag{6.63}$$

With similar calculation, one obtains, for the effective action up to operators of fourth power (with classical kinetic terms and choosing a renormalization scheme where the quartic self-coupling of the reduced model is just λT),

$$\begin{aligned}
L_{3D}^{pot} &= \frac{1}{2} m_3^2 \varphi^* \varphi + \frac{1}{2} m_D^2 \bar{A}_0^2 + \frac{\lambda T}{24} (\varphi^* \varphi)^2 + \frac{g_3^4 \beta}{24\pi^2} \bar{A}_0^4 + \frac{1}{2} \bar{g}^2 \bar{A}_0^2 \varphi^2, \\
L_{3D}^{kin} &= \frac{1}{4} \bar{F}_{ij} \bar{F}_{ij} + \frac{1}{2} D_i[A] \varphi^* D_i[A] \varphi + \frac{1}{2} (\partial_i \bar{A}_0)^2, \quad D_i[A] \varphi = (\partial_i + i g_3 \bar{A}_i) \varphi, \\
L_{3D}^{counter} &= -\frac{\Lambda}{2\pi^2} \left[\frac{1}{2} \varphi^* \varphi \left(3 g_3^2 + \frac{2}{3} \lambda \right) + \frac{1}{2} \bar{A}_0^2 g_3^2 \right].
\end{aligned} \tag{6.64}$$

The following notation is used:

$$m_D^2 = \frac{1}{3} g_3^2 T, \qquad m_3^2 = \frac{1}{24} \left(\frac{2}{3} \lambda + 3 g_3^2 \right) T, \tag{6.65}$$

and

$$\varphi = \sqrt{\beta} \Phi, \qquad \bar{A}_i = \sqrt{\beta} A_i, \qquad \bar{A}_0 = \sqrt{\beta} A_0, \qquad g_3^2 = g^2 T. \tag{6.66}$$

The expression of the coupling m_3^2 is given in terms of the renormalized quantities of the four-dimensional theory. Its explicit form depends on the renormalization conditions imposed on $U_{3D}(\Phi_0, A_0)$ [7].

A one-loop-accurate solution of the effective models offers some insight into the mechanism of the finite-temperature symmetry restoration. The most convenient choice for the evaluation of U_{3D} with one-loop accuracy on a constant background φ_0 is to choose the so-called 't Hooft gauge, which suppresses the A_L-φ_2 coupling ($A_{Li} = \hat{k}_i \hat{\mathbf{k}} \mathbf{A}$) in the quadratic part of the action (the last line below):

$$\begin{aligned}
S_{3D}^{(2)} = \int_k \Big[& \frac{1}{2} A_i^*(\mathbf{k}) (k^2 \delta_{ij} - k_i k_j) A_j(\mathbf{k}) + g_3^2 \varphi_0^2 |A_i(\mathbf{k})|^2 \\
& + \frac{1}{2} A_0^*(\mathbf{k}) (k^2 + m_D^2 + g_3^2 \varphi_0^2) A_0(\mathbf{k}) \\
& + \frac{1}{2} \varphi_\alpha^*(\mathbf{k}) \left(\left(k^2 + m_3^2 + \frac{\lambda}{6} \varphi_0^2 \right) \delta_{\alpha\beta} + \frac{\lambda}{3} \delta_{\alpha 1} \delta_{\beta 1} \varphi_0^2 \right) \varphi_\beta(\mathbf{k}) \\
& + \frac{i}{2} g_3 \varphi_0 \left(\mathbf{k} \mathbf{A}_\mathbf{L}^*(\mathbf{k}) \varphi_2(\mathbf{k}) - \varphi_2^*(\mathbf{k}) \mathbf{k} \mathbf{A}_\mathbf{L}(\mathbf{k}) \right) \Big].
\end{aligned} \tag{6.67}$$

The following gauge-fixing functional is chosen:

$$F = \nabla \mathbf{A}(x) - \xi g_3 \varphi_0 \varphi_2(x), \tag{6.68}$$

which gives for the gauge-fixed action, after adding to it $(1/2\xi)\int F^2$,

$$\begin{aligned} S_{3D}^{(2)'tHooft} = \int_k \Big[& \frac{1}{2} A_i^*(\mathbf{k}) \left(k^2 \delta_{ij} - k_i k_j \left(1 - \frac{1}{\xi} \right) + g_3^2 \varphi_0^2 \right) A_j(\mathbf{k}) \\ & + \frac{1}{2} A_0^*(\mathbf{k}) (k^2 + m_D^2 + g_3^2 \varphi_0^2) A_0(\mathbf{k}) \\ & + \frac{1}{2} \varphi_1^*(\mathbf{k}) \left(k^2 + m_3^2 + \left(\frac{\lambda}{6} + \xi g_3^2 \right) \varphi_0^2 \right) \varphi_1(\mathbf{k}) \\ & + \varphi_2^*(\mathbf{k}) \left(k^2 + m_3^2 + \frac{\lambda}{3} \varphi_0^2 \right) \varphi_2(\mathbf{k}) \Big]. \end{aligned} \tag{6.69}$$

The quadratic form is now diagonal; each degree of freedom independently contributes to the effective potential. One also has to take into account the opposite-sign contribution from the Fadeev–Popov determinant:

$$\mathrm{Det}(\triangle - \xi g_3^2 \varphi_0^2) = e^{\mathrm{Trlog}(\triangle - \xi g_3^2 \varphi_0^2)} = e^{V \int_k \ln(k^2 + \xi g_3^2 \varphi_0^2)}. \tag{6.70}$$

For definiteness, we choose $\xi = 1$ when the masses of the ghost and the transversal gauge boson become equal. These are the degrees of freedom that do not receive any thermal (Debye) mass. One checks explicitly that in the effective potential, the linear divergences ($\sim \Lambda$) are exactly canceled by the induced counterterm contributions. Finally, the finite contribution is rewritten in terms of four-dimensional quantities:

$$\begin{aligned} \beta U_{4D}(\Phi_0) = & \frac{1}{2} \left(m^2 + \frac{1}{24} T^2 \left(3g^2 + \frac{2}{3} \lambda \right) \right) \Phi_0^2 + \frac{\lambda}{24} \Phi_0^4 \\ & - \frac{1}{12\pi} T \Bigg[g^3 \Phi_0^3 + \left(m^2 + \frac{1}{24} T^2 \left(3g^2 + \frac{2}{3} \lambda \right) \right. \\ & \left. + \left(g^2 + \frac{\lambda}{6} \right) \Phi_0^2 \right)^{3/2} + \left(m^2 + \frac{1}{24} T^2 \left(3g^2 + \frac{2}{3} \lambda \right) + \frac{\lambda}{2} \Phi_0^2 \right)^{3/2} \\ & + \left(\frac{1}{3} g^2 T^2 + g^2 \Phi_0^2 \right)^{3/2} \Bigg]. \end{aligned} \tag{6.71}$$

The presence of the cubic terms is a clear signal for some sort of infinite resummation, since it is not analytic in the field amplitude. The potential is of "van der Waals type," since the coefficient of the sum of cubic contributions is negative. Were one to estimate the temperature-dependence of the effective potential without

the 3D contributions, the usual mean field argument would signal a second-order phase transition at T_c, where the thermal mass cancels the wrong sign $m^2 < 0$. The question of interest is, how intensive should the cubic piece be for turning this conclusion into one predicting a first-order phase transition?

This question is discussed as a last point of this section using the example of a simpler function, still reflecting the main features of the variation of the potential under the effect of changing temperature. Consider a generic potential parameterized as

$$U(\Phi) = A(T)\Phi^2 + B(T)\Phi^4 + C(T)\left(\Phi^2 + K^2(T)\right)^{3/2}, \qquad C(T) < 0. \tag{6.72}$$

Calculating the second derivative of U at the origin, one easily obtains the equation that determines the temperature below which the symmetric point becomes absolutely unstable:

$$V''(0) = 2A(T_2) + 3C(T_2)K(T_2) = 0. \tag{6.73}$$

For $T > T_2$, the first derivative vanishes at three points. One root is the origin; the other two are given as

$$\Phi_{\pm}^2(T) = \frac{1}{32B^2}\left[9C^2 - 16AB \pm 3|C|\left(9C^2 + 32(2B^2K^2 - AB)\right)^{3/2}\right]. \tag{6.74}$$

The temperature where

$$\Phi_+(T_1) = \Phi_-(T_1) \tag{6.75}$$

is the temperature where a metastable minimum appears first on decreasing the temperature. If $T_1 > T_2$, one sees how the nontrivial (metastable) minimum gets deeper until eventually it touches the Φ-axis. This temperature $T_2 < T_c < T_1$ defines the first-order transition temperature.

In Chap. 8, we shall analyze, along the lines sketched above, the electroweak transition. After discussing results from a gauge-invariant version of the optimized perturbation theory, we shall briefly describe the results of the nonperturbative (lattice) investigations.

References

1. L. Dolan, R. Jackiw, Phys. Rev. D **9**, 3320 (1974)
2. P. Ginsparg, Nucl. Phys. B **170**, 388 (1980)
3. A. Jakovác, Phys. Rev. D **53**, 4538 (1996)
4. K. Kajantie, M. Laine, K. Rummukainen, M. Shaposhnikov, Nucl. Phys. B **458**, 90 (1996)
5. A. Sakharov, J. Exp. Theor. Phys. **5**, 24 (1967)
6. K. Kajantie, K. Rummukainen, M. Shaposhnikov, Nucl. Phys. B **407**, 356 (1993)
7. A. Jakovác, K. Kajantie, A. Patkós, Phys. Rev. D **49**, 6810 (1994)

Chapter 7
Thermodynamics of the Strong Matter

The focus of this chapter is on the changing nature of the thermodynamic degrees of freedom characterizing the strong matter. The theories employed are variants of the effective meson–quark theories theoretically discussed in Chaps. 4 and 5 of these notes. Here we shall mostly rely on the renormalized equations derived previously. The discussion begins with the thermodynamics of the $\pi - \sigma$ system completed at a more advanced stage by quark degrees of freedom. In this family of models, the excitation spectra at zero temperature and baryon density are found with the help of a large-N solution, which allows one to determine the actual values of the couplings. The nature of the finite-temperature phase transformations and the behavior of the excitations in a neighborhood of the transition temperature follows, and finally, we turn to the effect of the finite baryo-chemical potential (μ_B) on the transition. The second model family (the three-flavor meson–quark model) is more complete, since it includes both the scalar and the pseudoscalar nonets. The process of zero-temperature parameterization was described in the OPT framework in Chap. 4. Here the change in the spectra at finite T and μ_B will be discussed. The scope of the investigations is expressed best in the form of a phase diagram (see Fig. 7.6), which exhibits the nature of the finite-temperature transition as established for different values of the baryo-chemical potential on arbitrarily chosen values of the mass of the Goldstone bosons (the pion and the kaon). In the second part of this chapter, we shall concentrate on the equation of state of the strong matter. The functional dependence of the pressure on the energy density plays a central role in any theoretical approach to high-energy heavy-ion experiments or the internal structure of compact astrophysical objects, such as neutron stars. Here the style of the discussion is closer to field-theory-motivated phenomenological model investigations than to searching for solutions using the formal rules of the relevant quantum field theories.

A. Jakovác, A. Patkós, *Resummation and Renormalization in Effective Theories of Particle Physics*, Lecture Notes in Physics 912,
DOI 10.1007/978-3-319-22620-0_7

7.1 The Thermodynamics of the $\pi - \sigma -$ Quark System

7.1.1 The $T = 0$ Excitation Spectra

Nontrivial phenomenology can be built on the LO solution of the Gell-Mann–Lévy linear sigma model discussed in Chap. 5. The input parameters used for fixing the renormalized couplings are the $T = 0$ mass of the pion $m_{G0} \approx 140\,\mathrm{MeV}$ and the decay constant $f_\pi \approx 90\,\mathrm{MeV}$ characterizing the weak decay of the charged pions. Also, one sets $N = 4$. Then applying the PCAC theorem to the pion decay and using Eqs. (5.50), (5.60), and (5.61), one arrives at the relations

$$v_0 = \frac{f_\pi}{\sqrt{N}}, \qquad m_{G0}^2 = \frac{h}{v_0}, \qquad m^2 = -\frac{\lambda}{6N} f_\pi^2 + m_{G0}^2 \left(1 - \frac{\lambda}{96\pi^2} \ln \frac{m_{G0}^2 e}{M_0^2}\right), \tag{7.1}$$

which determine the (renormalized) parameters v_0, h, m^2, using the explicit form of the finite M_0-dependent part of the tadpole integral. The zero of the inverse σ-propagator (5.64) continued to Minkowski metrics determines the mass of the sigma particle ($|\mathbf{p}| = 0$):

$$iG_{\sigma\sigma}^{-1}(p_0) = p_0^2 - m_{G0}^2 - \frac{\lambda_R}{3N} f_\pi^2 \frac{1}{1 - \frac{\lambda_R}{6} \mathscr{B}^F(p_0, m_{G0})} = 0. \tag{7.2}$$

Here one needs the finite part of the bubble integral:

$$\mathscr{B}^F(p_0, m_{G0}) = \frac{1}{16\pi^2} \left[\ln \frac{m_{G0}^2}{M_0^2} - \sqrt{1-x} \ln \frac{\sqrt{1-x} - 1}{\sqrt{1-x} + x} \right], \qquad x = \frac{m_{G0}^2}{p_0^2}. \tag{7.3}$$

It is notable that it has a finite limiting expression also in the chiral limit. This set of equations obeys the renormalization group invariance of the full solution. Namely, one can find a functional form of $\lambda(M_0^2)$ leading to the same m^2 for a fixed input f_π, m_{G0}, independent of M_0.

The model predicts the σ-mass as a function of λ. The physically interesting root of (7.2) is in the lower half-plane of the second complex Riemann sheet parameterized as $m_\sigma - i\Gamma_\sigma$. In the chiral case, the easiest approach is to search for it in the form

$$p_0 = M_0 e^{-i\varphi_0}, \qquad m_\sigma = M_0 \cos\varphi_0, \qquad \Gamma_\sigma = M_0 \sin\varphi_0. \tag{7.4}$$

If the pion mass is finite, one shifts the parameterization to the location of the $\sigma \to \pi\pi$ cut:

$$p_0 = 2m_{G0} + \bar{M}_0 e^{-i\bar{\varphi}_0}. \tag{7.5}$$

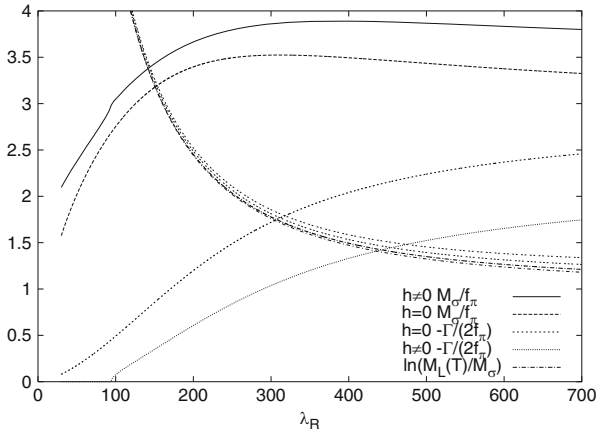

Fig. 7.1 The real and imaginary parts of the complex pole of the σ-propagator for $T = 0$. Results are presented both for the chiral limit and for a value of the explicit symmetry-breaking corresponding to realistic pion mass. Also is shown the purely imaginary Landau pole, which clearly sets a natural upper bound on λ (from [1])

In Fig. 7.1, the λ-dependence of the mass m_σ and the width Γ_σ are displayed both for $h = 0$ and $h \neq 0$. In the figure, a bunch of descending curves appears, which corresponds to the logarithm of the purely imaginary pole iM_L calculated in proportion of m_σ for several temperatures. It reflects the Landau-pole singularity of the scalar self-coupling discussed in Sect. 5.3. The theory makes sense only if the absolute scale of the Landau ghost lies much higher than the physical excitation spectra. This requirement clearly puts an upper limit on the allowed range of the renormalized self-couplings λ ($\lambda_{max} \approx 300$, since above this value $M_L/M_\sigma < \exp(1.5) \approx 4.5$). The same mechanism is at work in the standard model, where one has to include also the effect of the top quark in a realistic computation of the scale of the electroweak Landau singularity.

It is curious that the numerical solution of (7.2) displays a maximum. Apparently, the value of the σ-mass cannot exceed $4f_\pi$. This value is on the lower edge of the mass range, quoted by the Particle Data Group. It is below the value obtained from analyzing the phase shift in the isoscalar–scalar channel of the $\pi - \pi$ scattering in the framework of the chiral perturbation theory [2]. This remark raises a number of interesting questions: Does this upper bound becomes looser at NLO? Does there exist such an upper bound in extended versions of the linear σ-model containing more meson/quark fields?

The LO solution of the extended quark–meson model, discussed in Sect. 5.7, led to the σ-propagator (5.161). After Minkowskian continuation, one has to find the complex root of the following modified equation:

$$iG_{\sigma\sigma}^{-1}(q) = iG_{\pi}^{-1}(q) - \frac{\lambda}{3}v^2 \frac{1}{1 - \frac{\lambda}{6}\mathscr{B}^F(q, M_G)} + \frac{8g^4 N_c N_f}{N} v^2 \mathscr{B}^F(q, m_Q). \tag{7.6}$$

One can exploit the freedom to introduce into the fermionic renormalized bubble integral the renormalization scale M_{0F}, which is somewhat different from that used in the bosonic part (M_{0B}), although they should be chosen to be of same order of magnitude. One can attempt to tune the ratio $M_{0B}/M_{0F} \equiv \exp(\eta)$ to minimize the renormalization-scale-dependence of the characteristics of the thermal transition.

By the analyticity of the propagator, the spectral function defined with zero spatial momentum $\mathbf{q} = 0$ as

$$\rho_\sigma(\omega) = \frac{1}{\pi} \lim_{\epsilon \to 0} \mathrm{Im}\left[iG_{\sigma\sigma}(\omega + i\epsilon, 0)\right] \tag{7.7}$$

is sufficient to characterize fully the propagator through a dispersive representation. In Fig. 7.2, the ideal resonance-like shape is largely distorted, but the location of the maxima moves toward the phenomenologically more acceptable range due to the fermionic contribution.

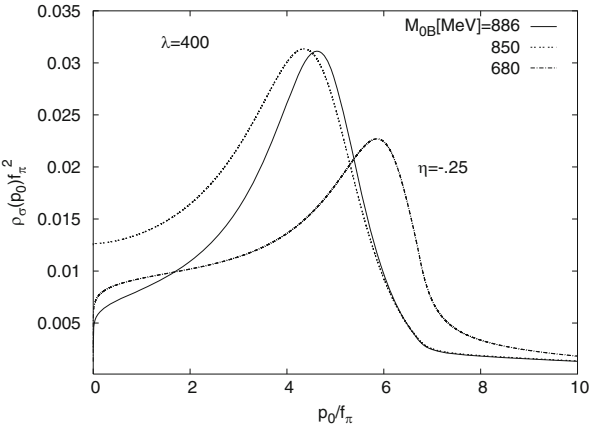

Fig. 7.2 The spectral function of the σ excitation at $T = 0$ in the quark–meson theory ($\eta = \ln(M_{0B}/M_{0F}) = -1/4$) for three somewhat different values of M_{0B} (from [3])

7.1.2 Change of the Ground State at Finite Temperature and Finite Density

In the $\pi - \sigma -$quark system at finite temperature, the pion tadpole receives a thermal Bose–Einstein contribution, and similar corrections appear in the quark tadpole characterized by the Fermi–Dirac distribution. The two will modify the equation of state (5.160) to

$$M_\pi^2(T) = m_R^2 + \frac{\lambda_R}{6}v^2(T) + \frac{\lambda_R}{96\pi^2}M_\pi^2(T)\ln\frac{M_\pi^2(T)e}{M_{0B}^2} - \frac{g^2N_c}{8\pi^2}M_Q^2(T)\ln\frac{M_Q^2(T)e}{M_{0F}^2}$$
$$+ \frac{\lambda_R T^2}{12\pi^2}\int_{M_\pi(T)/T}^{\infty} dy(e^y-1)^{-1}(y^2 - M_\pi^2(T)/T^2)^{1/2}$$
$$+ \frac{g^2N_cT^2}{\pi^2}\int_{M_Q(T)/T}^{\infty} dy(e^y+1)^{-1}(y^2 - M_Q^2(T)/T^2)^{1/2}. \tag{7.8}$$

First, one can analyze the chiral limit when $M_\pi = 0$. At the critical temperature T_c, the vacuum expectation value of σ vanishes ($M_Q(T_c) = gv(T_c) = 0$). Both integrals can be calculated, and one arrives at the equation

$$0 = m_R^2 + \left(\frac{\lambda_R}{6} + g^2N_c\right)\frac{T_c^2}{12}. \tag{7.9}$$

The case of nonzero baryo-chemical potential is obtained from (7.8) by replacing the Fermi–Dirac factor $(e^y+1)^{-1}$ in the last integral by $(ze^y+1)^{-1}+(e^y/z+1)^{-1}$, where $z = e^{\mu/T}$ is called *fugacity*. Then the integral over the Fermi–Dirac distribution can be performed term by term using an expansion of the integrand in powers of z. The result can be expressed in terms of a specific polylogarithmic function $Li_2(z)$. Making use of the identity (B.10), one arrives at the simple equation

$$m_R^2 + \left(\frac{\lambda_R}{6} + g^2N_c\right)\frac{T_c(\mu)^2}{12} + \frac{g^2N_c\mu^2}{4\pi^2} = 0. \tag{7.10}$$

The dependence of the critical temperature on the baryo-chemical potential can be deduced from comparing this equation with the previous one, (7.9), where $T_c = T_c(\mu = 0)$ is understood.

The line of second-order transitions changes into a first-order line at a tricritical point (TCP) where also the coefficient of the quartic ($\sim v^4$) term in the effective potential vanishes. This term is obtained by setting the derivative of the equation of state (7.8) with respect to v^2 to zero. This leads to the following analytic expression:

$$\frac{\lambda_R}{6} + \frac{g^4N_c}{4\pi^2}\left[\left(\frac{\partial}{\partial n}\left(\mathrm{Li}_n(-z) + \mathrm{Li}_n(-1/z)\right)\right)\Big|_{n=0} - \ln\frac{const.\times T_{TCP}}{M_0B}\right] = 0. \tag{7.11}$$

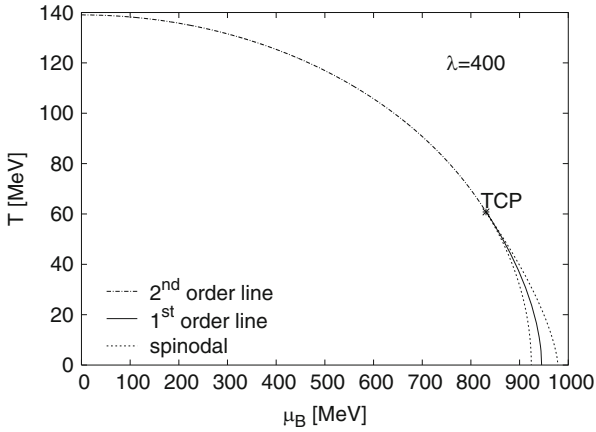

Fig. 7.3 The phase diagram in the $T-\mu$-plane ($M_{0B} = M_{0F} = 886\,\text{MeV}$). On the *left* from the tricritical point (TCP) the symmetric and the broken symmetry phases are separated by a second-order transition (*dashed*) *line*. On the two sides of the first-order line on the *right* of TCP, the (*dotted*) *lines* enclose the region of spinodal instability (from [3])

The root of this equation when combined with (7.10) determines the coordinates μ_{TCP}, T_{TCP} of the tricritical point. The solution with realistically chosen parameters is displayed in Fig. 7.3. In the case of explicit breaking of the chiral symmetry, the second-order line will change into a crossover region, and in place of TCP, a critical endpoint (CEP) of the first-order line appears. The location of the CEP for realistic pion mass is close to that of the TCP displayed in the figure. The existence of a CEP is largely debated in numerical simulations of QCD. The existing Monte Carlo simulations suffer from unknown systematic errors because of the negative weights associated with certain gauge configurations. The first numerical estimates of the CEP location [4] indicate lower μ_{CEP} and higher T_{CEP} values than what is obtained with the large-N approximation presented here. There are studies that have led to opposing the existence of the CEP [5]. The result presented here, however, is fully consistent with most the estimates derived to date from various versions of the effective chiral models [6–11].

7.2 The $U(3) \times U(3)$ Meson Model

An approximate solution of this broader model at $T = 0$, described in Chap. 4, relies on the optimized perturbation theory at the one-loop level. The renormalized couplings were determined exclusively with data from the pseudoscalar sector, avoiding the use of the scalar meson spectra, where the experimental knowledge is much less reliable.

Particularly important is the role of the optimization conditions (4.44) imposed on the π and K propagators. These equations are extended to finite T by evaluating the contributing one-loop self-energy diagrams as

$$\Sigma_M(p^2 = -m_\pi^2, m_i, \kappa) = \Sigma_M^{(T=0)}(p^2 = -m_\pi^2, m_i, \kappa) + \Sigma_M^{(T)}(p^2 = -m_\pi^2, m_i, \kappa), \tag{7.12}$$

where $M = \pi, K$ and one separates the $T = 0$ and $T \neq 0$ contributions. In principle, one should evaluate the self-energy self-consistently on the respective mass shells of the pion and the kaon. In practice, the computation is much simpler when one assumes that the momentum-dependence of the self-energies is negligible. Then the temperature-dependent part of the self-energies is computed at $p^2 = 0$. At this point, the bubble integrals can be expressed with help of tadpoles:

$$\mathscr{B}^F(p = 0, m_1, m_2) = \frac{\mathscr{T}^F(m_1, T) - \mathscr{T}^F(m_2, T)}{m_2^2 - m_1^2}. \tag{7.13}$$

As a consequence, the temperature-dependent corrections to the consistency conditions will consist of a linear combination of the T-dependent parts of the tadpole contributions evaluated with appropriate meson masses:

$$\begin{aligned}
m_\pi^2 &= -\mu^2 + 2(2f_1 + f_2)x^2 + 4f_1y^2 + 2gy \\
&\quad + Z_\pi \Sigma_\pi^{(1-loop,T=0)}(-m_\pi^2, m_i(m_\pi), \kappa) + \sum_{\alpha=\pi_i,\sigma_i} c_\alpha^\pi \mathscr{T}^F(m_i(m_\pi), T \neq 0), \\
m_K^2 &= -\mu^2 + 2(2f_1 + f_2)x^2 + 4f_1y^2 + 2gy - \sqrt{2}x(2f_2y - g) \\
&\quad + Z_K \Sigma_K^{(1-loop,T=0)}(-m_K^2, m_i(m_K), \kappa) \\
&\quad + \sum_{\alpha=\pi_i,\sigma_i} c_\alpha^K \mathscr{T}^F(m_i(m_K), T \neq 0).
\end{aligned} \tag{7.14}$$

The notation $m_i(m_\pi)$ or $m_i(m_K)$ emphasizes that in the equations, all meson masses are expressed with the help of the appropriately chosen Goldstone boson (for the η field, the 1-loop pole mass; for all others the tree-level masses were used in [12]).

When these equations are solved together with the Ward identities (4.48), one obtains the temperature-dependent quantities $x(T), y(T), m_\pi(T), m_K(T)$. Based on the PCAC relations (4.49), one determines also the temperature-dependence of f_π, f_K. The tree-level mass relations transfer the temperature-dependence of the Goldstone bosons on the masses of all other fields. The transition is well characterized by the variation of these quantities displayed in Fig. 7.4. The left-hand figure displays the variation of the nonstrange (x) and strange (y) order parameters in proportion to $f_\pi(T = 0)$ for four different choices of the renormalization scale (denoted in the figure by l) It is obvious that the crossover happens around $T = 200\,\text{MeV}$ and is dominated by the nonstrange order parameter. The variation of the renormalization scale only mildly influences the transition. In the right-hand figure,

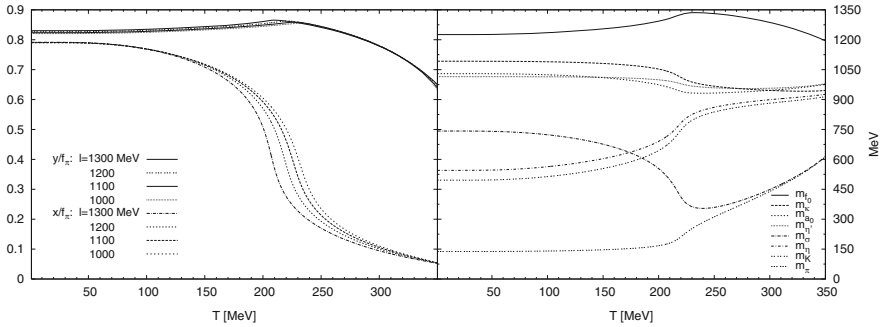

Fig. 7.4 *Left*: the T-variation of the order parameters x and y and the sensitivity to the choice of the renormalization scale. *Right*: the T-dependence of the masses in the pseudoscalar (π, K, η, η') and scalar $(\sigma, a_0, \kappa, f_0)$ multiplets (from [12])

the variation of the meson masses is displayed. Here one notices the masses of the parity partners from the scalar and pseudoscalar nonet approaching each other. The approximate degeneracy is realized well above the transition region ($T > 250$ MeV).

7.2.1 Phase Transition in the Three-Flavor Quark–Meson Model

For the determination of the temperature-dependence of the nonstrange ($x(T)$) and strange ($y(T)$) condensates, it is sufficient to consider in addition to the equations of state, the equation of the pion mass solved self-consistently. For convenience, Eqs. (4.54), (4.36) will be given here again, in a slightly more explicit form:

$$\begin{aligned}
\epsilon_x &= x(-\mu^2 + 2gy + 2(2f_1 + f_2)x^2 + 4f_1y^2) + \sum_i t_i^x \mathscr{T}^F(m_i(m_\pi) \\
&\quad -4g_F N_c M_u \mathscr{T}^F(M_u), \\
\epsilon_y &= y(-\mu^2 + 4f_1xy + 4(f_1 + f_2)y^2 + 4f_1x^2) + gx^2 + \sum_i t_i^y \mathscr{T}^F(m_i(m_\pi)) \\
&\quad -2\sqrt{2}g_F N_c M_s \mathscr{T}^F(M_s), \\
m_\pi^2 &= -\mu^2 + 2(2f_1 + f_2)x^2 + 4f_1y^2 + 2gy + \Sigma_\pi(p = 0, m_i(m_\pi), M_u). \quad (7.15)
\end{aligned}$$

Here also the fermionic tadpoles are expressed through bosonic tadpoles of mass M_Q, and in the evaluation of the meson contribution, the mass eigenbasis of the fields is used. All masses are expressed (as was explained in Chap. 4) through m_π.

The tadpole integrals are split into the sum of a $T = 0$ and a temperature-dependent part, where one has to choose carefully, where it is appropriate, between

the Bose–Einstein and the Fermi–Dirac distributions:

$$\mathscr{T}^F(m_i) = \mathscr{T}^F(m_i, T=0) + \frac{1}{2\pi^2}\int_{m_i}^{\infty} dE\sqrt{E^2 - m_i^2}\, n_{BE}(E/T),$$
$$\mathscr{T}^F(M_Q) = \mathscr{T}^F(M_Q, T=0) - \frac{1}{4\pi^2}\int_{M_Q}^{\infty} dE\sqrt{E^2 - M_Q^2}\,\left(n_{FD}((E+\mu_B)/T) + n_{FD}((E-\mu_B)/T)\right). \tag{7.16}$$

A discontinuous jump in $x(T)$ signals first-order transitions for large enough baryo-chemical potential μ_B. With diminishing μ_B, the gap diminishes, and at the CEP it vanishes. The line of first-order transitions exists for $\mu > \mu_{CEP}$, as appears in Fig. 7.5 (dashed line). Left from the CEP one observes finite maxima of the order parameter susceptibility $\chi \equiv dx/d\epsilon_x$. The location of these maxima in the $\mu_B - T$-plane draws a pseudocritical line (dashed line), which can be associated with the interval of rapid changes in the thermodynamic quantities. This is the crossover region. The pseudocritical line found with this approximate solution hits the $\mu_B = 0$-axis at $T_{cross}(\mu_B = 0) \approx 155\,\text{MeV}$, which agrees rather well with the crossover temperature region identified in Monte Carlo simulations of the full QCD [14, 15].

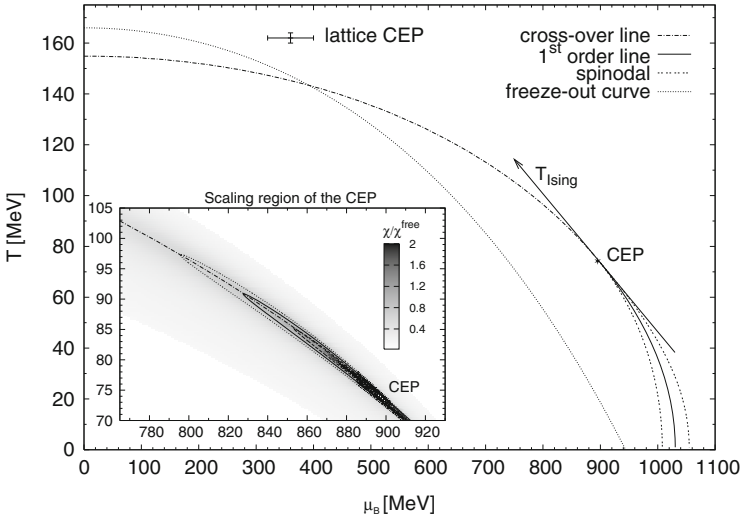

Fig. 7.5 Phase diagram of the three-flavor quark–meson model in the $T = \mu$-plane. In the insert, the scaling behavior of the baryo-chemical susceptibility is displayed. By its scaling exponent, the CEP of this model belongs to the universality class of the Ising model (from [13])

A scaling behavior of χ can be searched in the form of the following general parameterization:

$$\chi = (|\mu_B - \nu_{CEP}| \cos\alpha + |T - T_{CEP}| \sin\alpha)^{-\gamma} . \tag{7.17}$$

The angle α determines the orientation of the main scaling axes in the plane. In fact, one of the main axes lies along the tangential to the pseudocritical curve at the CEP. The value of the exponent γ is close to unity, which gives some evidence of the universality class of the second-order transition at the CEP belonging to the Ising class. In the inset of Fig. 7.5, the susceptibility is shown in proportion to the susceptibility of a free massless fermion gas. The darker region corresponds to the larger ratios. This graphical representation nicely depicts the main scaling direction.

7.2.2 *Dependence of the Nature of the Transition on the Masses of the Goldstone Fields*

Lattice simulations of the full QCD thermodynamics can be performed on a wide range of quark masses, which correspond to varying the masses of the light pseudoscalar Goldstone bosons. In the chiral limit (zero pion and kaon mass) and in a certain (unknown) mass region close to it, one expects a first-order transition between the phase of broken and restored chiral symmetry. It has been firmly established that the physical point in the $m_\pi - m_K$-plane lies outside this regime. It is located in the crossover region. Some effort has been invested in localizing the boundary of the first-order regime in numerical simulations, at least along the diagonal $m_\pi = m_K$ [16–18]. At present, no firmly accepted boundary mass is known even along this direction of higher mass degeneracy.

The existence and the location of the second-order phase boundary was first intensively studied in the framework of effective models at $\mu_B = 0$. The first computations [19] used just the one-loop-level equations (described above) and scanned through the (m_π, m_K)-plane using for the other couplings those values that arise in substituting into their expressions the actual pion and K-masses. It was realized that in the framework of the three-flavor nonlinear sigma model, the Goldstone masses influence the other masses and the weak decay constants rather subtly. In [20], the parameters of the linear model are fitted to the exact relations derived in the chiral perturbation theory. There is no space in the present notes to enter into a discussion of the details of matching the couplings in the two models. Only results obtained in the linear sigma model with the correctly tuned parameters will be discussed briefly below.

Figure 7.6 displays the boundary found with different parameterizations. The condition used for recognizing the second-order nature of the transition was the infinite response of the order parameter x to the variation of T at a fixed value of μ_B. The phase boundary could be constructed for $m_K > m_\pi$. The $m_\pi = m_K$ line

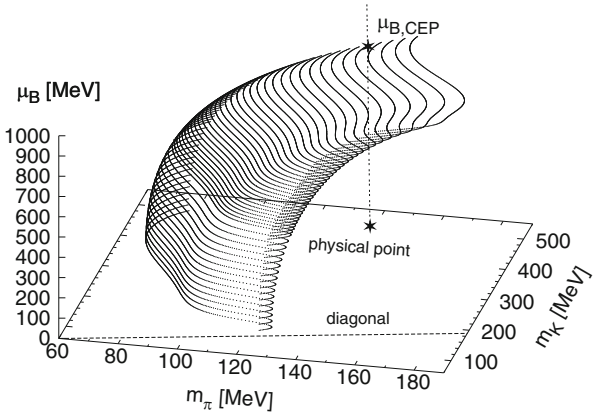

Fig. 7.6 The surface of second-order phase transitions in $\mu_B - m_\pi - m_K$ space. In the region to the *left* and above the surface, the restoration of chiral symmetry proceeds via first-order transitions below the surface via crossover. The physical points that might be reached in our actual world lie along the *vertical line* (from [13])

cannot be reached, since there, the parameterization based on having separate self-consistent gap equations for the pion and the kaon becomes singular. It also stays away from the $m_\pi = 0$ axis; in fact, for $m_K > 400\,\mathrm{MeV}$, the surface curves back and does not cross it at all.

The critical surface begins orthogonal to the $m_\pi - m_K$-plane. Then it bends rightward, and the equations definitely exclude an eventual bending backward. By this monotonic change, the existence of the CEP (as suggested by the figure) depends critically on the starting tendency of the bending near $m_B = 0$. The corresponding derivatives can be estimated in numerical simulations, avoiding the problem of negative weights.

7.3 Equation of State of the Strong Matter

In the previous sections, we discussed the spectrum and the description of the phase transition with the help of the effective action. For the bulk thermodynamics, the most relevant relation is the dependence of the free energy on the temperature and/or chemical potential (called the *equation of state*, EoS). In homogeneous systems, the complete thermodynamics is derived from this relation. In the remaining part of the chapter, we discuss the thermodynamics at zero chemical potential with the aim of achieving a physically fully adequate, analytic though phenomenological characterization.

The strong matter can be described in terms of qualitatively different degrees of freedom in the low- and high-temperature (energy-density) regimes. Although there is no strict phase transition between the two regimes, we shall speak about low- and high-temperature phases. Because of the continuous (crossover) nature of the transition, in principle the two regimes can be analytically continued from each phase to the other; but if one tries to use the degrees of freedom appropriate for

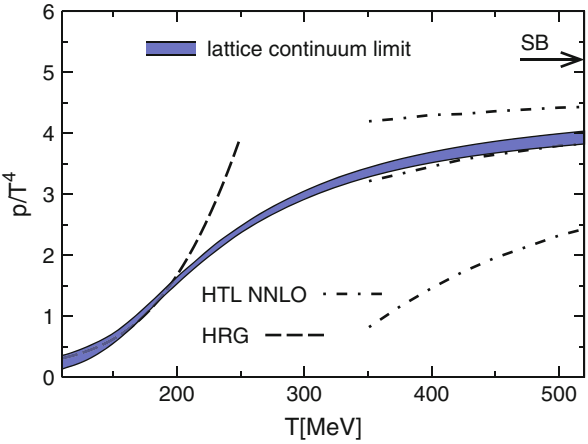

Fig. 7.7 The pressure of quark–hadron matter in $2+1$ flavor QCD by the numerical simulation of the BMW group [21]. The HRG approximation (*dashed line*) and the normalization-scale-dependent range covered by the perturbative results (the *dashed-dotted lines* corresponding to renormalization scales $\pi T, 2\pi T,\ 4\pi T$, respectively) are also shown here

a given phase to describe the other one, one typically gets very badly converging series.

No direct experimental measurements can be constructed for the EoS of QCD, but one can perform lattice MC simulations. After decade-long efforts, the most influential groups in the field of finite-temperature MC simulations provided results that are in reasonable agreement with each other [21, 22]; see Fig. 7.7. In view of the confidence in QCD as the exact theory of strong interactions, the results of numerical simulations can be accepted as the true behavior of the pressure of strongly interacting matter. The measured equation of state predicts a continuous transformation of the phases. This means that there is no discontinuity in any derivatives of the free energy, but only peaky but rounded structures can be observed in the temperature-dependence of the different thermodynamic susceptibilities. The position of the peak depends on the chosen observable. From the susceptibility of the chiral condensate, the best known result for the pseudocritical temperature is $T_c = 155\,\text{MeV}$ with a few MeV uncertainty. This value is referred to as the "critical" T_c in the sequel.

In the high-temperature phase, the degrees of freedom of the strong interaction are those that define QCD: quarks and gluons. At very high temperatures, the coupling constant of QCD is vanishingly small (asymptotic freedom), and so one expects that the free gas approximation will be valid. But this is true only for very high temperatures $T \sim 1000 T_c$. In the region where the temperature is just a few times T_c, the pressure reaches only about 80%–85% of the Stefan–Boltzmann limit corresponding to free quarks and gluons. This means that in the moderately, but not asymptotically, high temperature region, the interaction plays a crucial role in the quantitative description of the QCD pressure.

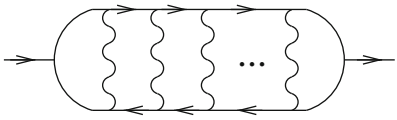

Fig. 7.8 A ladder diagram with arbitrary number of gluon ladders gives the same $\mathcal{O}(g^6)$ contribution to the self-energy: by adding an extra rung, the additional coupling factors from the two vertices are canceled by the inverse magnetic mass from the additional gluon propagator

The first theoretical tool to account for this behavior is perturbation theory. Straightforward perturbation theory with thermal masses but without any other optimization, however, shows very bad convergence features near T_c: the series of the computed quantities in different orders no longer converge. One needs better methods to obtain reliable results. In QCD, the most successfully used methods are dimensional reduction (DR) discussed in Chap. 6, and hard thermal loop (HTL) resummation [23], not discussed in these notes. Presently, the HTL perturbative results are three-loop accurate, while the DR results have reached the maximal g^5 accuracy. For higher precision, one necessarily encounters nonperturbative corrections present at each higher order. A nonperturbative resummation is needed to treat them, since starting from order g^6, the diagrams with increasing number of loops contribute at the same level (see Fig. 7.8). This is the so-called Linde problem [24].

A similar phenomenon appears also in the electroweak case (cf. Sect. 8.2). There one could take into account the resulting net effect by introducing an appropriate magnetic mass. In QCD, one can fix the g^6 terms by numerical simulations [25].

As a result, one gets stable results from both approximation procedures. As is customary in perturbation theory, these approximations still have some uncertainty, arising, for example, from the choice of the renormalization scale. The knowledge of some experimentally measured data allows one to select the procedure that best reproduces the data; cf. Fig. 7.9. The results very closely follow the lattice data; nevertheless, they do not show any signal for flattening toward low temperatures. Shortly after the pressure calculated in perturbation theory deviates from the MC data (in the lower left corner of the figure), it crosses zero, i.e., it apparently describes an unstable state of matter.

At low temperatures, we are in the hadronic phase, where the relevant degrees of freedom are the color neutral hadrons. From the point of view of thermodynamics, one starts with a free gas of hadrons. One faces here, however, the problem that most hadrons are not stable. It is not perfectly clear what should happen with a degree of freedom that decays before it can really be part of the thermal medium. We return to this problem below. The first approximation is certainly the assumption that all hadronic resonances can be taken into account as stable particles: this is the hadron resonance gas (HRG) limit. There, all hadronic resonances give a partial contribution to the total pressure in the form of an ideal quantum gas

$$P = \frac{T}{2\pi^2} \sum_n \int_0^\infty dp\, p^2 \left[(\mp) \ln \left(1 \mp e^{-E(p,m_n)/T} \right) \right], \tag{7.18}$$

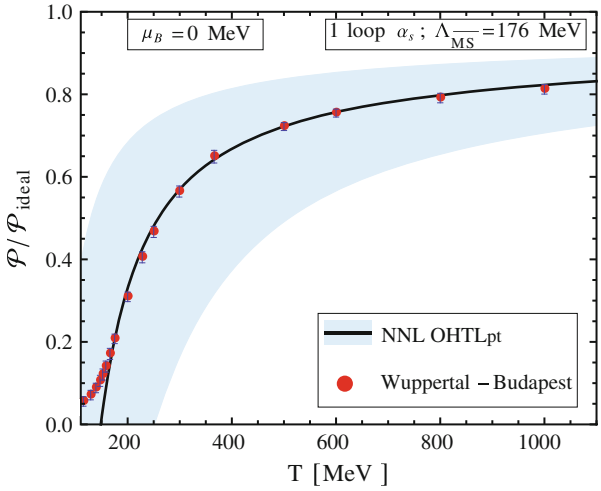

Fig. 7.9 The best perturbative results for the QCD pressure at high temperature from [23]. The shaded region is the variation of the perturbation theory under the change of the renormalization scale by a factor of 2

where the $\pm$ sign applies to bosonic/fermionic modes, and $E^2(p, m) = p^2 + m^2$. Within a nonrelativistic approximation (all hadrons are much heavier than the equivalent energy density corresponding to the actual low temperature), we can forget about the difference of statistics between bosons and fermions and have

$$P = \frac{T^2}{2\pi^2} \sum_n m_n^2 K_2(\beta m_n), \tag{7.19}$$

where K_2 is the modified Bessel function. The hadron masses are taken from experiments [26].

Although this approach seems to be oversimplified, it works surprisingly well, at least below a certain temperature that depends on the observable; for the pressure, it describes well the MC data up to $(1-1.2)T_c$ [21]. We should remark here, however, that the HRG pressure is a continuously increasing function that finally reaches the Stefan–Boltzmann (SB) limit belonging to the gas of hadrons, instead of the SB limit of the QCD degrees of freedom. Assuming the existence of infinitely many stable hadrons, one observes eventually a singular diverging behavior in the hadronic pressure. The reason is [27] that toward large masses, the density of hadronic resonances increases exponentially: $\varrho_H(m) \sim e^{m/T_H}$, where T_H is the Hagedorn temperature. This tendency can also be extracted from the experimental data [28]. There are several fits for the experimentally observed hadronic resonance density, for example those with powerlike prefactors in ρ_H, but already a simple exponential

does the expected job. Then the complete pressure behaves as

$$P \sim \int_0^\infty dm\, \varrho_H(m) e^{-m/T} = \int_0^\infty dm\, e^{-m(1/T - 1/T_H)}, \tag{7.20}$$

which is divergent when $T > T_H$. This singularity, called a Hagedorn singularity, signals the inapplicability of the hadronic description for temperatures higher than T_H.

Therefore, the validity range of the two descriptions, approaching the critical temperature from below and from above, are more or less overlapping, but not analytically related. If there were a first- or second-order phase transition between the two regimes, then we could simply stick those regimes together, changing description abruptly at T_c. From a purely phenomenological point of view, this can still be satisfactory, since it provides a good estimate for the pressure at any temperature.

However, for understanding the physics of the transition regime, and in particular to design a predictive strategy for applications in other physical situations, this dual approach is unsatisfactory. The phase transformation is continuous, and so we are pushed unavoidably to the conclusion that during the crossover regime, the excitations of the other phase appear continuously. The MC data display in dp/dT an inflection. But as we have emphasized, the pressure of the HRG is increasing monotonically, while the pressure of the HTL calculations decreases monotonically. These two facts suggest that within these approximation schemes, the continuous crossover to the other phase cannot be described. The precondition for the correct physical interpretation is an appropriate understanding of how the various degrees of freedom appear/disappear in the transient state of the system.

7.3.1 Characterization of the Excitations

Let us first discuss what kind of excitations or particles we want to describe. The notion of particles in several cases means free particles (for example in an ideal gas), or, as in scattering theory, the asymptotic states. But as we have stated before, the HRG approach takes into account all hadronic resonances, even those that live for a very short time. A particle with a finite lifetime cannot be an energy eigenstate; it is a collective excitation instead: we call them *quasiparticles*. The physical origin of the appearance of a quasiparticle is that the original free particle modes are mixed with the multiparticle modes of their environment, as was first demonstrated by the Weisskopf–Wigner approximation to the coupled atom + radiation system. The collective excitations maintain to some extent a nearly energy-eigenstate-like behavior to the degree that the real-time evolution of their response function is $\sim e^{-\gamma t} e^{-i\omega t}$. The quasiparticle properties, the damping rate γ, and the energy (mass)

ω depend on how the quasiparticle was formed. Consequently, they usually depend on the temperature/chemical potential.

The identification of quasiparticles therefore requires the observation of the characteristic asymptotic behavior of the response function $G_{ret}(t)$. Since the response function is perfectly described by the spectral function ϱ, the quasiparticle is best characterized as a peak in ϱ that behaves near the peak as a Lorentzian:

$$\varrho(k_0 \approx \omega) = \frac{A}{(k_0 - \omega)^2 + \gamma^2}. \tag{7.21}$$

Before proceeding further, we have to clarify here an interesting question of a general nature. A finite system always contains discrete energy levels E_n. Then the spectral function reads

$$\varrho(k_0) = \sum_n r_n \delta(k_0 - E_n) \tag{7.22}$$

with some spectral weights r_n. Now if the time evolution starts from an energy eigenstate, then it remains there $|n, t\rangle = e^{-iE_n t}|n\rangle$. There is no damping or decay whatsoever, and we get a stable system as in quantum mechanics. How, then, can we observe decays of the real excitations at all?

The answer stems from understanding the way in which the final state of the system is created. Consider a system having just two energy levels E_1 and E_2, and the initial state is composed of them coherently: $|\psi\rangle = c_1 |1\rangle + c_2 |2\rangle$. Then the expectation value of a Hermitian observable $\hat{O}$ at time t reads

$$\begin{aligned}\left\langle \hat{O} \right\rangle_\psi (t) = \left\langle \psi, t|\hat{O}|\psi, t \right\rangle = |c_1|^2 O_{11} \\ + |c_2|^2 O_{22} + (c_1^* c_2 e^{i(E_1 - E_2)t} + c_2^* c_1 e^{i(E_2 - E_1)t}) O_{12},\end{aligned} \tag{7.23}$$

where $O_{ij} = \left\langle i|\hat{O}|j \right\rangle$. If we want to determine whether just one of the energy levels was initially excited, or both, but we do not know the matrix elements exactly, then we should rely on the time evolution. If both energy levels are excited, we should observe a beat with frequency $\Delta E = |E_1 - E_2|$. The point is that we should monitor the evolution for a time duration minimally lasting $\Delta t \sim 1/\Delta E$ to be able to recognize that there is a time-dependence in at least one of the expectation values.

The creation of a state is just the reverse of the measurement process. A control process that forces the system to some initial state actually requires a preparation time $\Delta t \sim 1/\Delta E$.

The particle creation process, on the other hand, is rather fast. Therefore, although a quasiparticle peak consists of a large number of Dirac deltas (in a finite system), the dynamics is not able to pick up any of them to excite it separately. We can excite only an interval of the eigenstates located under the peak on an equal

footing. This leads to an intermediate "final" state

$$|\psi\rangle_{QP} \approx \sum_n c_n |n\rangle, \tag{7.24}$$

where the c_n coefficients express the degree of sensitivity of the creation process to the energy level $|n\rangle$. Its modulus $|c_n|^2$ is a spectral weight, describing the ability to create or measure an energy level. If we assign a quantum field to the creation/measurement, then $c_n = \left\langle n|\hat{\Phi}|0\right\rangle$. Then the overlap between the state $|\psi, t\rangle_{QP}$ and the initial state (i.e., the propagator) reads as

$$\langle\psi, 0|\psi, t\rangle_{QP} = \sum_n |c_n|^2 e^{-iE_n t} \approx \int \frac{d\omega}{2\pi}\, \varrho(\omega) e^{-i\omega t} = \varrho(t), \tag{7.25}$$

according to the definition of the spectral function (A.5). This formula, with the help of (7.21), yields the exponentially damped behavior in time.

Why is this argument relevant in the discussion of the changing nature of the degrees of freedom? Because it makes clear that the quasiparticles have nothing to do with single separate energy levels of the system. They are characterized only by their weighted density, i.e., the spectral function. Therefore, if the "degrees of freedom" change in a system, the appropriate quantity for the characterization of the change is provided by the spectral function.

All that has been said above applies only if the members of a set of energy eigenstates have the same quantum numbers. Otherwise, one easily chooses an operator $\hat{O}$ that is sensitive to a distinct value of a conserved quantity. Then in (7.23), $O_{11} \neq 0$, while the other matrix elements are zero, and so we easily can determine whether $c_1 = 0$. The same applies to particle creation: one usually calls a particle that carries well-defined values of the conserved quantities, i.e., it has definite quantum numbers, a quasiparticle.

Therefore, we can use different spectral functions for different quantum channels (superselection classes), i.e., for different sets of quantum numbers. But it makes no sense to assign more than one spectral function to the same quantum channel; more precisely, it would introduce tacitly a new quantum number, i.e., it would change the symmetry of the quantum system. The result is then a physically different system. The corollary therefore is that to each superselection class we can assign one, but only one, spectral function.

7.3.2 Spectral Functions and Thermodynamics

As we have seen, the excitations of the system should be characterized by the spectral functions. The next step is to examine how to extract the thermodynamics from a given set of spectral functions.

The complete partition function of the system is written as

$$Z = \sum_{n,q} e^{-\beta E_{n,q}}, \tag{7.26}$$

where q labels the distinct quantum channels and n is the index of the energy eigenstates in channel q. Usually, we do not know the exact spectral functions, except for quadratic (free) theories. In a free theory, the partition function can be evaluated, and we need only to know the dispersion relation of the one-particle channel: it determines all the other channels as well as the complete thermodynamics.

In our discussion, we assume that the interacting theory, after we have taken into account all sorts of interactions, finally behaves like a free theory with a modified particle spectrum. For low enough energy, in the strong interactions this assumption is certainly a good approximation to the thermodynamics, as the success of the HRG demonstrates. We will assume that this approach can also be consistently applied in the crossover regime, with much more distorted excitation spectra than in the low-energy regime.

For each system with a single degree of freedom, therefore, we will assume that there is a fundamental channel (similar to the original free particles of the system) with spectral function ϱ, and this determines the thermodynamics as well as the density of states of all the other channels. If there are bound states in the multiparticle channels, then these channels also should be treated as fundamental, where we must take care to avoid double counting.

Mathematically, these basic principles are implemented using a quadratic theory with a generic kernel $\mathscr{K}$, containing tunable parameters. Let us discuss a theory of scalar fields to avoid complications with the internal degrees of freedom. Then the action reads (compare to (2.65))

$$S[\varphi] = \frac{1}{2}\int d^4x\, \varphi(x)\mathscr{K}(i\partial)\,\varphi(x). \tag{7.27}$$

In Fourier space, we can write

$$S[\varphi] = \frac{1}{2}\int \frac{d^4p}{(2\pi)^4}\, \varphi^*(p)\mathscr{K}(p)\varphi(p). \tag{7.28}$$

The φ field is real, which in Fourier space means that $\varphi(-p) = \varphi^*(p)$. Since S is also real, the kernel must satisfy the relations $\mathscr{K}^*(p) = \mathscr{K}(-p) = \mathscr{K}(p)$. From the generic rules, we have for the retarded propagator and the spectral function

$$G^{(ra)}(p) = \mathscr{K}^{-1}(p_0 + i\varepsilon, \mathbf{p}), \qquad \varrho(p) = \operatorname*{Disc}_{p_0} iG^{(ra)}(p). \tag{7.29}$$

For the inverse relation, we can use the Kramers–Kronig relation (2.56), and then the relation between the kernel and the retarded Green's function. Finally, we obtain

$$\mathscr{K}(p) = \lim_{\varepsilon\to 0} \mathrm{Re}\left(\int \frac{d\omega}{2\pi}\,\frac{\varrho(\omega,\mathbf{p})}{p_0-\omega+i\varepsilon}\right)^{-1}. \tag{7.30}$$

One should ask whether the field theory defined with help of $\rho(\omega,\mathbf{p})$ is consistent. For an arbitrary kernel it is not, but it can be proven [29] that if the spectral function satisfies the generic properties discussed in Appendix A (namely that $\varrho(p_0>0,\mathbf{p})>0$, $\varrho(-p_0,\mathbf{p})=-\varrho(p_0,\mathbf{p})$) and it is normalized, then the field theory is consistent. If in addition, the spectral function is Lorentz-invariant, then the theory will be relativistically invariant, too. Therefore, the spectral function should be chosen as the input, and we should determine the kernel using the dispersion relation above.

Now we have a model theory that is capable of reproducing any spectra we want, at least in the fundamental channel. What is the thermodynamics it describes? It is best to start with the computation of the expectation value of the energy density. This quantity is the T_{00} component of the energy–momentum tensor, which is the Noether charge density generated by the time translation-invariance of the system. It is well defined microscopically. With the standard techniques, we arrive at the energy momentum tensor (cf. [29])

$$T_{\mu\nu}(x) = \frac{1}{2}\varphi(x)\,D_{\mu\nu}\mathscr{K}(i\partial)\,\varphi(x), \tag{7.31}$$

where

$$D_{\mu\nu}\mathscr{K}(i\partial) = \left[\left.\frac{\partial\mathscr{K}(p)}{\partial p^\mu}\right|_{p\to i\partial}\right]_{sym} i\partial_\nu - g_{\mu\nu}\mathscr{K}(i\partial), \tag{7.32}$$

and the symmetrized derivative is defined as

$$f(x)[(i\partial)^n]_{sym}g(x) = \frac{1}{n+1}\sum_{a=0}^{n}[(-i\partial)^a f(x)][(i\partial)^{n-a}g(x)]. \tag{7.33}$$

Although this expression is somewhat complicated, when we take its expectation, it becomes much simpler. For the expectation, we can use the KMS relation (2.49). Finally, we obtain

$$\varepsilon = \langle T_{00}\rangle = \frac{1}{2}\int \frac{d^4p}{(2\pi)^4}\,p_0\frac{\partial\mathscr{K}}{\partial p_0}\left(\frac{1}{2}+n(p_0)\right)\varrho(p), \tag{7.34}$$

where we also exploited the equation of motion $\mathscr{K}(p)\varrho(p) = 0$ (cf. (2.68)). If we use the expression of the free spectral function $\varrho(p) = (2\pi)\,\mathrm{sgn}\,p_0\delta(p^2-m^2)$ and the free kernel $\mathscr{K}(p) = p^2-m^2$, then we get back from this formula the ideal gas energy density (2.88). The integrand is symmetric, so it is enough to take into account the positive frequency part of $\mathscr{K}$ and omit the zero-point $1/2$ factor. This formula is not sensitive to the normalization of the spectral function (the normalization of $\mathscr{K}$ cancels it).

This result already suffices to recover the complete thermodynamics. In particular, the pressure reads

$$p = -\frac{1}{2}\int \frac{d^4p}{(2\pi)^4}\,\frac{\partial\mathscr{K}}{\partial p_0}\varrho(p)\,\ln(1-e^{-\beta p_0}). \tag{7.35}$$

We remark that an analogous formula can be derived using the generalized Beth–Uhlenbeck approach [30], where the imaginary time formula of the thermodynamic potential is expressed through the phase shifts.

7.3.3 (In)distinguishability of Particles and the Gibbs Paradox

Formula (7.34) has remarkable properties. First of all, if in a quantum channel there are Dirac-delta excitations with dispersion relation $p_0 = E_i(\mathbf{p})$, then the formula can be evaluated. In this case, the spectral function and the propagator are both additive:

$$\varrho(p)|_{p_0>0} = \sum_i 2\pi Z_i\delta(p_0 - E_i(\mathbf{p})), \qquad G^{(ra)}(p) = \sum_i \frac{Z_i}{p_0 + i\varepsilon - E_i(\mathbf{p})}, \tag{7.36}$$

where Z_i are the individual wave-function renormalization constants. The kernel is not additive, however, since it is $\mathscr{K} = 1/G$. Its derivative reads

$$\frac{\partial\mathscr{K}(p_0)}{\partial p_0} = -\frac{1}{G^2}\frac{\partial G}{\partial p_0} = \frac{1}{\left(\sum_i \dfrac{Z_i}{p_0 - E_i}\right)^2}\sum_i \frac{Z_i}{(p_0-E_i)^2}. \tag{7.37}$$

Because the spectral function is concentrated on the energy levels, in (7.34) we have to evaluate $p_0\mathscr{K}'(p_0)$ near these points. As can be easily seen,

$$\lim_{p_0\to E_i}\frac{\partial\mathscr{K}(p_0)}{\partial p_0} = \frac{1}{Z_i}. \tag{7.38}$$

Therefore, the Z_i factors drop out from the formula of the energy density. As a result, we obtain a sum of free energy densities

$$\varepsilon = \sum_n \varepsilon_0^{(n)}, \tag{7.39}$$

where $\varepsilon_0^{(n)}$ is the contribution to the free energy density from the nth particle.

This means in particular that a gas of N particles with the same quantum numbers, but with different masses, behaves as a mixture of N distinguishable particle species, despite the fact that all these particles are just peaks of the same spectral function.

In this case, therefore, the number of degrees of freedom was N, although the number of fundamental quantum channel was just one. The two numbers, therefore, can be different. For the characterization of the number of degrees of freedom of the system, we can introduce a somewhat heuristic measure:

$$N_{dof} = \int_0^\infty dp_0 \, \frac{\partial \mathscr{K}}{\partial p_0} \varrho(p_0). \tag{7.40}$$

This is a dimensionless quantity, and it gives N for the above example of the spectrum consisting of N Dirac-delta peaks.

As we see, the number of degrees of freedom as well as the complete energy density is a functional of the spectral function. This makes it possible to experience a dynamical change in the degrees of freedom. In this way, we can account also for the *Gibbs paradox*. In the original version of the paradox, Gibbs argued that the entropy of mixing two gases depends on whether the molecules of the gases are distinguishable. In the above example, we physically had a mixture of N species of Bose gases. We have seen that the number of species is explicitly measurable here (in contrast to the original "mixture entropy" problem), since, for example, at high temperature, the Stefan–Boltzmann limit of the total energy density is $N\pi^2 T^4/30$. Two species are distinguishable in the present formalism if in the spectrum we can find two distinct energy levels, if i.e., their masses are different. If the particles are free, then no matter what the mass difference (provided it is not zero) and the relative wave function renormalization constants may be, the two species are *always* distinguishable, yielding a factor of 2 in the Stefan–Boltzmann limit. The formulas (7.34) and (7.40) provide the analytic expressions reflecting the essence of the paradox: when two Dirac deltas merge into one, the resulting energy density or N_{dof} changes nonanalytically.

In reality, the quasiparticles always have a finite width, and this smoothens the nonanalytic behavior of ε and N_{dof}. An analytically calculable example is the case of two Lorentzians with the retarded propagator

$$G^{(ra)}(\omega) = \frac{Z}{\omega + i\Gamma} + \frac{Z}{\omega - E + i\Gamma}. \tag{7.41}$$

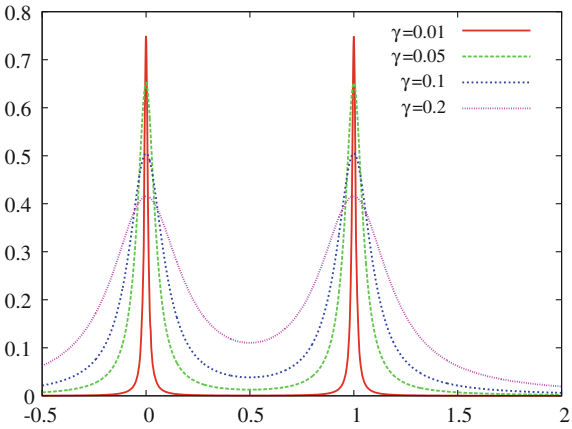

Fig. 7.10 Two nearby quasiparticle peaks with various widths, $\gamma = \Gamma/E$. The peaks are scaled with appropriately chosen Z to ensure optimal visibility

Physically, this describes two quasiparticles with mass difference E, and if they are independent, with lifetime Γ^{-1}. For simplicity, we take here the same width and same wave-function renormalization. The corresponding spectral function can be seen in Fig. 7.10.

What do we expect in this system? Assume that $\Gamma \neq 0$, but that it is small enough that a single peak can be considered a sufficiently long-lived quasiparticle. Now if $E \gg \Gamma$, then the two peaks are far from each other, and the system must behave as if it consisted of two Dirac-delta peaks as analyzed above. But when $E \ll \Gamma$, then in the spectrum, we cannot disentangle the two peaks. Since the physics is encoded in the spectrum, we expect that we have a system with a single degree of freedom. Therefore, we should see the continuous disappearance of a degree of freedom as the mass difference of the particles vanishes.

Exactly this picture arises when we calculate N_{dof}. One can perform the integral in (7.40), resulting in

$$N_{dof} = 1 + E^2 \frac{E^2 - 16\Gamma^2}{(E^2 + 16\Gamma^2)^2}. \tag{7.42}$$

This function is plotted in Fig. 7.11. If $E \to 0$, then $N_{dof} \to 1$, and if $E \to \infty$, then $N_{dof} \to 2$. Numerically, $E/\Gamma \sim \mathcal{O}(10)$ is the regime in which the effective number of degrees of freedom changes the fastest. We can also see a dip where $N_{dof} < 1$; this is a peculiarity of the simple quantity we defined.

7.3.4 *Melting of the Particles and Phenomenology of the Crossover Regime in QCD*

In a quantum field theory, the spectra consists not just of discrete energy levels, but also in each channel, a multiparticle continuum is present, the continuum of

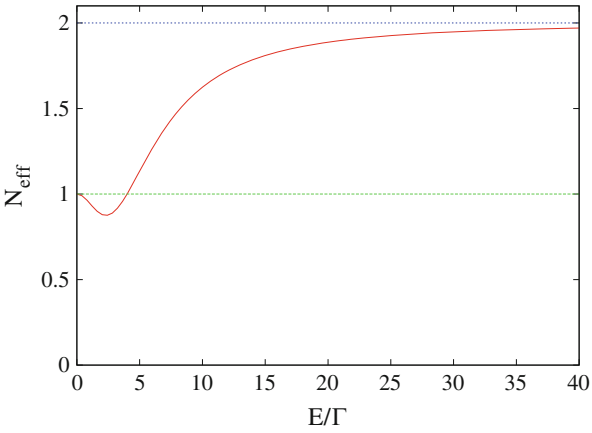

Fig. 7.11 The effective number of degrees of freedom for two peaks as a function of their energy difference scaled by the width. For large separation, we see two degrees of freedom; for zero separation, just one. This is the smooth version of the Gibbs paradox

the scattering states. Then the relevant physics scenario induced by an increase of the width of a particle is not the merging of two different particle species, but the merging of the quasiparticle into the continuum. Since the continuum contains many more states, the result of this process is that the particle peak becomes unidentifiable in the spectrum. Therefore, all the physical effects associated with the particle peak should also be suppressed, meaning that the particle has literally vanished from the ensemble. This process is called *particle melting*.

If we want to illustrate this process quantitatively, then we may use the trial spectral functions (cf. [31])

$$\varrho(p) = Z(\varrho_{Lor}(p) + \varrho_{cont}(p)), \tag{7.43}$$

where

$$\begin{aligned} \varrho_{Lor}(p) &= \frac{4h\gamma^2 p^2}{(p^2 - m^2)^2 + 4\gamma^2 p^2}, \\ \varrho_{cont}(p) &= \frac{p}{p^2 + m_{th}^2} \operatorname{Im} \sqrt{m_{th}^2 + iS - p^2}. \end{aligned} \tag{7.44}$$

In this parameterization, h is the height of the peak, γ is the peak width, Z is the wave-function renormalization constant. The continuum is modeled by a 2-particle spectral function with complex threshold mass $(m_{th}^2 + iS)$ and a correction prefactor is also introduced to ensure that the spectral function vanishes at $p = 0$. The overall normalization factor is not important, since it does not influence the physics. We depicted this spectral function with different γ values in Fig. 7.12, normalizing the quasiparticle peak height to unity for better visibility. We have chosen here $m = 1$, $m_{th} = 2$, with different γ values shown in the figure, and S that is consistent with the requirement that the quasiparticle width be the height of the spectral function at m.

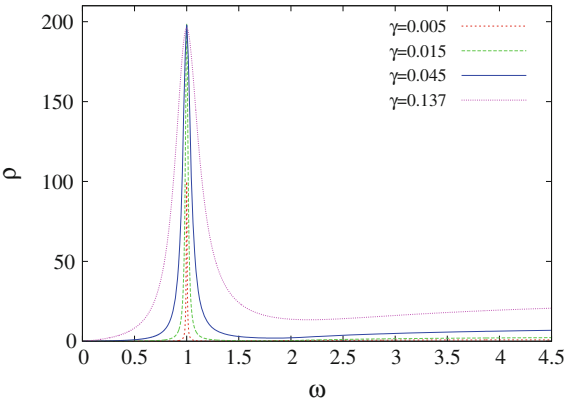

Fig. 7.12 Trial spectral functions containing a quasiparticle peak with different widths and a continuum. The quasiparticle peaks (at $m = 1$) are scaled to the same height for better visibility

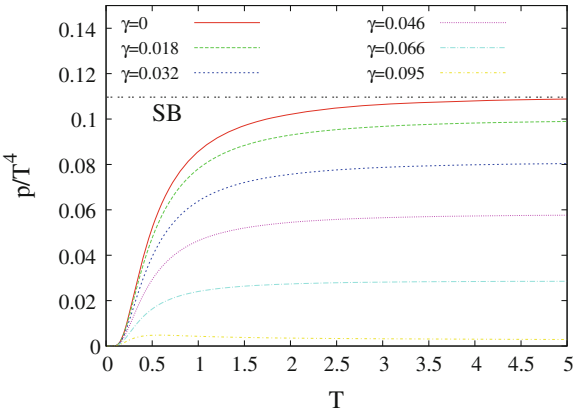

Fig. 7.13 The pressure calculated from trial spectral functions

Now we can use (7.35) to calculate the pressure of the system. We get the series of curves plotted in Fig. 7.13. What we see here is that the pressure in the melting process becomes smaller and smaller. In the limit $\gamma \to \infty$, we get zero pressure, and the particle has indeed become nonexistent from the point of view of thermodynamics. We can also observe that these curves can scale to each other by a multiplication

$$p(T) \approx p_0(T) N_{\mathit{eff}}, \tag{7.45}$$

where $p_0(T)$ is the pressure of the free particle gas with $\gamma = 0$, and N_{eff} is a more-or-less temperature-independent constant; cf. Fig 7.14. The coefficient N_{eff} can be interpreted as the effective number of thermodynamical degrees of freedom. It is the function(al) of the spectral parameters and does not depend directly on the temperature. In case of rather complicated trial spectral functions [32], a stretched exponential $N_{\mathit{eff}} = e^{-A\gamma^{\alpha}}$ was always a satisfactory fit.

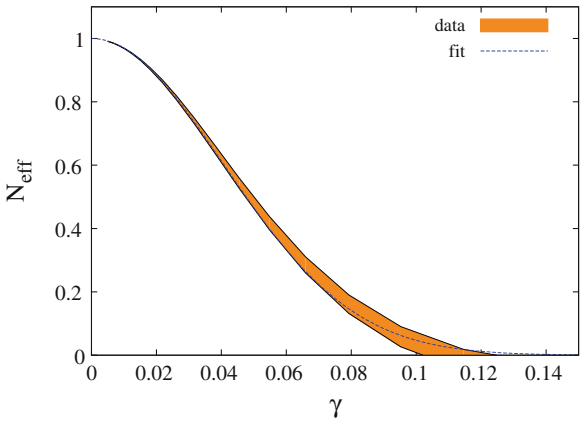

Fig. 7.14 The change in the effective number of degrees of freedom as a function of the quasiparticle peak width. The width of the band shows the temperature-dependence

The framework obtained through the analysis presented in the last three subsections can be used to draw a qualitative picture about the fate of the hadronic excitations in the crossover regime of QCD itself. According to the commonly accepted interpretation of the MC simulations [21, 22], all thermodynamic quantities are very well described by assuming a pure, phenomenologically composed hadron gas up to $T \sim T_c$. This would suggest that there are no QGP degrees of freedom present in this temperature range, at least that their contribution is not very important. On the other hand, above T_c, hadronic states are definitely observed [33–37], although these are not quasiparticle-like excitations. Combining these observations, one is tempted to suggest that in the spectral function of the partons of the QGP phase, there are no peaky structures below T_c (although other, scattering-like, states might still exist and even might dominate the continuum part of the spectral function in some channels). In the hadronic channels, one observes well identifiable peaks below T_c, and these do not disappear abruptly (discontinuously) at any well-defined temperature.

Analyzing these possibilities, one can propose a scenario whereby the hadrons vanish from the spectra by melting. The simplest approach is to assume that all hadrons melt in the same way. Therefore, one can adapt a common $N_{eff,hadron}$ for them. One has to treat the degrees of freedom of the QGP phase, too, again with a common $N_{eff,QGP}$. A natural expectation is that the width of the QGP excitations depends on the available hadronic resonances, for example $\gamma_{QGP} \sim N^{\alpha}_{eff,hadron}$, where α is a conveniently chosen power of order 1. Even with this simple scenario, one can obtain a smoothly varying spectral content through the crossover region instead of producing the Hagedorn singularity. This smooth variation can be nicely fitted to the MC observations. Figure 7.15 shows a scenario in which the hadrons survive for a very long time: they are present up to $T \sim 3T_c$ in the plasma, and they even give half of the pressure at $T \sim 2T_c$ [32].

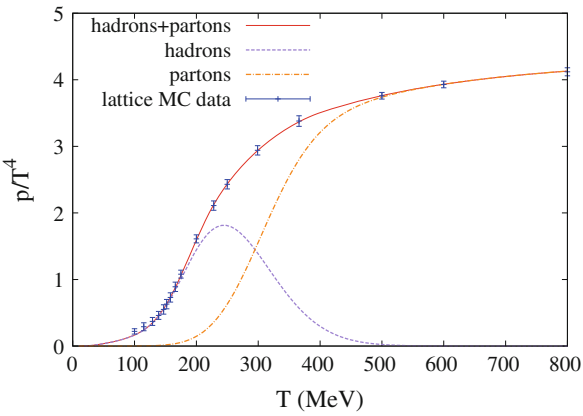

Fig. 7.15 A possible scenario for QCD crossover with melting hadrons, plotted with the MC measurements. Hadrons can survive in this scenario up to $\sim 3T_c$

Correspondingly, the QGP degrees of freedom appear only continuously, and they become the dominant degree of freedom of the plasma only beyond $\sim 2T_c$. In any case, the regime $T_c < T < 3T_c$ is a regime in which the standard quasiparticle picture cannot be applied; the interplay between the quasiparticle peak(s) and the continuum affects the physics crucially.

References

1. A. Patkós, Zs. Szép, P. Szépfalusy, Phys. Lett. B **537**, 77 (2002)
2. I. Caprini, G. Colangelo, H. Leutwyler, Phys. Rev. Lett. **96**, 132001 (2006)
3. A. Jakovác, A. Patkós, Zs. Szép, P. Szépfalusy, Phys. Lett. B **582**, 179 (2004)
4. Z. Fodor, S.D. Katz, J. High Energy Phys. **0404**, 050 (2004)
5. P. de Forcrand, O. Philipsen, J. High Energy Phys. **0701**, 077 (2007)
6. M. Asakawa, K. Yazaki, Nucl. Phys. A **504**, 668 (1989)
7. A. Barducci, R. Casalbuoni, G. Pettini, R. Gatto, Phys. Rev. D **49**, 426 (1994)
8. M.A. Halasz, A.D. Jackson, R.E. Shrock, M.A. Stephanov, J.J.M. Verbaarschot, Phys. Rev. D **58**, 096007 (1998)
9. O. Scavenius, A. Mocsy, I.N. Mishustin, D.H. Rischke, Phys. Rev. C **64**, 045202 (2001)
10. Y. Hatta, T. Ikeda, Phys. Rev. D **67**, 014028 (2003)
11. A. Barducci, R. Casalbuoni, G. Pettini, L. Ravagli, Phys. Rev. D **72**, 056002 (2005)
12. T. Herpay, Zs. Szép, Phys. Rev. D **74**, 025008 (2006)
13. P. Kovács, Zs. Szép, Phys. Rev. D **75**, 025015 (2007)
14. Y. Aoki, G. Endrődi, Z. Fodor, S.D. Katz, K.K. Szabó, Nature **443**, 675–678 (2006)
15. M. Cheng et al., [HotQCD Collaboration] Phys. Rev. D **74**, 054507 (2006)
16. F. Karsch, E. Laermann, C. Schmidt, Phys. Lett. B **520**, 41 (2001)
17. N.H. Christ, X. Liao, Nucl. Phys. Proc. Suppl. **119**, 514 (2003)
18. P. de Forcrand, O. Philipsen, Nucl. Phys. B **673**, 170 (2003)
19. H. Meyer-Ortmanns, B.-J. Schaefer, Phys. Rev. D **53**, 6586 (1996)
20. T. Herpay, A. Patkós, Zs. Szép, P. Szépfalusy, Phys. Rev. D **71**, 125017 (2005)
21. S. Borsanyi, Z. Fodor, C. Hoelbling, S.D. Katz, S. Krieg, K.K. Szabo, Phys. Lett. B **730**, 99 (2014)
22. A. Bazavov et al., [HotQCD Collaboration] Phys. Rev. D **90**(9), 094503 (2014)

23. J.O. Andersen, N. Haque, M.G. Mustafa, M. Strickland, N. Su, arXiv:1411.1253 [hep-ph] (2014)
24. A.D. Linde, Phys. Lett. B **96**, 289 (1980)
25. K. Kajantie, M. Laine, K. Rummukainen, Y. Schroder, J. High Energy Phys. **0304**, 036 (2003)
26. K.A. Olive et al. (Particle Data Group), Chin. Phys. C, **38**, 090001 (2014)
27. R. Hagedorn, Nuovo Cimento Suppl. **3**, 147 (1965)
28. W. Broniowski, W. Florkowski, L.Y. Glozman, Phys. Rev. D **70**, 117503 (2004)
29. A. Jakovac, Phys. Rev. D **86**, 085007 (2012)
30. D. Blaschke, D. Zablocki, M. Buballa, A. Dubinin, G. Roepke, Ann. Phys. **348**, 228 (2014)
31. A. Jakovac, Phys. Rev. D **88**, 065012 (2013)
32. T.S. Biro, A. Jakovac, Phys. Rev. D **90**, 094029 (2014)
33. S. Datta, F. Karsch, P. Petreczky, I. Wetzorke, Phys. Rev. D **69**, 094507 (2004)
34. T. Umeda, K. Nomura, H. Matsufuru, Eur. Phys. J. C **39S1**, 9 (2005)
35. M. Asakawa, T. Hatsuda, Phys. Rev. Lett. **92**, 012001 (2004)
36. A. Jakovac, P. Petreczky, K. Petrov, A. Velytsky, Phys. Rev. D **75**, 014506 (2007)
37. P. Petreczky, J. Phys. Conf. Ser. **402**, 012036 (2012)

Chapter 8
Finite-Temperature Restoration of the Brout–Englert–Higgs Effect

The origin of the matter–antimatter asymmetry of our cosmic neighborhood is one of the outstanding challenges faced at present by cosmology and particle physics. This asymmetry plays a central role in the successful modeling of the primordial nucleosynthesis (for a general introduction to particle-physics aspects of cosmology, see [1]). The observational estimation of the concentration of light elements of primordial origin can be interpreted with the help of the single asymmetry parameter

$$\eta_{baryon} = \frac{n_{baryon} - n_{anti-baryon}}{n_\gamma} \approx 6 \times 10^{-10}, \tag{8.1}$$

where n_γ is the photon number density and $n_{baryon}, n_{anti-baryon}$ are the respective densities of matter and antimatter. The estimate for this number was further sharpened with the help of the cosmic microwave background radiation data.

The common standpoint is that this feature of extreme importance for our very existence has a dynamic origin. It should have been generated from a symmetric initial state not later than when the spontaneous symmetry-breaking of the electroweak interactions occurred in the cooling universe.

There are three distinct necessary features that every quantum field theory has to possess for the generation of this asymmetry [2]:

- violation of the quark number (B) conservation;
- violation of the combined charge-conjugation–parity (CP) transformation symmetry;
- extended time interval during the cosmic evolution when quantum fields were far from thermal equilibrium.

A. Jakovác, A. Patkós, *Resummation and Renormalization in Effective Theories of Particle Physics*, Lecture Notes in Physics 912,
DOI 10.1007/978-3-319-22620-0_8

The standard model possesses the first two features. Anomalous processes transforming baryons into leptons were demonstrated to exist by 't Hooft [3]. A specific saddle-point solution of the field equations, called sphaleron, was constructed [4, 5], tunneling through which changes the baryon number of the ground state. The sustained presence of the nonzero baryon density generated by such processes requires the violation of the charge conjugation + parity symmetries, which is realized in the three-family structure of the standard model as predicted by Kobayashi and Maskawa [6]. The irreversibility of the processes generating the asymmetry could be due to a far-from-equilibrium state of the universe. The proposal that the electroweak phase transition, the onset of the Brout–Englert–Higgs (BEH) effect on cosmic scales. could be of a first-order nature and produce the necessary nonequilibrium stage was made in 1985 by Kuzmin et al. [7].

Early investigations based on summing the infrared-sensitive daisy-diagram contributions to the effective Higgs potential computed at the one-loop level [8, 9] have predicted persistently first-order transitions of gradually diminishing discontinuity in the Higgs vacuum condensate with increasing self-coupling of the Higgs field. Two-loop corrections turned out to be extremely large [10], raising doubts as to the reliability of the perturbative approach.

In this chapter, we describe first the results of the application of the optimized perturbation theory (OPT) to the electroweak phase transition as treated in the framework of the dimensionally reduced standard model. An optimized one-loop calculation led to the conclusion that the first-order nature of the transition has an endpoint when the quartic self-coupling of the Higgs sector exceeds the value corresponding to $M_{Higgs} \approx 100\,\mathrm{GeV/c^2}$ [11]. Since this conclusion hints at the necessity to extend the presently known elementary interactions beyond the standard model (BSM), it proved to be of great importance to obtain similar information from the exact solution of the reduced model relying on Monte Carlo simulations [12, 13]. The basis of the numerical investigations and the evidence confirming the existence of a critical endpoint of the first-order transition line will be summarized in the second part of the chapter.

8.1 The Reduced $SU(2)$ Symmetric Higgs + Gauge Model

The dimensionally reduced three-dimensional Higgs + gauge model with $SU(2)$ gauge symmetry has the following action:

$$S_{3D}[\boldsymbol{W}, \sigma, \boldsymbol{\pi}] = \int d^3x \,\mathrm{Tr}\left[\frac{1}{2} W_{ij} W_{ij} + (D_i \Phi)^\dagger D_i \Phi + m_3^2 \Phi^\dagger \Phi + 2\lambda_3^{BP} \left(\Phi^\dagger \Phi\right)^2\right], \tag{8.2}$$

where the trace is understood over the $SU(2)$ indices. For the fields, the following singlet–triplet representations are used:

$$\Phi = \frac{1}{2}\left(\sigma + i\vec{\tau}\vec{\pi}\right), \qquad W_i = \frac{1}{2}\vec{\tau}\vec{W}_i, \qquad D_i\Phi = (\partial_i - ig_3\vec{\tau}\vec{W}_i)\Phi. \tag{8.3}$$

(The conventions of [11] are followed, for which reason, the index BP, with reference to the initials of its authors, appears on the Higgs self-coupling.) The real fields $\sigma, \boldsymbol{\pi}$ are related nonlinearly to the four components of the complex doublet Φ_c used in the standard model:

$$\begin{aligned} \Phi_c^\dagger \Phi_c &= 2\mathrm{Tr}(\Phi^\dagger\Phi), \\ \vec{j}_i = i\frac{g_3}{2}\left[\Phi_c^\dagger\vec{\tau}\partial_i\Phi_c - (\partial_i\Phi_c)^\dagger\vec{\tau}\Phi_c\right] &= \frac{g_3}{2}\left[\partial_i\sigma\vec{\pi} - \sigma\partial_i\vec{\pi} - (\partial_i\vec{\pi})\times\vec{\pi}\right]. \end{aligned} \tag{8.4}$$

The first relation is the condition for the invariance of the local scalar potential; the second expresses the unchanged current of the scalar fields in the interaction with the gauge fields.

The lowest approximation to the dimensional reduction that leads to this form of the reduced action is arrived when after the nonstatic bosonic and fermionic modes, one integrates also over the static $\boldsymbol{W}_0$ fields. This process, realized at the one-loop level, determines the effective couplings $g_3, m_3^2, \lambda_3^{BP}$ and also the effective counterterms needed for finding the renormalized physical data of the model.

The integration over the nonstatic fields can be done in full conformity with the steps followed for the abelian Higgs + gauge model presented in Sect. 6.5. For the case of $SU(2)$ symmetry, the expression of the reduced action of the three-dimensional fields is the following [14, 15]:

$$\begin{aligned} S[\boldsymbol{W}_i, \boldsymbol{W}_0, \Phi] = \int d^3x \mathrm{Tr}\Big[& W_{ij}W_{ij} + (D_i\Phi)^\dagger D_i\Phi + \bar{m}_3^2\Phi^\dagger\Phi + 2\bar{\lambda}_3(\Phi^\dagger\Phi)^2 \\ & + (D_iA_0)^2 + m_D^2 W_0^2 + 2\lambda_W W_0^4 + 4h_3 W_0^2(\Phi^\dagger\Phi)\Big] \end{aligned} \tag{8.5}$$

($D_i = \partial_i - i\bar{g}_3 W_i$). Here the induced three-dimensional counterterms are not written out explicitly, and (without fermions)

$$\begin{aligned} & W_0 = \frac{1}{2}\vec{\tau}\vec{W}_0, \qquad m_D^2 = \frac{5}{6}g^2(\mu_T)T^2, \qquad \lambda_W = \frac{17g^4(\mu_T)T}{48\pi^2}, \qquad h_3 = \frac{1}{4}\bar{g}_3^2, \\ & \bar{g}_3^2 = g^2(\mu_T)T, \quad \bar{\lambda}_3 = \lambda(\mu_T)T, \quad \bar{m}_3^2 = m^2 + \left(\frac{3}{16}g^2(\mu_T) + \frac{1}{2}\lambda(\mu_T)\right)T^2, \end{aligned} \tag{8.6}$$

and μ_T denotes a special choice of the renormalization scale, which ensures the suppression of all logarithmic one-loop contributions to the expressions of $\bar{g}_3, \bar{\lambda}_3, \bar{m}_3^2$

(this is again a sort of optimization to avoid large contributions from perturbation theory; see Sect. 3.5.1).

For the second step of the one-loop integration, one separates the quadratic part of the W_0-dependent three-dimensional $SU(2)$ symmetric action on constant $\Phi_0, \bar{W}_i^a$ background [15]:

$$S_{W_0}^{(2)} = \frac{1}{2}\int_k W_0^a(-\mathbf{k}) \times \left[\left(k^2 + m_D^2 + h_3\Phi_0^2 + \bar{g}_3^2(\bar{W}_i^c)^2\right)\delta^{ab} - 2i\bar{g}_3\epsilon^{acb}k_i\bar{W}_i^c - \bar{g}_3^2\bar{W}_i^a\bar{W}_i^b\right] W_0^b(\mathbf{k}). \tag{8.7}$$

The electric potential receives a Debye screening mass m_D of $\mathcal{O}(gT)$, which is softer than the effective mass of the nonstatic Matsubara modes. Still, on reduction, this integral is infrared safe, and there is no need for gauge fixing. Below, evidence will be presented that the characteristic scale of the three-dimensional (magnetic) W_i-fluctuations is $\mathcal{O}(g^2T)$.

The contribution of the W_0-integration to (8.2) is obtained by expanding the result of the integration up to fourth power in the 3D field variables with the following result:

$$\Delta_{W_0}U[\Phi_0, \bar{W}_i^a] = -\frac{1}{4\pi}\left(m_D^2 + \frac{1}{4}\bar{g}_3^2\Phi_0^2\right)^{3/2} + \frac{\bar{g}_3^4}{96\pi}\frac{(\vec{\bar{W}}_i \times \vec{\bar{W}}_j)^2}{\left(m_D^2 + \bar{g}_3^2\Phi_0^2/4\right)^{1/2}} + \mathcal{O}(\bar{A}_i^6). \tag{8.8}$$

The second term on the right-hand side is readily completed to a gauge-invariant correction of the three-dimensional pure gauge action:

$$\frac{1}{4}F_{ij}^aF_{ij}^a \to \frac{1}{4\mu}F_{ij}^aF_{ij}^a, \qquad \frac{1}{\mu} = 1 + \frac{1}{24\pi}\frac{\bar{g}_3^2}{\left(m_D^2 + \bar{g}_3^2\Phi_0^2/4\right)^{1/2}}. \tag{8.9}$$

The leading (Φ_0-independent) piece of this induced magnetic susceptibility can be absorbed into a field rescaling, but it is then reflected in the final relation of g_3^2 to the four-dimensional gauge coupling. Also, the first term of the correction is expanded up to Φ_0^4 and modifies both $\bar{m}_3^2$ and $\bar{\lambda}_3$.

Here we give the finite parts of the relations of the couplings of the three-dimensional Higgs + gauge system derived in [14, 15] for the case of pure $SU(2)$ Higgs + gauge theory, taking into account also the effects of W_0:

$$m_3^2 = \bar{m}_3^2 - \frac{3\bar{g}_3^2m_D}{16\pi} + \mathcal{O}(g^4, \lambda^2),$$
$$\lambda_3^{BP} = \bar{\lambda}_3 - \frac{3\bar{g}_3^4}{128\pi m_D} + \mathcal{O}(g^4, \lambda^2), \qquad g_3^2 = \bar{g}_3^2\left(1 - \frac{\bar{g}_3^2}{24\pi m_D}\right). \tag{8.10}$$

The zero of m_3^2 determines the temperature where the effective squared mass of the Higgs field changes sign (it contains the negative renormalized squared mass parameter m^2), which in the mean field approximation would give the critical temperature of a continuous (second-order) transition. In a better approximation, one decides about the nature and the location of the transition after solving the effective three-dimensional theory with static field fluctuations taken into account.

8.2 Optimized Perturbation Theory for the Electroweak Phase Transition

A gauge-independent formulation of the OPT to the effective Higgs + gauge theory has been put forward in [11]. The Lagrangian is first expanded around the scalar background as $\sigma = v + \sigma'$ and supplemented with the gauge-fixing term

$$L_{GF} = \frac{1}{2\xi}\left(\partial_i W_i^a + \xi\frac{g}{2}v\pi^a\right)^2. \tag{8.11}$$

The full Lagrangian (the 3D counterterms not written out explicitly) includes also the contribution of the anticommuting ghost triplet c^a representing the Fadeev–Popov determinant of the reduced theory:

$$\begin{aligned}
L = {} & \frac{1}{4}\vec{W}_{ij}\vec{W}_{ij} + \frac{1}{2\xi}(\partial_i\vec{W}_i)^2 + \frac{g_3^2}{8}v^2\vec{W}_i^2 + \frac{g_3^2}{4}v\sigma'\vec{W}_i^2 + \vec{j}_i\vec{W}_i \\
& + \frac{1}{2}(\partial_i\sigma')^2 + \lambda_3^{BP}v^2\sigma'^2 + \frac{1}{2}(\partial_i\vec{\pi})^2 + \xi\frac{g_3^2}{8}v^2\vec{\pi}^2 \\
& + \frac{1}{2}(m_3^2 + \lambda_3^{BP}v^2)(\sigma'^2 + \vec{\pi}^2 + 2v\sigma') \\
& + \frac{g_3^2}{8}\vec{W}_i^2(\sigma'^2 + \vec{\pi}^2) + \lambda_3^{BP}v\sigma'(\sigma'^2 + \vec{\pi}^2) \\
& + \frac{\lambda_3^{BP}}{4}(\sigma'^2 + \vec{\pi}^2)^2 + \frac{1}{2}m_3^2v^2 + \frac{1}{4}\lambda_3^{BP}v^2 \\
& + \partial_i\vec{c}^*\partial_i c + \xi\frac{g_3^2}{4}v^2\vec{c}^*\vec{c} + g_3\partial_i\vec{c}^*(\vec{W}_i\times\vec{c}) \\
& + \xi\frac{g_3^2}{4}v\left(\sigma'\vec{c}^*\vec{c} + \vec{c}^*(\vec{\pi}\times\vec{c})\right).
\end{aligned} \tag{8.12}$$

For a one-loop computation in the 3D perturbation theory, one obtains for the gauge field the following propagators, some of them explicitly depending on the gauge-fixing parameter ξ:

$$D_{ij}^{ab}(p) = \delta_{ab}\left[D_T(p)P_{ij}^T + D_L(p)P_{ij}^L\right], \quad P_{ij}^T = \delta_{ij} - \frac{p_i p_j}{p^3}, \quad P_{ij}^L = \frac{p_i p_j}{p^2},$$
$$D_T^{-1} = p^2 + \frac{g_3^2}{4}v^2, \quad D_L^{-1} = \xi^{-1}\left(p^2 + \xi\frac{g_3^2}{4}v^2\right). \tag{8.13}$$

The Higgs fields and the ghost propagators are partly degenerate:

$$(\Delta_\pi^{-1})^{ab} = (\Delta_c^{-1})^{ab} = \delta_{ab}\left(p^2 + \xi\frac{g_3^2}{4}v^2\right), \qquad \Delta_\sigma^{-1} = p^2 + m_3^2 + 3\lambda_3^{BP}v^2. \tag{8.14}$$

Here it is appropriate to recall the idea of OPT: one replaces in the propagators the tree-level masses by the optimal mass parameter (attention: this parameter does not necessarily coincide with the true mass of the exact solution):

$$\frac{g_3^2}{4}v^2 = M_W^2 - \delta M_W^2, \qquad m_3^2 + 3\lambda_3^{BP}v^2 = M_H^2 - \delta M_H^2. \tag{8.15}$$

This replacement is done also in the masses proportional to the gauge-fixing parameter ξ. The optimization of the σ mass and of the transversal vector mass parameters is expressed then by requiring the on-shell suppression of the one-loop self-energy correction to the chosen masses:

$$\delta M_W^2 + \Pi_T(p^2 = -M_W^2, M_H, M_W, \xi) = 0,$$
$$\delta M_H^2 + \Sigma(p^2 = -M_H^2, M_W, M_H, \xi) = 0, \tag{8.16}$$

where $\Pi_T(p^2)$ is the coefficient function of the transversal part of the polarization tensor of the $\boldsymbol{W}_i$ field, and $\Sigma(p^2)$ is the self-energy of σ'. The linear divergences occurring in the one-loop calculation of these functions are automatically canceled by the induced counterterms.

However, the equations resulting from simply copying the OPT scenario worked out for scalar theories in Chap. 4 would depend explicitly on the gauge-fixing parameter. The clever idea suggested in [11] was to achieve gauge independence by appropriate resummations of the three- and four-point couplings of (8.12). The resulting gauge-invariant piece chosen for the resummed one-loop computation emerges by replacing m_3^2 and λ_3^{BP} through the "exact" mass parameters:

$$L_{resum} = \mathrm{Tr}\left[\frac{1}{2}W_{ij}W_{ij} + (D_i\Phi)^\dagger D_i\Phi + \frac{1}{2}M_H^2\Phi^\dagger\Phi + \frac{g_3^2M_H^2}{4M_W^2}(\Phi^\dagger\Phi)^2\right], \tag{8.17}$$

supplemented with the gauge-fixing term

$$L_{GF,resum} = \frac{1}{2\xi}\left(\partial_i W_i^a + \xi M_W \pi^a\right)^2 . \tag{8.18}$$

Also, the shift of the σ-field is parameterized through the optimal parameters:

$$\sigma = \sigma' + \frac{2M_W}{g_3}. \tag{8.19}$$

The terms completing L_{resum} to the original L are shifted to the interaction piece, which should be included only at the next (two-loop) order. In this way, one explicitly checks in the one-loop gap equations the cancellation of the ξ-dependent contributions to the Higgs and gauge self-energies on the respective mass shells:

$$\begin{aligned}\Sigma(p^2 = -M_H^2) = g_3^2\Bigg[&\frac{3v}{2g_3 M_W}(m_3^2 + \lambda_3^{BP} v^2) + \frac{3}{4M_W^2}(4M_W^2 + M_H^2)\mathscr{T}_3(M_W^2)\\ &+\frac{3}{8M_W^2}\left(8M_W^4 - 4M_W^2 M_H^2 + M_H^4\right)\mathscr{B}_3(-M_H^2, M_W^2, M_W^2)\\ &+\frac{3M_H^2}{4M_W^2}\mathscr{T}_3(M_H^2) + \frac{9M_H^4}{8M_W^2}\mathscr{B}_3(-M_H^2, M_H^2, M_H^2)\Bigg].\end{aligned} \tag{8.20}$$

$$\begin{aligned}\Pi_T(p^2 = -M_W^2) = g_3^2\Bigg[&\frac{M_W}{g_3 M_H^2} v(m_3^2 + \lambda_3^{BP} v^2) + \left(\frac{3M_W^2}{M_H^2} - \frac{M_H^2}{8M_W^2} - \frac{1}{2}\right)\mathscr{T}_3(M_W^2)\\ &+\left(\frac{M_H^2}{8M_W^2} + \frac{1}{2}\right)\mathscr{T}_3(M_H^2) - \frac{63}{64}M_W^2\mathscr{B}_3(-M_W^2, M_W^2, M_W^2)\\ &+\left(M_W^2 - \frac{1}{2}M_H^2 + \frac{M_H^4}{8M_W^2}\right)\mathscr{B}_3(-M_W^2, M_W^2, M_H^2)\Bigg].\end{aligned} \tag{8.21}$$

Here $\mathscr{T}_3(\mu^2)$ is the tadpole integral in the three-dimensional theory computed with propagator masses $\mu^2 = M_H^2, M_W^2$. Its linearly divergent piece is taken care of by the induced counterterms; only its finite part is to be included into the gap equations. The first argument of the three-dimensional bubble diagram $\mathscr{B}_3$ gives the value of the momentum where it is evaluated ($p^2 = -M_W^2, -M_H^2$). The second and third arguments give the propagator masses appearing on the two lines of the bubble.

The missing input into the two equations comes from the equation of state, which determines the physical value of the background v. This equation arises from averaging the fluctuating part of the σ-field to zero: $\langle\sigma'\rangle = 0$. This equation turns out to be mildly ξ-dependent:

$$v(m_3^2 + \lambda_3^{BP} v^2) = -\frac{3}{4} g_3 M_W \left(4\mathscr{T}_3(M_W^2) + \frac{M_H^2}{M_W^2} \left(\mathscr{T}_3(\xi M_W^2) + \mathscr{T}_3(M_H^2) \right) \right). \tag{8.22}$$

The integrals $\mathscr{T}_3$ and $\mathscr{B}_3$ can be calculated easily in analytic form. Taking into account the fact that only the one-particle-irreducible diagrams contribute, one obtains, after the cancellation of the linear divergences, the following explicit form for the gap equations plus the equation of state:

$$\begin{aligned} M_W^2 &= \frac{g_3^2}{4} v^2 + M_W g_3^2 f(z), \qquad M_H^2 = m_3^2 + 3\lambda_3^{BP} v^2 + M_H g_3^2 F(z), \\ v(m_3^2 + \lambda_3^{BP} v^2) &= \frac{3}{16\pi} g_3 \left(4M_W^2 + \sqrt{\xi} M_H^2 + \frac{M_H^3}{M_W} \right), \end{aligned} \tag{8.23}$$

where the explicit form of the two functions $f(z), F(z)$ depending on $z = M_W/M_H$ can be found in the original publication [11]. Note that $F(z)$ becomes complex for $z < 1/2$, signaling the decay of σ into two W's. In the physically interesting region, each term in each of the equations is real, and one has to search for real solutions v, M_W, M_H.

The numerical solution of the set of three equations was found by fixing values of $x = \lambda_3^{BP}/g_3^2$. The quantities $v/g_3, M_H/g_3^2, M_W/g_3^2$ were evaluated as functions of $y \equiv m_3^2/g_3^4$. This variation corresponds to that induced by the temperature, since the reduced-mass parameter m_3^2 changes sign at some $T = T_{barrier}$. Negative values of x correspond to the broken symmetry phase, large positive values to the phase of restored symmetry.

The dependence on the gauge-fixing parameter ξ is negligible for small values of λ_3^{BP}/g_3^2. Therefore, in this region one safely can choose the Landau gauge $\xi = 0$. The variation of the scaled order parameter v/g_3 is displayed in Fig. 8.1, where the continuous line gives the result for $\lambda_3^{BP}/g_3^2 = 1/128$, which (estimating by the tree-level relations) corresponds to the $T = 0$ mass relation $M_{H0} \approx M_{W0}/4$ (here and below, the $T = 0$ masses receive an extra lower "0" index in order to distinguish them from the temperature-dependent masses). The order parameter has large values for $y < 0$, which monotonically decrease as y approaches zero. This branch of the solution is stopped at some maximal value in the region $y > 0$. In the symmetric phase, the value of the order parameter is nonzero but takes very small values almost independently of y. The two overlapping branches of the order parameter solutions near $y = 0$ demonstrate the coexistence of two minima in the free energy density. The computation is optimized for the masses and not for the corresponding effective potential. Therefore, it is doubtful whether one can decide which solution is the stable one at a given y.

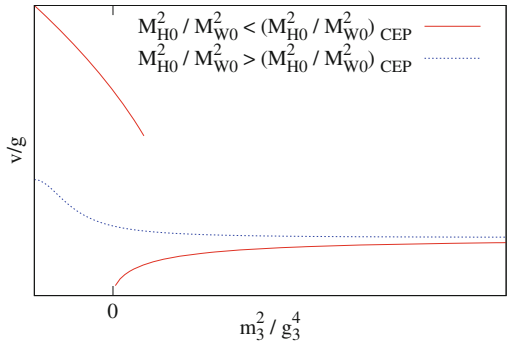

Fig. 8.1 Variation of the order parameter v/g with m_3^2/g_3^4 for two values of $8\lambda^{BP}/g^2 \approx M_{H0}^2/M_{W0}^2$ (after [11])

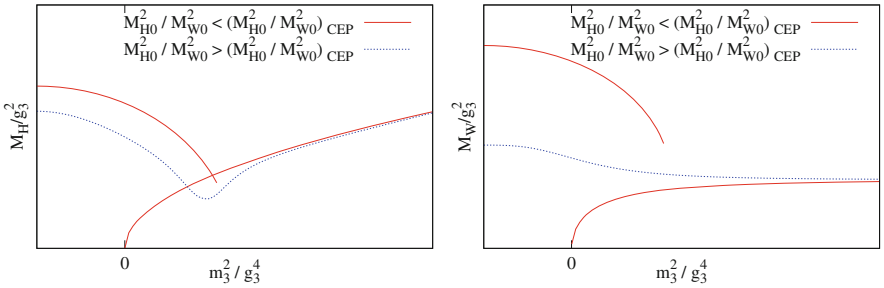

Fig. 8.2 Variation of the scaled Higgs mass M_H/g_3^2 (*left*) and the scaled vector mass M_W/g_3^2 (*right*) with m_3^2/g_3^4 for two values of $8\lambda^{BP}/g^2 \approx M_{H0}^2/M_{W0}^2$ (after [11])

One can perform also an ordinary one-loop renormalized perturbative calculation that gives vanishing v in the symmetric phase, while it has a nonzero solution in the broken symmetry phase approximating quite well the solution of the gap equations. This calculation corresponds to the pioneering investigation of Kirzhnits and Linde [16], who concluded that for small Higgs masses, the electroweak phase transition is of first-order nature.

When repeating the analysis for $\lambda_3^{BP}/g_3^2 = 1/8$ (or $M_{H0} \approx M_{W0}$), one finds (dashed line) a continuously varying scaled order parameter over the whole range of m_3^2/g_3^4 (the perturbative calculation makes no sense for $y > 0$). This is a clear message from a continuous crossover transition.

The crossover nature of the transition in the second case is further supported by the variation of the masses in the two cases. In the left-hand figure of Fig. 8.2 one recognizes the abrupt jump downward of the Higgs mass in passing through y_c (continuous line), which clearly hints at a first-order transition ($M_{H0} \approx M_{W0}/4$). The dashed line corresponds to nearly equal Higgs and vector masses, and in the broken-symmetry phase, one observes the Higgs mass passing through a nonzero minimum, signaling the presence of a pseudocritical temperature.

The branch of the nonperturbatively computed vector mass (the right-hand figure) for $M_{H0} \approx M_{W0}/4$ begins close to the perturbative value in the broken phase and ends discontinuously at some $y > 0$ near zero. Another branch grows for $y > 0$ from zero, which at large y approaches from below a small, but definitely nonzero, constant value as opposed to the expectation based on perturbation theory. When $M_{H0} \approx M_{W0}$ (dashed line), the two sections appear to form a unique continuous curve, displaying the same nonzero asymptotic value for large y. This effect is related to the nonperturbative dynamics of the gauge sector and defines a high-temperature scale of $\mathcal{O}(g_3^2) \sim \mathcal{O}(g^2 T)$. The constant-high-temperature asymptotics hint at the existence of magnetic screening in nonabelian pure gauge theories like QCD. The existence of the magnetic mass has been long debated [17–19], but one should not forget that an OPT-based evidence in favor of finite-range magnetic screening could be an artifact arising from the restricted set of optimizable parameters.

One can also compare the results with the simple perturbative one-loop mass calculations. The close, almost quantitative agreement of the perturbatively calculated Higgs and vector masses with the result of the gap equations is obvious in the broken-symmetry phase for smaller Higgs mass. The two results are also not too far from each other in the high-temperature phase concerning the scalar mass. For nearly equal vector and scalar masses, the quality of the agreement deteriorates even in the broken-symmetry phase when one approaches $y = 0$. In the symmetric phase, only the Higgs mass is nonzero in the perturbative framework, but again its value diverges from the solution of the gap equation for asymptotically large temperatures.

The location of the transition (λ_c^{BP}/g^2) from the first-order phase transition to the crossover-type variation lies between the two values of λ_3^{BP}/g_3^2 analyzed here. Since the results for $M_{W0} \approx M_{H0}$ become increasingly ξ-sensitive, especially in the region $y \approx 0$, one cannot draw reliable quantitative conclusions about the accuracy of the one-loop location of the transition $(\lambda_c^{BP}/g^2 \approx 0.0406)$. Taking into account all the uncertainties of the approximate solution, one can, however, safely claim that the first-order nature of the electroweak transition changes into a smooth crossover somewhere for $M_{H0} \leq M_{W0}$. Since the mass of the Higgs particle discovered at CERN is outside this region, one has to abandon the idea of the electroweak generation of the matter–antimatter asymmetry, under the condition that this conclusion becomes supported by more accurate mappings of the electroweak phase structure.

The accurate localization of the endpoint of the first-order line of electroweak phase transitions was found with the help of Monte Carlo simulations. It will be reviewed with emphasis on the results obtained in the framework of resummed (dimensionally reduced) effective models in the next section.

8.3 Results from the Numerical Simulation of the Electroweak Model Reduced with One-Loop Accuracy

In the lattice regularization of (8.2), the gauge field $W_j(x)$ is replaced by the link variable $U_{x,j} = \exp(ig_3 W_j(x)a)$, pointing from the lattice site x to $x + ae_j$ (a is the lattice constant; e_j is the unit vector along the $j(= 1, 2, 3)$-axis). The Wilson action of the gauge field is proportional to the $SU(2)$-trace of the plaquette variable $U_{P(jl)}(x) = U^{\dagger}_{x,l} U^{\dagger}_{x+ae_l,j} U_{x+ae_j,l} U_{x,j}$. The scalar multiplet is parameterized in the same way as in (8.3); the Higgs self-coupling will be redefined in this section as $\lambda_3 = 6\lambda_3^{BP}$. The lattice regularized action in this notation is given as [13, 20]

$$S_{lat} = \frac{1}{2} \sum_x \mathrm{Tr}\Big[\beta \sum_{jl} U_{P(jl)} + 4 \sum_j \Phi^{\dagger}(x) U_{x,j} \Phi(x + ae_j) - \frac{2}{\kappa} \Phi^{\dagger}(x)\Phi(x) - \frac{2\lambda_{3L}}{3} \left(\Phi^{\dagger}(x)\Phi(x)\right)^2\Big]. \tag{8.24}$$

The dimensional couplings of the effective theory given at one-loop accuracy in the previous section are related to the dimensionless couplings of (8.24) as

$$\begin{aligned} &\Theta \equiv aT, \quad \beta = \frac{4}{g_3^2 a}, \quad \lambda_{3L} = \lambda_3 a, \\ &\frac{1}{\kappa} = m_3^2 a^2 + 6 - \Theta \Sigma(L) \left(\frac{3}{2} g^2 + \lambda - \frac{15 g^3}{32\pi} \sqrt{\frac{5}{6}}\right), \\ &\Sigma(\infty) = 0.252731. \end{aligned} \tag{8.25}$$

Note that in the coefficient of the so-called hopping term (κ^{-1}), also a size-dependent ($\sim \Sigma(L)$) piece is present beyond the additive contribution ($+6$) arising from the discretization of the kinetic term. This contribution to the squared mass or $(\kappa^2 a^2)^{-1}$ is linearly divergent near the continuum ($\sim 1/a$) and replaces the previous induced counterterm, generated now by evaluating the three-dimensional tadpole integral on a cubic lattice with lattice constant a.

There exist detailed introductory textbooks helping the reader to gain deeper insight into the technology of lattice field theory [21, 22]. Here we proceed by presenting the findings of [13] without entering into any technical details. The correspondence of the lattice couplings to the four-dimensional couplings was fixed by setting $\Theta = 1$, that is, $a = 1/T$, and choosing $\beta = 9$. This choice determines g_3^2, and by the one-loop relation, the four-dimensional renormalized gauge coupling g. The simulation has been realized for a number of λ_3 values. By its one-loop expression, one obtains, in the knowledge of g, the corresponding values of the Higgs self-coupling λ in four dimensions.

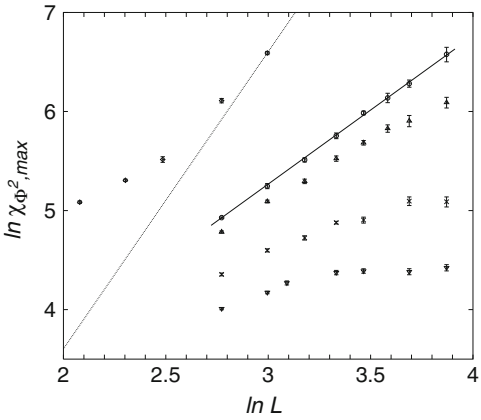

Fig. 8.3 Variation of the maxima of the field-length susceptibility (8.26) with the lattice size for $L = 8$ to $L = 48$ for five different values of λ_3 (from [13])

Using the physical value of the vacuum condensate $v = 246\,\text{GeV}$, one can use the corresponding tree-level expressions to estimate the W and Higgs masses. The set of variables corresponds to fixing the W-mass near its physical value and investigating the nature of the symmetry-restoring transition for various Higgs masses. For each set of couplings, one tunes κ, which corresponds to tuning $|m^2|/T^2$. The goal is to find the maximum of certain thermodynamic susceptibilities of the system. The corresponding value of κ, called κ_{max}, characterizes the temperature (in units of the renormalized mass) where the system turns from the broken-symmetry regime into the symmetric phase.

A widely used class of signatures allowing distinction between first-order transitions and crossovers is the finite-size behavior of various susceptibilities. In Fig. 8.3, the size-dependence of

$$\chi_{\Phi^2} = \text{Volume} \times \langle (\Phi^\dagger \Phi - \langle \Phi^\dagger \Phi \rangle)^2 \rangle \tag{8.26}$$

is plotted on a log-log diagram. For a first-order transition, χ_{Φ^2} should increase with the size of the lattice system as $V = L^3$, while for a crossover, it should tend to a constant. The figure clearly reveals that for $\lambda_3 = 0.170190$ (the upper left group of points), with increasing volume the variation of the susceptibilities approaches a linear behavior in V. The lower three sequences of points obviously tend to constants. These measurements were done for $\lambda_3 = 0.313860, 0.401087, 0.498579$, respectively. A power law behavior with nontrivial power (critical exponent) is observed for $\lambda_3 = 0.291275$, which is the accepted signal for a second-order transition. The corresponding Higgs self-coupling is the point separating the first-order and crossover regimes.

Another method for finding the critical endpoint is to study the behavior of the partition function when κ is continued to complex values [23]. The partition function of the complexified theory displays a number of zeros (κ_0). With increasing size L,

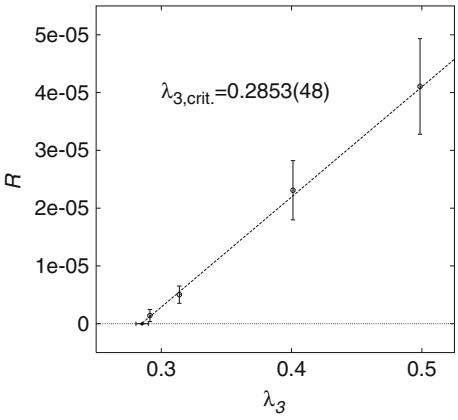

Fig. 8.4 Variation of the constant R of (8.27) with λ_3 extrapolated linearly to $R = 0$. The horizontal interval gives the error of the extrapolation but does not reflect the systematic error from the one-loop mapping (from [13])

the imaginary part of $\kappa_{0,min}$, the zero lying the closest to the real κ-axis, exhibits the scaling behavior

$$\mathrm{Im}(\kappa_{0,min}) = CL^{-(1/\nu)} + R(\lambda_3). \tag{8.27}$$

The range of λ_3 values where $R \neq 0$ corresponds to the crossover-type transitions where the partition function does not contain any nonanalytic behavior. The critical power exponent ν characterizes the vanishing of the Higgs mass in the critical endpoint ($R(\lambda_{3c}) = 0$) as a function of the temperature. In Fig. 8.4, the variation of the constant R is plotted for four larger values of λ_3 and is extrapolated to the point below which it vanishes. The critical endpoint was located as $\lambda_{3c} = 0.2853(48)$ quite close to the value found from analyzing the field susceptibility. Using the one-loop relations for the couplings and the corresponding expression of the Higgs mass, the critical Higgs mass value was estimated as $m_{Hc} = 75.4(6)$.

The intriguing question of the existence of a magnetic screening mass in the symmetric (high-T) phase has been also investigated. For this study, the asymptotic behavior of the $W - W$ correlator was extracted from a lattice simulation of the model with Landau-gauge fixing. The variation with κ of the dimensionless W mass ($M_W a$), extracted as the inverse characteristic length of the exponential decrease of the correlator, is seen in Fig. 8.5. For $\kappa < \kappa_c$, i.e., in the high-T phase, the existence of a constant screening mass has been clearly demonstrated.

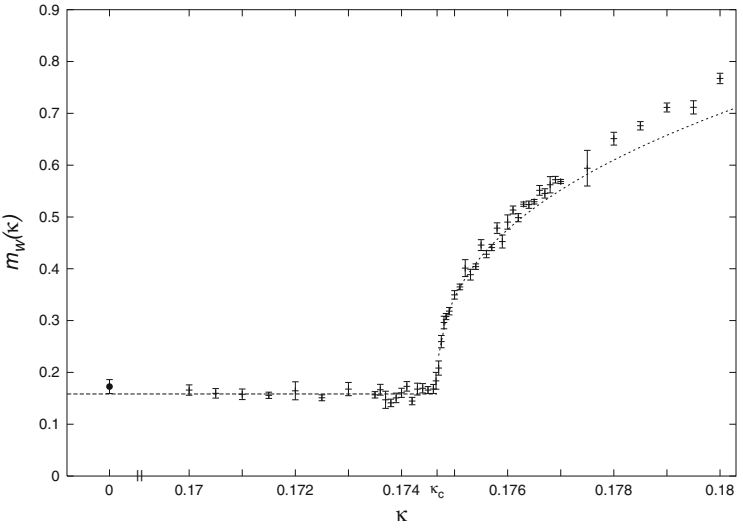

Fig. 8.5 Variation of the magnetic mass with the temperature (low κ values correspond to high temperatures (from [13]))

8.4 On the High-Accuracy Determination of the Critical Higgs Mass

The field theory defined in (8.2) is superrenormalizable. This means that only the operator m_3^2 requires a counterterm, and the couplings λ_3, g_3^2 are renormalization group invariants within the three-dimensional model. Moreover, only one- and two-loop Feynman diagrams provide divergent contributions. Therefore, the counterterm can be determined exactly by analyzing a finite number of diagrams. Its structure is the following:

$$\delta m_3^2 = f_{1m}\Sigma_{lin} + f_{2m}\Sigma_{log}. \tag{8.28}$$

The first term shows up as an induced counterterm in the coefficient of Φ_0^2 when one expands the one-loop nonstatic + W_0 contribution to the effective potential computed on constant-Φ_0 background. If one solves the reduced model also perturbatively, this induced counterterm ensures the finiteness of the potential or of any other observable. But when one treats the reduced model with the method of lattice field theory, one finds the necessary counterterm by analyzing the lattice version of the tadpole integral supplemented with the requirement that it should provide the same finite part as with momentum cutoff regularization. This gives the last term in the expression of κ^{-1} in (8.25).

The two-loop divergence comes from the so-called setting-sun diagrams, which are logarithmically divergent. The divergent piece has the following expression

when calculated on a lattice (compare to Appendix C.2):

$$\Sigma_{log} = \frac{1}{16\pi^2}\left(\log\frac{6}{a\mu_3} + 0.09\right). \tag{8.29}$$

The finite piece again stems from requiring the same finite parts as calculated with momentum cutoff regularization. Collecting all the diagrams, for the coefficient of Σ_{log} one obtains

$$f_{2m} = \frac{51}{16}g_3^4 + 9\lambda_3^{BP}g_3^2 - 12\lambda_3^{BP2}. \tag{8.30}$$

The renormalization of the logarithmic divergences necessarily introduces a new scale (independent of the renormalization scale generated in the $4D \to 3D$ reduction step), denoted by μ_3. One has an exact renormalization group equation

$$\frac{\partial m_3^2(\mu_3)}{\partial \log\mu_3} = -\frac{1}{16\pi^2}f_{2m} \to m_3^2(\mu_3) = \frac{1}{16\pi^2}f_{2m}\log\frac{\Lambda_m}{\mu_3}, \tag{8.31}$$

where Λ_m is a renormalization group invariant constant of integration. This constant is found by comparing the two-loop effective potential calculated with couplings λ_3^{BP}, m_3^2 in three dimensions and the two-loop finite-temperature potential calculated directly in four dimensions. This comparison implies that at high temperatures, Λ_m will be predominantly proportional to T. Then, similarly to the optimal choice μ_T considerably simplifying the expression of $\bar{m}_3^2$, one chooses the scale μ_3 optimally.

There is an additional source of "counterterms" that comes from the difference of finite two-loop contributions of double-scoop type, calculated respectively in the continuum and the lattice schemes. These terms for the $SU(2)$ group give an additional counterterm to (8.25) [24]:

$$\frac{1}{16\pi^2}\left[f_{2m}\Sigma_{log} + 5.0g_3^4 + 5.2\lambda_3 g_3^2\right]. \tag{8.32}$$

A high-precision Monte Carlo simulation of the three-dimensional Higgs + gauge model was performed [12] for several values of the ratio $x = \lambda_3^{BP}/g_3^2$. The zero-temperature W-mass was chosen near its physical value by setting $v = 246\,\text{GeV}$ and $g = 2/3$. The variation of the temperature was realized by varying $y = m_3^2/g_3^4$. These two dimensionless variables have been expressed with the tree-level zero temperature Higgs mass $m_H^2 = \lambda v^2/3$ and the ratio m_H^2/T^2. Including also the counterterm contributions just discussed above, the following relations were used for analyzing the data:

$$\begin{aligned} x &= -0.00550 + 0.12622h^2, \\ y &= 0.39818 + 0.15545h^2 - 0.00190h^4 - 2.58088\frac{m_H^2}{T^2}, \end{aligned} \tag{8.33}$$

where $h = m_H/(80.6\,\text{GeV})$.

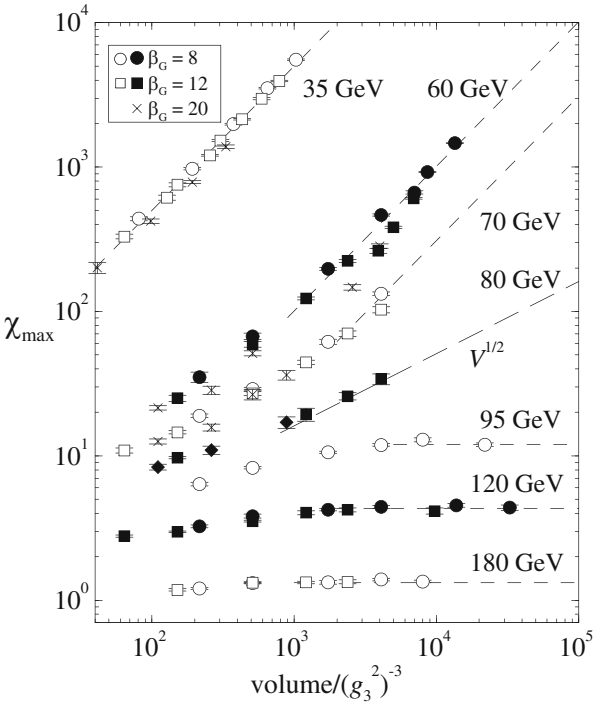

Fig. 8.6 Variation of the field-length susceptibility with the lattice size for $L = 8$ to $L = 64$ for seven different values of λ_3 (from [12])

The simulations covered the range $m_H \in 35$–$180\,\text{GeV}$. Three different lattice spacings were used to control possible discretization errors. The volume-dependence of the susceptibility (8.26) was studied for lattice sizes $L = 12, 16, 24, 32, 48, 64$. In Fig. 8.6, the variation of the maximal values $\chi_{\max}$ with the lattice volume is displayed. It is clear that the curves in the $m_H = 35, 60, 70\,\text{GeV}$ cases signal a first-order transition, while those of 95, 120, 180 GeV correspond to a crossover. The slope of the $m_H = 80\,\text{GeV}$ data seems to follow a nontrivial scaling exponent. Therefore, the conclusion was (in agreement with [13]) that the endpoint is located below $m_H \approx 80\,\text{GeV}$.

The investigation of the nature of the electroweak symmetry restoration was performed also in [25] using the reduced three-dimensional effective model. These authors obtained $m_{Hc} = 67.0(8)\,\text{GeV}$ for the critical Higgs mass. All these investigations done in the dimensionally reduced effective model are compatible among each other and also with the result of Csikor et al. obtained by simulating the original finite-temperature four-dimensional model [26].

The conclusion of the intensive study of the $SU(2)$ symmetric Higgs + gauge model in the middle of the 1990s can be best summarized through the phase diagram of electroweak theory in the $T_c - M_H$-plane as it appears in Fig. 8.7.

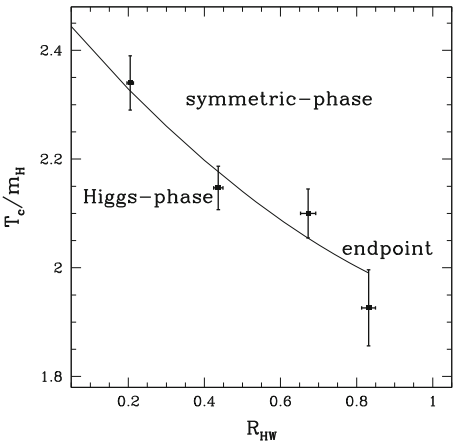

Fig. 8.7 The phase diagram of the $SU(2)$ symmetric Higgs + Gauge theory ($R_{HW} = m_H/m_W$, from [26])

References

1. E.W. Kolb, M.S. Turner, *The Early Universe* (Addison-Wesley, New York, 1990)
2. A. Sakharov, J. Exp. Theor. Phys. **5**, 24 (1967)
3. G. t'Hooft, Phys. Rev. D **14**, 3432 (1976)
4. N. Manton, Phys. Rev. D **28**, 2019 (1983)
5. F. Klinkhamer, N. Manton, Phys. Rev. D **30**, 2212 (1984)
6. M. Kobayashi, T. Maskawa, Prog. Theor. Phys. **49**, 652 (1973)
7. V.A. Kuzmin, V.A. Rubakov, M.E. Shaposhnikov, Phys. Lett. B **155**, 36 (1985)
8. G.W. Anderson, L.J. Hall, Phys. Rev. D **45**, 2685 (1992)
9. M. Carrington, Phys. Rev. D **45**, 2933 (1992)
10. Z. Fodor, A. Hebecker, Nucl. Phys. B **432**, 127 (1994)
11. W. Buchmuller, O. Philipsen, Nucl. Phys. B **443**, 47 (1995)
12. K. Kajantie, M. Laine, K. Rummukainen, M. Shaposhnikov, Phys. Rev. Lett. **77**, 2887 (1996)
13. F. Karsch, T. Neuhaus, A. Patkós, J. Rank, Proceedings of Lattice 96 international conference. Nucl. Phys. Proc. Suppl. **53**, 623 (1997)
14. K. Farakos, K. Kajantie, K. Rummukainen, M. Shaposhnikov, Nucl. Phys. B **425**, 67 (1994)
15. A. Jakovác, K. Kajantie, A. Patkós, Phys. Rev. D **49**, 6810 (1994)
16. D.A. Kirzhnits, A.D. Linde, Phys. Lett. B **72**, 471 (1972)
17. G. Alexanian, V.P. Nair, Phys. Lett. B **352**, 435 (1995)
18. A. Patkós, P. Petreczky, Zs. Szép, Eur. Phys. J. **C5**, 337 (1998)
19. F. Eberlein, Phys. Lett. B **439**, 130 (1998)
20. F. Karsch, T. Neuhaus, A. Patkós, J. Rank, Nucl. Phys. B **474**, 217 (1996)
21. I. Montvay, G. Münster, *Quantum Fields on Lattice* (Cambridge University Press, Cambridge, 1994)
22. H.J. Rothe, *Lattice Gauge Theories: An Introduction*, 4th edn. (World Scientific, Singapore, 2012)
23. C.N. Yang, T.D. Lee, Phys. Rev. **87**, 404 (1952)
24. M. Laine, Nucl. Phys. B **451**, 484 (1995)
25. M- Gürtler, E.-M. Ilgenfritz, A. Schiller, Nucl. Phys. Proc. Suppl. **63**, 566 (1998)
26. F. Csikor, Z. Fodor, J. Heitger, Phys. Rev. Lett. **82**, 21 (1999)

Appendix A
The Spectral Function

We briefly mention some properties of the spectral function.

A.1 Sum Rules

Expressed with operators, we have

$$\varrho_{AB}(x) = \frac{1}{Z_0} \operatorname{Tr}\left[e^{-\beta H}[A(x), B(0)]_\alpha\right], \tag{A.1}$$

i.e., this is the expectation of the (anti)commutator of the two operators. For fundamental fields, the (anti)commutator is just a Dirac delta (cf. (2.8)), which implies

$$\varrho_{A\Pi}(t = 0, \mathbf{x}) = i\delta(\mathbf{x}), \qquad \int \frac{dk_0}{2\pi} \varrho_{A\Pi}(k_0, \mathbf{k}) = i; \tag{A.2}$$

this is the basic form of sum rules. In general, the (anti)commutator of a local operator at equal times must be proportional to $\delta(\mathbf{x})$, but the proportionality constant can be complicated. Thus in the generic sum rule, the right-hand side is not just i, but in addition, a (temperature-dependent) constant can appear.

A.2 Positivity

Using the time translation-invariance of the equilibrium and the properties of the (anti)commutators, it is easy to show that $\varrho^*_{AB}(k) = \varrho_{B^\dagger A^\dagger}(k)$, which means that $\varrho^*_{AA^\dagger}(k) = \varrho_{AA^\dagger}(k)$, i.e., the spectral function is real for $B = A^\dagger$. Moreover,

A. Jakovác, A. Patkós, *Resummation and Renormalization in Effective Theories of Particle Physics*, Lecture Notes in Physics 912,
DOI 10.1007/978-3-319-22620-0

$\varrho_{AB}(-k) = -\alpha\varrho_{BA}(k)$, which means that the spectral function is antisymmetric for $B = A$.

Continuing with the real spectral functions $\varrho_{AA^\dagger}$, we can insert into the definition a complete system with states $\langle Pn|$, where P is the four-vector of the energy and momentum, and n is the eigenvalue of N, the operator of a conserved charge. We obtain

$$\begin{aligned}
&\mathrm{Tr}\, e^{-\beta(H-\mu N)}[A(x), A^\dagger(0)]_\alpha = \sum_{Pn} \left\langle Pn \left| e^{-\beta(H-\mu N)}[A(x), A^\dagger(0)]_\alpha \right| Pn \right\rangle \\
&= \sum_{PP'nn'} \left(e^{-\beta(E-\mu n)} - \alpha e^{-\beta(E'-\mu n')} \right) \left\langle Pn \left| A(x) \right| P'n' \right\rangle \left\langle P'n' \left| A^\dagger(0) \right| Pn \right\rangle \\
&= \sum_{PP'nn'} \left(e^{-\beta(E-\mu n)} - \alpha e^{-\beta(E'-\mu n')} \right) e^{i(P-P')x} |\left\langle Pn \left| A(0) \right| P'n' \right\rangle|^2, \qquad \text{(A.3)}
\end{aligned}$$

where we have used $A(x) = e^{iPx}A(0)e^{-iPx}$. If A has a definite charge q, then $n' + q = n$ must be true. In Fourier space, we have

$$\varrho_{AA^\dagger}(k) = \sum_{PP'nn'} e^{-\beta(E-\mu n)} \left(1 - \alpha e^{-\beta(k_0+\mu q)}\right) (2\pi)^4 \delta(k + P - P') |\left\langle Pn \left| A(0) \right| P'n' \right\rangle|^2. \qquad \text{(A.4)}$$

This form shows that for $k_0 + \mu q > 0$, the spectral function is strictly positive.

The same formula also demonstrates that the spectral function is a sum of Dirac deltas, at values of k, where two energy eigenstates satisfy the equality $P' = P + k$. At zero temperature and chemical potential, only the $E = 0$ ground state remains, where

$$\varrho_{AA^\dagger}(k_0 > 0)|_{T=\mu=0} = \sum_P C_k (2\pi)^4 \delta(k - P), \qquad \text{(A.5)}$$

where $C_k = |\left\langle kq \left| A(0) \right| 0 \right\rangle|^2$. This is proportional to the density of states.

Appendix B
Computation of the Basic Diagrams

Here we summarize the results of the computation of the tadpole and the bubble diagrams in a one-component bosonic or fermionic theory.

B.1 Tadpole Integral

The contribution of the tadpole diagram (see the first diagram of Fig. 2.2) is momentum-independent, and so it yields the same result in every formalism. In real space, the diagram is proportional to $G^{(33)}(x = 0)$. This will be considered the tadpole integral with the definition

$$\mathscr{T} = \alpha G^{(33)}(x = 0). \tag{B.1}$$

We can write it in the imaginary time formalism as

$$\mathscr{T} = \alpha T \sum\!\!\!\!\!\!\int \frac{d^3p}{(2\pi)^3} \frac{1}{\omega_n^2 + \omega_p^2}, \tag{B.2}$$

where $\omega_n = 2\pi n$ or $(2n + 1)\pi$ for the bosonic or fermionic case, respectively. We do not perform the sum, instead we use the line of argument of Eq. (2.82): using the definition in (2.42), we obtain

$$\begin{aligned} \mathscr{T} &= \int \frac{d^4p}{(2\pi)^4} \left(\frac{\alpha}{2} + n_\alpha(p_0 - \mu)\right) \varrho_0(p) \\ &= \int \frac{d^3\mathbf{p}}{(2\pi)^3 2\omega_p} \left(\alpha + n_\alpha(\omega_p - \mu) + n_\alpha(\omega_p + \mu)\right). \end{aligned} \tag{B.3}$$

A. Jakovác, A. Patkós, *Resummation and Renormalization in Effective Theories of Particle Physics*, Lecture Notes in Physics 912,
DOI 10.1007/978-3-319-22620-0

It naturally splits into a zero- and finite-temperature/chemical potential part:

$$\mathscr{T} = \alpha \mathscr{T}_0 + \frac{1}{2}\left[\mathscr{T}_{T,\mu} + \mathscr{T}_{T,-\mu}\right], \qquad \mathscr{T}_0 = \mathscr{T}\big|_{\mu=T=0}. \tag{B.4}$$

Here $\mathscr{T}_0$ is UV divergent. We need to regularize the integral in order to be able to handle it. With momentum cutoff, we have

$$\mathscr{T}_0 = \frac{1}{2}\int \frac{d^3\mathbf{p}}{(2\pi)^3}\,\frac{1}{\sqrt{p^2+m^2}} = \frac{1}{4\pi^2}\int_0^\Lambda \frac{dpp^2}{\sqrt{p^2+m^2}} = \frac{\Lambda^2}{8\pi^2} - \frac{m^2}{16\pi^2}\ln\frac{4\Lambda^2}{em^2}. \tag{B.5}$$

We can also apply dimensional regularization (cf. Appendix B.3) to compute its value:[1]

$$\frac{\mu^{2\varepsilon}}{2}\int \frac{d^{3-2\varepsilon}p}{(2\pi)^{3-2\varepsilon}}\,\left(p^2+m^2\right)^{-1/2} = \frac{m^2}{16\pi^2}\left(-\frac{1}{\varepsilon} + \gamma_E - 1 + \ln\frac{m^2}{4\pi\mu^2} + \mathscr{O}(\varepsilon)\right), \tag{B.6}$$

where γ_E is the Euler constant, $\gamma_E = 0.577216$.

The quantity $\mathscr{T}_{T,\mu}$ is UV finite, due to the exponential suppression of the distribution functions. For the evaluation, we change the integration variable $p \to x = \beta p$, and obtain

$$\mathscr{T}_{T,\mu} = \frac{T^2}{2\pi^2}\int_0^\infty dx\,\frac{x^2}{\gamma}\,\frac{1}{e^{\gamma-\beta\mu}-\alpha}, \qquad \gamma = \sqrt{x^2+(\beta m)^2}. \tag{B.7}$$

The only analytic problem with this integral is a pole for the bosonic ($\alpha = 1$) case for $\mu > m$. Therefore, the bosonic expression $\mathscr{T}$ is defined only in the range $-m < \mu < m$, just as for the thermodynamics itself.

In the convergent regimes, one can study different limits. The small-temperature regime is common for the bosonic and fermionic cases:

$$\begin{aligned}\mathscr{T}_{T\ll\mu,m} &= \frac{T^2}{2\pi^2}\int_{\beta m}^\infty dx\,e^{-x+\beta\mu}\sqrt{x^2-(\beta m)^2} = \frac{mT}{2\pi^2}K_1(\beta m)e^{\beta\mu} \\ &\approx \frac{1}{m}\left(\frac{mT}{2\pi}\right)^{3/2} e^{-\beta(m-\mu)}.\end{aligned} \tag{B.8}$$

[1] Usually, it is computed in $4-2\varepsilon$ dimensions, using Wick rotation; but the result is the same.

For the leading order of the small-mass expansion, we also can get analytic expressions by formally substituting $m = 0$:

$$\mathscr{T}_{T,\mu}(m=0) = \frac{T^2}{2\pi^2}\int_0^\infty dx\,\frac{x}{e^{-\beta\mu}e^x - \alpha} = \frac{\alpha T^2}{2\pi^2}\mathrm{Li}_2(\alpha e^{\beta\mu}), \tag{B.9}$$

where Li_2 is the dilogarithm (Spence's) function. In the bosonic case, the pole is regularized by principal value integration. Using the identity [1]

$$\mathrm{Li}_2(z) + \mathrm{Li}_2(1/z) = -\frac{\pi^2}{6} - \frac{1}{2}\ln^2(-z), \tag{B.10}$$

one obtains

$$\frac{1}{2}\left[\mathscr{T}_{T,\mu}(m=0) + \mathscr{T}_{T,-\mu}(m=0)\right] = \begin{cases} \dfrac{T^2}{12} - \dfrac{\mu^2}{8\pi^2} & \text{for } \alpha = 1 \\ \dfrac{T^2}{24} + \dfrac{\mu^2}{8\pi^2} & \text{for } \alpha = -1. \end{cases} \tag{B.11}$$

Note that for the $\alpha = 1$ bosonic case, only $|\mu| < m$ is the physical domain.

The next terms of the small-mass expansion come from the expansion of the Bose–Einstein or Fermi–Dirac distribution. We will compute the function [2]

$$I^\varepsilon_\alpha(z) = \int_0^\infty \frac{dx\,e^{-\varepsilon x}}{\gamma}\,\frac{1}{e^{-\beta\mu}e^\gamma - \alpha}, \qquad \gamma^2 = x^2 + z^2. \tag{B.12}$$

It is connected to the tadpole as

$$\frac{d\mathscr{T}_{T,\mu}}{dm^2} = -\frac{1}{4\pi^2}I_\alpha(\beta m). \tag{B.13}$$

We work out only the $\mu = 0$ case.

In the bosonic case, the expansion of the distribution function reads

$$\frac{1}{e^\gamma - 1} = \frac{1}{\gamma} - \frac{1}{2} + 2\sum_{n=1}^\infty \frac{\gamma}{\gamma^2 + (2\pi n)^2}. \tag{B.14}$$

We note that the first term is the contribution of the zeroth (static) Matsubara mode. We have

$$I_+^\varepsilon(z) = \int_0^\infty dx \left(\frac{x^\varepsilon}{\gamma^2} - \frac{x^\varepsilon}{2\gamma} + 2\sum_{n=1}^\infty \frac{x^\varepsilon}{x^2 + z^2 + (2\pi n)^2} \right). \tag{B.15}$$

In the first term, we can take $\varepsilon = 0$, which yields $\pi/(2z)$. The second term is similar to the zero-temperature result

$$-\frac{1}{2}\int_0^\infty dx\, x^\varepsilon (x^2+z^2)^{-1/2} = -\frac{z^\varepsilon}{4\sqrt{\pi}}\Gamma(-\frac{\varepsilon}{2})\Gamma(\frac{1+\varepsilon}{2}) = \frac{1}{2\varepsilon} + \frac{1}{2}\ln\frac{z}{2}. \tag{B.16}$$

In the last term, we can take $z = 0$ and obtain

$$\begin{aligned} 2\sum_{n=1}^\infty \int_0^\infty dx \frac{x^\varepsilon}{x^2 + (2\pi n)^2} &= \sum_{n=1}^\infty \frac{\pi^\varepsilon (2n)^{-1+\varepsilon}}{\cos \varepsilon\pi/2} \\ &= \frac{(2\pi)^\varepsilon \zeta(1-\varepsilon)}{2\cos\varepsilon\pi/2} = -\frac{1}{2\varepsilon} + \frac{\gamma_E}{2} - \frac{1}{2}\ln(2\pi), \end{aligned} \tag{B.17}$$

where ζ is the Riemann zeta function. We then have

$$I_+(z) = \frac{\pi}{2z} + \frac{1}{2}\ln\frac{z}{4\pi} + \frac{\gamma_E}{2}. \tag{B.18}$$

In the fermionic case, we write

$$\frac{1}{e^\gamma + 1} = \frac{1}{2} - 2\sum_{n=1}^\infty \frac{\gamma}{\gamma^2 + ((2n+1)\pi)^2}. \tag{B.19}$$

Here there is no $1/\gamma$ term, since there is no zeroth Matsubara mode. The first term is the same as before; the second term yields

$$\begin{aligned} &2\sum_{n=1}^\infty \int_0^\infty dx \frac{x^\varepsilon}{x^2 + ((2n+1)\pi)^2} = \sum_{n=1}^\infty \frac{\pi^\varepsilon (2n+1)^{-1+\varepsilon}}{\cos\varepsilon\pi/2} = \frac{\pi^\varepsilon(2-2^\varepsilon)\zeta(1-\varepsilon)}{2\cos\varepsilon\pi/2} \\ &= -\frac{1}{2\varepsilon} + \frac{\gamma_E}{2} - \frac{1}{2}\ln\frac{\pi}{2}. \end{aligned} \tag{B.20}$$

Then we have

$$I_-(z) = -\frac{\gamma_E}{2} - \frac{1}{2}\ln\frac{z}{\pi}. \tag{B.21}$$

To have the result for the tadpole integral, we integrate (B.13). We obtain for bosons

$$\mathscr{T}_T^+ = \frac{T^2}{12} - \frac{mT}{4\pi} - \frac{m^2}{16\pi^2}\left[\ln\frac{m^2}{c_+^2T^2} - 1\right], \tag{B.22}$$

for fermions

$$\mathscr{T}_T^- = \frac{T^2}{24} + \frac{m^2}{16\pi^2}\left[\ln\frac{m^2}{c_-^2T^2} - 1\right]. \tag{B.23}$$

The constant terms are

$$\begin{aligned} \ln c_+ &:= -\gamma_E + \ln 4\pi = 1.95381, \qquad c_+ = 7.05551 \\ \ln c_- &:= -\gamma_E + \ln \pi = 0.567514, \qquad c_- = 1.7638. \end{aligned} \tag{B.24}$$

Therefore in the high-temperature expansion, we have

$$\begin{aligned} &\text{bosons with cutoff :} && \mathscr{T} = \frac{\Lambda^2}{8\pi^2} + \frac{T^2}{12} - \frac{mT}{4\pi} - \frac{m^2}{16\pi^2}\ln\frac{\Lambda^2}{d_+^2T^2} \\ &\text{bosons with dim.reg. :} && \mathscr{T} = \frac{T^2}{12} - \frac{mT}{4\pi} - \frac{m^2}{16\pi^2}\left[\frac{1}{\varepsilon} - \gamma_E + \ln\frac{4\pi\mu^2}{c_+^2T^2}\right], \\ &\text{fermions with cutoff :} && \mathscr{T} = -\frac{\Lambda^2}{8\pi^2} + \frac{T^2}{24} + \frac{m^2}{16\pi^2}\ln\frac{\Lambda^2}{d_-^2T^2} \\ &\text{fermions with dim.reg. :} && \mathscr{T} = \frac{T^2}{24} + \frac{m^2}{16\pi^2}\left[\frac{1}{\varepsilon} - \gamma_E + \ln\frac{4\pi\mu^2}{c_-^2T^2}\right], \end{aligned} \tag{B.25}$$

where

$$\begin{aligned} \ln d_+ &= -\gamma_E + 1 + \ln 2\pi = 2.26066, \quad d_+ = 9.58943, \\ \ln d_- &= -\gamma_E + 1 + \ln\frac{\pi}{2} = 0.874367, \quad d_- = 2.39736. \end{aligned} \tag{B.26}$$

B.2 The Bubble Diagram

Similarly to the tadpole case, we just define the basic integral. In imaginary time, this corresponds to the expression

$$\mathscr{I}_E(x) = \alpha G_{33}(m_1, x)G_{33}(m_2, x), \tag{B.27}$$

where $\alpha = -1$ if both propagating particles are fermions. This formula is true if two different particles propagate on the two lines. In this note we discuss only the case in which the particles are identical and there is no chemical potential in the system.

In Fourier space, it reads

$$\mathscr{I}_E(q) = \alpha T \sum\!\!\!\!\!\!\int \frac{d^3p}{(2\pi)^3} \frac{1}{(\omega_n^2 + \omega_{1p}^2)((q_0 - \omega_n)^2 + \omega_{2(\mathbf{q}-\mathbf{p})}^2)}. \tag{B.28}$$

One can tell immediately the result of the integral for the $q = 0$ case. There we have

$$\mathscr{I}_E(q) = \alpha T \sum\!\!\!\!\!\!\int \frac{d^3p}{(2\pi)^3} \frac{1}{(\omega_n^2 + p^2 + m^2)^2} = -\frac{\partial \mathscr{T}}{\partial m^2}. \tag{B.29}$$

At zero temperature, we can use (B.5) or (B.6), and we have with cutoff

$$\mathscr{I}_E^{T=0}(0) = -\frac{\partial}{\partial m^2}\left[\frac{m^2}{16\pi^2}\ln\frac{em^2}{4\Lambda^2}\right] = \frac{1}{16\pi^2}\left[\ln\frac{4\Lambda^2}{em^2} - 1\right] \tag{B.30}$$

and with dimensional regularization

$$\begin{aligned}\mathscr{I}_E^{T=0}(0) &= -\frac{\partial}{\partial m^2}\left[\frac{m^2}{16\pi^2}\left(-\frac{1}{\varepsilon} + \gamma_E - 1 + \ln\frac{m^2}{4\pi\mu^2}\right)\right] \\ &= \frac{1}{16\pi^2}\left(\frac{1}{\varepsilon} - \gamma_E - \ln\frac{m^2}{4\pi\mu^2}\right).\end{aligned} \tag{B.31}$$

The finite-temperature correction reads, using (B.13),

$$\mathscr{I}_E^T(0) = \frac{1}{4\pi^2} I_\alpha(\beta m, \mu = 0). \tag{B.32}$$

At high temperatures, we can use (B.25) and write

$$\begin{aligned}&\text{bosons with cutoff :} && \mathscr{I}_E(0) = \frac{T}{8\pi m} + \frac{1}{16\pi^2}\ln\frac{\Lambda^2}{d_+^2 T^2} \\ &\text{bosons with dim.reg. :} && \mathscr{I}_E(0) = \frac{T}{8\pi m} + \frac{1}{16\pi^2}\left[\frac{1}{\varepsilon} - \gamma_E + \ln\frac{4\pi\mu^2}{c_+^2 T^2}\right], \\ &\text{fermions with cutoff :} && \mathscr{I}_E(0) = -\frac{1}{16\pi^2}\ln\frac{\Lambda^2}{d_-^2 T^2} \\ &\text{fermions with dim.reg. :} && \mathscr{I}_E(0) = -\frac{1}{16\pi^2}\left[\frac{1}{\varepsilon} - \gamma_E + \ln\frac{4\pi\mu^2}{c_-^2 T^2}\right].\end{aligned} \tag{B.33}$$

To obtain the momentum-dependence, we change to real time, and write the retarded expression

$$i\mathscr{I}^{(ar)}(q) = 2\int \frac{d^4p}{(2\pi)^4}\left[iG^{(rr)}(p)iG^{(ra)}(q-p)\right]. \tag{B.34}$$

This is a causal function, so it can be reproduced from its discontinuity. We obtain

$$\underset{q_0}{\text{Disc}}\, i\mathscr{I}^{(ar)}(q) = \int \frac{d^4p}{(2\pi)^4}\varrho(p)\varrho(q-p)(1+n(p_0)+n(q_0-p_0)). \tag{B.35}$$

Using the free spectral function and the notation $k = q - p$, we have

$$\begin{aligned}&\text{Disc}\, i\mathscr{I}(q)\\ &= \int \frac{d^3\mathbf{p}}{(2\pi)^3}\,\frac{(2\pi)}{4\omega_p\omega_k}\Big[\left[\delta(q_0-\omega_p-\omega_k)-\delta(q_0+\omega_p+\omega_k)\right]\left[1+n_p+n_k\right]\\ &\qquad +\left[\delta(q_0-\omega_p+\omega_k)-\delta(q_0+\omega_p-\omega_k)\right]\left[n_k-n_p\right]\Big].\end{aligned} \tag{B.36}$$

We see that $\text{Disc}\, i\mathscr{I}(-q_0,\mathbf{q}) = \text{Disc}\, i\mathscr{I}(q_0,\mathbf{q})$, so it is enough to work out the $q_0 > 0$ case. We obtain

$$\begin{aligned}\text{Disc}\, i\mathscr{I}(q_0>0,\mathbf{q}) = \int \frac{d^3\mathbf{p}}{(2\pi)^3}\,\frac{(2\pi)}{4\omega_p\omega_k}\Big[&\delta(q_0-\omega_p-\omega_k)\left[1+n_p+n_k\right]\\ &+2\delta(q_0-\omega_p+\omega_k)\left[n_k-n_p\right]\Big].\end{aligned} \tag{B.37}$$

This integral depends on the angle between $\mathbf{p}$ and $\mathbf{q}$. We change from $\cos\theta \to k$ with the help of the relation

$$k^2 = q^2+p^2+2qpx \quad\Rightarrow\quad pdx = \frac{k}{q}dk, \qquad |q-p| < k < q+p, \tag{B.38}$$

which means that k, p, q forms a triangle. This means that

$$\begin{aligned}\text{Disc}\, i\mathscr{I}(k) \;= \frac{1}{8\pi k}\int_0^\infty dqdp\,\Theta_\Delta(k,p,q)\frac{pq}{\omega_p\omega_q}\Big[&\delta(k_0-\omega_p-\omega_q)(1+n_p+n_q)\\ &+2\delta(k_0-\omega_p+\omega_q)(n_q-n_p)\Big]\end{aligned}$$

$$= \frac{1}{8\pi k}\int_0^\infty dp\frac{p}{\omega_p}\int_{\omega_-}^{\omega_+} d\omega_q \Big[\delta(k_0-\omega_p-\omega_q)(1+n_p+n_q) + 2\delta(k_0-\omega_p+\omega_q)(n_q-n_p)\Big]$$

$$= \frac{1}{8\pi k}\int_m^\infty d\omega\Big[\Theta(\omega_+ > k_0-\omega > \omega_-)(1+n(\omega)+n(k_0-\omega)) + 2\Theta(\omega_+ > \omega-k_0 > \omega_-)(n(\omega-k_0)-n(\omega))\Big], \quad \text{(B.39)}$$

where $\omega_\pm^2 = (k\pm p)^2+m^2$. The constraints taking into account both theta functions can be summarized as

$$\begin{aligned} &\omega_+ > |k_0-\omega| > \omega_- \\ &|K^2-2k_0\omega| < 2kp \\ &4K^2\omega^2 - 4K^2k_0\omega + K^4 - 4k^2m^2 < 0. \end{aligned} \quad \text{(B.40)}$$

The positions of the zeros are

$$\Omega^\pm = \frac{1}{2}\left(k_0 \pm k\sqrt{1-\frac{4m^2}{K^2}}\right). \quad \text{(B.41)}$$

This is real if $K^2 > 4m^2$ or $K^2 < 0$. The solution of the inequality then reads

$$\begin{aligned} K^2 > 4m^2 \quad &\Rightarrow \quad \Omega_+ > \omega > \Omega_- \\ K^2 < 0 \quad &\Rightarrow \quad \Omega_+ < \omega \quad \text{or} \quad \omega < \Omega_-. \end{aligned} \quad \text{(B.42)}$$

Since $\Omega_- < 0$ if $K^2 < 0$, this term does not contribute in the integration range $[m,\infty]$. In the other cases, one can prove that for $K^2 > 4m^2$, we have $\Omega_- > m$, and for $K^2 < 0$, we have $\Omega_+ > m$. Taking into account that we still have $k_0-\Omega_+ = \Omega_-$, we obtain

$$\begin{aligned} \text{Disc}\, i\mathscr{I}(k) \;&= \frac{1}{8\pi}\Theta(K^2>4m^2)\sqrt{1-\frac{4m^2}{K^2}} \\ &+\frac{1}{4\pi k}\left(\Theta(K^2>4m^2)+\Theta(K^2<0)\right)\int_{|\Omega_-|}^{\Omega_+} d\omega n(\omega). \end{aligned} \quad \text{(B.43)}$$

The integral can be performed:

$$\begin{aligned}\text{Disc}\, i\mathscr{I}(k) &= \frac{1}{8\pi}\Theta(K^2 > 4m^2)\sqrt{1-\frac{4m^2}{K^2}} + \\ &+\frac{1}{4\pi k}\left(\Theta(K^2 > 4m^2) + \Theta(K^2 < 0)\right)\ln\frac{1-e^{-\beta\Omega_+}}{1-e^{-\beta|\Omega_-|}}. \quad \text{(B.44)}\end{aligned}$$

At zero temperature, we have only the first term: this yields a branch cut starting at $2m$ with a square-root threshold behavior. This corresponds to the creation of two real particles. At finite temperature, the amplitude of the branch cut is modified, and we also obtain a contribution below the light cone ($K^2 < 0$). This latter term is allowed because the finite temperature leads to Lorentz invariance-breaking (it singles out a rest frame). The name of this contribution is Landau damping.

We can study some limiting cases:

- For small q_0, the Landau damping reads

$$\text{Disc}\, i\mathscr{I}(q_0 \ll q) = \frac{q_0}{4\pi q} n\left(\frac{q}{2}\sqrt{1+\frac{4m^2}{q^2}}\right). \quad \text{(B.45)}$$

- For small q, the finite-temperature correction to the zero-temperature result reads

$$\frac{1}{4\pi}\Theta(Q^2 > 4m^2)\sqrt{1-\frac{4m^2}{Q^2}}\, n\left(\frac{q_0}{2}\right). \quad \text{(B.46)}$$

- At high temperature ($T \gg m, q_0, q$), the second term reads

$$\frac{T}{4\pi q}\left(\Theta(Q^2 > 4m^2) + \Theta(Q^2 < 0)\right)\ln\left|\frac{q_0+q\gamma}{q_0-q\gamma}\right|, \qquad \gamma = \sqrt{1-\frac{4m^2}{Q^2}}. \quad \text{(B.47)}$$

Once we know the discontinuity, we can recover the original function using the Kramers–Kronig relation. The only problem is that the zero-temperature part goes to a constant at large q_0 value, and therefore, the Kramers–Kronig integral does not converge. To overcome this difficulty, we calculate the contribution directly at zero temperature at finite momenta. We write for the 11 part

$$i\mathscr{I}_{T=0}(q) = -\int\frac{d^4p}{(2\pi)^4}\,\frac{1}{(p^2-m^2+i\varepsilon)((q-p)^2-m^2+i\varepsilon)}. \quad \text{(B.48)}$$

Wick rotation is performed with the rule

$$\int\frac{dp_0}{2\pi}f(p_0) = i\int\frac{dp_{0E}}{2\pi}f(ip_{0E}), \quad \text{(B.49)}$$

and we apply Feynman parameterization:

$$\mathscr{I}_{T=0}(q) = -\int_0^1 dx \int \frac{d^4p_E}{(2\pi)^4} \frac{1}{(p_E^2 + m^2 + q_E^2 x(1-x))^2}. \tag{B.50}$$

We now use 4D momentum cutoff to evaluate this expression. With $z = p_E^2$ we obtain

$$\begin{aligned}\mathscr{I}_{T=0}(q) &= -\frac{1}{16\pi^2}\int_0^1 dx \int_0^{\Lambda^2} dz \frac{z}{(z + m^2 + q_E^2 x(1-x))^2} \\ &= -\frac{1}{16\pi^2}\left(\ln\frac{\Lambda^2}{m^2} - 1\right) + \frac{1}{16\pi^2}\int_0^1 dx \ln\frac{m^2 + q_E^2 x(1-x))^2}{m^2}. \end{aligned} \tag{B.51}$$

This means that

$$\mathscr{I}_{T=0}(q) = \mathscr{I}_{T=0}(q=0) + \frac{1}{16\pi^2}\int_0^1 dx \ln\frac{m^2 - q^2 x(1-x)}{m^2}. \tag{B.52}$$

This formula should be true independently of the chosen regularization. Therefore, the full expression can be written as

$$\begin{aligned}\mathscr{I}^{(ra)}(q) = \; & \mathscr{I}_{T=0}(q=0) + \frac{1}{16\pi^2}\int_0^1 dx \ln\frac{m^2 - q^2 x(1-x)}{m^2}\Bigg|_{q_0+i\varepsilon} \\ & + \int_{-\infty}^{\infty}\frac{d\omega}{2\pi}\frac{\mathrm{Disc}\, i\mathscr{I}_T(\omega, \mathbf{q})}{q_0 - \omega + i\varepsilon}, \end{aligned} \tag{B.53}$$

where in the second line, only the finite-T part of the discontinuity has to be taken into account.

B.3 Dimensional Regularization

The basic idea of dimensional regularization is that we evaluate the integrals in arbitrary dimension and identify the divergences by the poles of the result in going to integer dimensions.

The basic input to dimensional regularization is that the surface of a d-dimensional sphere $K_d = \frac{2\pi^{d/2}}{\Gamma(d/2)}$ is an analytic function of the dimension. Therefore, a rotationally invariant integrand can be rewritten as

$$\begin{aligned}\mu^{2\varepsilon}\int\frac{d^{d-2\varepsilon}p}{(2\pi)^{d-2\varepsilon}} &= \frac{2(4\pi\mu^2)^{\varepsilon}}{(4\pi)^{d/2}\Gamma(d/2-\varepsilon)}\int dp\, p^{d-1-2\varepsilon}\\ &= \frac{(4\pi\mu^2)^{\varepsilon}}{(4\pi)^{d/2}\Gamma(d/2-\varepsilon)}\int dz\, z^{d/2-\varepsilon-1},\end{aligned} \tag{B.54}$$

where in the last term, we performed the change of integration variable $z = p^2$. Note that $d = 1$ is also a possible choice.

We need the quantity μ of mass dimension to maintain the original engineering dimension of the integral. Its numerical value is arbitrary, and its appearance is an unavoidable consequence of the presence of divergences (in the case of cutoff regularization, the cutoff itself provides this scale).

One of the most common integrals reads

$$\int_0^\infty dz\, z^{a-1}(M^2+z)^{-b} = (M^2)^{a-b}\,\frac{\Gamma(b-a)\Gamma(a)}{\Gamma(b)}. \tag{B.55}$$

The properties of the gamma functions are

$$\begin{aligned}&\Gamma(z) = \int_0^\infty dx\, x^{z-1}\, e^{-x}\\ &\Gamma(z+1) = z\Gamma(z)\\ &\Gamma(1) = \Gamma(2) = 1,\ \Gamma(1/2) = \sqrt{\pi}\\ &\Gamma(\varepsilon) = \frac{1}{\varepsilon} - \gamma_E + \varepsilon\left(\frac{\gamma_E^2}{2} + \frac{\pi^2}{12}\right)\\ &\Gamma(-1+\varepsilon) = -\frac{1}{\varepsilon} + \gamma_E - 1 - \varepsilon\left(1 - \gamma_E + \frac{\gamma_E^2}{2} + \frac{\pi^2}{12}\right).\end{aligned} \tag{B.56}$$

Finally, we often need the expansion

$$X^{\varepsilon} = e^{\varepsilon \ln X} = 1 + \varepsilon \ln X + \frac{\varepsilon^2}{2}(\ln X)^2. \tag{B.57}$$

Chapter C
Integrals Relevant for Dimensional Reduction

C.1 Nonstatic Sum-Integrals

The high-temperature expansion of the nonstatic contribution to the free-energy density of the massive ideal gas in powers of M^2/T^2 can be related to the mass expansion of the nonstatic tadpole integral up to an unimportant constant term:

$$I(M) = T\sum_{n\neq 0}\int p^{(\Lambda)}\log(\beta^2(\omega_n^2+p^2+M^2)) = I_0 + I_1M^2 + I_2M^4 + \ldots,$$

$$I'(M) = T\sum_{n\neq 0}\int p^{(\Lambda)}\frac{1}{\omega_n^2+p^2+M^2} = I_1 + 2I_2M^2 + 3I_3M^4 + \ldots. \qquad \text{(C.1)}$$

The three-dimensional integrals are computed with sharp momentum cutoff Λ with the result [3]

$$I_1 = I_1^{(2)}\Lambda^2 + I_1^{(1)}\Lambda T + I_1^{(0)}T^2, \qquad I_1^{(1)} = \frac{1}{8\pi^2}, \quad I_1^{(1)} = -\frac{1}{2\pi^2}, \quad I_1^{(0)} = \frac{1}{12},$$

$$I_2 = I_2^{(ln)}\ln\frac{\Lambda}{T} + I_2^{(0)}, \qquad I_2^{(ln)} = -\frac{1}{16\pi^2}, \quad I_2^{(0)} = \frac{1}{16\pi^2}[1+\ln(2\pi)-\gamma_E],$$

$$I_3 = \frac{\zeta(3)}{192\pi^4T^2}. \qquad \text{(C.2)}$$

A. Jakovác, A. Patkós, *Resummation and Renormalization in Effective Theories of Particle Physics*, Lecture Notes in Physics 912,
DOI 10.1007/978-3-319-22620-0

The nonstatic bubble integral can be reduced to a one-variable integral plus some analytic terms:

$$\begin{aligned}
\mathscr{B}^{nonstatic}(\mathbf{k}) &= T\sum_{n\neq 0}\int p^{(\Lambda)}\frac{1}{(\omega_n^2+\mathbf{p}^2)(\omega_n^2+(\mathbf{p}+\mathbf{k})^2)}\\
&= 2I_2^{(0)} + B(k/T) + F(k/\Lambda),\\
B(\kappa) &= \frac{1}{4\pi^2}\int_0^\infty \frac{dy}{y}\left(1-\frac{y}{\kappa}\ln\left|\frac{\kappa+2y}{\kappa-2y}\right|\right)\left(\frac{1}{e^y+1}+\frac{1}{2}-\frac{1}{y}\right)\\
F(x) &= \left(\frac{2}{x}-1\right)\ln\left(1-\frac{x}{2}\right)+1.
\end{aligned} \tag{C.3}$$

The expansion coefficients of the "setting-sun" integral are introduced as

$$\begin{aligned}
&T^2\sum_{l,n,m\neq 0}\int_{p_1}^{(\Lambda)}\int_{p_2}^{(\Lambda)}\int_{p_3}^{(\Lambda)}\frac{(2\pi)^3\delta(\mathbf{p_1}+\mathbf{p_2}+\mathbf{p_3})\delta_{n_1+n_2+n_3,0}}{(\omega_l^2+\omega_{p_1}^2)(\omega_m^2+\omega_{p_2}^2)(\omega)_m^2+\omega_{p_3}^2)}\\
&= K_0 + K_1M^2 + K_2M^4 + \ldots
\end{aligned} \tag{C.4}$$

$$\begin{aligned}
K_0 &= K_0^{(2)}\Lambda^2 + K_0^{(1)}\Lambda T + K_0^{(ln)}T^2\ln\frac{\Lambda}{T} + K_0^{(0)}T^2,\\
K_1 &= K_1^{(2ln)}\left(\ln\frac{\Lambda}{T}\right)^2 + K_1^{(ln)}\ln\frac{\Lambda}{T} + K_1^{(0)},
\end{aligned} \tag{C.5}$$

and they are computed mostly numerically:

$$\begin{aligned}
&K_0^{(2)} = 0.0001041333, \quad K_0^{(1)} = -0.0029850437, \quad K_0^{(ln)} = \frac{5}{32\pi^2}\\
&K_0^{(0)} = -0.0152887686, \quad K_1^{(2ln)} = -\frac{3}{128\pi^4}, \quad K_1^{(ln)} = 0.001087971.
\end{aligned} \tag{C.6}$$

C.2 Three-Dimensional Integrals

The integrals that are relevant for the one-loop computation of the effective potential in three dimensions are the following:

$$\int p^{(\Lambda)} \log(p^2 + M^2) = 2J_1 M^2 \Lambda + 2J_0 M^3, \quad J_1 = \frac{1}{4\pi^2}, \quad J_0 = -\frac{1}{12\pi}$$

$$\int_{p_1}^{(\Lambda)} \int_{p_2}^{(\Lambda)} \int_{p_3}^{(\Lambda)} \frac{(2\pi)^3 \delta(\mathbf{p_1} + \mathbf{p_2} + \mathbf{p_3})}{(p_1^2 + M^2)(p_2^2 + M^2)(p_3^2 + M^2)} = L^{(ln)} \log \frac{\Lambda^2}{9M^2} + L^{(0)},$$

$$L^{(ln)} = \frac{1}{32\pi^2}, \quad L_0 = 0.00670322. \tag{C.7}$$

References

1. A. Besser, Finite and p-adic polylogarithms. Compos. Math. **130**, 215–223 (2002)
2. L. Dolan, R. Jackiw, Phys. Rev. D **9**, 3320 (1974)
3. A. Jakovác, Phys. Rev. D **53**, 4538 (1996)